iScience

CellPress

Article

Enantioselective Copper-Catalyzed Cyanation of Remote C(sp^3)-H Bonds Enabled by 1,5-Hydrogen Atom Transfer

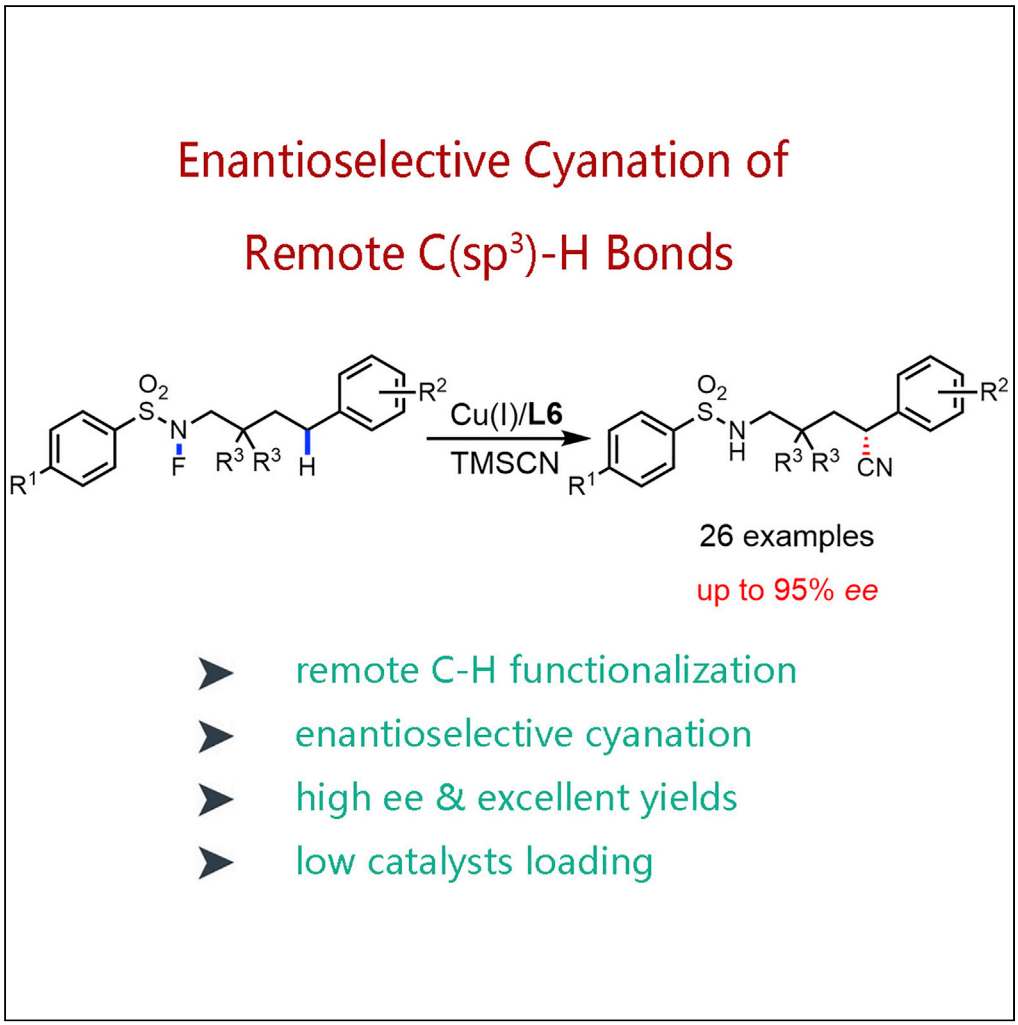

Cheng-Yu Wang, Zi-Yang Qin, Yu-Ling Huang, Ruo-Xing Jin, Quan Lan, Xi-Sheng Wang

xswang77@ustc.edu.cn

HIGHLIGHTS

Remote C-H functionalization

Enantioselective cyanation

High *ee* and excellent yields

Low catalysts loading

Wang et al., iScience *21*, 490–498
November 22, 2019
https://doi.org/10.1016/j.isci.2019.10.048

iScience

CellPress

Article

Enantioselective Copper-Catalyzed Cyanation of Remote C(sp^3)-H Bonds Enabled by 1,5-Hydrogen Atom Transfer

Cheng-Yu Wang,[1,2] Zi-Yang Qin,[1,2] Yu-Ling Huang,[1] Ruo-Xing Jin,[1] Quan Lan,[1] and Xi-Sheng Wang[1,3,*]

SUMMARY

The direct functionalization of C(sp^3)-H bonds has led to the development of methods to access molecules or intermediates from basic chemicals in an atom- and step-economic fashion. Nevertheless, achieving high levels of chemo-, regio-, and enantioselectivity in these reactions remains challenging due to the ubiquity and low reactivity of C(sp^3)-H bonds. Herein, we report an unprecedented protocol for enantioselective cyanation of remote C(sp^3)-H bonds. With chiral Box-Cu complex as the catalyst, the reaction of N-fluorosulfonamide furnishes the corresponding products in excellent yields and high enantiomeric excess (*ee*) under mild reaction conditions. A radical relay pathway involving 1,5-hydrogen atom transfer (1,5-HAT) of N-center radicals followed by enantioselective cyanation of the *in situ*-formed benzyl radicals is proposed. This enantioselective copper-catalyzed cyanation thus offers insights into an efficient way for the synthesis of bioactive molecules for drug discovery.

INTRODUCTION

Synthesizing functional molecules in a rapid, efficient, and convenient manner still represents a significant challenge in organic synthesis (McMurry et al., 2011; Gutekunst and Baran, 2011; Yamaguchi et al., 2012; Karimov and Hartwig, 2018). The past several decades have witnessed the renaissance of C-H bond functionalization, which thus offers a unique solution for facile synthesis of functional molecules from basic chemicals (Giri et al., 2009; Colby et al., 2010; Lyons and Sanford, 2010; Newhouse and Baran, 2011; Sun et al., 2011; Wencel-Delord et al., 2011; Wendlandt et al., 2011; Liu et al., 2015; Davies and Morton, 2016; Rao and Shi, 2016; Liang and Jiao, 2017; Yang et al., 2017; Dong et al., 2017; Gensch et al., 2018). Specifically, the direct functionalization of C(sp^3)-H bonds has led to the development of methods to access molecules or intermediates from simple starting materials in an atom- and step-economic fashion (Zhang et al., 2011; Baudoin, 2011; Rouquet and Chatani, 2013; Xie et al., 2014; Liu and Groves, 2015; He et al., 2016, 2017; Hartwig, 2016; Yi et al., 2017; Saint-Denis et al., 2018). Nevertheless, achieving high levels of chemo-, regio-, and enantioselectivity in these reactions remains challenging due to the ubiquity and low reactivity of C(sp^3)-H bonds. To date, one efficient approach to asymmetric C(sp^3)-H functionalization was the enantioselective insertion of chiral metallocarbene (Davies and Beckwith, 2003; Doyle et al., 2010; Davies and Morton, 2011; Davies and Manning, 2008; Lu and Zhang, 2011; Zheng and You, 2014; Schafer and Blakey, 2015; Newton et al., 2017) or metallonitrene (Davies and Manning, 2008; Lu and Zhang, 2011; Zheng and You, 2014; Schafer and Blakey, 2015; Newton et al., 2017; Müller and Fruit, 2003; Collet et al., 2011) species *in situ* generated into C-H bonds. The other known approach was transition-metal-catalyzed C(sp^3)-H activation, which involves a stereocontrolled C-H cleavage to generate an enantioenriched organometallic intermediate for further functionalization (Saint-Denis et al., 2018). Despite recent advances in both approaches, the efficient and practical methods for enantioselective functionalization of remote C(sp^3)-H bonds are still less developed.

As an alternative tactic, hydrogen-atom abstraction via radical path has long been used as a powerful tool to activate the C(sp^3)-H bonds. Of note is a radical relay strategy for enantioselective functionalization of allylic (Zhou and Andrus, 2002) and benzylic (Zhang et al., 2016, 2019a, 2019b, 2019c; Wang et al., 2018) C-H bonds has recently been developed, in which a benzylic or allylic radical generated by hydrogen-atom abstraction underwent asymmetric functionalization by a chiral copper catalysis. Although inert C(sp^3)-H bonds are almost impossible to distinguish from other aliphatic C-H bonds on the alkyl side chain, 1,n-hydrogen-atom transfer strategy offers us a reliable solution to selectively cleave the remote C(sp^3)-H bonds in a high chemo- and regioselective path. Starting from the pioneering work of Hofmann (Hofmann,

[1]Hefei National Laboratory for Physical Sciences at the Microscale and Department of Chemistry, Center for Excellence in Molecular Synthesis of CAS, University of Science and Technology of China, 96 Jinzhai Road, Hefei, Anhui 230026, P. R. China

[2]These authors contributed equally

[3]Lead Contact

*Correspondence: xswang77@ustc.edu.cn

https://doi.org/10.1016/j.isci.2019.10.048

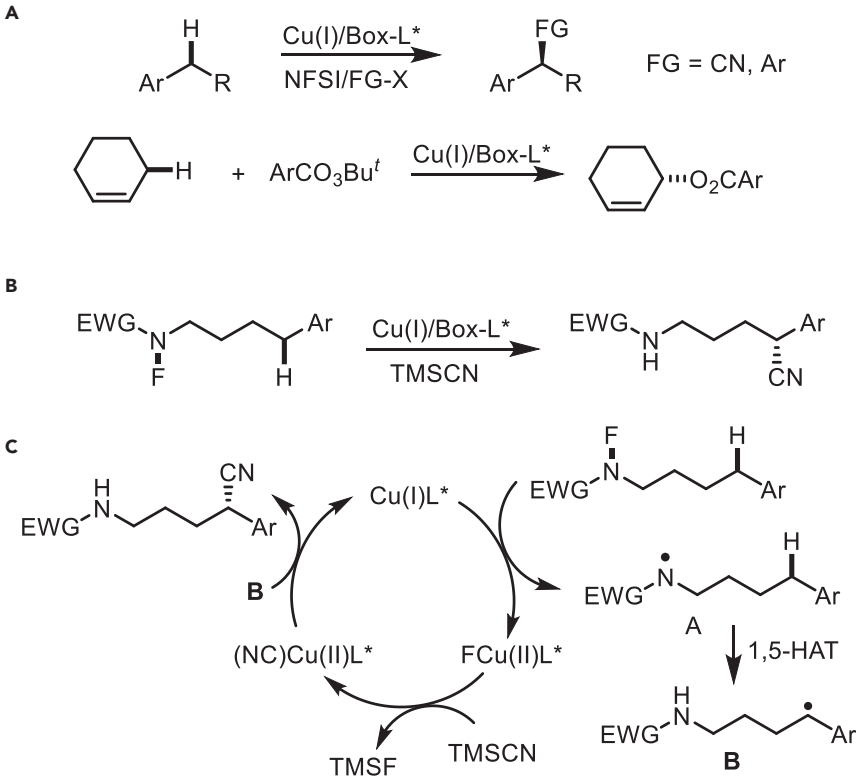

Scheme 1. Enantioselective C(sp^3)-H Functionalization via Reductive Elimination from Chiral Transition-Metal Catalyst

(A) Previous work: copper-catalyzed benzylic or allylic C-H functionaliztions.

(B) This work: copper-catalyzed remote C(sp^3)-H cyanation enabled by 1,5-HAT.

(C) Proposed mechanism.

1883), known as Hofmann–Löffler–Freytag (HLF) reaction with N-haloamines used as precursors to generate N-centered radical (Hofmann, 1883; Löffler and Freytag, 1909; Wolff, 1963; Neale, 1971; Mackiewicz and Furstoss, 1978), the selective cleavage of remote C(sp^3)-H bonds *via* 1,5-HAT process is well documented (Robertson et al., 2001; Čeković, 2003; Chiba and Chen, 2014; Stateman et al., 2018; Chu and Rovis, 2016, 2018; Martínez and Muñiz, 2015; Wappes et al., 2016; Choi et al., 2016; Xia et al., 2018; Na and Alexanian, 2018). Although the early examples utilize transition metal to facilitate electron transfer, to further expand the scope of this remote C(sp^3)-H functionalization process, many domino processes involving a metal-catalyzed cross-coupling pathway have developed (Scheme 1A) (Zhou and Andrus, 2002; Zhang et al., 2016, 2019a, 2019b, 2019c; Wang et al., 2018; Groendyke et al., 2016; Li et al., 2018; Liu et al., 2019; Bao et al., 2019). With the generation of N-centered radical initiating remote hydrogen transfer, the following cross-coupling reactions enabled by the recapture of *in situ*-generated carbon radical could be achieved with transition metals (Groendyke et al., 2016; Li et al., 2017, 2018; Liu et al., 2019; Bao et al., 2019; Zhang et al., 2019a, 2019b, 2019c; Yu et al., 2014). As our continuous efforts on selective cleavage of remote aliphatic C(sp^3)-H *via* a 1,5-HAT process (Scheme 1B) (Wang et al., 2017a, 2017b), we envisioned that the recapture of *in situ*-generated carbon radical of 1,5-HAT by chiral metal catalyst, followed by reductive elimination from the chiral metal complex would realize enantioselective C(sp^3)–H functionalizations, thus providing a convenient entry to optically pure δ-cyano amines and their pharmaceutical derivatives (Figure 1) (Sugimoto et al., 2000; van de Waterbeemd et al., 2001; Abdel-Rahman et al., 2002). More recently, the remote C(sp^3)-H functionalization was accomplished by the groups of Zhu (Bao et al., 2019) and Nagib (Zhang et al., 2019a, 2019b; 2019c), whereas the enantioselective remote C(sp^3)-H cyanation reaction of excellent yield and high *ee* still remains as an unsolved problem.

Herein, we described the first example of N-radical initiated enantioselective copper-catalyzed cyanation of remote C(sp^3)-H bonds with excellent yield and high enantioselectivity (up to 95% *ee*). This asymmetric

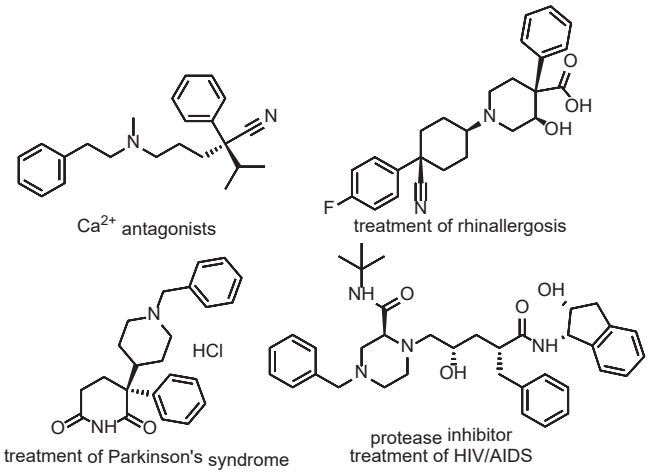

Figure 1. Pharmaceuticals Containing Chiral δ-cyano Amines and Their Derivatives

reaction has demonstrated high catalytic reactivity, excellent regio- and enantioselective control, low catalyst loading, mild conditions, and broad scope. The key to success is the recapture of the alkyl radical generated by selective cleavage of C(sp^3)-H bond *via* 1,5-HAT with Box-Cu catalyst resulting in chiral copper cyanide for stereoselective reductive elimination (Wang et al., 2018). This radical relay strategy will offer a solution for regio- and enantioselective functionalization of remote C(sp^3)-H bonds and provides an efficient way for facile synthesis of chiral δ-cyano amines and their pharmaceutical derivatives.

RESULTS AND DISCUSSION

Optimization of the Enantioselective Copper-Catalyzed Cyanation

Our initial investigation commenced with N-fluorosulfonamide**1a** used as the pilot substrate, along with trimethylsilyl cyanide (TMSCN) used as the coupling partner in the presence of a catalytic amount of $Cu(MeCN)_4PF_6$ (3 mol%) at room temperature. To our delight, the desired cyanation product **2a** was obtained in 62% yield and 78% *ee* when chiral bis(oxazoline) ligand **L1** was used (Entry 1, Table 1). To improve the enantioselectivity of this reaction, various chiral bis(oxazoline) ligands were next investigated. Gratifyingly, indanyl amino alcohol-derived bis(oxazoline) ligands (**L2**-**L7**) could afford almost the same good *ee* and normally satisfactory yield, whereas Pybox (**L8**) gave only trace amount of **2a** (Entries 2–8). Lowering the reaction temperature to 10°C could further improve the *ee* to 90%, albeit with a relatively lower yield (52%, Entry 9). A careful investigation of various copper salts with the optimal bis(oxazoline) ligand (**L6**) were next performed, which indicated that a variety of Cu(I) and Cu(II) sources (Entries 10–12) gave higher *ee*, but with a low overall yield. Although a majority of H-abstraction byproduct of nitrogen was found after the reaction had run for 24 h, we proposed decreasing catalyst loading might improve the mass balance by reducing the amount of H-abstraction byproducts and allowing for a higher yield (Shu et al., 2017). As expected, lower catalyst loading to 1 mol% remarkably increased the yield to about 80% without a decline in *ee* (Entries 13–14).

To further improve the yield of this transformation, solvent effect was next studied with 1 mol% of CuSCN used as the catalyst, which showed DCE was the optimal solvent with excellent yield and a slightly lower *ee* (99% yield, 90% *ee*, Entry 17). Interestingly, a lower concentration and an enhancement of the ratio of ligand to copper salts (2/1) could slightly improve the *ee* to 92% (Entries 19–21), whereas further reducing the reaction temperature to 0°C resulted in an obvious drop in yield and 29% of **1a** recovered from the reaction system (Entry 22). The absolute configuration of product **2a** was assigned as (R) by single crystal X-ray diffraction.

Scope of the Enantioselective Copper-Catalyzed Cyanation

With the optimal reaction conditions in hand, we next explored the scope of this enantioselective cyanation of remote C(sp^3)-H bonds (Figure 2). First, with respect to substituted benzenesulfonyl protecting groups ($ArSO_2$), both electron-donating (**1b**-**1c**) and electron-withdrawing (**1d**-**1e**) substituents (R1) at para-position of the aryl rings gave the desired product in good to excellent yield along with excellent *ee*, among

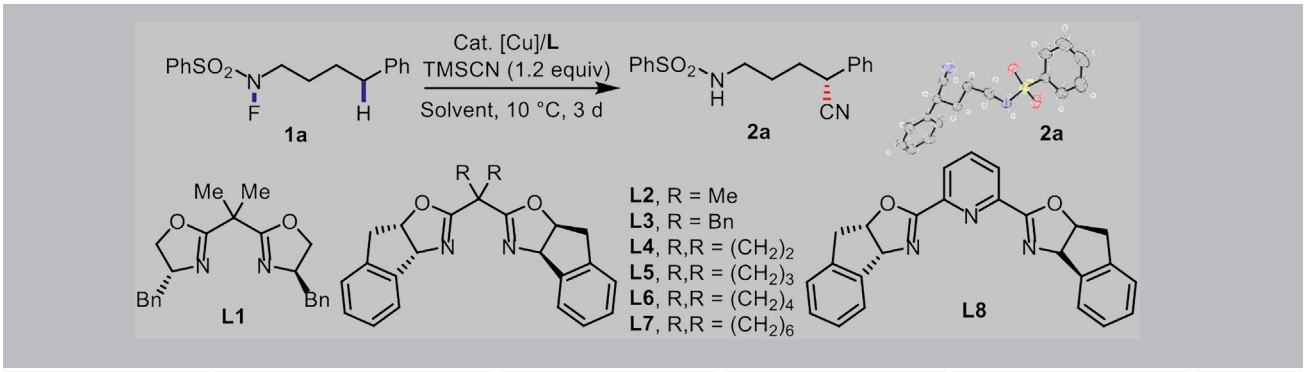

Entry	Cu cat.	Ligand	Solvent	Yield (%)	*ee* (%)
1	$Cu(MeCN)_4PF_6$	L1	DCM	62	78
2	$Cu(MeCN)_4PF_6$	L2	DCM	75	86
3	$Cu(MeCN)_4PF_6$	L3	DCM	33	87
4	$Cu(MeCN)_4PF_6$	L4	DCM	58	86
5	$Cu(MeCN)_4PF_6$	L5	DCM	70	87
6	$Cu(MeCN)_4PF_6$	L6	DCM	73	89
7	$Cu(MeCN)_4PF_6$	L7	DCM	33	87
8	$Cu(MeCN)_4PF_6$	L8	DCM	trace	–
9[a]	$Cu(MeCN)_4PF_6$	L6	DCM	52	90
10[a]	CuSCN	L6	DCM	43	92
11[a]	$Cu(OAc)_2$	L6	DCM	43	92
12[a]	CuI	L6	DCM	30	92
13[a,b]	CuSCN	L6	DCM	81	91
14[a,b]	$Cu(OAc)_2$	L6	DCM	78	92
15[a,b]	CuSCN	L6	MeCN	39	81
16[a,b]	CuSCN	L6	PhCl	84	88
17[a,b]	CuSCN	L6	DCE	99	90
18[a,b]	$Cu(OAc)_2$	L6	DCE	91	90
19[a,b,c]	CuSCN	L6	DCE	92	91
20[a,c,d]	CuSCN	L6	DCE	98	91
21[a,c,e]	CuSCN	L6	DCE	99	92
22[a,e,f]	CuSCN	L6	DCE	64	92

Table 1. Optimization of Reaction Conditions

Reaction conditions: **1a** (0.1 mmol, 1.0 equiv), TMSCN (1.2 equiv), Cu cat. (3 mol%), **L** (3.6 mol%), solvent (1.0 mL), rt, 2 d, Ar. Yields were determined by ^{1}HNMR analysis using CH_2Br_2 as internal standard. The *ee* values were determined by HPLC analysis on a chiral stationary phase.

DCM, dichloromethane; THF, tetrahydrofuran; DCE, 1,2-dichloroethane; Ac, acetyl.

[a]10°C, 3 days.

[b]Cu cat. (1 mol%), L6 (1.2 mol%).

[c]Solvent (2.0 mL).

[d]CuSCN (1 mol%), L6 (1.5 mol%).

[e]CuSCN (1 mol%), L6 (2 mol%).

[f]0°C.

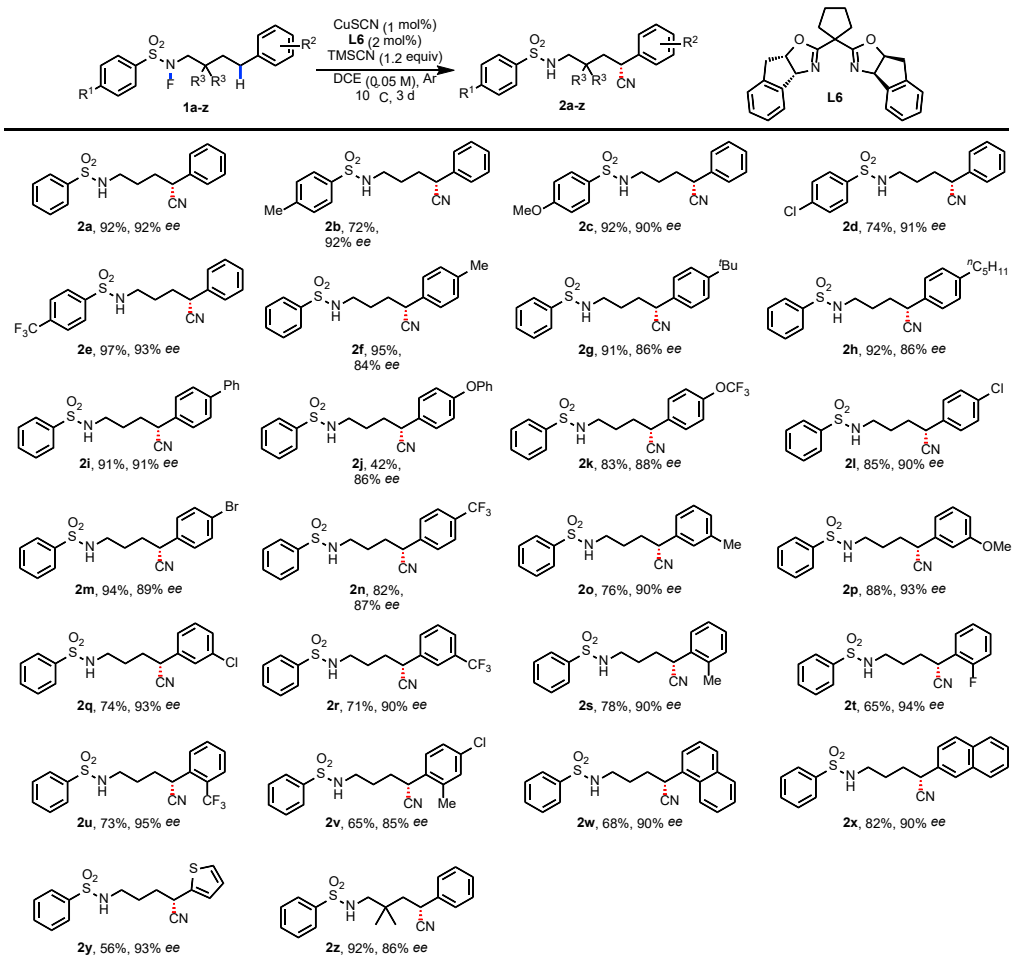

Figure 2. Substrate Scope of Enantioselective Copper-Catalyzed Remote C(sp^3)-H Cyanation

Reaction conditions: **1** (0.2 mmol, 1.0 equiv), TMSCN (1.2 equiv), CuSCN (1 mol%), **L6** (2 mol%), DCE (4.0 mL), 10°C, 3 d, Ar. Isolated yields. The *ee* values were determined by HPLC analysis on a chiral stationary phase.

which para-CF_3 substituted substrate performed best with 97% yield and 93% *ee*. Considering the common availability and low cost, benzenesulfonyl group was selected as the N-protecting group to investigate the substituent effect (R2) of the aromatic ring linked to the alkyl chain. A variety of N-fluorosulfonamides **1** installed with ortho-, meta-, and para-substituents on the aryl rings were smoothly cyanated on the benzylic position in this asymmetric catalytic system, furnishing the corresponding products **2** with satisfactory yields and high *ee* (up to 95%). Both electron-donating, including Me (**2f**, **2o**, **2s**), $^nC_5H_{11}$ (**2h**), ^{t}Bu (**2g**), PhO (**2j**), and MeO (**2p**), and electron-withdrawing groups, including F (**2t**), Cl (**2l**, **2q**), Br (**2m**), and CF_3 (**2n**, **2r**, **2u**), were well compatible with the optimized conditions. Notably, Br (**2m**) as well as inert halides including F and Cl on the aromatic ring offered the synthetic potential for further transformations through transition-metal-catalyzed cross-coupling methods. Moreover, polycyclic arenes, such as naphthalene (**2w**-**2x**), and heteroaromatic ring, such as thiophene (**2y**), were well tolerated in this reaction with high *ee* and good yield. To our surprise, the incorporation of two methyl groups to the alkyl chain to induce the Thorpe-Ingold effect failed to give higher *ee* (**2z**), possibly because the increased steric hindrance of the methyl groups hampered the stereo control of chiral copper catalyst.

Mechanistic Studies

To gain some insights into the mechanism of this asymmetric cyanation of remote C(sp^3)-H bonds, we next carried out a series of control experiments. Firstly, the addition of 2.0 equiv of 2,2,6,6-tetramethyl-1-piperidinyloxy (TEMPO) into the standard conditions completely inhibited the reaction, and **1a** was

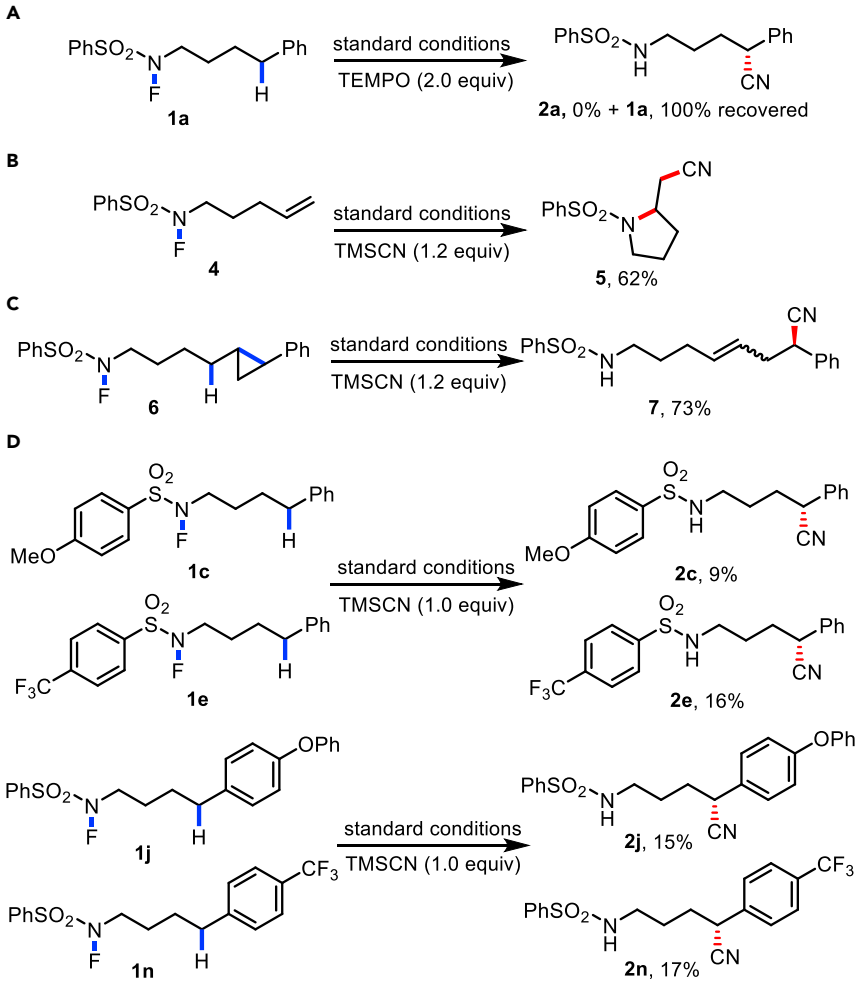

Scheme 2. Mechanistic Studies

(A) The radical trapping experiment with TEMPO.

(B) N-radical trapping experiment.

(C) Radical clock experiment.

(D) Competition experiments.

100% recovered from the reaction system (Scheme 2A), which was consistent with our previously noted hypothesis that this reaction may proceed *via* a radical path (Scheme 1). Although the coupling product of TEMPO and **1a** was not isolated, compounds **4** and **6** had been designed and synthesized to trap the corresponding radicals. Accordingly, the subjection of alkene **4** into the reaction system afforded 5-exo cyclization product **5** in 62% yield, indicating an N-centered radical was involved in the catalytic cycle (Scheme 2B). Meanwhile, a radical clock experiment with **6** furnished the ring-opening product **7** in 73% yield, which suggested a carbon-centered radical generated *via* N-radical initiated 1,5-HAT (Scheme 2C). Secondly, competition experiments had been performed using N-fluorosulfonamide substrates with different substituents on respective aryl ring. Indeed, a competition experiment between **1c** and **1e** with para-OMe or CF_3 groups on the aryl rings in the arylsulfonyl protecting groups showed that trifluoromethylated substrate reacted faster than methoxylated substrate (16% yield to 9% yield). On the other hand, the competition experiment between **1j** and **1n** with para-OPh or CF_3 groups on the alkylated aryl rings afforded the desired products **2j** and **2n** in almost the same yields (15% and 17%, Scheme 2D). All these results indicated that a copper-involved single electron transfer process for the cleavage of N-F bond might be the rate-determining step (Zhang et al., 2016, 2019a; Shu et al., 2017; Shekhar et al., 2018, 2019b, 2019c). It should be noted that besides our proposed mechanism as shown in Scheme 1C, an alternative

mechanism involving the direct cyano group enantioselective transfer from chiral copper cyanide could not be excluded at this stage (Liu et al., 2018; Xiao et al., 2019).

Conclusion

In summary, we have developed a nitrogen-centered radical-initiated enantioselective copper-catalyzed cyanation of remote C(sp^3)-H bonds with high yield and enantioselectivity (up to 95% *ee*). This method has demonstrated high catalytic reactivity, excellent regio- and enantioselective control, low catalyst loading, mild conditions, and broad scope. This radical relay strategy will offer a solution for region- and enantioselective functionalization of remote C(sp^3)-H bonds and provides an efficient way for facile synthesis of chiral δ-cyano amines and their pharmaceutical derivatives. Mechanistic studies indicate that this transformation undergoes a radical relay pathway involving a 1,5-HAT process. Further exploration on enantioselective functionalizations of remote C(sp^3)-H bonds are currently ongoing in our laboratory.

Limitations of the Study

Starting materials were cyanated only on the benzylic position under the current reaction conditions.

METHODS

All methods can be found in the accompanying Transparent Methods supplemental file.

DATA AND CODE AVAILABILITY

The structures of **2a** reported in this article have been deposited in the Cambridge Crystallographic Data Center under accession numbers CCDC: 1911620.

SUPPLEMENTAL INFORMATION

Supplemental Information can be found online at https://doi.org/10.1016/j.isci.2019.10.048.

ACKNOWLEDGMENTS

We gratefully acknowledge the Strategic Priority Research Program of the Chinese Academy of Sciences (Grant No. XDB20000000), the National Basic Research Program of China (973 Program 2015CB856600), and the National Science Foundation of China (21971228, 21772187) for financial support. During the revision of our manuscript, we are informed that a similar work has just been accepted by Chem, see: Chem, xx, xx-xx (2019).

AUTHOR CONTRIBUTIONS

C.-Y. W. and Z.-Y. Q. designed and performed the experiments. Y.-L. H., R.-X. J., and Q. L. helped to complete the experiments. X.-S. W. directed the project and wrote the manuscript. All authors interpreted the results on the manuscript.

DECLARATION OF INTERESTS

The authors declare no competing interests.

Received: September 2, 2019
Revised: September 25, 2019
Accepted: October 23, 2019
Published: November 22, 2019

REFERENCES

Abdel-Rahman, H.M., Al-karamany, G.S., El-Koussi, N.A., Youssef, A.F., and Kiso, Y. (2002). HIV protease inhibitors: peptidomimetic drugs and future perspectives. Curr. Med. Chem. *9*, 1905–1922.

Bao, X., Wang, Q., and Zhu, J. (2019). Dual photoredox/copper catalysis for the remote C(sp^3)-H functionalization of alcohol and alkyl halides by *N*-alkoxypyridinium salts. Angew. Chem. Int. Ed. *58*, 2139–2143, Only one enantioselective example was reported in this work (74% yield & 86% ee).

Baudoin, O. (2011). Transition metal-catalyzed arylation of unactivated C(sp^3)-H bonds. Chem. Soc. Rev. *40*, 4902–4911.

Čeković, Ž. (2003). Reactions of δ-carbon radicals generated by 1,5-hydrogen transfer to alkoxyl radicals. Tetrahedron *59*, 8073–8090.

Chiba, S., and Chen, H. (2014). sp^3 C-H oxidation by remote *H*-radical shift with oxygen- and nitrogen-radicals: a recent update. Org. Biomol. Chem. *12*, 4051–4060.

Choi, G.J., Zhu, Q., Miller, D.C., Gu, C.J., and Knowles, R.R. (2016). Catalytic alkylation of remote C-H bonds enabled by proton-coupled electron transfer. Nature *539*, 268–271.

Chu, J.C.K., and Rovis, T. (2016). Amide-directed photoredox-catalysed C-C bond formation at unactivatedsp^3 C-H bonds. Nature *539*, 272–275.

Chu, J.C.K., and Rovis, T. (2018). Complementary strategies for directed C(sp^3)-H functionalization: a comparison of transition-metal-catalyzed activation, hydrogen atom transfer, and carbine/nitrene transfer. Angew. Chem. Int. Ed. *57*, 62–101.

Colby, D.A., Bergman, R.G., and Ellman, J.A. (2010). Rhodium-catalyzed C-C bond formation *via* heteroatom-directed C-H bond activation. Chem. Rev. *110*, 624–655.

Collet, F., Lescot, C., and Dauban, P. (2011). Catalytic C-H amination: the stereoselectivity issue. Chem. Soc. Rev. *40*, 1926–1936.

Davies, H.M.L., and Beckwith, R.E.J. (2003). Catalytic enantioselective C-H activation by means of metal-carbenoid-induced C-H insertion. Chem. Rev. *103*, 2861–2904.

Davies, H.M.L., and Manning, J.R. (2008). Catalytic C-H functionalization by metal carbenoid and nitrenoid insertion. Nature *451*, 417–424.

Davies, H.M.L., and Morton, D. (2011). Guiding principles for site selective and stereoselective intermolecular C-H functionalization by donor/acceptor rhodium carbenes. Chem. Soc. Rev. *40*, 1857–1869.

Davies, H.M.L., and Morton, D. (2016). Recent advances in C-H functionalization. J. Org. Chem. *81*, 343–350.

Dong, Z., Ren, Z., Thompson, S.J., Xu, Y., and Dong, G. (2017). Transition-metal-catalyzed C-H alkylation using alkenes. Chem. Rev. *117*, 9333–9403.

Doyle, M.P., Duffy, R., Ratnikov, M., and Zhou, L. (2010). Catalytic carbine insertion into C-H bonds. Chem. Rev. *110*, 704–724.

Gensch, T., James, M.J., Dalton, T., and Glorius, F. (2018). Increasing catalyst efficiency in C-H activation catalysis. Angew. Chem. Int. Ed. *57*, 2296–2306.

Giri, R., Shi, B.F., Engle, K.M., Maugel, N., and Yu, J.-Q. (2009). Transition metal-catalyzed C-H activation reactions: diastereoselectivity and enantioselectivity. Chem. Soc. Rev. *38*, 3242–3272.

Groendyke, B.J., AbuSalim, D.I., and Cook, S.P. (2016). Iron-catalyzed, fluoroamide-directed C-H fluorination. J. Am. Chem. Soc. *138*, 12771–12774.

Gutekunst, W.R., and Baran, P.S. (2011). C-H functionalization logic in total synthesis. Chem. Soc. Rev. *40*, 1976–1991.

Hartwig, J.T. (2016). Evolution of C-H bond functionalization from methane to methodology. J. Am. Chem. Soc. *138*, 2–24.

He, G., Wang, B., Nack, W.A., and Chen, G. (2016). Syntheses and transformations of α-amino acids *via* palladium-catalyzed auxiliary-directed sp^3 C-H functionalization. Acc. Chem. Res. *49*, 635–645.

He, J., Wasa, M., Chan, K.S.L., Shao, Q., and Yu, J.-Q. (2017). Palladium-catalyzed transformations of alkyl C-H bonds. Chem. Rev. *117*, 8754–8786.

Hofmann, A.W. (1883). Ueber die einwirkung des broms in alkalischer lösung auf die amine. Ber. Dtsch. Chem. Ges. *16*, 558–560.

Karimov, R.R., and Hartwig, J.F. (2018). Transition-metal-catalyzed selective functionalization of C(sp^3)-H bonds in natural products. Angew. Chem. Int. Ed. *57*, 4234–4241.

Li, T., Yu, P., Du, Y.-M., Lin, J.-S., Zhi, Y., and Liu, X.-Y. (2017). Enantioselectiveα-C-H functionalization of amides with indoles triggered by radical trifluoromethylation of alkenes: highly selective formation of C-CF$_3$ and C-C bonds. J. Fluor. Chem. *203*, 214–217.

Li, Z., Wang, Q., and Zhu, J. (2018). Copper-catalyzed arylation of remote C(sp^3)-H bonds in carboxamides and sulfonamides. Angew. Chem. Int. Ed. *57*, 13288–13292.

Liang, Y.-F., and Jiao, N. (2017). Oxygenation *via* C-H/C-C bond activation with molecular oxygen. Acc. Chem. Res. *50*, 1640–1653.

Liu, W., and Groves, J.T. (2015). Manganese catalyzed C-H halogenation. Acc. Chem. Res. *48*, 1727–1735.

Liu, B., Hu, F., and Shi, B.-F. (2015). Recent advances on esters synthesis *via* transition-metal catalyzed C-H functionalization. ACS Catal. *5*, 1863–1881.

Liu, Z., Chen, H., Lv, Y., Tan, X., Shen, H., Yu, H.-Z., and Li, C. (2018). Radical carbofluorination of unactivated alkenes with fluoride ions. J. Am. Chem. Soc. *140*, 6169–6175.

Liu, Z., Xiao, H., Zhang, B., Shen, H., Zhu, L., and Li, C. (2019). Copper-catalyzed remote C(sp^3)-H trifluoromethylation of carboxamides and sulfonamides. Angew. Chem. Int. Ed. *58*, 2510–2513.

Lu, H., and Zhang, X.P. (2011). Catalytic C-H functionalization by metalloporphyrins: recent developments and future directions. Chem. Soc. Rev. *40*, 1899–1909.

Lyons, T.W., and Sanford, M.S. (2010). Palladium-catalyzed ligand-directed C-H functionalization reactions. Chem. Rev. *110*, 1147–1169.

Löffler, K., and Freytag, C. (1909). Übereineneuebildungsweise von N-alkyliertenpyrrolidinen. Ber. Dtsch. Chem. Ges. *42*, 3427–3431.

Mackiewicz, P., and Furstoss, R. (1978). Radicauxamidyl: structure et reativite. Tetrahedron *34*, 3241–3260.

Martínez, C., and Muñiz, K. (2015). An iodine-catalyzed Hofmann-Löffler reaction. Angew. Chem. Int. Ed. *54*, 8287–8291.

McMurry, L., O'Hara, F., and Gaunt, M.J. (2011). Recent developments in natural product synthesis using metal-catalysed C-H bond functionalization. Chem. Soc. Rev. *40*, 1885–1898.

Müller, P., and Fruit, C. (2003). Enantioselective catalytic aziridinations and asymmetric nitrene insertions into CH bonds. Chem. Rev. *103*, 2905–2920.

Na, C.G., and Alexanian, E.J. (2018). A general approach to site-specific, intramolecular C-H functionalization using dithiocarbamates. Angew. Chem. Int. Ed. *57*, 13106–13109.

Neale, R.S. (1971). Nitrogen radical as synthesis intermediates. *N*-halamide rearrangements and additions to unsaturated hydrocarbons. Synthesis *3*, 1–15.

Newhouse, T., and Baran, P.S. (2011). If C-H bonds could talk: selective C-H bond oxidation. Angew. Chem. Int. Ed. *50*, 3362–3374.

Newton, C.J., Wang, S.-G., Oliveira, C.C., and Cramer, N. (2017). Catalytic enantioselective transformations involving C-H bond cleavage by transition-metal complexes. Chem. Rev. *117*, 8908–8976.

Rao, W.-H., and Shi, B.-F. (2016). Recent advances in copper-mediated chelation-assisted functionalization of unactivated C-H bonds. Org. Chem. Front. *3*, 1028–1047.

Robertson, J., Pillai, J., and Lush, R.K. (2001). Radical translocation reactions in synthesis. Chem. Soc. Rev. *30*, 94–103.

Rouquet, G., and Chatani, N. (2013). Catalytic functionalization of C(sp^2)-H and C(sp^3)-H bonds by using bidentate directing groups. Angew. Chem. Int. Ed. *52*, 11726–11743.

Saint-Denis, T.G., Zhu, R.-Y., Chen, G., Wu, Q.-F., and Yu, J.-Q. (2018). Enantioselective C(sp^3)-H bond activation by chiral transition metal catalysts. Science *359*, eaao4798.

Schafer, A.G., and Blakey, S.B. (2015). Ir-catalyzed enantioselective group transfer reactions. Chem. Soc. Rev. *44*, 5969–5980.

Shekhar, K.C., Dhungana, R., Shrestha, B., Thapa, S., Khanal, N., Basnet, P., Lebrun, R.W., and Giri, R. (2018). J. Am. Chem. Soc. *140*, 9801–9805.

Shu, W., Genoux, A., Li, Z., and Nevado, C. (2017). γ-Functionalization of amines through visible-light-mediated, redox-neutral C-C bond cleavage. Angew. Chem. Int. Ed. *56*, 10521–10524.

Stateman, L.M., Nakafuku, K.M., and Nagib, D.A. (2018). Remote C-H functionalization *via* selective hydrogen atom transfer. Synthesis *50*, 1569–1586.

Sugimoto, H., Yamanish, Y., Iimura, Y., and Kawakami, Y. (2000). Donepezil hydrochloride (E2020) and other acetylcholinesterase inhibitors. Curr. Med. Chem. *7*, 303–339.

Sun, C.-L., Li, B.-J., and Shi, Z.-J. (2011). Direct C-H transformation *via* iron catalysis. Chem. Rev. *111*, 1293–1314.

Wang, R., Jin, R.-X., Qin, Z.-Y., Bian, K.-J., and Wang, X.-S. (2017a). Novel and facile synthesis of 1-benzazepines*via* copper-catalyzed oxidative C(sp^3)-H/C(sp^2)-H cross-coupling. Chem. Commun. *53*, 12229–12232.

Wang, R., Li, Y., Jin, R.-X., and Wang, X.-S. (2017b). Copper-catalyzed oxidative C(sp^3)-H/

C(sp^2)-H cross-coupling *en route* to carbocyclic rings. Chem. Sci. *8*, 3838–3842.

Wang, F., Chen, P., and Liu, G. (2018). Copper-catalyzed radical relay for asymmetric radical transformation. Acc. Chem. Res. *51*, 2036–2046.

Wappes, E.A., Fosu, S.C., Chopko, T.C., and Nagib, D.A. (2016). Triiodide-mediated δ-amination of secondary C-H bonds. Angew. Chem. Int. Ed. *55*, 9974–9978.

van de Waterbeemd, H., Smith, D.A., Beaumont, K., and Walker, D.K. (2001). Property-based design: optimization of drug absorption and pharmacokinetics. J. Med. Chem. *44*, 1313–1333.

Wencel-Delord, J., Dröge, T., Liu, F., and Glorius, F. (2011). Towards mild metal-catalyzed C-H bond activation. Chem. Soc. Rev. *40*, 4740–4761.

Wendlandt, A.E., Suess, A.M., and Stahl, S.S. (2011). Copper-catalyzed aerobic oxidation C-H functionalizations: trends and mechanistic insights. Angew. Chem. Int. Ed. *50*, 11062–11087.

Wolff, M.E. (1963). Cyclization of *N*-halogenated amines (the Hofmann-Löffler reaction). Chem. Rev. *63*, 55–64.

Xia, Y., Wang, L., and Studer, A. (2018). Site-selective remote radical C-H functionalization of unactivated C-H bonds in amides using sulfone reagents. Angew. Chem. Int. Ed. *57*, 12940–12944.

Xiao, H., Shen, H., Zhu, L., and Li, C. (2019). Copper-catalyzed radical aminotrifluoromethylation of alkenes. J. Am. Chem. Soc. *141*, 11440–11445.

Xie, J., Pan, C., Abdukader, A., and Zhu, C. (2014). Gold-catalyzed C(sp^3)-H bond functionalization. Chem. Soc. Rev. *43*, 5245–5256.

Yamaguchi, J., Yamaguchi, A.D., and Itami, K. (2012). C-H bond functionalization: emerging synthetic tool for natural products and pharmaceuticals. Angew. Chem. Int. Ed. *51*, 8960–9009.

Yang, Y., Lan, J., and You, J. (2017). Oxidative C-H/C-H coupling reactions between two (hetero) arenes. Chem. Rev. *117*, 8787–8863.

Yi, H., Zhang, G., Wang, H., Huang, Z., Wang, J., Singh, A.K., and Lei, A. (2017). Recent advances in radical C-H activation/radical crossing-coupling. Chem. Rev. *117*, 9016–9085.

Yu, P., Lin, J.-S., Li, L., Zheng, S.-C., Xiong, Y.-P., Zhao, L.-J., Tan, B., and Liu, X.-Y. (2014). Enantioselective C-H bond functionalization triggered by radical trifluoromethylation of unactivated alkene. Angew. Chem. Int. Ed. *53*, 11890–11894.

Zhang, S.-Y., Zhang, F.-M., and Tu, Y.-Q. (2011). Direct sp^3α-C-H activation and functionalization of alcohol and ether. Chem. Soc. Rev. *40*, 1937–1949.

Zhang, W., Wang, F., McCann, S.D., Wang, D., Chen, P., Stahl, S.S., and Liu, G. (2016). Enantioselectivecyanation of benzylic C-H bonds *via* copper-catalyzed radical relay. Science *353*, 1014–1018.

Zhang, W., Wu, L., Chen, P., and Liu, G. (2019a). Enantioselectivearylation of benzylic C-H bonds by copper-catalyzed radical relay. Angew. Chem. Int. Ed. *58*, 6425–6429.

Zhang, Z., Stateman, L.M., and Nagib, D.A. (2019b). δC-H (hetero)arylation*via* Cu-catalyzed radical relay. Chem. Sci. *10*, 1207–1211, Only one enantioselective example was reported in this work (59% yield & 65% ee).

Zhang, K.-F., Bian, K.-J., Li, C., Sheng, J., Li, Y., and Wang, X.-S. (2019c). Nickel-catalyzed carbofluoroalkylation of 1, 3-enynes to access structurally diverse fluoroalkylatedallenes. Angew. Chem. Int. Ed. *58*, 5069–5074.

Zheng, C., and You, S.-L. (2014). Recent development of direct asymmetric functionalization of inert C-H bonds. RSC Adv. *4*, 6173–6214.

Zhou, Z., and Andrus, M.B. (2002). Highly enantioselective copper-bisoxazoline-catalyzed allylic oxidation of cyclic olefin with *tert*-Butyl *p*-nitroperbenzoate. J. Am. Chem. Soc. *124*, 8806–8807.

ISCI, Volume *21*

Supplemental Information

Enantioselective Copper-Catalyzed Cyanation of Remote C(sp^3)-H Bonds Enabled by 1,5-Hydrogen Atom Transfer

Cheng-Yu Wang, Zi-Yang Qin, Yu-Ling Huang, Ruo-Xing Jin, Quan Lan, and Xi-Sheng Wang

Supporting Information
For

Enantioselective Copper-Catalyzed Cyanation of Remote C(sp3)-H Bonds Enabled by 1,5-Hydrogen Atom Transfer

Cheng-Yu Wang[+], Zi-Yang Qin[+], Yu-Ling Huang, Ruo-Xing Jin, Quan Lan and Xi-Sheng Wang *

Hefei National Laboratory for Physical Sciences at the Microscale and Department of Chemistry,
Center for Excellence in Molecular Synthesis of CAS,
University of Science and Technology of China,
96 Jinzhai Road, Hefei, Anhui 230026, China

Tabel of Contents

Transparent Methods

I. General Information

NMR spectra were recorded on Bruker-400 MHz NMR spectrometer (400 MHz for ^{1}H; 101 MHz for ^{13}C and 376 MHz for ^{19}F {^{1}H, ^{13}C decoupled}). ^{1}H NMR spectra were referenced relative to internal $Si(Me)_4$ (TMS) at δ 0.00 ppm. ^{13}C NMR spectra were recorded at ambient temperature on Bruker-400 (100 MHz) spectrometers and are referenced relative to $CDCl_3$ at δ 77.16 ppm. The ^{13}C NMR spectra were obtained with ^{1}H decoupling. Data for ^{1}H, ^{13}C, ^{19}F NMR are recorded as follows: chemical shift (δ, ppm), multiplicity (s = singlet, d = doublet, t = triplet, m = multiplet, q = quartet, quint = quintet, br = broad), integration, and coupling constant (Hz). High resolution mass spectra were recorded on P-SIMS-Gly of BrukerDaltonics Inc. using ESI-TOF (electrospray ionization-time of flight). High performance liquid chromatography was performed on shimadzu Series HPLC, using AD-H, OD-H, AS-H chiral column eluted with a mixture of hexane and isopropyl alcohol. TMSCN was purchased from energy-chemical, CuSCN was purchased from TCI. And DCE was purchased from J&K Chemical Reagent Co., Ltd.

II. Tables of the Optimization of Reaction Conditions of Enantioselective Copper-catalyzed Cyanation

Table S1. Solvent Screening[a], related to **Table 1**.

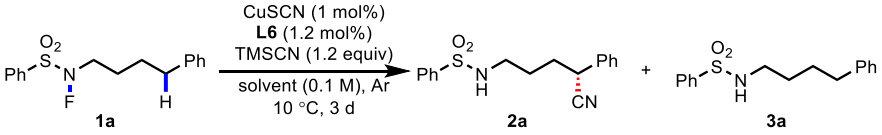

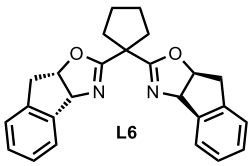

Entry	solvent	**2a**[b]	**3a**[b]	*ee*[c]
1	MeCN	39%	40%	81%
2	DCE	99%	8%	90%
3	THF	20%	78%	89%
4	PhCl	84%	15%	88%
5	$PhCF_3$	84%	14%	87%
6	DCM	78%	26%	91%

[a] Reation conditions: **1a** (0.1 mmol. 1.0 equiv), CuSCN (1 mol%), **L6** (1.2 mol%), TMSCN (1.2 equiv), solvent (1.0 mL), Ar, 10 °C, 3 d.
[b] Yields detected by crude ^{1}H NMR with CH_2Br_2 as internal standard.
[c] Enantiomeric excess (*ee*) values detected by HPLC on a chiral stationary phase.

Table S2. Catalyst Screening[a], related to **Table 1**.

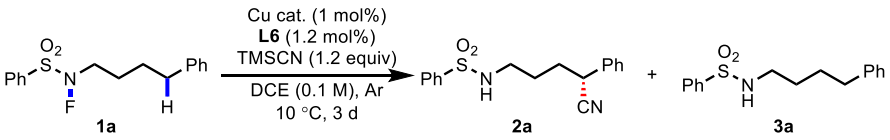

Entry	solvent	**2a**[b]	**3a**[b]	*ee*[c]
1	CuI	69%	23%	90%
2	CuCN	51%	32%	88%
3	$Cu(MeCN)_4PF_6$	trace	0%	-
4	$Cu(OAc)_2$	91%	13%	90%
5	$Cu(acac)_2$	70%	21%	90%
6	$Cu(OTf)_2$	0%	0%	-

[a] Reation conditions: **1a** (0.1 mmol. 1.0 equiv), Cu cat. (1 mol%), **L6** (1.2 mol%), TMSCN (1.2 equiv), DCE (1.0 mL), Ar, 10 °C, 3 d.
[b] Yields detected by crude ^{1}H NMR with CH_2Br_2 as internal standard.
[c] Enantiomeric excess (*ee*) values detected by HPLC on a chiral stationary phase.

Table S3. Loading of Catalyst Screening[a], related to **Table 1**.

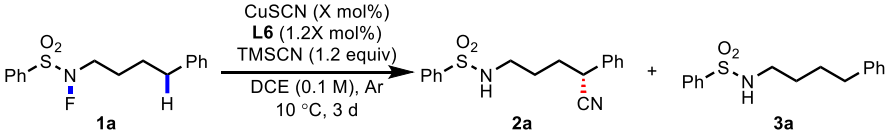

Entry	X	**2a**[b]	**3a**[b]	*ee*[c]
1	0.5	86%	11%	89%
2	1.5	60%	30%	90%
3	2.0	55%	20%	91%

[a] Reation conditions: **1a** (0.1 mmol. 1.0 equiv), CuSCN (X mol%), **L6** (1.2X mol%), TMSCN (1.2 equiv), DCE (1.0 mL), Ar, 10 °C, 3 d.
[b] Yields detected by crude ^{1}H NMR with CH_2Br_2 as internal standard.
[c] Enantiomeric excess (*ee*) values detected by HPLC on a chiral stationary phase.

Table S4. Concentration Screening[a], related to **Table 1**.

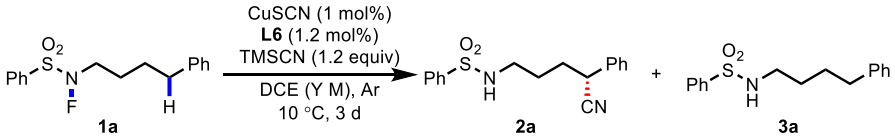

Entry	Y	**1a**[b]	**2a**[b]	**3a**[b]	*ee*[c]
1	0.05	0%	92%	13%	91%
2	0.2	45%	22%	12%	90%

[a] Reation conditions: **1a** (0.1 mmol. 1.0 equiv), CuSCN (1 mol%), **L6** (1.2 mol%), TMSCN (1.2 equiv), Ar, 10 °C, 3 d.
[b] Yields detected by crude ^{1}H NMR with CH_2Br_2 as internal standard.
[c] Enantiomeric excess (*ee*) values detected by HPLC on a chiral stationary phase.

Table S5. Ligand Screening[a], related to **Table 1**.

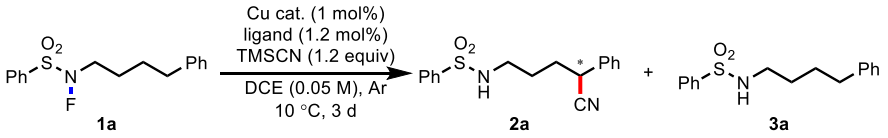

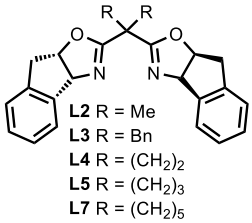

Entry	ligand	**2a**[b]	**3a**[b]	ee[c]
1	**L2**	92%	16%	88%
2	**L3**	72%	5%	87%
3	**L4**	98%	4%	87%
4	**L5**	89%	15%	91%
5	**L7**	74%	25%	82%

[a] Reation conditions: **1a** (0.1 mmol. 1.0 equiv), CuSCN (1 mol%), ligand (1.2 mol%), TMSCN (1.2 equiv), Ar, DCE (2.0 mL), 10 °C, 3 d.
[b] Yields detected by crude ^{1}H NMR with CH_2Br_2 as internal standard.
[c] Enantiomeric excess (ee) values detected by HPLC on a chiral stationary phase.

Table S6. Loading of Ligand Screening[a], related to **Table 1**.

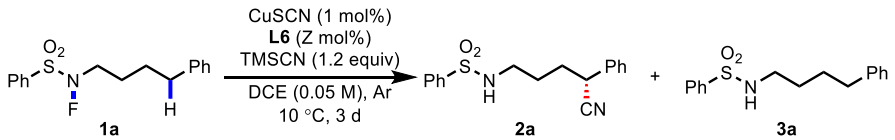

Entry	Z	**2a**[b]	**3a**[b]	*ee*[c]
1	1.5	98%	4%	91%
2	2.0	99%	5%	92%

[a] Reation conditions: **1a** (0.1 mmol. 1.0 equiv), CuSCN (1 mol%), **L6** (Z mol%), TMSCN (1.2 equiv), Ar, DCE (2.0 mL), 10 °C, 3 d.
[b] Yields detected by crude ^{1}H NMR with CH_2Br_2 as internal standard.
[c] Enantiomeric excess (*ee*) values detected by HPLC on a chiral stationary phase.

Table S7. Temperature Screening[a] , related to **Table 1**.

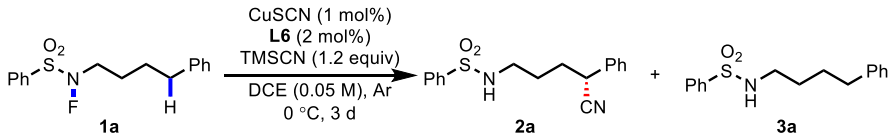

Entry	**1a**[b]	**2a**[b]	**3a**[b]	*ee*[c]
1	29%	64%	4%	92%

[a] Reation conditions: **1a** (0.1 mmol. 1.0 equiv), CuSCN (1 mol%), **L6** (2 mol%), TMSCN (1.2 equiv), Ar, DCE (2.0 mL), 0 °C, 3 d.
[b] Yields detected by crude ^{1}H NMR with CH_2Br_2 as internal standard.
[c] Enantiomeric excess (*ee*) values detected by HPLC on a chiral stationary phase.

Table S8. Controlling Experiments[a] , related to **Table 1**.

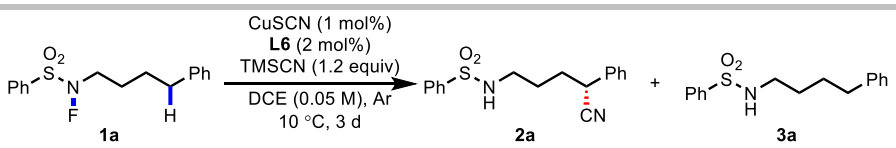

Entry	Reaction conditions	**2a**[b]	**3a**[b]	*ee*[c]
1	w/o CuSCN	0%	0%	-
2	w/o **L6**	trace	0%	-

[a] Reation conditions: **1a** (0.1 mmol. 1.0 equiv), CuSCN (1 mol%), **L6** (2 mol%), TMSCN (1.2 equiv), Ar, DCE (2.0 mL), 0 °C, 3 d.

[b] Yields detected by crude ^{1}H NMR with CH_2Br_2 as internal standard.

[c] Enantiomeric excess (*ee*) values detected by HPLC on a chiral stationary phase.

III. Experimental procedures and data

1. Synthesis of Starting Materials

General Procedure A − N-F sulfonamides

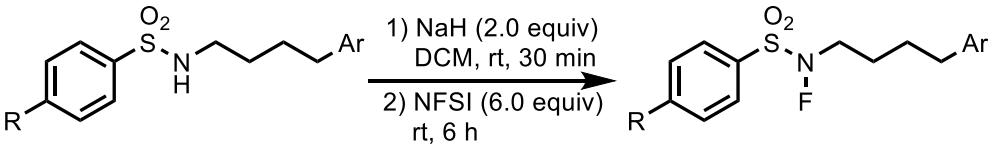

Synthesized according to a reported procedure (Wang et al., 2017): In a 100 mL round-bottomed flask, to a stirred suspension of NaH (6 mmol, 60 wt% in mineral oil) in anhydrous CH_2Cl_2 (24 mL), a solution of sulfonamide (3 mmol) in anhydrous CH_2Cl_2 (6 mL) was slowly added at room temperature under an N_2 atmosphere. After stirring for 30 min, N-fluorobenzenesulfonimide (NFSI, 5.67 g, 18 mmol) was added. The reaction mixture was stirred for another 6 h. Upon completion, the reaction was quenched by the addition of water. The mixture was extracted with DCM (3 × 30 mL) and the organic layers were combined, washed with brine, and dried over anhydrous Na_2SO_4. The crude mixture was filtered through celite and concentrated. The resulting residue was purified by column chromatography on silica gel with a gradient eluent of petroleum ether and ethyl acetate.

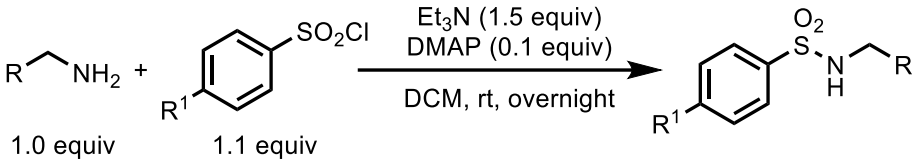

Synthesized according to a reported procedure (Zhang et al., 2019). To a clean, dry round bottom flask was added a magnetic stir bar and primary amine (1 equiv) under nitrogen at RT. The substrate was dissolved in DCM [0.2 M], followed by addition of freshly distilled triethylamine (1.5 equiv), 4-Dimethylaminopyridine (0.1 equiv) and p-toluenesulfonyl chloride (1.1 equiv) were subsequently added. The reaction was allowed to stir at room temperature overnight. H_2O was added to the reaction and the aqueous layer was extracted DCM (3 × 100 mL). The combined organic layers were washed with brine, dried over Na_2SO_4, and concentrated in vacuo. The crude material was purified by silica gel chromatography.

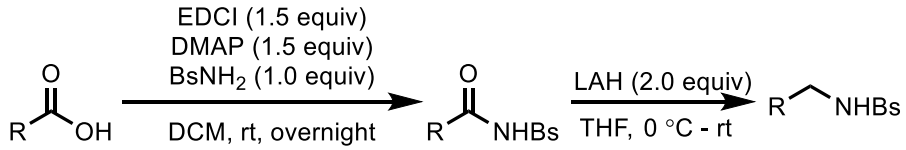

Synthesized according to a reported procedure (Zhang et al., 2019). To a clean, dry round bottom flask was added a magnetic stir bar, the starting carboxylic acid (1.0 equiv), 4-Dimethylaminopyridine (1.5 equiv) and benzenesulfonamide (1.0 equiv) under nitrogen at room temperature. The mixture was

dissolved in DCM, followed by addition of EDCI (1.5 equiv). The reaction was allowed to stir at room temperature overnight. Upon completion, 4N HCl was added, the organic phase was collected, and the aqueous layer was extracted three times with DCM. The combined organic phase was washed with brine, dried over Na_2SO_4, and concentrated *in vacuo*. The crude mixture was then taken onto the reduction step.

To a dry round bottom flask, was added a magnetic stir bar, the starting amide (1.0 equiv), and lithium aluminum hydride (2.0 equiv) under nitrogen. Reaction was cooled to 0 ℃ and slowly dissolved in THF. The reaction was monitored by TLC and upon consumption of starting material, the mixture was cooled to 0 ℃ and quenched carefully by addition of a 1 M solution of sodium hydroxide. The reaction was allowed to warm to room temperature and stirred for 20 minutes. The mixture was filtered through celite and the resulting clear solution was dried over Na_2SO_4 and concentrated *in vacuo*. Final substrates were purified by silica gel chromatography.

2. Synthesis of Products

General Procedure B − Enantioselective 1,5-HAT cyanation

Preparation of catalyst solution A. To a 25 mL sealed tube, CuSCN (1.1 mg, 0.009 mmol), chiral bisoxazoline ligand (***1R***, ***2S***) – **L6** (6.9 mg, 0.018 mmol) were added in degassed DCE (18.0 mL) under Ar atmosphere. The tube was sealed with a Teflon-lined cap, then the mixture was stirred at room temperature for 30 minutes. The **solution A** was used immediately.

To a sealed tube, **solution A** (4.0 mL), TMSCN (23.8 mg, 30 μL, 0.24 mmol, 1.2 equiv) and substrate were sequentially added under Ar atmosphere. The tube was sealed with a Teflon-lined cap, and the mixture was stirred at 10 ℃ for three days. After the reaction was completed, the mixture was concentrated. Then the residue was purified by silica gel chromatography with petroleumether and ethylacetate (PE/EA = 5:1) to afford the product.

3. Analytical data for compounds

1. **N-F sulfonamides:**

N-fluoro-N-(4-phenylbutyl)benzenesulfonamide (**1a**)

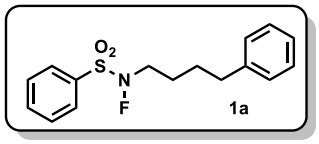

Prepared following general procedure A the reaction mixture was purified by column chromatography (petroleum ether/ethyl acetate = 19/1 as the eluent) as a yellow solid (664 mg, 72% yield). ^{1}H NMR (400 MHz, Chloroform-*d*) δ 7.99 – 7.88 (m, 2H), 7.78 – 7.69 (m, 1H), 7.65 – 7.56 (m, 2H), 7.31 – 7.23 (m, 2H), 7.22 – 7.11 (m, 3H), 3.23 (dt, *J* = 40.7, 6.4 Hz, 2H), 2.63 (t, *J* = 7.0 Hz, 2H), 1.83 – 1.66 (m, 4H). ^{13}C NMR (101 MHz, Chloroform-*d*) δ 141.80, 135.00, 132.11, 130.04, 129.40, 128.49, 126.03, 53.60 (d, *J* = 12.5 Hz), 35.41, 28.41, 25.97. ^{19}F NMR (376 MHz, Chloroform-*d*) δ -49.82 (t, *J* = 40.6 Hz). HRMS (ESI) (*m/z*): $[M+Na]^+$ calcd. for $C_{16}H_{18}FNO_2SNa$: 330.0940, found: 330.0914.

N-fluoro-4-methyl-N-(4-phenylbutyl)benzenesulfonamide (**1b**)

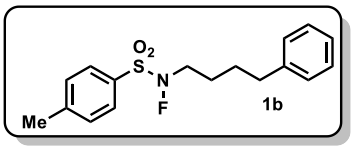

Prepared following general procedure A the reaction mixture was purified by column chromatography (petroleum ether/ethyl acetate = 19/1 as the eluent) as a light yellow solid (571 mg, 59% yield). The NMR spectra were identical to the reference.[2]

N-fluoro-4-methoxy-N-(4-phenylbutyl)benzenesulfonamide (**1c**)

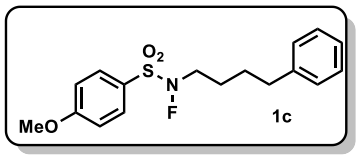

Prepared following general procedure A the reaction mixture was purified by column chromatography (petroleum ether/ethyl acetate = 19/1 as the eluent) as a yellow solid (597 mg, 62% yield). The NMR spectra were identical to the reference.[2]

4-chloro-N-fluoro-N-(4-phenylbutyl)benzenesulfonamide (**1d**)

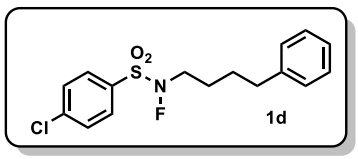

Prepared following general procedure A the reaction mixture was purified by column chromatography (petroleum ether/ethyl acetate = 19/1 as the eluent) as a light yellow solid (655 mg, 64% yield). ^{1}H NMR (400 MHz, Chloroform-*d*) δ 7.84 – 7.75 (m, 2H), 7.55 – 7.46 (m, 2H), 7.25 – 7.16 (m, 2H), 7.15 – 7.03 (m, 3H), 3.17 (dt, *J* = 40.5, 5.6 Hz, 2H), 2.56 (t, *J* = 6.2 Hz, 2H), 1.77 – 1.56 (m, 4H). ^{13}C NMR (101 MHz, Chloroform-*d*) δ 142.01, 141.74, 131.39, 130.62, 129.81, 128.51, 128.48, 126.06, 53.50 (d, *J* = 12.5 Hz), 35.40, 28.37, 25.93. ^{19}F NMR (376 MHz, Chloroform-*d*) δ -49.50 (t, *J* = 40.5 Hz). HRMS (ESI) (*m/z*): $[M+Na]^+$ calcd. for $C_{16}H_{17}ClFNO_2SNa$: 364.0550, found: 364.0524.

N-fluoro-N-(4-phenylbutyl)-4-(trifluoromethyl)benzenesulfonamide (**1e**)

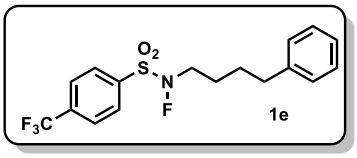

Prepared following general procedure A the reaction mixture was purified by column chromatography (petroleum ether/ethyl acetate = 19/1 as the eluent) as a light yellow solid (617 mg, 55% yield). ^{1}H NMR (400 MHz, Chloroform-*d*) δ 8.07 (d, *J* = 8.2 Hz, 2H), 7.87 (d, *J* = 8.3 Hz, 2H), 7.31 – 7.25 (m, 2H), 7.22 – 7.12 (m, 3H), 3.28 (dt, *J* = 40.3, 6.5 Hz, 2H), 2.64 (t, *J* = 7.0 Hz, 2H), 1.83 – 1.70 (m, 4H). ^{13}C NMR (101 MHz, Chloroform-*d*) δ 141.70, 136.54 (q, *J* = 33.3 Hz), 136.00, 130.61, 128.54, 128.50, 126.55 (q, *J* = 3.6 Hz), 126.10, 123.08 (q, *J* = 273.2 Hz), 53.39 (d, *J* = 12.6 Hz), 35.40, 28.35,

25.93. ^{19}F NMR (376 MHz, Chloroform-*d*) δ -49.57 (t, *J* = 40.3 Hz), -63.36 (s). HRMS (ESI) (*m/z*): $[M+Na]^+$ calcd. for $C_{17}H_{17}F_4NO_2SNa$: 398.0814, found: 398.0790.

N-fluoro-N-(4-(p-tolyl)butyl)benzenesulfonamide (**1f**)

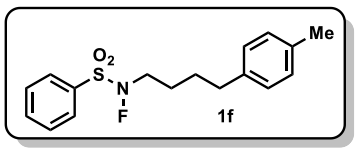

Prepared following general procedure A the reaction mixture was purified by column chromatography (petroleum ether/ethyl acetate = 19/1 as the eluent) as a light yellow oil (439 mg, 46% yield). ^{1}H NMR (400 MHz, Chloroform-*d*) δ 7.98 – 7.89 (m, 2H), 7.78 – 7.70 (m, 1H), 7.65 – 7.57 (m, 2H), 7.12 – 7.01 (m, 4H), 3.23 (dt, *J* = 40.7, 6.5 Hz, 2H), 2.59 (t, *J* = 7.0 Hz, 2H), 2.31 (s, 3H), 1.79 – 1.67 (m, 4H). ^{13}C NMR (101 MHz, Chloroform-*d*) δ 138.72, 135.48, 134.99, 132.16, 130.05, 129.39, 129.18, 128.37, 53.61 (d, *J* = 12.5 Hz), 34.96, 28.53, 25.97, 21.13. ^{19}F NMR (376 MHz, Chloroform-*d*) δ -49.86 (t, *J* = 40.7 Hz). HRMS (ESI) (*m/z*): $[M+Na]^+$ calcd. for $C_{17}H_{20}FNO_2SNa$: 344.1096, found: 344.1086.

N-(4-(4-(tert-butyl)phenyl)butyl)-N-fluorobenzenesulfonamide (**1g**)

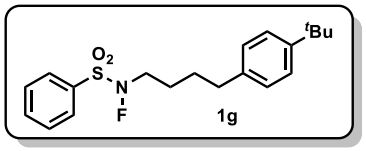

Prepared following general procedure A the reaction mixture was purified by column chromatography (petroleum ether/ethyl acetate = 19/1 as the eluent) as a light yellow oil (373 mg, 34% yield). ^{1}H NMR (400 MHz, Chloroform-*d*) δ 7.99 – 7.90 (m, 2H), 7.78 – 7.70 (m, 1H), 7.65 – 7.56 (m, 2H), 7.29 (d, *J* = 8.3 Hz, 2H), 7.09 (d, *J* = 8.2 Hz, 2H), 3.24 (dt, *J* = 40.7, 6.4 Hz, 2H), 2.60 (t, *J* = 7.1 Hz, 2H), 1.83 – 1.67 (m, 4H), 1.30 (s, 9H). ^{13}C NMR (101 MHz, Chloroform-*d*) δ 148.83, 138.73, 135.00, 132.17, 130.06, 129.40, 128.14, 125.38, 53.62 (d, *J* = 12.5 Hz), 34.86, 34.49, 31.54, 28.42, 26.06. ^{19}F NMR (376 MHz, Chloroform-*d*) δ -49.79 (t, *J* = 40.7 Hz). HRMS (ESI) (*m/z*): $[M+Na]^+$ calcd. for $C_{20}H_{26}FNO_2SNa$: 386.1566, found: 386.1570.

N-fluoro-N-(4-(4-pentylphenyl)butyl)benzenesulfonamide (**1h**)

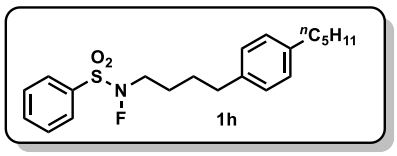

Prepared following general procedure A the reaction mixture was purified by column chromatography (petroleum ether/ethyl acetate = 19/1 as the eluent) as a white solid (581 mg, 51% yield). ^{1}H NMR (400 MHz, Chloroform-*d*) δ 8.00 – 7.85 (m, 2H), 7.78 – 7.68 (m, 1H), 7.66 – 7.54 (m, 2H), 7.14 – 6.96 (m, 4H), 3.23 (dt, *J* = 40.7, 6.0 Hz, 2H), 2.67 – 2.47 (m, 4H), 1.82 – 1.66 (m, 4H), 1.65 – 1.52 (m, 2H), 1.40 – 1.23 (m, 4H), 0.88 (t, *J* = 6.3 Hz, 3H). ^{13}C NMR (101 MHz, Chloroform-*d*) δ 140.62, 138.92, 134.99, 132.16, 130.05, 129.39, 128.51, 128.34, 53.63 (d, *J* = 12.5 Hz), 35.65, 35.00, 31.69, 31.40, 28.49, 26.01, 22.69, 14.18. ^{19}F NMR (376 MHz, Chloroform-*d*) δ -49.83 (t, *J* = 40.7 Hz). HRMS (ESI) (*m/z*): $[M+Na]^+$ calcd. for $C_{21}H_{28}FNO_2SNa$: 400.1722, found: 400.1714.

N-(4-([1,1'-biphenyl]-4-yl)butyl)-N-fluorobenzenesulfonamide (**1i**)

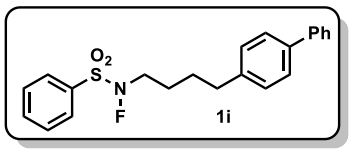

Prepared following general procedure A the reaction mixture was purified by column chromatography (petroleum ether/ethyl acetate = 19/1 as the eluent) as a white solid (520 mg, 45% yield). ^{1}H NMR (400 MHz, Chloroform-*d*) δ 7.98 – 7.90 (m, 2H), 7.77 – 7.71 (m, 1H), 7.64 – 7.55 (m, 4H), 7.51 (d, *J* = 8.0 Hz, 2H), 7.46 – 7.39 (m, 2H), 7.35 – 7.29 (m, 1H), 7.23 (d, *J* = 8.0 Hz, 2H), 3.26 (dt, *J* = 40.7, 6.2 Hz, 2H), 2.68 (t, *J* = 6.8 Hz, 2H), 1.83 – 1.75 (m, 4H). ^{13}C NMR (101 MHz, Chloroform-*d*) δ 141.14, 140.94, 139.03, 135.02, 132.15, 130.06, 129.41, 128.93, 128.86, 127.25, 127.18, 127.12, 53.60 (d, *J* = 12.5 Hz), 35.05, 28.39, 26.02. ^{19}F NMR (376 MHz, Chloroform-*d*) δ -

49.79 (t, *J* = 40.7 Hz). HRMS (ESI) (*m/z*): $[M+Na]^+$ calcd. for $C_{22}H_{22}FNO_2SNa$: 406.1253, found: 406.1250.

N-fluoro-N-(4-(4-phenoxyphenyl)butyl)benzenesulfonamide (**1j**)

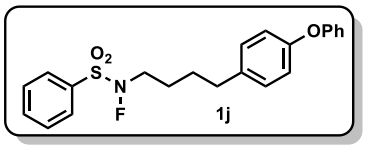

Prepared following general procedure A the reaction mixture was purified by column chromatography (petroleum ether/ethyl acetate = 19/1 as the eluent) as a light yellow oil (332 mg, 28% yield). ^{1}H NMR (400 MHz, Chloroform-*d*) δ 8.02 – 7.87 (m, 2H), 7.80 – 7.69 (m, 1H), 7.68 – 7.56 (m, 2H), 7.36 – 7.29 (m, 2H), 7.15 – 7.04 (m, 3H), 7.03 – 6.96 (m, 2H), 6.96 – 6.88 (m, 2H), 3.25 (dt, *J* = 40.7, 6.3 Hz, 2H), 2.62 (t, *J* = 6.9 Hz, 2H), 1.86 – 1.64 (m, 4H). ^{13}C NMR (101 MHz, Chloroform-*d*) δ 157.70, 155.34, 136.80, 135.03, 132.15, 130.07, 129.81, 129.70, 129.42, 123.08, 119.17, 118.66, 53.59 (d, *J* = 12.5 Hz), 34.71, 28.55, 25.96. ^{19}F NMR (376 MHz, Chloroform-*d*) δ -49.81 (t, *J* = 40.6 Hz). HRMS (ESI) (*m/z*): $[M+Na]^+$ calcd. for $C_{22}H_{22}FNO_3SNa$: 422.1202, found: 422.1197.

N-fluoro-N-(4-(4-(trifluoromethoxy)phenyl)butyl)benzenesulfonamide (**1k**)

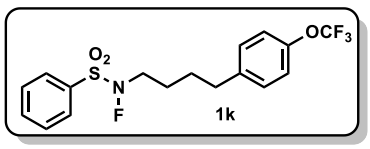

Prepared following general procedure A the reaction mixture was purified by column chromatography (petroleum ether/ethyl acetate = 19/1 as the eluent) as a colourless oil (835 mg, 71% yield). ^{1}H NMR (400 MHz, Chloroform-*d*) δ 7.98 – 7.90 (m, 2H), 7.79 – 7.70 (m, 1H), 7.66 – 7.58 (m, 2H), 7.17 (d, *J* = 8.7 Hz, 2H), 7.11 (d, *J* = 8.2 Hz, 2H), 3.24 (dt, *J* = 40.6, 6.0 Hz, 2H), 2.64 (t, *J* = 6.8 Hz, 2H), 1.82 – 1.66 (m, 4H). ^{13}C NMR (101 MHz, Chloroform-*d*) δ 147.56, 140.55, 135.07, 132.05, 130.04, 129.71, 129.43, 121.09, 120.62 (q, *J* = 256.5 Hz), 53.52 (d, *J* = 12.5 Hz), 34.72, 28.32, 25.89. ^{19}F NMR (376 MHz, Chloroform-*d*) δ -49.82 (t, *J* = 40.6 Hz), -57.92 (s). HRMS (ESI) (*m/z*): $[M+Na]^+$ calcd. for $C_{17}H_{17}F_4NO_3SNa$: 414.0763, found: 414.0773.

N-(4-(4-chlorophenyl)butyl)-N-fluorobenzenesulfonamide (**1l**)

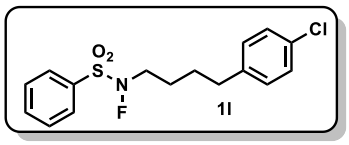

Prepared following general procedure A the reaction mixture was purified by column chromatography (petroleum ether/ethyl acetate = 19/1 as the eluent) as a light yellow oil (483 mg, 47% yield). ^{1}H NMR (400 MHz, Chloroform-*d*) δ 8.00 – 7.88 (m, 2H), 7.79 – 7.70 (m, 1H), 7.67 – 7.56 (m, 2H), 7.23 (d, *J* = 8.4 Hz, 2H), 7.08 (d, *J* = 8.4 Hz, 2H), 3.23 (dt, *J* = 40.6, 6.3 Hz, 2H), 2.60 (t, *J* = 7.0 Hz, 2H), 1.81 – 1.65 (m, 4H). ^{13}C NMR (101 MHz, Chloroform-*d*) δ 140.22, 135.05, 132.06, 131.73, 130.03, 129.83, 129.42, 128.58, 53.51 (d, *J* = 12.5 Hz), 34.74, 28.27, 25.86. ^{19}F NMR (376 MHz, Chloroform-*d*) δ -49.81 (t, *J* = 40.6 Hz). HRMS (ESI) (*m/z*): $[M+Na]^+$ calcd. for $C_{16}H_{17}ClFNO_2SNa$: 364.0550, found: 364.0548.

N-(4-(4-bromophenyl)butyl)-N-fluorobenzenesulfonamide (**1m**)

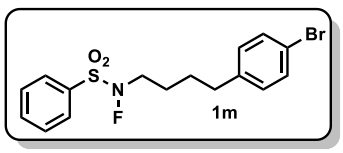

Prepared following general procedure A the reaction mixture was purified by column chromatography (petroleum ether/ethyl acetate = 19/1 as the eluent) as a light yellow oil (243 mg, 21% yield). ^{1}H NMR (400 MHz, Chloroform-*d*) δ 7.98 – 7.88 (m, 2H), 7.79 – 7.70 (m, 1H), 7.67 – 7.58 (m, 2H), 7.38 (d, *J* = 8.4 Hz, 2H), 7.03 (d, *J* = 8.4 Hz, 2H), 3.23 (dt, *J* = 40.6, 6.4 Hz, 2H), 2.59 (t, *J* = 7.0 Hz, 2H), 1.81 – 1.65 (m, 4H). ^{13}C NMR (101 MHz, Chloroform-*d*) δ 140.74, 135.05, 132.10, 131.55, 130.26, 130.04, 129.42, 119.77, 53.49 (d, *J* = 12.5 Hz), 34.81, 28.21, 25.87. ^{19}F NMR (376 MHz,

Chloroform-*d*) δ -49.75 (t, *J* = 40.5 Hz). HRMS (ESI) (*m/z*): $[M+Na]^+$ calcd. for $C_{16}H_{17}BrFNO_2SNa$: 408.0045, found: 408.0040.

N-fluoro-N-(4-(4-(trifluoromethyl)phenyl)butyl)benzenesulfonamide (**1n**)

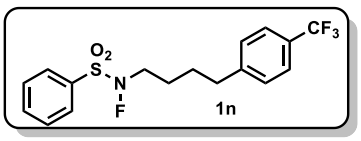

Prepared following general procedure A the reaction mixture was purified by column chromatography (petroleum ether/ethyl acetate = 19/1 as the eluent) as a colourless oil (474 mg, 42% yield). ^{1}H NMR (400 MHz, Chloroform-*d*) δ 8.01 – 7.85 (m, 2H), 7.79 – 7.71 (m, 1H), 7.65 – 7.58 (m, 2H), 7.53 (d, *J* = 8.0 Hz, 2H), 7.27 (d, *J* = 7.4 Hz, 2H), 3.25 (dt, *J* = 40.5, 5.8 Hz, 2H), 2.70 (t, *J* = 6.6 Hz, 2H), 1.89 – 1.63 (m, 4H). ^{13}C NMR (101 MHz, Chloroform-*d*) δ 145.92, 135.08, 132.06, 130.04, 129.44, 128.80, 128.44 (q, *J* = 32.3 Hz), 125.44 (q, *J* = 3.8 Hz), 124.44 (q, *J* = 271.8 Hz), 53.45 (d, *J* = 12.4 Hz), 35.24, 28.10, 25.89. ^{19}F NMR (376 MHz, Chloroform-*d*) δ -49.81 (t, *J* = 40.5 Hz), -62.30 (s). HRMS (ESI) (*m/z*): $[M+Na]^+$ calcd. for $C_{17}H_{17}F_4NO_2SNa$: 398.0814, found: 398.0815.

N-fluoro-N-(4-(m-tolyl)butyl)benzenesulfonamide (**1o**)

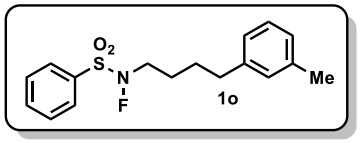

Prepared following general procedure A the reaction mixture was purified by column chromatography (petroleum ether/ethyl acetate = 19/1 as the eluent) as a light yellow oil (447 mg, 46% yield). ^{1}H NMR (400 MHz, Chloroform-*d*) δ 8.00 – 7.86 (m, 2H), 7.78 – 7.69 (m, 1H), 7.67 – 7.54 (m, 2H), 7.16 (t, *J* = 7.5 Hz, 1H), 7.07 – 6.88 (m, 3H), 3.23 (dt, *J* = 40.7, 5.9 Hz, 2H), 2.59 (t, *J* = 6.6 Hz, 2H), 2.31 (s, 3H), 1.81 – 1.66 (m, 4H). ^{13}C NMR (101 MHz, Chloroform-*d*) δ 141.74, 138.02, 134.99, 132.09, 130.02 (d, *J* = 0.6 Hz), 129.39, 129.30, 128.37, 126.75, 125.48, 53.63 (d, *J* = 12.7 Hz), 35.33, 28.42, 26.01, 21.51. ^{19}F NMR (376 MHz, Chloroform-*d*) δ -49.83 (t, *J* = 40.7 Hz). HRMS (ESI) (*m/z*): $[M+Na]^+$ calcd. for $C_{17}H_{20}FNO_2SNa$: 344.1096, found: 344.1092.

N-fluoro-N-(4-(3-methoxyphenyl)butyl)benzenesulfonamide (**1p**)

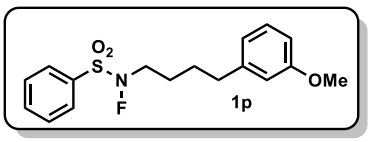

Prepared following general procedure A the reaction mixture was purified by column chromatography (petroleum ether/ethyl acetate = 19/1 as the eluent) as a light yellow oil (476 mg, 47% yield). ^{1}H NMR (400 MHz, Chloroform-*d*) δ 8.00 – 7.90 (m, 2H), 7.78 – 7.70 (m, 1H), 7.66 – 7.56 (m, 2H), 7.19 (t, *J* = 7.8 Hz, 1H), 6.82 – 6.64 (m, 3H), 3.79 (s, 3H), 3.23 (dt, *J* = 40.7, 6.3 Hz, 2H), 2.61 (t, *J* = 6.9 Hz, 2H), 1.80 – 1.68 (m, 4H). ^{13}C NMR (101 MHz, Chloroform-*d*) δ 159.75, 143.43, 135.00, 132.08, 130.02 (d, *J* = 0.5 Hz), 129.45, 129.39, 120.90, 114.23, 111.30, 55.25, 53.60 (d, *J* = 12.7 Hz), 35.43, 28.26, 25.95. ^{19}F NMR (376 MHz, Chloroform-*d*) δ -49.82 (t, *J* = 40.7 Hz). HRMS (ESI) (*m/z*): $[M+Na]^+$ calcd. for $C_{17}H_{20}FNO_3SNa$: 360.1046, found: 360.1053.

N-(4-(3-chlorophenyl)butyl)-N-fluorobenzenesulfonamide (**1q**)

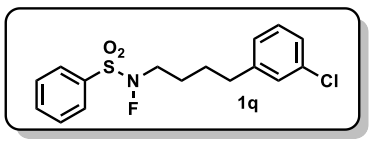

Prepared following general procedure A the reaction mixture was purified by column chromatography (petroleum ether/ethyl acetate = 19/1 as the eluent) as a light yellow oil (498 mg, 49% yield). ^{1}H NMR (400 MHz, Chloroform-*d*) δ 8.00 – 7.90 (m, 2H), 7.78 – 7.71 (m, 1H), 7.67 – 7.57 (m, 2H), 7.23 – 7.12 (m, 3H), 7.09 – 7.00 (m, 1H), 3.23 (dt, *J* = 40.6, 6.1 Hz, 2H), 2.61 (t, *J* = 6.9 Hz, 2H), 1.81 – 1.67 (m, 4H). ^{13}C NMR (101 MHz, Chloroform-*d*) δ 143.83, 135.05, 134.22, 132.05, 130.04, 129.76, 129.42, 128.58, 126.71, 126.25, 53.50 (d, *J* = 12.7 Hz), 35.08, 28.14, 25.88. ^{19}F NMR (376 MHz, Chloroform-*d*) δ -49.78 (t, *J* = 40.6 Hz). HRMS (ESI) (*m/z*): $[M+Na]^+$ calcd. for

$C_{16}H_{17}ClFNO_2SNa$: 364.0550, found: 364.0555.

N-fluoro-N-(4-(3-(trifluoromethyl)phenyl)butyl)benzenesulfonamide (**1r**)

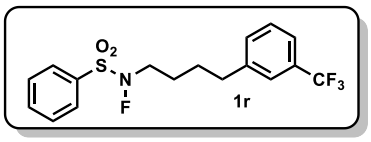

Prepared following general procedure A the reaction mixture was purified by column chromatography (petroleum ether/ethyl acetate = 19/1 as the eluent) as a light yellow oil (588 mg, 52% yield). ^{1}H NMR (400 MHz, Chloroform-*d*) δ 8.01 – 7.88 (m, 2H), 7.79 – 7.71 (m, 1H), 7.66 – 7.58 (m, 2H), 7.50 – 7.29 (m, 4H), 3.25 (dt, *J* = 40.5, 6.2 Hz, 2H), 2.70 (t, *J* = 7.1 Hz, 2H), 1.86 – 1.67 (m, 4H). ^{13}C NMR (101 MHz, Chloroform-*d*) δ 142.69, 135.08, 132.04, 131.91 (d, *J* = 1.1 Hz), 130.78 (q, *J* = 32.0 Hz), 130.05, 129.44, 128.94, 125.13 (q, *J* = 3.8 Hz), 124.34 (q, *J* = 273.3 Hz), 122.98 (q, *J* = 3.8 Hz), 53.48 (d, *J* = 12.5 Hz), 35.25, 28.23, 25.93. ^{19}F NMR (376 MHz, Chloroform-*d*) δ -49.77 (t, *J* = 40.5 Hz), -62.54 (s). HRMS (ESI) (*m/z*): $[M+Na]^+$ calcd. for $C_{17}H_{17}F_4NO_2SNa$: 398.0814, found: 398.0812.

N-fluoro-N-(4-(o-tolyl)butyl)benzenesulfonamide (**1s**)

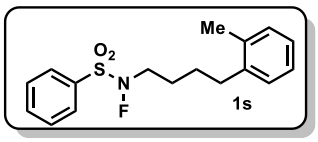

Prepared following general procedure A the reaction mixture was purified by column chromatography (petroleum ether/ethyl acetate = 19/1 as the eluent) as a light yellow oil (580 mg, 60% yield). ^{1}H NMR (400 MHz, Chloroform-*d*) δ 7.98 – 7.90 (m, 2H), 7.78 – 7.71 (m, 1H), 7.66 – 7.57 (m, 2H), 7.16 – 7.06 (m, 4H), 3.26 (dt, *J* = 40.7, 6.7 Hz, 2H), 2.62 (t, *J* = 7.7 Hz, 2H), 2.29 (s, 3H), 1.85 – 1.75 (m, 2H), 1.74 – 1.65 (m, 2H). ^{13}C NMR (101 MHz, Chloroform-*d*) δ 140.02, 135.93, 135.01, 132.15, 130.35, 130.05, 129.40, 128.91, 126.17, 126.07, 53.60 (d, *J* = 12.5 Hz), 32.78, 27.24, 26.32, 19.41. ^{19}F NMR (376 MHz, Chloroform-*d*) δ -49.83 (t, *J* = 40.7 Hz). HRMS (ESI) (*m/z*): $[M+Na]^+$ calcd. for $C_{17}H_{20}FNO_2SNa$: 344.1096, found: 344.1090.

N-fluoro-N-(4-(2-fluorophenyl)butyl)benzenesulfonamide (**1t**)

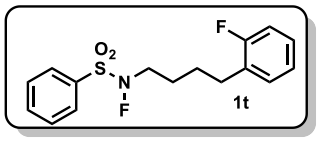

Prepared following general procedure A the reaction mixture was purified by column chromatography (petroleum ether/ethyl acetate = 19/1 as the eluent) as a light yellow oil (529 mg, 54% yield). ^{1}H NMR (400 MHz, Chloroform-*d*) δ 8.00 – 7.87 (m, 2H), 7.78 – 7.70 (m, 1H), 7.66 – 7.56 (m, 2H), 7.20 – 7.12 (m, 2H), 7.09 – 6.93 (m, 2H), 3.25 (dt, *J* = 40.6, 6.4 Hz, 2H), 2.66 (t, *J* = 6.7 Hz, 2H), 1.81 – 1.68 (m, 4H). ^{13}C NMR (101 MHz, Chloroform-*d*) δ 161.21 (d, *J* = 244.5 Hz), 135.02, 132.11, 130.71 (d, *J* = 5.1 Hz), 130.05, 129.41, 128.57 (d, *J* = 15.9 Hz), 127.80 (d, *J* = 8.1 Hz), 124.11 (d, *J* = 3.5 Hz), 115.34 (d, *J* = 22.2 Hz), 53.54 (d, *J* = 12.5 Hz), 28.55 (d, *J* = 2.3 Hz), 27.21, 25.99. ^{19}F NMR (376 MHz, Chloroform-*d*) δ -49.77 (t, *J* = 40.9 Hz), -118.70 – -119.10 (m). HRMS (ESI) (*m/z*): $[M+Na]^+$ calcd. for $C_{16}H_{17}F_2NO_2SNa$: 348.0846, found: 348.0852.

N-fluoro-N-(4-(2-(trifluoromethyl)phenyl)butyl)benzenesulfonamide (**1u**)

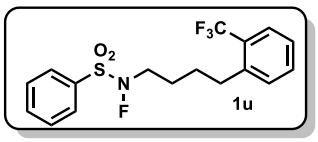

Prepared following general procedure A the reaction mixture was purified by column chromatography (petroleum ether/ethyl acetate = 19/1 as the eluent) as a light yellow oil (563 mg, 50% yield). ^{1}H NMR (400 MHz, Chloroform-*d*) δ 8.02 – 7.87 (m, 2H), 7.78 – 7.71 (m, 1H), 7.69 – 7.55 (m, 3H), 7.50 – 7.41 (m, 1H), 7.34 – 7.26 (m, 2H), 3.26 (dt, *J* = 40.6, 6.5 Hz, 2H), 2.79 (t, *J* = 7.5 Hz, 2H), 1.89 – 1.67 (m, 4H). ^{13}C NMR (101 MHz, Chloroform-*d*) δ 140.67, 135.06, 132.03, 131.91, 131.04, 130.05, 129.43, 128.45 (q, *J* = 29.7 Hz), 126.17, 126.05 (q, *J* = 5.8 Hz), 124.72 (q, *J* = 274.8 Hz), 53.57 (d, *J* = 12.5 Hz),

32.13 (d, *J* = 1.6 Hz), 28.71, 26.32. ^{19}F NMR (376 MHz, Chloroform-*d*) δ -49.76 (t, *J* = 40.6 Hz), -59.56 (s). HRMS (ESI) (*m/z*): $[M+Na]^+$ calcd. for $C_{17}H_{17}F_4NO_2SNa$: 398.0814, found: 398.0811.

N-(4-(4-chloro-2-methylphenyl)butyl)-N-fluorobenzenesulfonamide (**1v**)

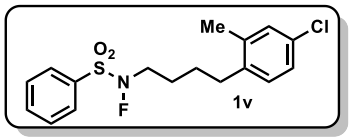

Prepared following general procedure A the reaction mixture was purified by column chromatography (petroleum ether/ethyl acetate = 19/1 as the eluent) as a yellow solid (577 mg, 54% yield). ^{1}H NMR (400 MHz, Chloroform-*d*) δ 8.00 – 7.90 (m, 2H), 7.79 – 7.71 (m, 1H), 7.69 – 7.58 (m, 2H), 7.15 – 7.05 (m, 2H), 7.05 – 6.98 (m, 1H), 3.25 (dt, *J* = 40.6, 6.7 Hz, 2H), 2.58 (t, *J* = 7.6 Hz, 2H), 2.26 (s, 3H), 1.86 – 1.72 (m, 2H), 1.72 – 1.61 (m, 2H). ^{13}C NMR (101 MHz, Chloroform-*d*) δ 138.48, 137.86, 135.06, 132.10, 131.51, 130.17, 130.13, 130.05, 129.43, 126.03, 53.50 (d, *J* = 12.5 Hz), 32.20, 27.12, 26.20, 19.33. ^{19}F NMR (376 MHz, Chloroform-*d*) δ -49.81 (t, *J* = 40.6 Hz). HRMS (ESI) (*m/z*): $[M+Na]^+$ calcd. for $C_{17}H_{19}ClFNO_2SNa$: 378.0707, found: 378.0710.

N-fluoro-N-(4-(naphthalen-1-yl)butyl)benzenesulfonamide (**1w**)

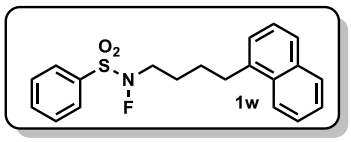

Prepared following general procedure A the reaction mixture was purified by column chromatography (petroleum ether/ethyl acetate = 19/1 as the eluent) as a yellow solid (752 mg, 70% yield). ^{1}H NMR (400 MHz, Chloroform-*d*) δ 7.99 (d, *J* = 8.1 Hz, 1H), 7.91 (d, *J* = 7.4 Hz, 2H), 7.86 – 7.81 (m, 1H), 7.73 – 7.66 (m, 2H), 7.57 (t, *J* = 7.8 Hz, 2H), 7.52 – 7.43 (m, 2H), 7.37 (t, *J* = 7.6 Hz, 1H), 7.28 (d, *J* = 6.8 Hz, 1H), 3.24 (dt, *J* = 40.7, 6.3 Hz, 2H), 3.08 (t, *J* = 7.1 Hz, 2H), 1.94 – 1.73 (m, 4H). ^{13}C NMR (101 MHz, Chloroform-*d*) δ 137.85, 135.00, 133.99, 132.03, 131.82, 130.00, 129.38, 128.91, 126.86, 126.13, 125.94, 125.61, 125.59, 123.76, 53.60 (d, *J* = 12.5 Hz), 32.55, 27.72, 26.38. ^{19}F NMR (376 MHz, Chloroform-*d*) δ -49.67 (t, *J* = 40.7 Hz). HRMS (ESI) (*m/z*): $[M+Na]^+$ calcd. for $C_{20}H_{20}FNO_2SNa$: 380.1096, found: 380.1091.

N-fluoro-N-(4-(naphthalen-2-yl)butyl)benzenesulfonamide (**1x**)

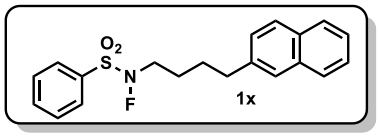

Prepared following general procedure A the reaction mixture was purified by column chromatography (petroleum ether/ethyl acetate = 19/1 as the eluent) as a yellow solid (834 mg, 78% yield). ^{1}H NMR (400 MHz, Chloroform-*d*) δ 7.91 (d, *J* = 7.5 Hz, 2H), 7.81 – 7.73 (m, 3H), 7.71 (t, *J* = 7.5 Hz, 1H), 7.63 – 7.53 (m, 3H), 7.49 – 7.38 (m, 2H), 7.33 – 7.26 (m, 1H), 3.24 (dt, *J* = 40.6, 6.5 Hz, 2H), 2.79 (t, *J* = 7.1 Hz, 2H), 1.90 – 1.68 (m, 4H). ^{13}C NMR (101 MHz, Chloroform-*d*) δ 139.29, 134.99, 133.68, 132.13, 132.06, 130.01, 129.38, 128.08, 127.72, 127.53, 127.28, 126.54, 126.06, 125.31, 53.62 (d, *J* = 12.5 Hz), 35.53, 28.22, 25.99. ^{19}F NMR (376 MHz, Chloroform-*d*) δ -49.82 (t, *J* = 40.6 Hz). HRMS (ESI) (*m/z*): $[M+Na]^+$ calcd. for $C_{20}H_{20}FNO_2SNa$: 380.1096, found: 380.1093.

N-fluoro-N-(4-(thiophen-2-yl)butyl)benzenesulfonamide (**1y**)

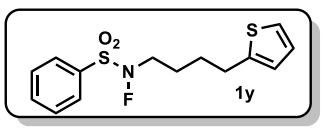

Prepared following general procedure A the reaction mixture was purified by column chromatography (petroleum ether/ethyl acetate = 19/1 as the eluent) as a yellow oil (417 mg, 42% yield). ^{1}H NMR (400 MHz, Chloroform-*d*) δ 7.94 (d, *J* = 7.8 Hz, 2H), 7.74 (t, *J* = 7.5 Hz, 1H), 7.61 (t, *J* = 7.8 Hz, 2H), 7.11 (d, *J* = 5.1 Hz, 1H), 6.97 – 6.83 (m, 1H), 6.77 (d, *J* = 3.3 Hz, 1H), 3.24 (dt, *J* = 40.5, 6.0 Hz, 2H), 2.85 (t, *J* = 6.6 Hz, 2H), 1.90 – 1.68 (m, 4H). ^{13}C NMR (101 MHz, Chloroform-*d*) δ 144.52, 135.03, 132.03, 130.03, 129.41, 126.87, 124.46, 123.23, 53.46 (d, *J* = 12.5 Hz), 29.41, 28.73, 25.76. ^{19}F NMR (376 MHz, Chloroform-*d*) δ -

49.83 (t, J = 40.5 Hz). HRMS (ESI) (*m/z*): $[M+Na]^+$ calcd. for $C_{14}H_{16}FNO_2S_2Na$: 336.0504, found: 336.0506.

N-(2,2-dimethyl-4-phenylbutyl)-N-fluorobenzenesulfonamide (**1z**)

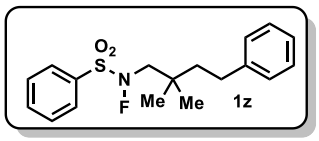

Prepared following general procedure A the reaction mixture was purified by column chromatography (petroleum ether/ethyl acetate = 19/1 as the eluent) as a white solid (653 mg, 65% yield). ^{1}H NMR (400 MHz, Chloroform-*d*) δ 7.99 – 7.90 (m, 2H), 7.78 – 7.71 (m, 1H), 7.66 – 7.58 (m, 2H), 7.30 – 7.25 (m, 2H), 7.21 – 7.13 (m, 3H), 3.10 (d, J = 44.2 Hz, 2H), 2.60 – 2.52 (m, 2H), 1.68 – 1.61 (m, 2H), 1.05 (s, 6H). ^{13}C NMR (101 MHz, Chloroform-*d*) δ 142.69, 134.96, 132.68, 129.92, 129.44, 128.52, 128.46, 125.88, 62.85 (d, J = 10.6 Hz), 42.42, 34.69, 30.44, 25.76. ^{19}F NMR (376 MHz, Chloroform-*d*) δ -36.35 (t, J = 44.2 Hz). HRMS (ESI) (*m/z*): $[M+Na]^+$ calcd. for $C_{18}H_{22}FNO_2SNa$: 358.1253, found: 358.1242.

N-fluoro-N-(pent-4-en-1-yl)benzenesulfonamide (**4**)

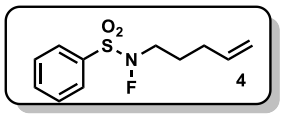

Prepared following general procedure A the reaction mixture was purified by column chromatography (petroleum ether/ethyl acetate = 19/1 as the eluent) as a yellow oil (565 mg, 77% yield). ^{1}H NMR (400 MHz, Chloroform-*d*) δ 8.00 – 7.90 (m, 2H), 7.79 – 7.71 (m, 1H), 7.67 – 7.57 (m, 2H), 5.87 – 5.66 (m, 1H), 5.12 – 4.96 (m, 2H), 3.25 (dt, J = 40.5, 6.9 Hz, 2H), 2.18 (q, J = 7.0 Hz, 2H), 1.82 (quint, J = 7.3 Hz, 2H). ^{13}C NMR (101 MHz, Chloroform-*d*) δ 136.97, 135.02, 132.18, 130.05, 129.41, 116.09, 53.02 (d, J = 12.5 Hz), 30.59, 25.53. ^{19}F NMR (376 MHz, Chloroform-*d*) δ -49.87 (t, J = 40.6 Hz). HRMS (ESI) (*m/z*): $[M+Na]^+$ calcd. for $C_{11}H_{14}FNO_2SNa$: 266.0627, found: 266.0616.

N-fluoro-N-(4-(2-phenylcyclopropyl)butyl)benzenesulfonamide (**6**)

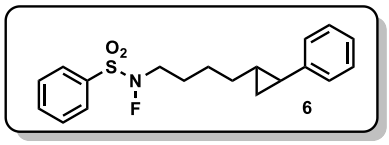

Prepared following general procedure A (1.1 mmol scale) the reaction mixture was purified by column chromatography (petroleum ether/ethyl acetate = 19/1 as the eluent) as a light yellow oil (214 mg, 56% yield). ^{1}H NMR (400 MHz, Chloroform-*d*) δ 8.00 – 7.87 (m, 2H), 7.78 – 7.69 (m, 1H), 7.66 – 7.57 (m, 2H), 7.26 – 7.20 (m, 2H), 7.16 – 7.09 (m, 1H), 7.07 – 6.96 (m, 2H), 3.23 (dt, J = 40.6, 6.9 Hz, 2H), 1.83 – 1.70 (m, 2H), 1.64 – 1.50 (m, 3H), 1.45 – 1.37 (m, 2H), 1.05 – 0.93 (m, 1H), 0.92 – 0.84 (m, 1H), 0.79 – 0.70 (m, 1H). ^{13}C NMR (101 MHz, Chloroform-*d*) δ 143.80, 134.99, 132.18, 130.06, 129.40, 128.38, 125.68, 125.38, 53.78 (d, J = 12.5 Hz), 33.96, 26.55, 26.20, 23.55, 23.36, 16.23. ^{19}F NMR (376 MHz, Chloroform-*d*) δ -49.85 (t, J = 40.6 Hz). HRMS (ESI) (*m/z*): $[M+Na]^+$ calcd. for $C_{19}H_{22}FNO_2SNa$: 370.1253, found: 370.1248.

2. **Products:**

(R)-N-(4-cyano-4-phenylbutyl)benzenesulfonamide (**2a**)

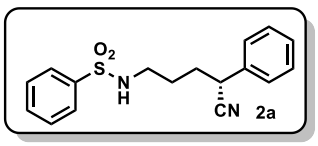

Prepared following general procedure B the reaction mixture was purified by column chromatography (petroleum ether/ethyl acetate = 5/1 as the eluent) to afford the product **2a** (58.0 mg, 92% yield, 92% *ee*) as a white solid. ^{1}H NMR (400 MHz, Chloroform-*d*) δ 7.88 – 7.80 (m, 2H), 7.62 – 7.55 (m, 1H), 7.55 – 7.47 (m, 2H), 7.40 – 7.30 (m, 3H), 7.30 – 7.26 (m, 2H), 4.95 – 4.55 (m, 1H), 3.80 (t, J = 7.3 Hz, 1H), 3.07 – 2.91 (m, 2H), 2.00 – 1.85 (m, 2H), 1.71 – 1.58 (m, 2H). ^{13}C NMR (101 MHz, Chloroform-

d) δ 139.80, 135.36, 132.94, 129.36, 129.28, 128.35, 127.31, 127.07, 120.53, 42.41, 36.84, 32.72, 27.10. HRMS (ESI) (*m/z*): $[M+Na]^+$ calcd. for $C_{17}H_{18}N_2O_2SNa$: 337.0987, found: 337.0987.

$[\alpha]_D^{20.0}$ = 14.70 (c 0.71, $CHCl_3$). HPLC (OD-H, 0.46*25 cm, 5 μm, hexane/isopropanol = 7/3, flow 0.5 mL/min, detection at 214 nm) retention time = 20.08 min (minor) and 21.71 min (major).

(R)-N-(4-cyano-4-phenylbutyl)-4-methylbenzenesulfonamide (**2b**)

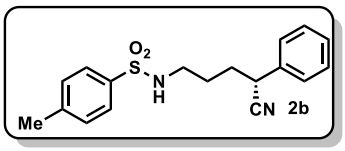

Prepared following general procedure B the reaction mixture was purified by column chromatography (petroleum ether/ethyl acetate = 5/1 as the eluent) to afford the product **2b** (47.5 mg, 72% yield, 91% *ee*) as a white solid. ^{1}H NMR (400 MHz, Chloroform-*d*) δ 7.72 (t, *J* = 7.9 Hz, 2H), 7.42 – 7.32 (m, 3H), 7.32 – 7.24 (m, 4H), 4.76 (t, *J* = 6.2 Hz, 1H), 3.79 (t, *J* = 7.3 Hz, 1H), 3.04 – 2.89 (m, 2H), 2.42 (s, 3H), 2.00 – 1.82 (m, 2H), 1.71 – 1.58 (m, 2H). ^{13}C NMR (101 MHz, Chloroform-*d*) δ 143.75, 136.78, 135.39, 129.93, 129.25, 128.30, 127.30, 127.13, 120.57, 42.35, 36.82, 32.71, 27.06, 21.66. HRMS (ESI) (*m/z*): $[M+Na]^+$ calcd. for $C_{18}H_{20}N_2O_2SNa$: 351.1143, found: 351.1151.

$[\alpha]_D^{20.0}$ = 10.08 (c 0.57, $CHCl_3$). HPLC (OD-H, 0.46*25 cm, 5 μm, hexane/isopropanol = 7/3, flow 0.5 mL/min, detection at 214 nm) retention time = 20.17 min (minor) and 21.88 min (major).

(R)-N-(4-cyano-4-phenylbutyl)-4-methoxybenzenesulfonamide (**2c**)

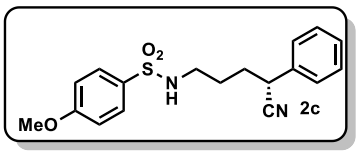

Prepared following general procedure B the reaction mixture was purified by column chromatography (petroleum ether/ethyl acetate = 5/1 to 3/1 as the eluent) to afford the product **2c** (63.5 mg, 92% yield, 90% *ee*) as a yellow solid. ^{1}H NMR (400 MHz, Chloroform-*d*) δ 7.77 (d, *J* = 9.0 Hz, 2H), 7.39 – 7.30 (m, 3H), 7.30 – 7.26 (m, 2H), 6.97 (d, *J* = 9.0 Hz, 2H), 4.76 (t, *J* = 6.4 Hz, 1H), 3.86 (s, 3H), 3.80 (t, *J* = 7.4 Hz, 1H), 3.02 – 2.89 (m, 2H), 1.98 – 1.83 (m, 2H), 1.68 – 1.58 (m, 2H). ^{13}C NMR (101 MHz, Chloroform-*d*) δ 163.04, 135.39, 131.29, 129.22, 128.27, 127.28, 120.61, 114.45, 55.74, 42.28, 36.80, 32.71, 26.98. HRMS (ESI) (*m/z*): $[M+Na]^+$ calcd. for $C_{18}H_{20}N_2O_3SNa$: 367.1092, found: 367.1082.

$[\alpha]_D^{20.0}$ = 21.03 (c 0.50, $CHCl_3$). HPLC (OD-H, 0.46*25 cm, 5 μm, hexane/isopropanol = 7/3, flow 0.5 mL/min, detection at 214 nm) retention time = 27.64 min (minor) and 29.80 min (major).

(R)-4-chloro-N-(4-cyano-4-phenylbutyl)benzenesulfonamide (**2d**)

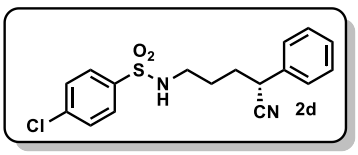

Prepared following general procedure B the reaction mixture was purified by column chromatography (petroleum ether/ethyl acetate = 5/1 as the eluent) to afford the product **2d** (51.7 mg, 74% yield, 91% *ee*) as a white solid. ^{1}H NMR (400 MHz, Chloroform-*d*) δ 7.77 (d, *J* = 8.7 Hz, 2H), 7.47 (d, *J* = 8.7 Hz, 2H), 7.40 – 7.31 (m, 3H), 7.30 – 7.26 (m, 2H), 4.84 (t, *J* = 6.4 Hz, 1H), 3.82 (t, *J* = 7.3 Hz, 1H), 3.05 – 2.92 (m, 2H), 1.99 – 1.85 (m, 2H), 1.73 – 1.58 (m, 2H). ^{13}C NMR (101 MHz, Chloroform-*d*) δ 139.42, 138.34, 135.24, 129.64, 129.30, 128.55, 128.39, 127.27, 120.54, 42.44, 36.85, 32.69, 27.07. HRMS (ESI) (*m/z*): $[M+Na]^+$ calcd. for $C_{17}H_{17}ClN_2O_2SNa$: 371.0597, found: 371.0591.

$[\alpha]_D^{20.0}$ = 13.10 (c 1.0, $CHCl_3$). HPLC (OD-H, 0.46*25 cm, 5 μm, hexane/isopropanol = 7/3, flow 0.5 mL/min, detection at 214 nm) retention time = 20.62 min (minor) and 22.13 min (major).

(R)-N-(4-cyano-4-phenylbutyl)-4-(trifluoromethyl)benzenesulfonamide (**2e**)

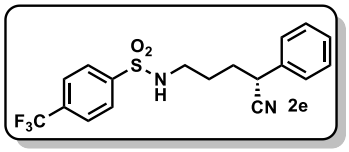

Prepared following general procedure B the reaction mixture was purified by column chromatography (petroleum ether/ethyl acetate = 5/1 as the eluent) to afford the product **2e** (74.1 mg, 97% yield, 93% *ee*) as a colourless oil. ^{1}H NMR (400 MHz, Chloroform-*d*) δ 7.96 (d, *J* = 8.2 Hz, 2H), 7.77 (d, *J* = 8.2 Hz, 2H), 7.40 – 7.31 (m, 3H), 7.30 – 7.26 (m, 2H), 4.92 (t, *J* = 6.3 Hz, 1H), 3.83 (t, *J* = 7.3 Hz, 1H), 3.10 – 2.93 (m, 2H), 1.99 – 1.89 (m, 2H), 1.73 – 1.62 (m, 2H). ^{13}C NMR (101 MHz, Chloroform-*d*) δ 143.47, 135.20, 134.61 (q, *J* = 33.1 Hz), 129.32, 128.43, 127.61, 127.26, 126.53 (q, *J* = 3.7 Hz), 123.28 (q, *J* = 272.9 Hz), 120.53, 42.52, 36.86, 32.68, 27.13. ^{19}F NMR (376 MHz, Chloroform-*d*) δ -63.11 (s). HRMS (ESI) (*m/z*): $[M+Na]^+$ calcd. for $C_{18}H_{17}F_3N_2O_2SNa$: 405.0861, found: 405.0871. $[\alpha]_D^{20.0}$ = 11.51 (c 1.0, $CHCl_3$). HPLC (AS-H, 0.46*25 cm, 5 μm, hexane/isopropanol = 8/2, flow 0.5 mL/min, detection at 214 nm) retention time = 56.98 min (major) and 69.90 min (minor).

(R)-N-(4-cyano-4-(p-tolyl)butyl)benzenesulfonamide (**2f**)

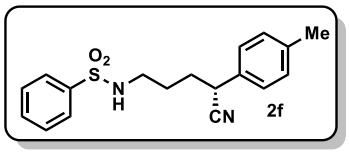

Prepared following general procedure B the reaction mixture was purified by column chromatography (petroleum ether/ethyl acetate = 5/1 as the eluent) to afford the product **2f** (62.4 mg, 95% yield, 84% *ee*) as a white solid. ^{1}H NMR (400 MHz, Chloroform-*d*) δ 7.89 – 7.79 (m, 2H), 7.62 – 7.54 (m, 1H), 7.54 – 7.46 (m, 2H), 7.20 – 7.11 (m, 4H), 5.02 – 4.86 (m, 1H), 3.74 (t, *J* = 7.3 Hz, 1H), 3.06 – 2.86 (m, 2H), 2.34 (s, 3H), 1.94 – 1.83 (m, 2H), 1.68 – 1.56 (m, 2H). ^{13}C NMR (101 MHz, Chloroform-*d*) δ 139.78, 138.10, 132.87, 132.31, 129.87, 129.31, 127.15, 127.04, 120.76, 42.39, 36.40, 32.66, 27.01, 21.16. HRMS (ESI) (*m/z*): $[M+Na]^+$ calcd. for $C_{18}H_{20}N_2O_2SNa$: 351.1143, found: 351.1140.

$[\alpha]_D^{20.0}$ = 14.60 (c 0.70, $CHCl_3$). HPLC (AD-H, 0.46*25 cm, 5 μm, hexane/isopropanol = 8/2, flow 0.5 mL/min, detection at 214 nm) retention time = 30.62 min (minor) and 34.30 min (major).

(R)-N-(4-(4-(tert-butyl)phenyl)-4-cyanobutyl)benzenesulfonamide (**2g**)

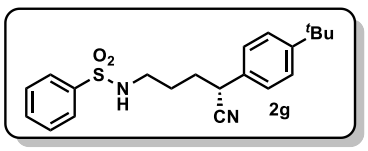

Prepared following general procedure B the reaction mixture was purified by column chromatography (petroleum ether/ethyl acetate = 5/1 as the eluent) to afford the product **2g** (67.2 mg, 91% yield, 86% *ee*) as a white solid. ^{1}H NMR (400 MHz, Chloroform-*d*) δ 7.89 – 7.82 (m, 2H), 7.60 – 7.55 (m, 1H), 7.54 – 7.47 (m, 2H), 7.37 (d, *J* = 8.3 Hz, 2H), 7.20 (d, *J* = 8.3 Hz, 2H), 4.87 (t, *J* = 6.0 Hz, 1H), 3.76 (t, *J* = 7.3 Hz, 1H), 3.06 – 2.90 (m, 2H), 2.00 – 1.81 (m, 2H), 1.70 – 1.58 (m, 2H), 1.31 (s, 9H). ^{13}C NMR (101 MHz, Chloroform-*d*) δ 151.36, 139.81, 132.89, 132.26, 129.33, 127.06, 126.98, 126.17, 120.74, 42.44, 36.38, 34.68, 32.66, 31.38, 27.09. HRMS (ESI) (*m/z*): $[M+Na]^+$ calcd. for $C_{21}H_{26}N_2O_2SNa$: 393.1613, found: 393.1609.

$[\alpha]_D^{20.0}$ = 13.20 (c 0.61, $CHCl_3$). HPLC (OD-H, 0.46*25 cm, 5 μm, hexane/isopropanol = 8/2, flow 0.5 mL/min, detection at 214 nm) retention time = 19.71 min (minor) and 22.73 min (major).

(R)-N-(4-cyano-4-(4-pentylphenyl)butyl)benzenesulfonamide (**2h**)

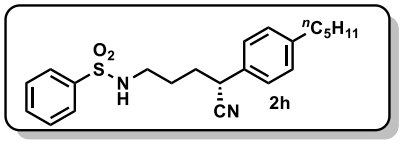

Prepared following general procedure B the reaction mixture was purified by column chromatography (petroleum ether/ethyl acetate = 5/1 as the eluent) to afford the product **2h** (70.8 mg, 92% yield, 86% *ee*) as a white solid. ^{1}H NMR (400 MHz, Chloroform-*d*) δ 7.88 – 7.81

(m, 2H), 7.61 – 7.55 (m, 1H), 7.54 – 7.47 (m, 2H), 7.20 – 7.13 (m, 4H), 4.82 (t, *J* = 6.2 Hz, 1H), 3.75 (t, *J* = 7.3 Hz, 1H), 3.04 – 2.92 (m, 2H), 2.59 (t, *J* = 7.8 Hz, 2H), 2.00 – 1.81 (m, 2H), 1.90 (q, *J* = 7.4 Hz, 2H), 1.67 – 1.55 (m, 2H), 1.39 – 1.28 (m, 4H), 0.89 (t, *J* = 6.9 Hz, 3H). ^{13}C NMR (101 MHz, Chloroform-*d*) δ 143.20, 139.86, 132.88, 132.49, 129.33, 129.24, 127.17, 127.07, 120.75, 42.44, 36.50, 35.61, 32.71, 31.57, 31.16, 27.10, 22.63, 14.14. HRMS (ESI) (*m/z*): $[M+Na]^+$ calcd. for $C_{22}H_{28}N_2O_2SNa$: 407.1769, found: 407.1765.

$[\alpha]_D^{20.0}$ = 11.58 (c 0.60, $CHCl_3$). HPLC (OD-H, 0.46*25 cm, 5 μm, hexane/isopropanol = 8/2, flow 0.5 mL/min, detection at 214 nm) retention time = 20.22 min (minor) and 21.85 min (major).

(R)-N-(4-([1,1'-biphenyl]-4-yl)-4-cyanobutyl)benzenesulfonamide (**2i**)

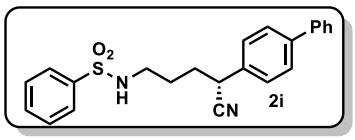

Prepared following general procedure B the reaction mixture was purified by column chromatography (petroleum ether/ethyl acetate = 5/1 to 3/1 as the eluent) to afford the product **2i** (71.4 mg, 91% yield, 91% *ee*) as a white solid. ^{1}H NMR (400 MHz, Chloroform-*d*) δ 7.89 – 7.81 (m, 2H), 7.61 – 7.54 (m, 5H), 7.53 – 7.42 (m, 4H), 7.40 – 7.32 (m, 3H), 4.80 (t, *J* = 6.2 Hz, 1H), 3.85 (t, *J* = 7.3 Hz, 1H), 3.08 – 2.93 (m, 2H), 2.07 – 1.86 (m, 2H), 1.76 – 1.59 (m, 2H). ^{13}C NMR (101 MHz, Chloroform-*d*) δ 141.32, 140.26, 139.80, 134.28, 132.93, 129.35, 129.01, 127.94, 127.78, 127.75, 127.18, 127.07, 120.52, 42.41, 36.51, 32.67, 27.10. HRMS (ESI) (*m/z*): $[M+Na]^+$ calcd. for $C_{23}H_{22}N_2O_2SNa$: 413.1300, found: 413.1292.

$[\alpha]_D^{20.0}$ = 12.24 (c 0.50, $CHCl_3$). HPLC (AD-H, 0.46*25 cm, 5 μm, hexane/isopropanol = 8/2, flow 0.5 mL/min, detection at 214 nm) retention time = 43.66 min (minor) and 55.78 min (major).

(R)-N-(4-cyano-4-(4-phenoxyphenyl)butyl)benzenesulfonamide (**2j**)

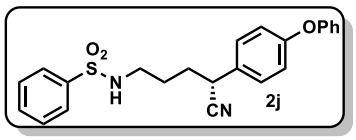

Prepared following general procedure B the reaction mixture was purified by column chromatography (petroleum ether/ethyl acetate = 5/1 as the eluent) to afford the product **2j** (34.5 mg, 42% yield, 86% *ee*) as a yellow oil. ^{1}H NMR (400 MHz, Chloroform-*d*) δ 7.88 – 7.81 (m, 2H), 7.59 (t, *J* = 7.0 Hz, 1H), 7.52 (t, *J* = 7.7 Hz, 2H), 7.36 (t, *J* = 7.7 Hz, 2H), 7.23 (d, *J* = 8.5 Hz, 2H), 7.14 (t, *J* = 7.4 Hz, 1H), 6.99 (dd, *J* = 15.0, 8.4 Hz, 4H), 4.73 (t, *J* = 6.3 Hz, 1H), 3.78 (t, *J* = 7.4 Hz, 1H), 3.07 – 2.93 (m, 2H), 1.92 (t, *J* = 7.7 Hz, 2H), 1.73 – 1.57 (m, 2H). ^{13}C NMR (101 MHz, Chloroform-*d*) δ 157.53, 156.72, 139.85, 132.95, 130.01, 129.86, 129.37, 128.74, 127.08, 123.90, 120.59, 119.36, 119.21, 42.42, 36.19, 32.76, 27.14. HRMS (ESI) (*m/z*): $[M+Na]^+$ calcd. for $C_{23}H_{22}N_2O_3SNa$: 429.1249, found: 429.1248.

$[\alpha]_D^{20.0}$ = 7.03 (c 0.34, $CHCl_3$). HPLC (OD-H, 0.46*25 cm, 5 μm, hexane/isopropanol = 8/2, flow 0.5 mL/min, detection at 214 nm) retention time = 46.47 min (major) and 54.01 min (minor).

(R)-N-(4-cyano-4-(4-(trifluoromethoxy)phenyl)butyl)benzenesulfonamide (**2k**)

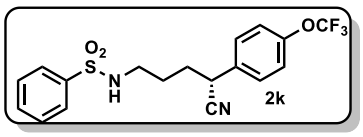

Prepared following general procedure B the reaction mixture was purified by column chromatography (petroleum ether/ethyl acetate = 5/1 as the eluent) to afford the product **2k** (66.5 mg, 83% yield, 88% *ee*) as a white solid. ^{1}H NMR (400 MHz, Chloroform-*d*) δ 7.91 – 7.78 (m, 2H), 7.63 – 7.55 (m, 1H), 7.55 – 7.47 (m, 2H), 7.33 (d, *J* = 8.3 Hz, 2H), 7.21 (d, *J* = 8.2 Hz, 2H), 5.03 – 4.71 (m, 1H), 3.85 (t, *J* = 7.3 Hz, 1H), 3.11 – 2.91 (m, 2H), 2.03 – 1.83 (m, 2H), 1.75 – 1.58 (m, 2H). ^{13}C NMR (101 MHz, Chloroform-*d*) δ 148.96, 139.64, 134.00, 132.87, 129.26, 128.75, 126.93, 121.62, 120.19 (q,

J = 247.4 Hz), 119.98, 42.14, 36.09, 32.54, 26.95. ^{19}F NMR (376 MHz, Chloroform-*d*) δ -57.89 (s). HRMS (ESI) (*m/z*): $[M+Na]^+$ calcd. for $C_{18}H_{17}F_3N_2O_3SNa$: 421.0810, found: 421.0812.

$[\alpha]_D^{20.0}$ = 10.66 (c 0.70, $CHCl_3$). HPLC (OD-H, 0.46*25 cm, 5 μm, hexane/isopropanol = 8/2, flow 0.5 mL/min, detection at 214 nm) retention time = 21.52 min (minor) and 24.11 min (major).

(R)-N-(4-(4-chlorophenyl)-4-cyanobutyl)benzenesulfonamide (**2l**)

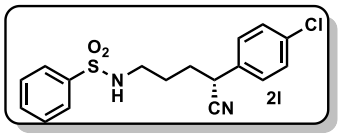

Prepared following general procedure B the reaction mixture was purified by column chromatography (petroleum ether/ethyl acetate = 5/1 as the eluent) to afford the product **2l** (59.5 mg, 85% yield, 90% *ee*) as a white solid. ^{1}H NMR (400 MHz, Chloroform-*d*) δ 7.88 – 7.80 (m, 2H), 7.62 – 7.56 (m, 1H), 7.54 – 7.47 (m, 2H), 7.32 (d, *J* = 8.4 Hz, 2H), 7.22 (d, *J* = 8.4 Hz, 2H), 5.05 (s, 1H), 3.80 (t, *J* = 7.4 Hz, 1H), 3.04 – 2.92 (m, 2H), 1.96 – 1.84 (m, 2H), 1.69 – 1.57 (m, 2H). ^{13}C NMR (101 MHz, Chloroform-*d*) δ 139.71, 134.27, 133.89, 132.95, 129.42, 129.35, 128.69, 127.01, 120.17, 42.24, 36.20, 32.55, 26.95. HRMS (ESI) (*m/z*): $[M+Na]^+$ calcd. for $C_{17}H_{17}ClN_2O_2SNa$: 371.0597, found: 371.0597.

$[\alpha]_D^{20.0}$ = 11.12 (c 0.79, $CHCl_3$). HPLC (OD-H, 0.46*25 cm, 5 μm, hexane/isopropanol = 8/2, flow 0.5 mL/min, detection at 214 nm) retention time = 29.17 min (minor) and 31.98 min (major).

(R)-N-(4-(4-bromophenyl)-4-cyanobutyl)benzenesulfonamide (**2m**)

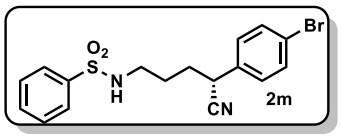

Prepared following general procedure B the reaction mixture was purified by column chromatography (petroleum ether/ethyl acetate = 5/1 as the eluent) to afford the product **2m** (74.1 mg, 94% yield, 89% *ee*) as a white solid. ^{1}H NMR (400 MHz, Chloroform-*d*) δ 7.90 – 7.80 (m, 2H), 7.62 – 7.56 (m, 1H), 7.55 – 7.44 (m, 4H), 7.16 (d, *J* = 8.4 Hz, 2H), 4.98 (s, 1H), 3.79 (t, *J* = 7.4 Hz, 1H), 3.06 – 2.91 (m, 2H), 2.00 – 1.80 (m, 2H), 1.70 – 1.56 (m, 2H). ^{13}C NMR (101 MHz, Chloroform-*d*) δ 139.72, 134.41, 132.97, 132.40, 129.36, 129.01, 127.02, 122.36, 120.07, 42.25, 36.28, 32.51, 26.97. HRMS (ESI) (*m/z*): $[M+Na]^+$ calcd. for $C_{17}H_{17}BrN_2O_2SNa$: 415.0092, found: 415.0092.

$[\alpha]_D^{20.0}$ = 8.75 (c 1.0, $CHCl_3$). HPLC (OD-H, 0.46*25 cm, 5 μm, hexane/isopropanol = 8/2, flow 0.5 mL/min, detection at 214 nm) retention time = 31.50 min (minor) and 35.10 min (major).

(R)-N-(4-cyano-4-(4-(trifluoromethyl)phenyl)butyl)benzenesulfonamide (**2n**)

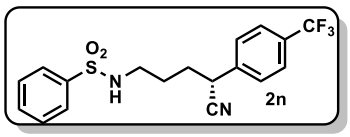

Prepared following general procedure B the reaction mixture was purified by column chromatography (petroleum ether/ethyl acetate = 5/1 as the eluent) to afford the product **2n** (63.0 mg, 82% yield, 87% *ee*) as a yellow solid. ^{1}H NMR (400 MHz, Chloroform-*d*) δ 7.89 – 7.81 (m, 2H), 7.65 – 7.55 (m, 3H), 7.54 – 7.48 (m, 2H), 7.43 (d, *J* = 8.1 Hz, 2H), 5.04 (s, 1H), 3.91 (dd, *J* = 8.5, 6.3 Hz, 1H), 3.10 – 2.91 (m, 2H), 2.05 – 1.86 (m, 2H), 1.72 – 1.61 (m, 2H). ^{13}C NMR (101 MHz, Chloroform-*d*) δ 139.70, 139.40, 133.00, 130.69 (q, *J* = 32.8 Hz), 129.38, 127.81, 127.02, 126.27 (q, *J* = 3.7 Hz), 123.87 (q, *J* = 273.1 Hz), 119.82, 42.20, 36.62, 32.53, 27.01. ^{19}F NMR (376 MHz, Chloroform-*d*) δ -62.68 (s). HRMS (ESI) (*m/z*): $[M+Na]^+$ calcd. for $C_{18}H_{17}F_3N_2O_2SNa$: 405.0861, found: 405.0862.

$[\alpha]_D^{20.0}$ = 9.15 (c 0.60, $CHCl_3$). HPLC (OD-H, 0.46*25 cm, 5 μm, hexane/isopropanol = 8/2, flow 0.5 mL/min, detection at 214 nm) retention time = 23.44 min (minor) and 26.75 min (major).

(R)-N-(4-cyano-4-(m-tolyl)butyl)benzenesulfonamide (**2o**)

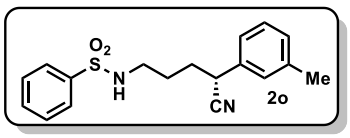

Prepared following general procedure B the reaction mixture was purified by column chromatography (petroleum ether/ethyl acetate = 5/1 as the eluent) to afford the product **2o** (50.1 mg, 76% yield, 90% *ee*) as a yellow oil. ^{1}H NMR (400 MHz, Chloroform-*d*) δ 7.87 – 7.81 (m, 2H), 7.61 – 7.55 (m, 1H), 7.54 – 7.47 (m, 2H), 7.24 (t, *J* = 7.6 Hz, 1H), 7.15 – 7.03 (m, 3H), 4.80 (s, 1H), 3.74 (t, *J* = 7.3 Hz, 1H), 3.04 – 2.93 (m, 2H), 2.35 (s, 3H), 1.96 – 1.85 (m, 2H), 1.70 – 1.59 (m, 2H). ^{13}C NMR (101 MHz, Chloroform-*d*) δ 139.84, 139.12, 135.26, 132.90, 129.33, 129.12, 129.07, 127.95, 127.07, 124.35, 120.67, 42.44, 36.78, 32.71, 27.12, 21.49. HRMS (ESI) (*m/z*): $[M+Na]^+$ calcd. for $C_{18}H_{20}N_2O_2SNa$: 351.1143, found: 351.1142.

$[\alpha]_D^{20.0}$ = 14.95 (c 0.60, $CHCl_3$). HPLC (OD-H, 0.46*25 cm, 5 μm, hexane/isopropanol = 8/2, flow 0.5 mL/min, detection at 214 nm) retention time = 23.46 min (minor) and 26.59 min (major).

(R)-N-(4-cyano-4-(3-methoxyphenyl)butyl)benzenesulfonamide (**2p**)

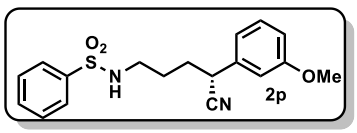

Prepared following general procedure B the reaction mixture was purified by column chromatography (petroleum ether/ethyl acetate = 5/1 to 3/1 as the eluent) to afford the product **2p** (60.5 mg, 88% yield, 93% *ee*) as a yellow oil. ^{1}H NMR (400 MHz, Chloroform-*d*) δ 7.87 – 7.81 (m, 2H), 7.60 – 7.55 (m, 1H), 7.54 – 7.47 (m, 2H), 7.26 (t, *J* = 7.9 Hz, 1H), 6.87 – 6.80 (m, 3H), 4.85 (t, *J* = 5.8 Hz, 1H), 3.81 (s, 3H), 3.76 (t, *J* = 7.36 Hz, 1H), 3.03 – 2.93 (m, 2H), 1.95 – 1.87 (m, 2H), 1.68 – 1.59 (m, 2H). ^{13}C NMR (101 MHz, Chloroform-*d*) δ 160.19, 139.83, 136.80, 132.90, 130.32, 129.33, 127.05, 120.49, 119.54, 113.69, 113.13, 55.46, 42.40, 36.80, 32.59, 27.07. HRMS (ESI) (*m/z*): $[M+Na]^+$ calcd. for $C_{18}H_{20}N_2O_3SNa$: 367.1092, found: 367.1102.

$[\alpha]_D^{20.0}$ = 11.36 (c 0.80, $CHCl_3$). HPLC (OD-H, 0.46*25 cm, 5 μm, hexane/isopropanol = 8/2, flow 0.5 mL/min, detection at 214 nm) retention time = 39.34 min (minor) and 45.54 min (major).

(R)-N-(4-(3-chlorophenyl)-4-cyanobutyl)benzenesulfonamide (**2q**)

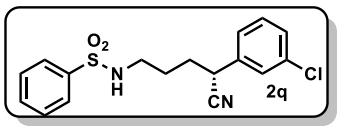

Prepared following general procedure B the reaction mixture was purified by column chromatography (petroleum ether/ethyl acetate = 5/1 as the eluent) to afford the product **2q** (51.6 mg, 74% yield, 93% *ee*) as a yellow oil. ^{1}H NMR (400 MHz, Chloroform-*d*) δ 7.90 – 7.80 (m, 2H), 7.63 – 7.56 (m, 1H), 7.56 – 7.47 (m, 2H), 7.33 – 7.27 (m, 3H), 7.22 – 7.15 (m, 1H), 4.86 (t, *J* = 6.3 Hz, 1H), 3.80 (dd, *J* = 8.4, 6.4 Hz, 1H), 3.11 – 2.91 (m, 2H), 2.00 – 1.82 (m, 2H), 1.74 – 1.56 (m, 2H). ^{13}C NMR (101 MHz, Chloroform-*d*) δ 139.75, 137.30, 135.12, 132.99, 130.58, 129.38, 128.64, 127.51, 127.05, 125.55, 119.93, 42.29, 36.48, 32.55, 27.05. HRMS (ESI) (*m/z*): $[M+Na]^+$ calcd. for $C_{17}H_{17}ClN_2O_2SNa$: 371.0597, found: 371.0601.

$[\alpha]_D^{20.0}$ = 13.75 (c 0.70, $CHCl_3$). HPLC (OD-H, 0.46*25 cm, 5 μm, hexane/isopropanol = 8/2, flow 0.5 mL/min, detection at 214 nm) retention time = 27.74 min (minor) and 32.43 min (major).

(R)-N-(4-cyano-4-(3-(trifluoromethyl)phenyl)butyl)benzenesulfonamide (**2r**)

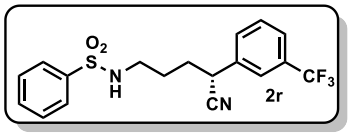

Prepared following general procedure B the reaction mixture was purified by column chromatography (petroleum ether/ethyl acetate = 5/1 as the eluent) to afford the product **2r** (54.1 mg, 71% yield, 90% *ee*) as a yellow oil. ^{1}H NMR (400 MHz, Chloroform-*d*) δ 7.89 – 7.81 (m, 2H), 7.62 – 7.56

(m, 2H), 7.56 – 7.47 (m, 5H), 4.90 (s, 1H), 3.91 (dd, *J* = 8.6, 6.3 Hz, 1H), 3.08 – 2.95 (m, 2H), 2.04 – 1.86 (m, 2H), 1.76 – 1.61 (m, 2H). ^{13}C NMR (101 MHz, Chloroform-*d*) δ 139.77, 136.55, 133.00, 131.74 (q, *J* = 32.7 Hz), 130.79, 129.94, 129.38, 127.05, 125.35 (q, *J* = 3.7 Hz), 124.13 (q, *J* = 3.7 Hz), 123.79 (q, *J* = 272.6 Hz), 119.79, 42.26, 36.72, 32.66, 27.14. ^{19}F NMR (376 MHz, Chloroform-*d*) δ -62.68 (s). HRMS (ESI) (*m/z*): $[M+Na]^+$ calcd. for $C_{18}H_{17}F_3N_2O_2SNa$: 405.0861, found: 405.0859.

$[\alpha]_D^{20.0}$ = 4.48 (c 0.60, $CHCl_3$). HPLC (OD-H, 0.46*25 cm, 5 μm, hexane/isopropanol = 8/2, flow 0.5 mL/min, detection at 214 nm) retention time = 20.85 min (minor) and 23.16 min (major).

(R)-N-(4-cyano-4-(o-tolyl)butyl)benzenesulfonamide (**2s**)

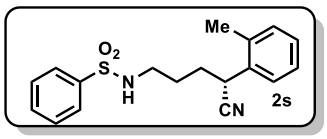

Prepared following general procedure B the reaction mixture was purified by column chromatography (petroleum ether/ethyl acetate = 5/1 as the eluent) to afford the product **2s** (51.5 mg, 78% yield, 90% *ee*) as a light yellow solid. ^{1}H NMR (400 MHz, Chloroform-*d*) δ 7.88 – 7.80 (m, 2H), 7.60 – 7.54 (m, 1H), 7.54 – 7.47 (m, 2H), 7.38 – 7.31 (m, 1H), 7.25 – 7.19 (m, 2H), 7.19 – 7.14 (m, 1H), 4.88 (t, *J* = 6.2 Hz, 1H), 3.94 (t, *J* = 7.3 Hz, 1H), 3.11 – 2.91 (m, 2H), 2.31 (s, 3H), 2.00 – 1.82 (m, 2H), 1.74 – 1.56 (m, 2H). ^{13}C NMR (101 MHz, Chloroform-*d*) δ 139.72, 135.07, 133.67, 132.91, 131.20, 129.33, 128.35, 127.43, 127.05, 126.97, 120.84, 42.50, 33.73, 31.27, 27.26, 19.24. HRMS (ESI) (*m/z*): $[M+Na]^+$ calcd. for $C_{18}H_{20}N_2O_2SNa$: 351.1143, found: 351.1148.

$[\alpha]_D^{20.0}$ = 32.73 (c 0.60, $CHCl_3$). HPLC (OD-H, 0.46*25 cm, 5 μm, hexane/isopropanol = 8/2, flow 0.5 mL/min, detection at 214 nm) retention time = 30.22 min (minor) and 34.51 min (major).

(R)-N-(4-cyano-4-(2-fluorophenyl)butyl)benzenesulfonamide (**2t**)

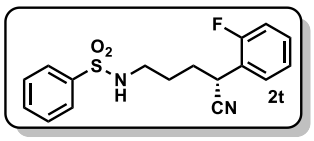

Prepared following general procedure B the reaction mixture was purified by column chromatography (petroleum ether/ethyl acetate = 5/1 as the eluent) to afford the product **2t** (42.9 mg, 65% yield, 94% *ee*) as a yellow oil. ^{1}H NMR (400 MHz, Chloroform-*d*) δ 7.89 – 7.81 (m, 2H), 7.62 – 7.55 (m, 1H), 7.55 – 7.48 (m, 2H), 7.44 – 7.37 (m, 1H), 7.37 – 7.29 (m, 1H), 7.22 – 7.14 (m, 1H), 7.12 – 7.04 (m, 1H), 4.63 (t, *J* = 6.3 Hz, 1H), 4.07 (t, *J* = 7.3 Hz, 1H), 3.01 (q, *J* = 6.7 Hz, 2H), 1.98 – 1.87 (m, 2H), 1.74 – 1.58 (m, 2H). ^{13}C NMR (101 MHz, Chloroform-*d*) δ 159.80 (d, *J* = 247.6 Hz), 139.85, 132.91, 130.36 (d, *J* = 8.3 Hz), 129.34, 129.01 (d, *J* = 3.1 Hz), 127.08, 125.01 (d, *J* = 3.7 Hz), 122.61 (d, *J* = 14.0 Hz), 119.71, 116.06 (d, *J* = 21.4 Hz), 42.44, 31.27, 30.79 (d, *J* = 3.3 Hz), 27.20. ^{19}F NMR (376 MHz, Chloroform-*d*) δ -118.14 – -118.34 (m). HRMS (ESI) (*m/z*): $[M+Na]^+$ calcd. for $C_{17}H_{17}FN_2O_2SNa$: 355.0892, found: 355.0895.

$[\alpha]_D^{20.0}$ = 14.77 (c 0.50, $CHCl_3$). HPLC (AD-H, 0.46*25 cm, 5 μm, hexane/isopropanol = 8/2, flow 0.5 mL/min, detection at 214 nm) retention time = 29.23 min (minor) and 33.90 min (major).

(R)-N-(4-cyano-4-(2-(trifluoromethyl)phenyl)butyl)benzenesulfonamide (**2u**)

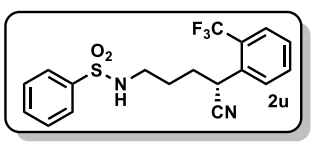

Prepared following general procedure B the reaction mixture was purified by column chromatography (petroleum ether/ethyl acetate = 5/1 as the eluent) to afford the product **2u** (55.6 mg, 73% yield, 95% *ee*) as a yellow oil. ^{1}H NMR (400 MHz, Chloroform-*d*) δ 7.88 – 7.82 (m, 2H), 7.70 – 7.65 (m, 1H), 7.64 – 7.54 (m, 3H), 7.54 – 7.42 (m, 3H), 4.77 (s, 1H), 4.08 (dd, *J* = 9.1, 5.7 Hz, 1H), 3.06 – 2.97 (m, 2H), 1.98 – 1.84 (m, 2H), 1.84 – 1.72 (m, 1H), 1.70 – 1.58 (m, 1H). ^{13}C NMR (101 MHz, Chloroform-*d*) δ 139.84, 134.37, 133.04, 132.92, 129.59, 129.34, 128.68, 127.71 (q, *J* = 30.4 Hz), 127.09, 126.67 (q, *J* =

5.5 Hz), 124.01 (q, *J* = 273.8 Hz), 120.18, 42.49, 33.47 (q, *J* = 2.3 Hz), 33.32, 27.67. ^{19}F NMR (376 MHz, Chloroform-*d*) δ -58.82 (s). HRMS (ESI) (*m/z*): $[M+Na]^+$ calcd. for $C_{18}H_{17}F_3N_2O_2SNa$: 405.0861, found: 405.0855.

$[\alpha]_D^{20.0}$ = 18.90 (c 0.71, $CHCl_3$). HPLC (AD-H, 0.46*25 cm, 5 μm, hexane/isopropanol = 8/2, flow 0.5 mL/min, detection at 214 nm) retention time = 20.36 min (minor) and 23.87 min (major).

(R)-N-(4-(4-chloro-2-methylphenyl)-4-cyanobutyl)benzenesulfonamide (**2v**)

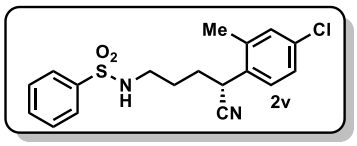

Prepared following general procedure B the reaction mixture was purified by column chromatography (petroleum ether/ethyl acetate = 5/1 as the eluent) to afford the product **2v** (47.3 mg, 65% yield, 85% *ee*) as a yellow oil. ^{1}H NMR (400 MHz, Chloroform-*d*) δ 7.95 – 7.80 (m, 2H), 7.65 – 7.47 (m, 3H), 7.35 – 7.15 (m, 3H), 4.90 (s, 1H), 3.92 (t, *J* = 7.3 Hz, 1H), 3.12 – 2.90 (m, 2H), 2.29 (s, 3H), 1.96 – 1.78 (m, 2H), 1.78 – 1.60 (m, 2H). ^{13}C NMR (101 MHz, Chloroform-*d*) δ 139.74, 137.10, 134.03, 132.95, 132.28, 131.07, 129.35, 128.83, 127.05, 120.40, 42.42, 33.30, 31.15, 27.19, 19.16. HRMS (ESI) (*m/z*): $[M+Na]^+$ calcd. for $C_{18}H_{19}ClN_2O_2SNa$: 385.0753, found: 385.0753.

$[\alpha]_D^{20.0}$ = 19.91 (c 0.67, $CHCl_3$). HPLC (OD-H, 0.46*25 cm, 5 μm, hexane/isopropanol = 8/2, flow 0.5 mL/min, detection at 214 nm) retention time = 30.23 min (minor) and 32.25 min (major).

(R)-N-(4-cyano-4-(naphthalen-1-yl)butyl)benzenesulfonamide (**2w**)

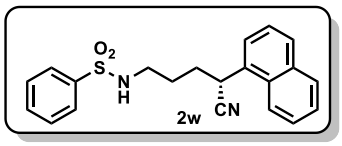

Prepared following general procedure B the reaction mixture was purified by column chromatography (petroleum ether/ethyl acetate = 5/1 as the eluent) to afford the product **2w** (49.4 mg, 68% yield, 90% *ee*) as a yellow oil. ^{1}H NMR (400 MHz, Chloroform-*d*) δ 7.92 – 7.87 (m, 2H), 7.85 – 7.79 (m, 3H), 7.63 – 7.50 (m, 4H), 7.50 – 7.42 (m, 3H), 4.73 (t, *J* = 6.3 Hz, 1H), 4.56 (dd, *J* = 8.8, 5.3 Hz, 1H), 3.08 – 2.92 (m, 2H), 2.16 – 1.92 (m, 2H), 1.81 – 1.66 (m, 2H). ^{13}C NMR (101 MHz, Chloroform-*d*) δ 139.71, 134.12, 132.89, 130.99, 129.94, 129.44, 129.30, 129.23, 127.22, 127.05, 126.34, 125.63, 125.52, 122.17, 120.80, 42.49, 33.90, 31.55, 27.34. HRMS (ESI) (*m/z*): $[M+Na]^+$ calcd. for $C_{21}H_{20}N_2O_2SNa$: 387.1143, found: 387.1139.

$[\alpha]_D^{20.0}$ = 52.21 (c 0.50, $CHCl_3$). HPLC (AD-H, 0.46*25 cm, 5 μm, hexane/isopropanol = 8/2, flow 0.5 mL/min, detection at 214 nm) retention time = 48.28 min (major) and 64.37 min (minor).

(R)-N-(4-cyano-4-(naphthalen-2-yl)butyl)benzenesulfonamide (**2x**)

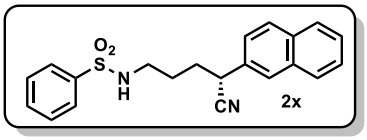

Prepared following general procedure B the reaction mixture was purified by column chromatography (petroleum ether/ethyl acetate = 5/1 as the eluent) to afford the product **2x** (60.1 mg, 82% yield, 90% *ee*) as a white solid. ^{1}H NMR (400 MHz, Chloroform-*d*) δ 7.86 – 7.78 (m, 5H), 7.77 – 7.73 (m, 1H), 7.55 – 7.48 (m, 3H), 7.48 – 7.41 (m, 2H), 7.33 (dd, *J* = 8.5, 1.8 Hz, 1H), 4.90 (t, *J* = 6.2 Hz, 1H), 3.95 (t, *J* = 7.2 Hz, 1H), 3.05 – 2.91 (m, 2H), 2.05 – 1.93 (m, 2H), 1.69 – 1.60 (m, 2H). ^{13}C NMR (101 MHz, Chloroform-*d*) δ 139.75, 133.31, 132.91, 132.87, 132.57, 129.29, 129.27, 127.97, 127.82, 127.01, 126.88, 126.69, 126.42, 124.72, 120.58, 42.38, 36.92, 32.49, 27.02. HRMS (ESI) (*m/z*): $[M+Na]^+$ calcd. for $C_{21}H_{20}N_2O_2SNa$: 387.1143, found: 387.1140.

$[\alpha]_D^{20.0}$ = 15.25 (c 0.67, $CHCl_3$). HPLC (OD-H, 0.46*25 cm, 5 μm, hexane/isopropanol = 8/2, flow 0.5 mL/min, detection at 214 nm) retention time = 48.95 min (minor) and 55.55 min (major).

(S)-N-(4-cyano-4-(thiophen-2-yl)butyl)benzenesulfonamide (**2y**)

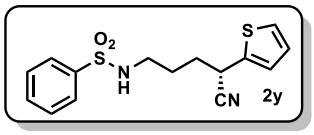

Prepared following general procedure B the reaction mixture was purified by column chromatography (petroleum ether/ethyl acetate = 5/1 as the eluent) to afford the product **2y** (36.2 mg,56% yield, 93% *ee*) as a yellow oil. ^{1}H NMR (400 MHz, Chloroform-*d*) δ 7.88 – 7.83 (m, 2H), 7.62 – 7.56 (m, 1H), 7.56 – 7.48 (m, 2H), 7.28 – 7.24 (m, 1H), 7.05 – 7.00 (m, 1H), 6.99 – 6.93 (m, 1H), 4.83 (t, *J* = 5.9 Hz, 1H), 4.08 (t, *J* = 7.2 Hz, 1H), 3.04 – 2.96 (m, 2H), 2.07 – 1.94 (m, 2H), 1.77 – 1.60 (m, 2H). ^{13}C NMR (101 MHz, Chloroform-*d*) δ 139.76, 137.30, 132.95, 129.37, 127.26, 127.08, 126.44, 125.80, 119.64, 42.35, 32.75, 32.07, 26.95. HRMS (ESI) (*m/z*): $[M+Na]^+$ calcd. for $C_{15}H_{16}N_2O_2S_2Na$: 343.0551, found: 343.0549.

$[\alpha]_D^{20.0}$ = 18.59 (c 0.30, $CHCl_3$). HPLC (AD-H, 0.46*25 cm, 5 μm, hexane/isopropanol = 8/2, flow 0.5 mL/min, detection at 214 nm) retention time = 37.54 min (minor) and 41.14 min (major).

(R)-N-(4-cyano-2,2-dimethyl-4-phenylbutyl)benzenesulfonamide (**2z**)

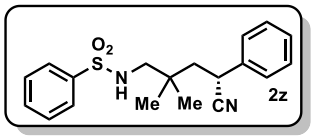

Prepared following general procedure B the reaction mixture was purified by column chromatography (petroleum ether/ethyl acetate = 5/1 as the eluent) to afford the product **2z** (68.5 mg, 92% yield, 86% *ee*) as a white solid. ^{1}H NMR (400 MHz, Chloroform-*d*) δ 7.90 – 7.81 (m, 2H), 7.61 – 7.55 (m, 1H), 7.54 – 7.48 (m, 2H), 7.39 – 7.29 (m, 5H), 4.91 (t, *J* = 7.2 Hz, 1H), 3.82 (dd, *J* = 10.6, 3.8 Hz, 1H), 2.85 (dd, *J* = 13.1, 8.2 Hz, 1H), 2.71 (dd, *J* = 13.1, 6.3 Hz, 1H), 1.98 (dd, *J* = 14.4, 10.6 Hz, 1H), 1.75 (dd, *J* = 14.5, 3.9 Hz, 1H), 1.05 (s, 3H), 1.00 (s, 3H). ^{13}C NMR (101 MHz, Chloroform-*d*) δ 139.76, 137.17, 132.93, 129.37, 128.20, 127.35, 127.04, 122.04, 52.64, 45.38, 34.77, 32.64, 25.69, 25.13. HRMS (ESI) (*m/z*): $[M+Na]^+$ calcd. for $C_{19}H_{22}N_2O_2SNa$: 365.1300, found: 365.1302.

$[\alpha]_D^{20.0}$ = 12.35 (c 0.50, $CHCl_3$). HPLC (OD-H, 0.46*25 cm, 5 μm, hexane/isopropanol = 7/3, flow 0.5 mL/min, detection at 214 nm) retention time = 13.26 min (minor) and 17.62 min (major).

Mechanistic Studies

1. Procedure of the radical trapping experiment with TEMPO:

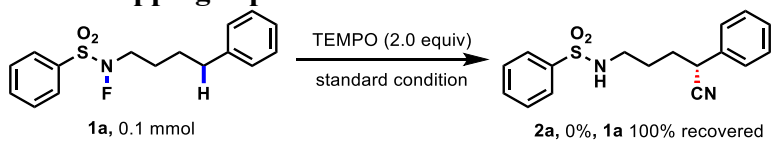

Scheme S1. The radical trapping experiment with TEMPO, related to **Scheme 2**.

To a sealed tube containing TEMPO, **solution A** (2.0 mL), TMSCN (11.9 mg, 15 μL, 0.12 mmol, 1.2 equiv) and **1a** (0.1 mmol, 1.0 equiv) were sequentially added under Ar atmosphere. The tube was sealed with a Teflon-lined cap, and the mixture was stirred at 10 ℃ for three days. After the reaction was completed, the mixture was concentrated. Then the residue was purified by silica gel chromatography with petroleumether and ethylacetate (PE/EA = 5:1) to afford the product.

2. Procedure of competition experiments:

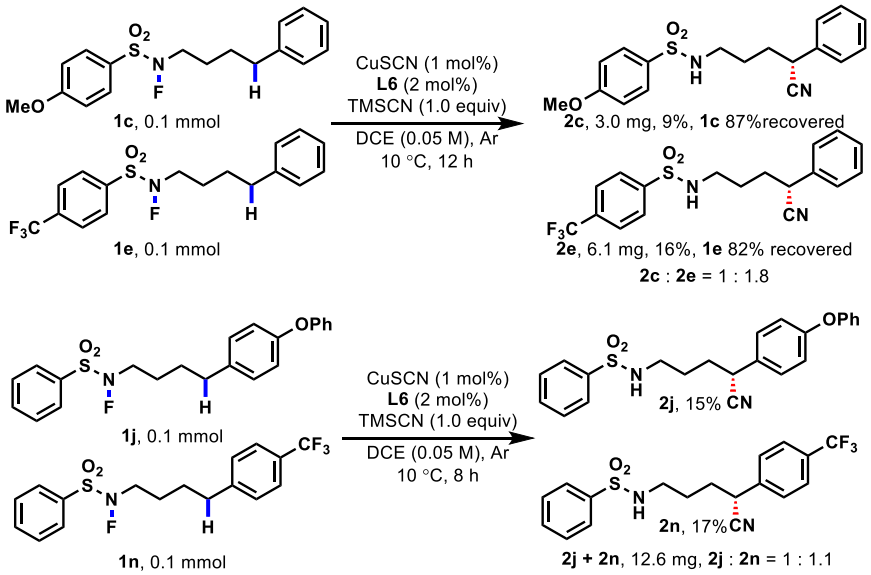

Scheme S2. Competitive experiments, related to **Scheme 2**.

To a sealed tube, **solution A** (2.0 mL), TMSCN (9.9 mg, 12.5 μL, 0.10 mmol, 1.0 equiv), **1c** (0.1 mmol, 1.0 equiv) and **1e** (0.1 mmol, 1.0 equiv) were sequentially added under Ar atmosphere. The tube was sealed with a Teflon-lined cap, and the mixture was stirred at 10 ℃ for 12 h. After the reaction was completed, the mixture was concentrated. Then the residue was purified by silica gel chromatography with petroleumether and ethylacetate (PE/EA = 5:1) to afford the product.

To a sealed tube, **solution A** (2.0 mL), TMSCN (9.9 mg, 12.5 μL, 0.10 mmol, 1.0 equiv), **1j** (0.1 mmol, 1.0 equiv) and **1n** (0.1 mmol, 1.0 equiv) were sequentially added under Ar atmosphere. The tube was sealed with a Teflon-lined cap, and the mixture was stirred at 10 ℃ for 8 h. After the reaction was completed, the mixture was concentrated. Then the residue was purified by silica gel chromatography with petroleumether and ethylacetate (PE/EA = 5:1) to afford the product.

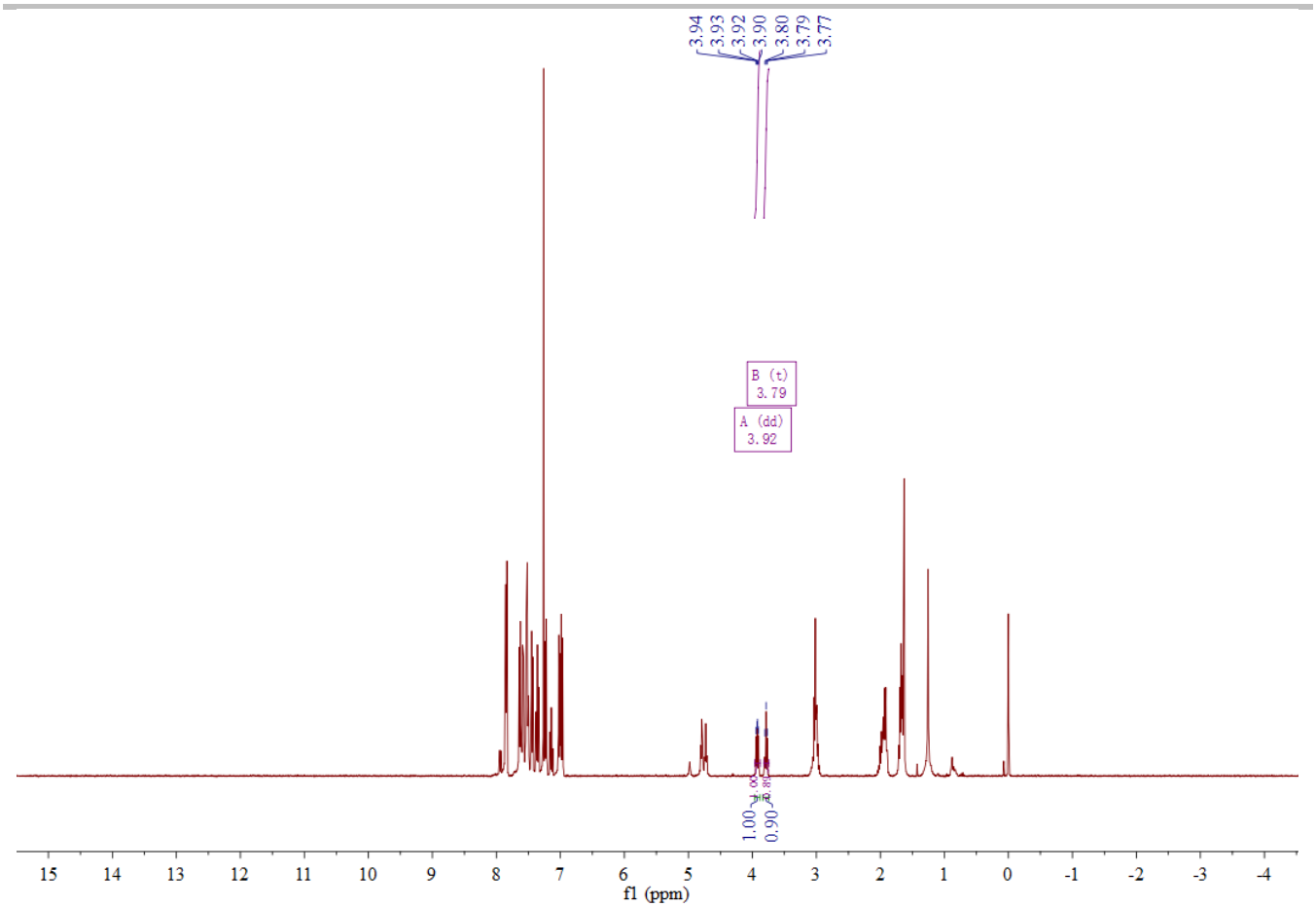

Figure S1. ^{1}H NMR spectrum of the mixture of **2j** and **2n**, related to **Scheme 2**.

3. Procedure of 5-exo cyclization reaction:

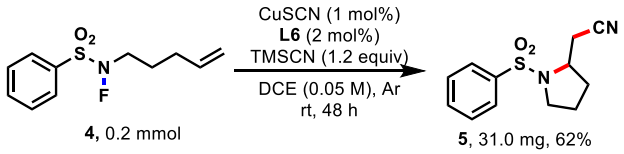

Scheme S3. 5-exo cycliztion reaction, related to **Scheme 2**.

To a sealed tube, **solution A** (4.0 mL), TMSCN (23.8 mg, 30.0 uL, 0.24 mmol, 1.2 equiv), **4** (0.2 mmol, 1.0 equiv) were sequentially added under Ar atmosphere. The tube was sealed with a Teflon-lined cap, and the mixture was stirred at room temperature for two days. After the reaction was completed, the mixture was concentrated. Then the residue was purified by silica gel chromatography with petroleumether and ethylacetate (PE/EA = 5:1) to afford the product.

2-(1-(phenylsulfonyl)pyrrolidin-2-yl)acetonitrile (**5**)

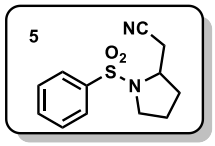

^{1}H NMR (400 MHz, Chloroform-*d*) δ 7.89 – 7.82 (m, 2H), 7.69 – 7.62 (m, 1H), 7.61 – 7.54 (m, 2H), 3.90 – 3.78 (m, 1H), 3.52 (dt, *J* = 10.2, 5.9 Hz, 1H), 3.19 (dt, *J* = 10.1, 7.1 Hz, 1H), 2.90 (dd, *J* = 16.8, 3.6 Hz, 1H), 2.81 (dd, *J* = 16.8, 7.9 Hz, 1H), 2.03 – 1.93 (m, 1H), 1.90 (q, *J* = 7.0 Hz, 2H), 1.66 – 1.58 (m, 1H). ^{13}C NMR (101 MHz, Chloroform-*d*) δ 136.77, 133.34, 129.46, 127.61, 117.52, 56.11, 49.72, 31.37, 25.40, 24.02. HRMS (ESI) (*m/z*): $[M+Na]^+$ calcd. for $C_{12}H_{14}N_2O_2SNa$: 273.0674, found: 273.0675.

4. Procedure of radical clock experiment:

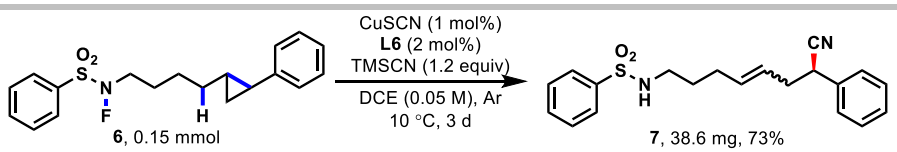

Scheme S4. Radical clock experiment, related to **Scheme 2**.

To a sealed tube **solution A** (3.0 mL), TMSCN (17.9 mg, 22.5 μL, 0.18 mmol, 1.2 equiv) and **6** (0.15 mmol, 1.0 equiv) were sequentially added under Ar atmosphere. The tube was sealed with a Teflon-lined cap, and the mixture was stirred at 10 ℃ for three days. After the reaction was completed, the mixture was concentrated. Then the residue was purified by silica gel chromatography with petroleumether and ethylacetate (PE/EA = 5:1) to afford the product.

(R)-N-(7-cyano-7-phenylhept-4-en-1-yl)benzenesulfonamide (**7**)

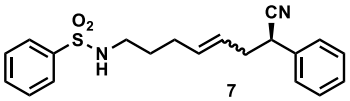

^{1}H NMR (400 MHz, Chloroform-*d*) δ 7.92 – 7.82 (m, 2H), 7.63 – 7.56 (m, 1H), 7.56 – 7.49 (m, 2H), 7.40 – 7.28 (m, 5H), 5.55 – 5.32 (m, 2H), 4.59 (s, 1H), 3.80 (t, *J* = 7.2 Hz, 1H), 3.01 – 2.84 (m, 2H), 2.53 (t, *J* = 6.9 Hz, 2H), 2.03 (q, *J* = 6.6 Hz, 2H), 1.59 – 1.45 (m, 2H). ^{13}C NMR (101 MHz, Chloroform-*d*) δ 140.08, 135.37, 134.10, 132.74, 129.25, 129.16, 128.23, 127.42, 127.14, 125.56, 120.59, 42.54, 38.93, 38.10, 29.35, 29.10. HRMS (ESI) (*m/z*): $[M+Na]^+$ calcd. for $C_{20}H_{22}N_2O_2SNa$: 377.1300, found: 377.1304.

References:

Wang, D., Wu, L., Wang, F., Wan, X., Chen, P., Lin, Z., Liu, G. Asymmetric copper-catalyzed intermolecular aminoarylation of styrenes: efficient access to optical 2,2-diarylethylamines. *J. Am. Chem. Soc.* **139**, 6811-6814 (2017).
Zhang, Z., Stateman, L. M., Nagib, D. A. δ C–H (hetero)arylation *via* Cu-catalyzed radical relay. *Chem. Sci*. **10**, 1207-1211 (2019).

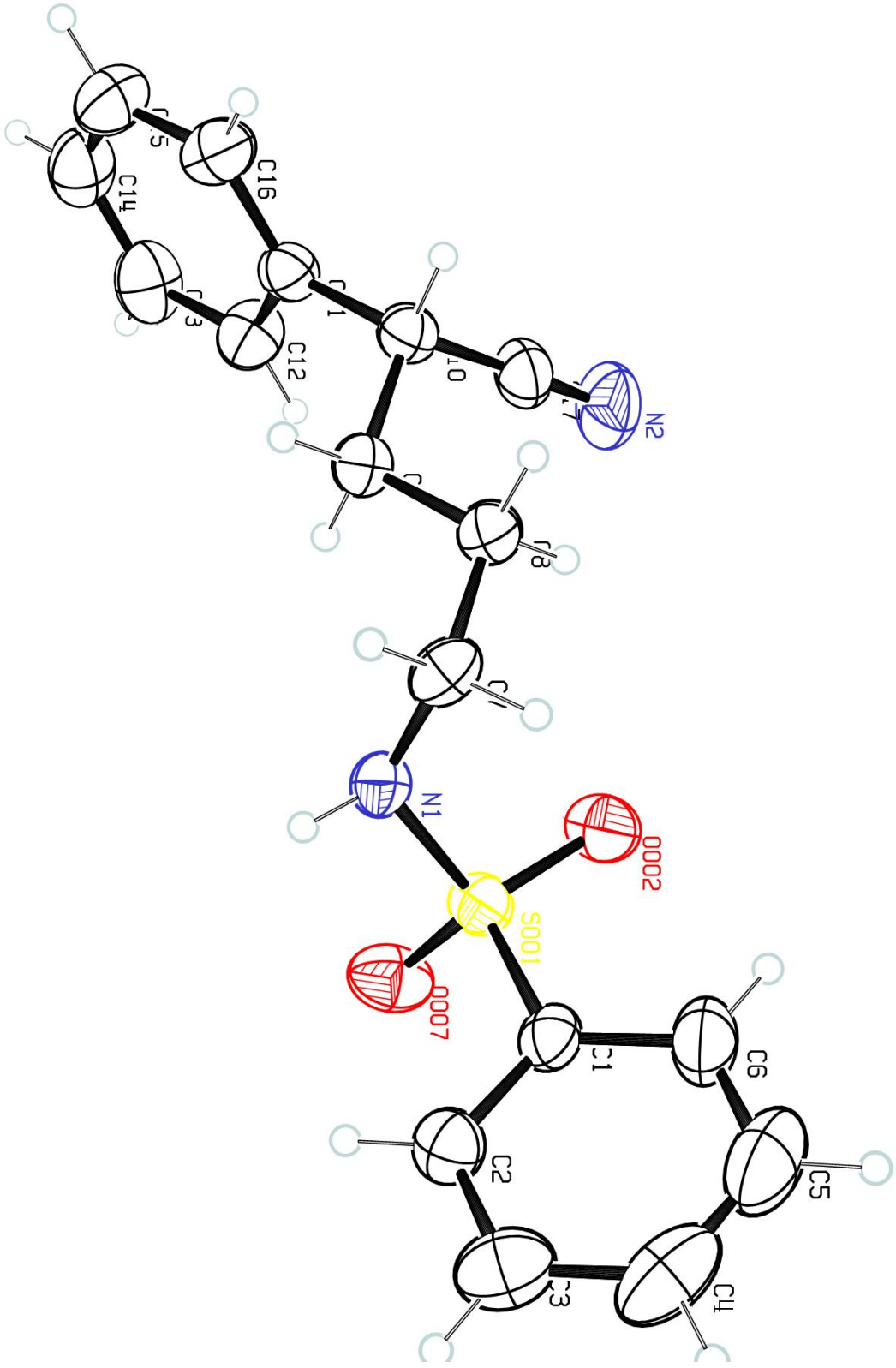

Figure S2. X-Ray crystal data of **2a**, related to **Figure 2**

Table 9 Crystal data and structure refinement for **2a**, related to **Figure 2.**

Identification code	2a
Empirical formula	$C_{17}H_{18}N_2O_2S$
Formula weight	314.39
Temperature/K	293(2)

Crystal system	orthorhombic
Space group	$P2_12_12_1$
a/Å	8.93873(10)
b/Å	10.13670(8)
c/Å	18.31766(18)
α/°	90
β/°	90
γ/°	90
Volume/Å^3	1659.75(3)
Z	4
ρ_{calc}g/cm^3	1.258
μ/mm^{-1}	1.799
F(000)	664.0
Crystal size/mm^3	0.3 × 0.3 × 0.2
Radiation	CuKα (λ = 1.54184)
2Θ range for data collection/°	9.656 to 147.836
Index ranges	$-10 \leq h \leq 11$, $-12 \leq k \leq 12$, $-22 \leq l \leq 22$
Reflections collected	15923
Independent reflections	3313 [R_{int} = 0.0252, R_{sigma} = 0.0146]
Data/restraints/parameters	3313/0/199
Goodness-of-fit on F^2	1.114
Final R indexes [I>=2σ (I)]	R_1 = 0.0344, wR_2 = 0.1209
Final R indexes [all data]	R_1 = 0.0353, wR_2 = 0.1236
Largest diff. peak/hole / e Å^{-3}	0.16/-0.37
Flack parameter	0.009(6)

Table 10 Fractional Atomic Coordinates (×10^4) and Equivalent Isotropic Displacement Parameters (Å^2×10^3) for **2a**. U_{eq} is defined as 1/3 of of the trace of the orthogonalised U_{IJ} tensor, related to **Figure 2**.

Atom	***x***	***y***	***z***	**U(eq)**
S001	-4627.8(6)	-1386.4(5)	-2339.6(3)	56.6(2)
O002	-5617(2)	-262.1(18)	-2362.4(14)	79.9(6)
N1	-5654(2)	-2680.6(18)	-2370.3(11)	58.0(4)
C1	-3707(3)	-1337(2)	-1493.1(12)	55.2(5)
C11	-10477(3)	-3162(2)	-4098.7(12)	57.0(5)
C9	-8704(3)	-2991(2)	-3008.3(12)	57.1(5)
O007	-3511(2)	-1512(3)	-2887.8(11)	81.3(6)
C8	-8381(3)	-2306(2)	-2287.6(13)	58.8(5)
C10	-10138(3)	-2483(2)	-3377.4(13)	56.4(5)
C7	-6986(3)	-2815(2)	-1913.9(12)	61.0(6)
C13	-10029(5)	-3464(4)	-5380.9(16)	90.5(10)
C17	-10031(3)	-1046(3)	-3478.7(14)	69.4(7)
N2	-9918(4)	56(2)	-3550.9(19)	99.5(10)
C3	-1792(5)	-2174(4)	-713.5(17)	88.3(9)
C12	-9728(4)	-2818(3)	-4727.1(15)	75.3(7)
C16	-11516(4)	-4156(3)	-4122.9(17)	76.3(7)

C14	-11085(5)	-4438(4)	-5405(2)	93.1(11)
C6	-4100(5)	-399(3)	-981.7(19)	86.1(9)
C15	-11810(5)	-4799(4)	-4778(3)	97.9(11)
C4	-2195(6)	-1232(5)	-197.1(18)	105.2(15)
C2	-2563(3)	-2237(3)	-1365.9(14)	66.9(6)
C5	-3307(6)	-360(5)	-330(2)	112.7(15)

Table 11 Anisotropic Displacement Parameters ($Å^2 \times 10^3$) for **2a**. The Anisotropic displacement factor exponent takes the form: $-2\pi^2[h^2a^{*2}U_{11}+2hka^*b^*U_{12}+\ldots]$, related to **Figure 2**.

Atom	U_{11}	U_{22}	U_{33}	U_{23}	U_{13}	U_{12}
S001	52.1(3)	48.7(3)	69.0(3)	5.9(2)	2.7(2)	-1.6(2)
O002	65.7(10)	41.6(7)	132.5(16)	15.8(9)	-5.7(12)	-0.9(8)
N1	56.9(10)	43.1(8)	73.9(10)	-4.1(7)	-4.9(9)	1.4(7)
C1	56.8(11)	47.4(9)	61.5(10)	-4.8(8)	5.8(9)	-10.2(9)
C11	52.4(12)	55.8(10)	62.9(11)	2.5(8)	-3.4(10)	4.2(9)
C9	56.4(12)	50.6(10)	64.1(11)	-2.5(8)	-0.4(9)	0.5(9)
O007	63.2(12)	115.2(17)	65.4(9)	11.1(9)	6.7(8)	-2.9(12)
C8	55.0(12)	58.4(11)	63.1(11)	-7.0(9)	4.2(10)	-4.4(9)
C10	51.0(12)	55.5(11)	62.6(11)	-0.6(8)	5.6(9)	-0.2(9)
C7	70.2(14)	53.4(11)	59.4(11)	3.7(9)	-7.1(10)	-14.6(10)
C13	115(3)	95(2)	62.1(13)	-3.2(13)	0.7(15)	16(2)
C17	72.8(18)	57.8(12)	77.5(13)	-5.8(11)	-0.3(13)	12.8(11)
N2	124(3)	55.3(13)	119(2)	-4.7(13)	-6(2)	15.6(14)
C3	89(2)	99(2)	77.7(16)	18.6(16)	-16.1(16)	-15.0(19)
C12	85.6(19)	73.2(15)	67.2(13)	0.1(11)	5.2(13)	-9.2(15)
C16	70.8(16)	73.7(15)	84.6(16)	2.8(13)	-8.4(15)	-10.9(14)
C14	104(3)	93(2)	82.4(19)	-21.7(16)	-29.7(19)	17.6(19)
C6	92(2)	75.6(16)	90.9(18)	-27.5(15)	18.0(17)	-3.8(16)
C15	87(2)	91(2)	115(3)	-22(2)	-22(2)	-12(2)
C4	139(4)	112(3)	63.8(14)	1.5(17)	-14.2(19)	-52(3)
C2	72.2(15)	63.1(12)	65.5(12)	1.4(11)	-1.4(11)	0.9(12)
C5	140(4)	117(3)	81(2)	-38(2)	14(3)	-25(3)

Table 12 Bond Lengths for **2a**, related to **Figure 2**.

Atom	Atom	Length/Å	Atom	Atom	Length/Å
S001	O002	1.4433(19)	C8	C7	1.513(3)
S001	N1	1.6016(19)	C10	C17	1.472(3)
S001	C1	1.756(2)	C13	C12	1.391(4)
S001	O007	1.421(2)	C13	C14	1.366(6)
N1	C7	1.461(3)	C17	N2	1.129(4)
C1	C6	1.381(3)	C3	C4	1.391(6)
C1	C2	1.390(4)	C3	C2	1.381(4)
C11	C10	1.520(3)	C16	C15	1.390(5)

C11	C12	1.376(4)	C14	C15	1.370(7)
C11	C16	1.371(4)	C6	C5	1.389(6)
C9	C8	1.519(3)	C4	C5	1.353(7)
C9	C10	1.538(3)			

Table 13 Bond Angles for **2a**, related to **Figure 2.**

Atom	**Atom**	**Atom**	**Angle/°**	**Atom**	**Atom**	**Atom**	**Angle/°**
O002	S001	N1	107.14(11)	C11	C10	C9	113.37(19)
O002	S001	C1	106.89(13)	C17	C10	C11	110.6(2)
N1	S001	C1	108.82(10)	C17	C10	C9	109.4(2)
O007	S001	O002	118.72(14)	N1	C7	C8	112.40(18)
O007	S001	N1	107.70(13)	C14	C13	C12	120.1(3)
O007	S001	C1	107.29(12)	N2	C17	C10	178.5(4)
C7	N1	S001	121.51(16)	C2	C3	C4	119.4(4)
C6	C1	S001	120.0(2)	C11	C12	C13	120.5(3)
C6	C1	C2	121.7(3)	C11	C16	C15	120.1(3)
C2	C1	S001	118.31(18)	C13	C14	C15	119.5(3)
C12	C11	C10	121.1(2)	C1	C6	C5	118.2(4)
C16	C11	C10	119.7(2)	C14	C15	C16	120.6(4)
C16	C11	C12	119.2(3)	C5	C4	C3	121.1(3)
C8	C9	C10	112.8(2)	C3	C2	C1	118.8(3)
C7	C8	C9	113.2(2)	C4	C5	C6	120.7(4)

Table 14 Hydrogen Atom Coordinates ($Å \times 10^4$) and Isotropic Displacement Parameters ($Å^2 \times 10^3$) for **2a**, related to **Figure 2**.

Atom	***x***	***y***	***z***	**U(eq)**
H1	-5108.69	-3377.48	-2339.08	70
H9A	-8800.19	-3931.39	-2922.99	68
H9B	-7865.15	-2856.69	-3335.77	68
H8A	-8269.39	-1367.14	-2375.01	71
H8B	-9228.68	-2426.65	-1964.05	71
H10	-10976.48	-2656.57	-3046.07	68
H7A	-6835.46	-2331.35	-1462.77	73
H7B	-7125.64	-3737.04	-1790.83	73
H13	-9510.61	-3233.46	-5802.07	109
H3	-1011.25	-2756.37	-620.13	106
H12	-9016.6	-2149.67	-4714.63	90
H16	-12024.14	-4400.07	-3701.04	92
H14	-11309.5	-4851.88	-5844.58	112
H6	-4874.57	191.83	-1071.3	103
H15	-12506.2	-5480.93	-4789.51	117
H4	-1690.14	-1201.77	246.64	126
H2	-2321.38	-2870.68	-1713.79	80
H5	-3544.5	272.51	19.35	135

NMR Spectra of New Compounds (^{1}H NMR, ^{19}F NMR, ^{13}C NMR)

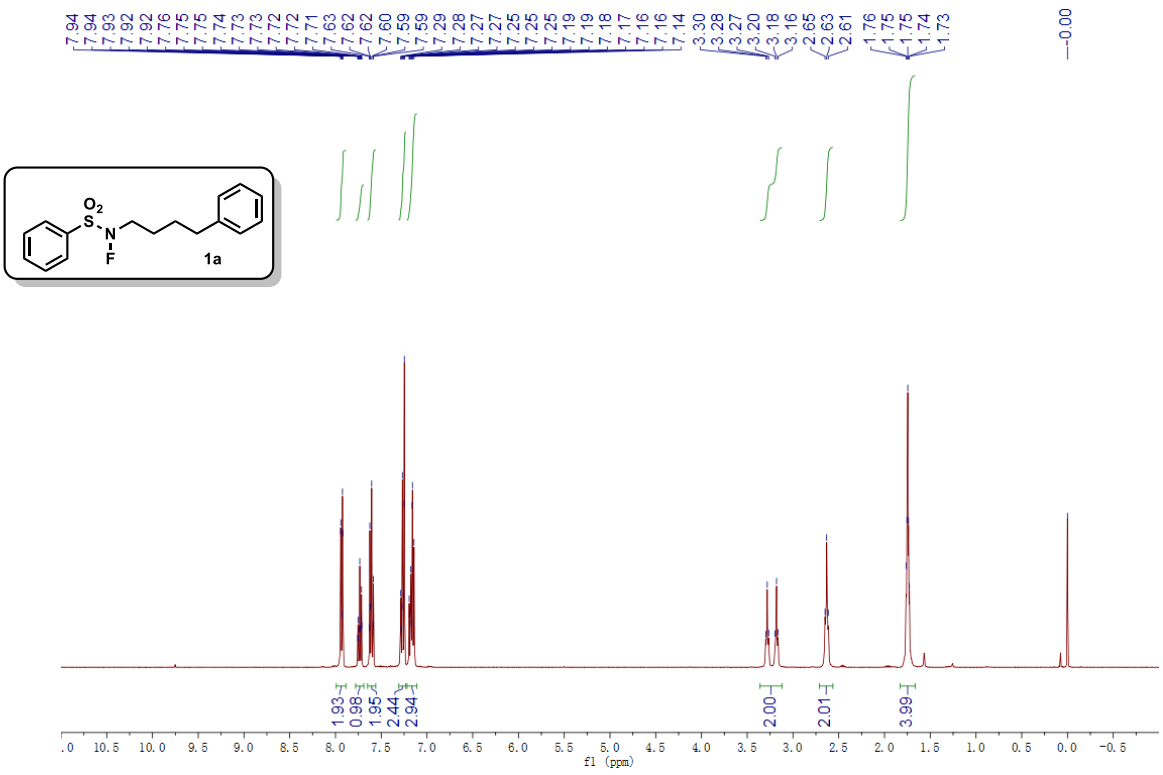

Figure S3. ^{1}H NMR of **1a**, related to Figure 2.

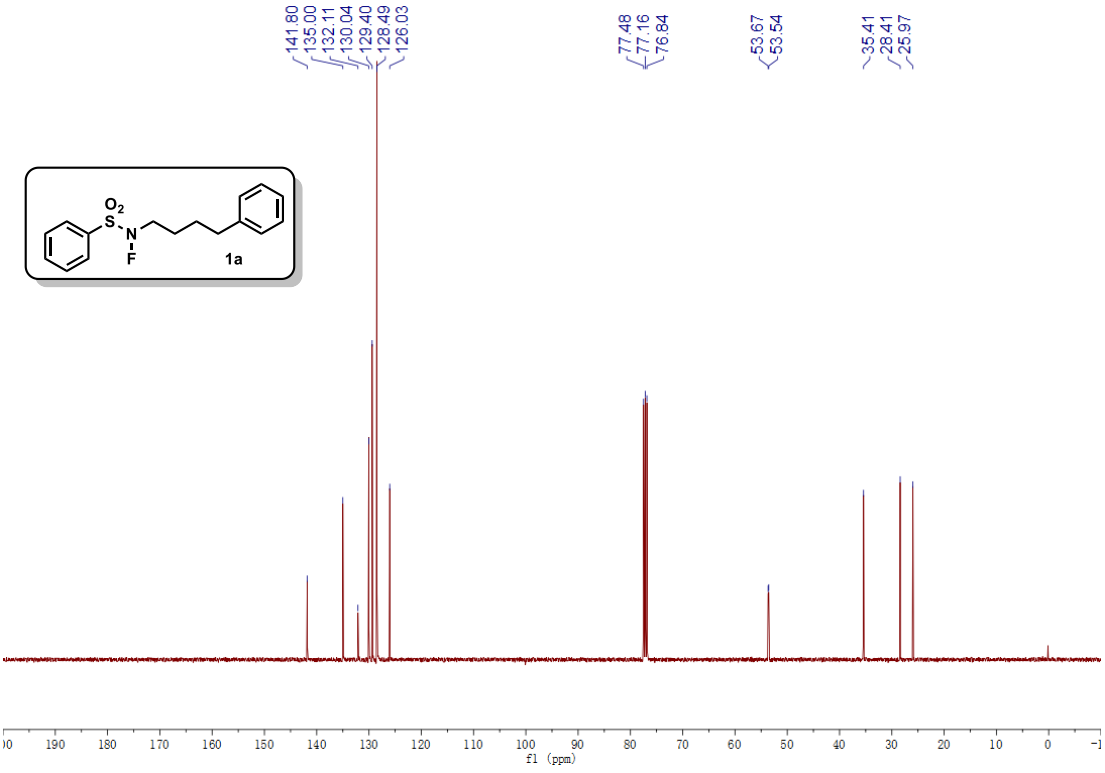

Figure S4. ^{13}C NMR of **1a**, related to Figure 2.

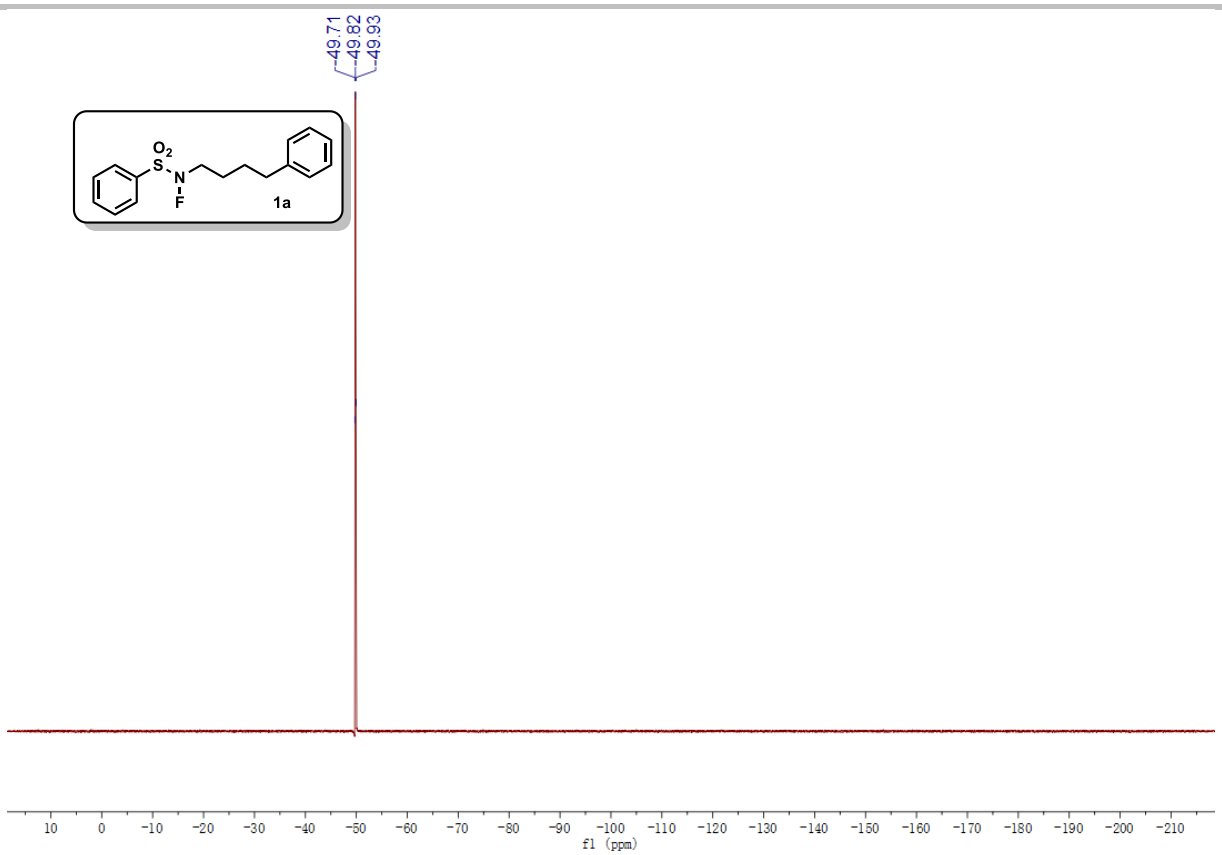

Figure S5. ^{19}F NMR of **1a**, related to Figure 2.

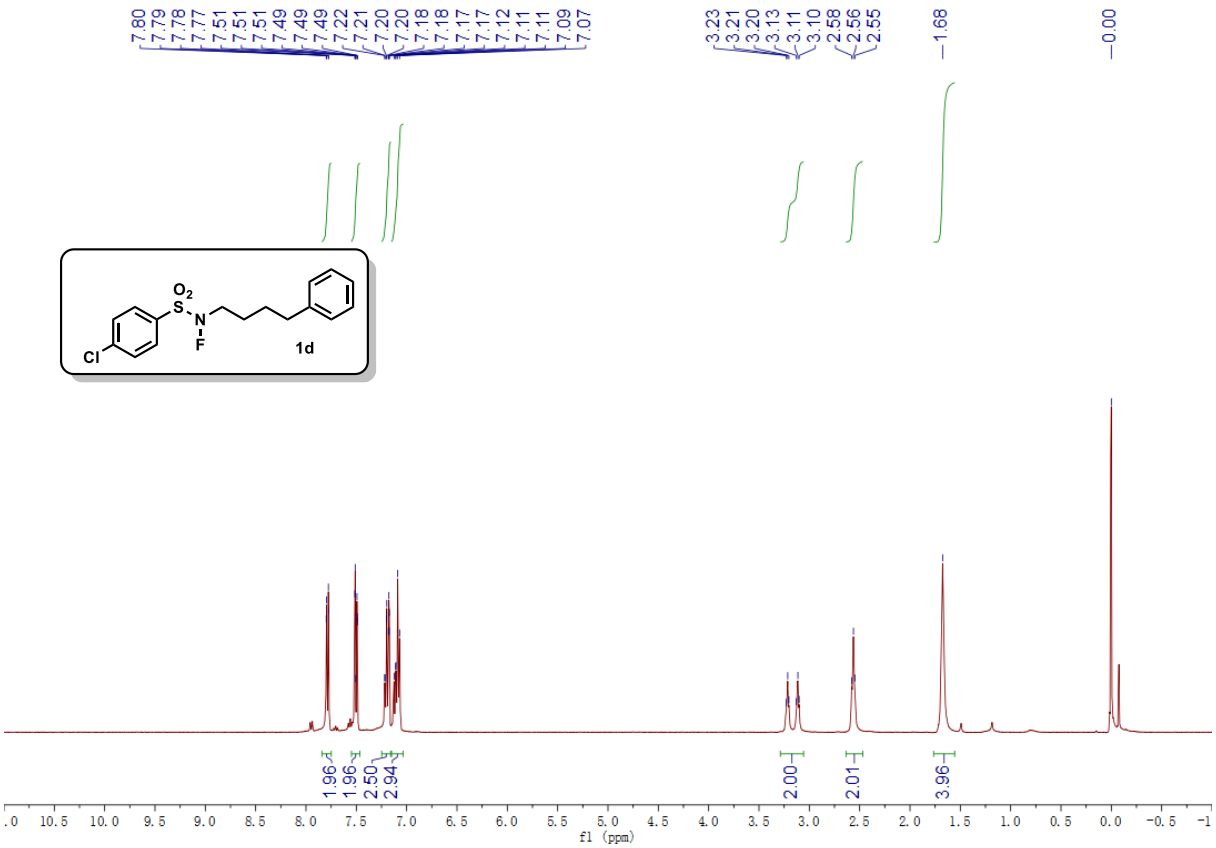

Figure S6. ^{1}H NMR of **1d**, related to Figure 2.

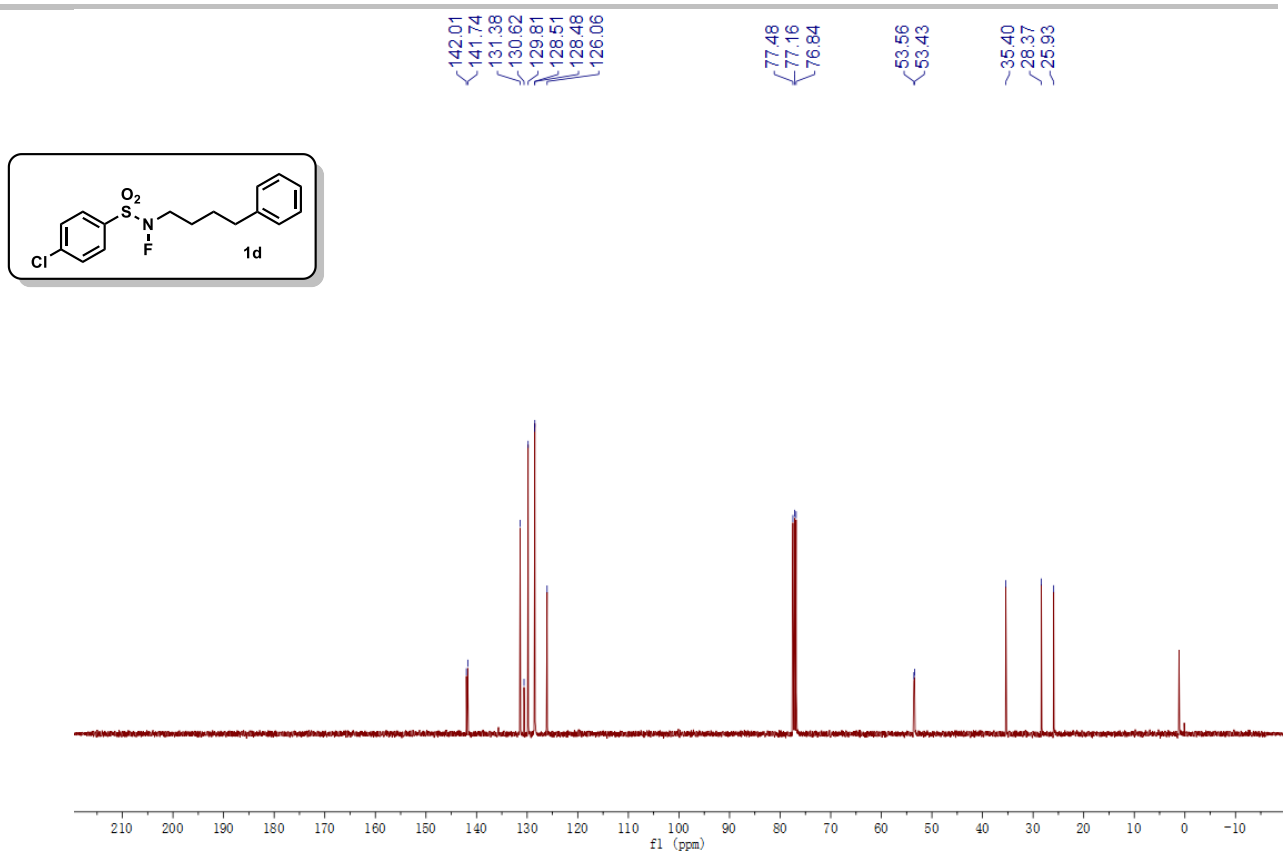

Figure S7. ^{13}C NMR of **1d**, related to Figure 2.

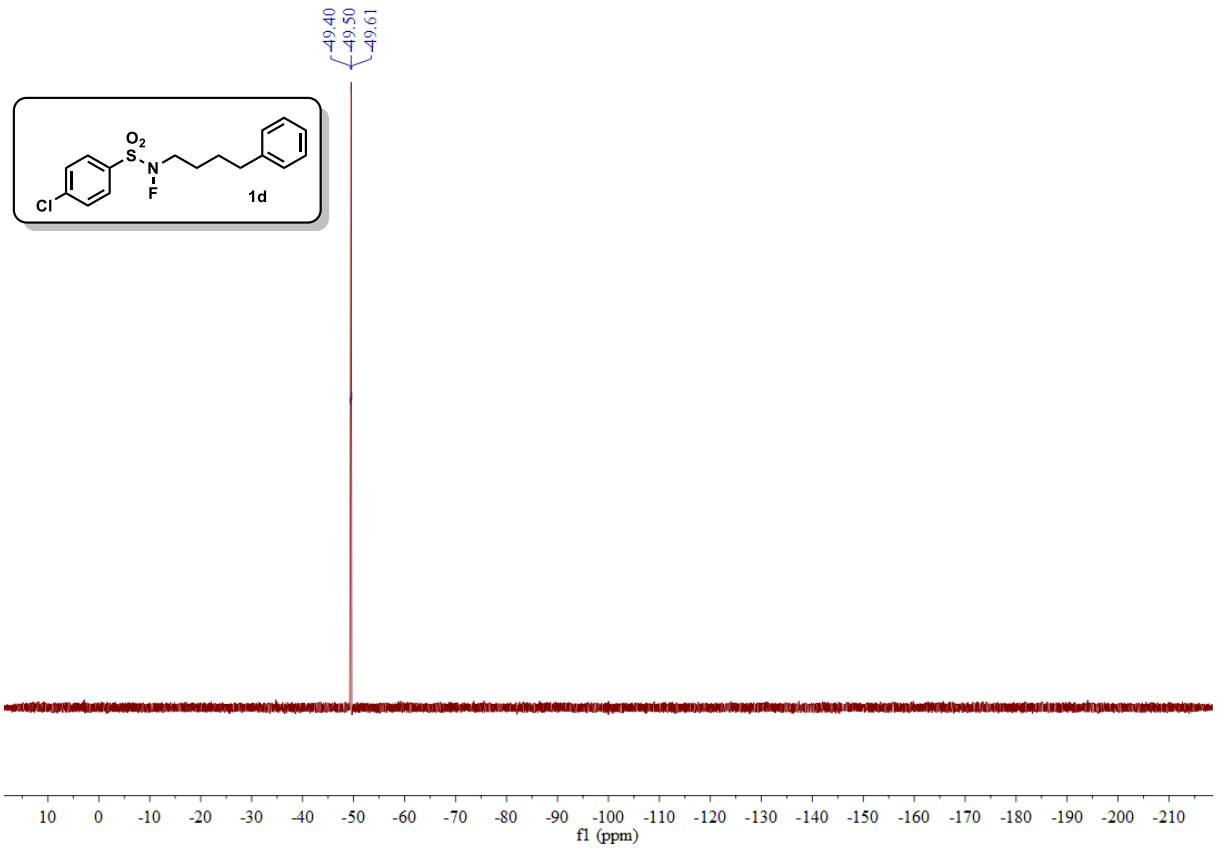

Figure S8. ^{19}F NMR of **1d**, related to Figure 2.

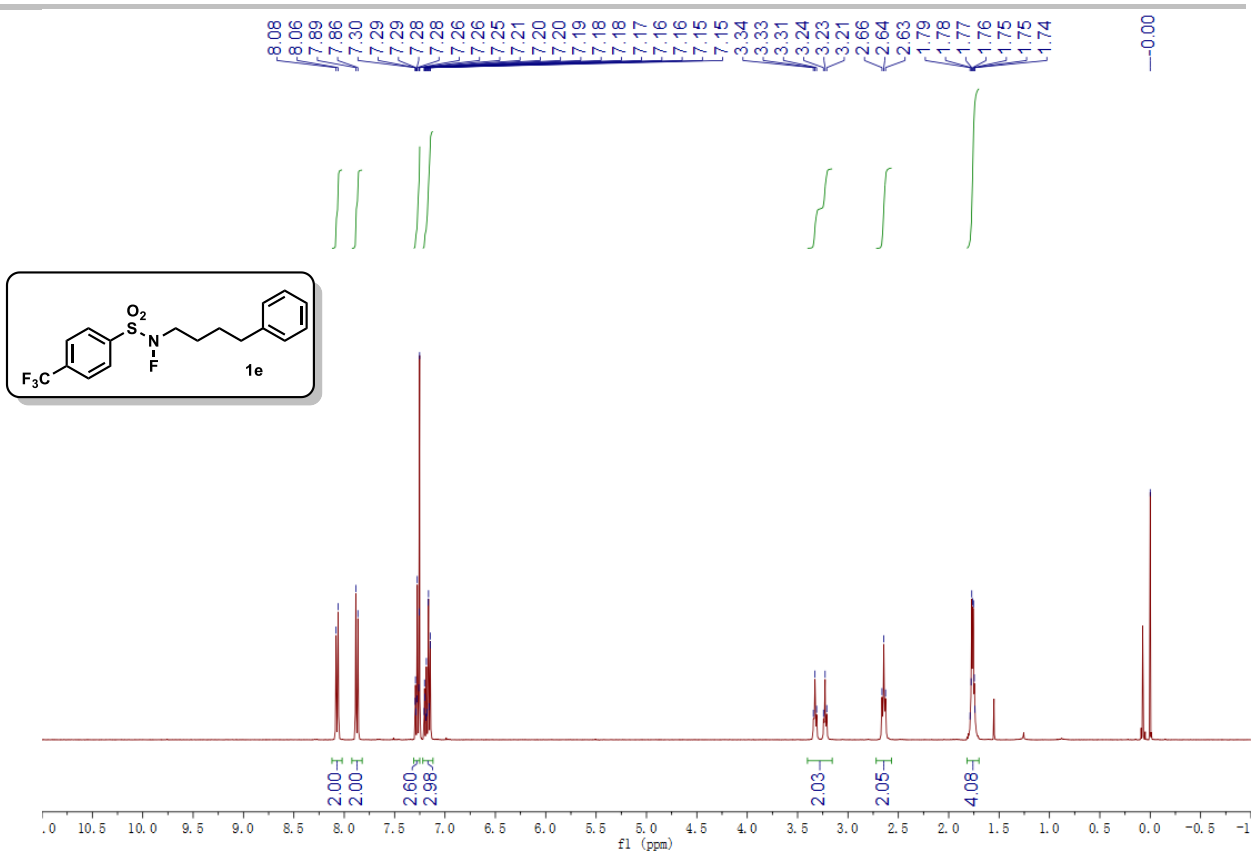

Figure S9. ^{1}H NMR of **1e**, related to Figure 2.

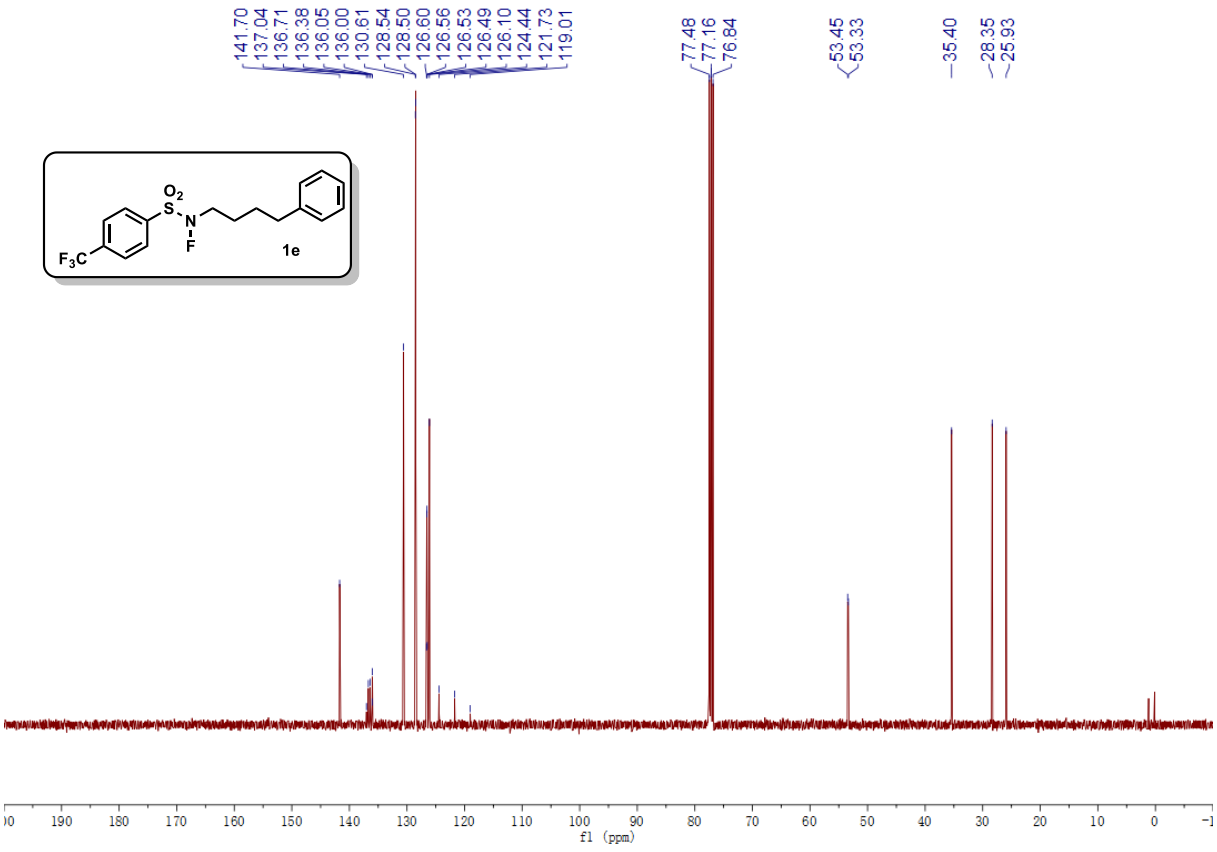

Figure S10. ^{13}C NMR of **1e**, related to Figure 2.

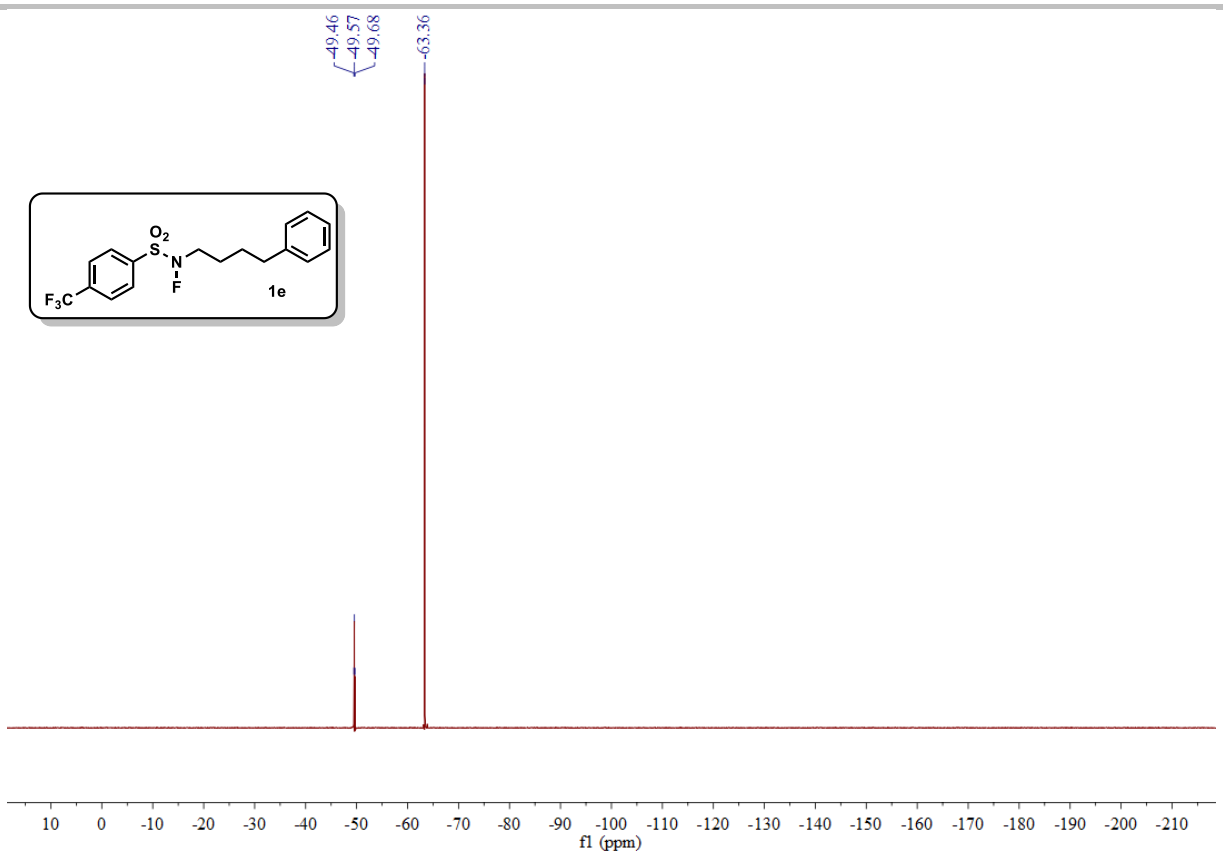

Figure S11. ^{19}F NMR of **1e**, related to Figure 2.

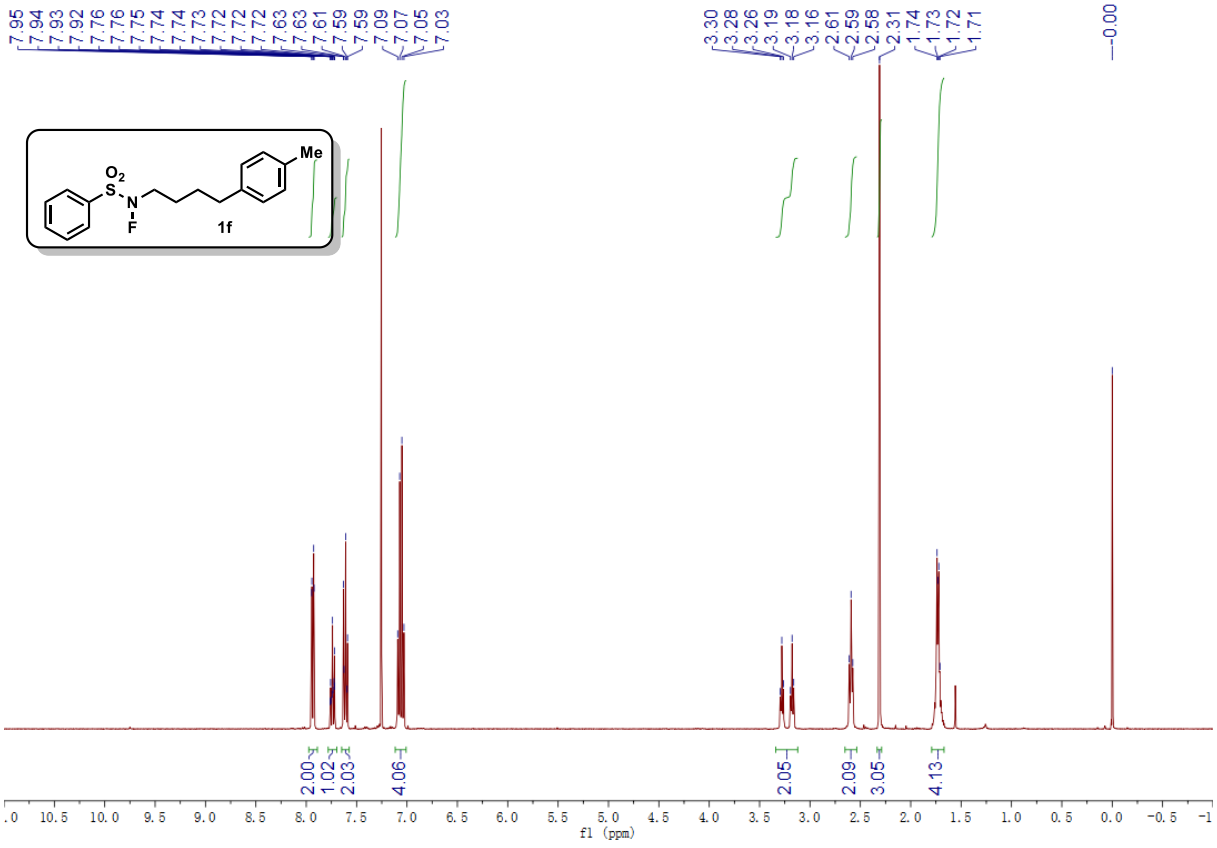

Figure S12. ^{1}H NMR of **1f**, related to Figure 2.

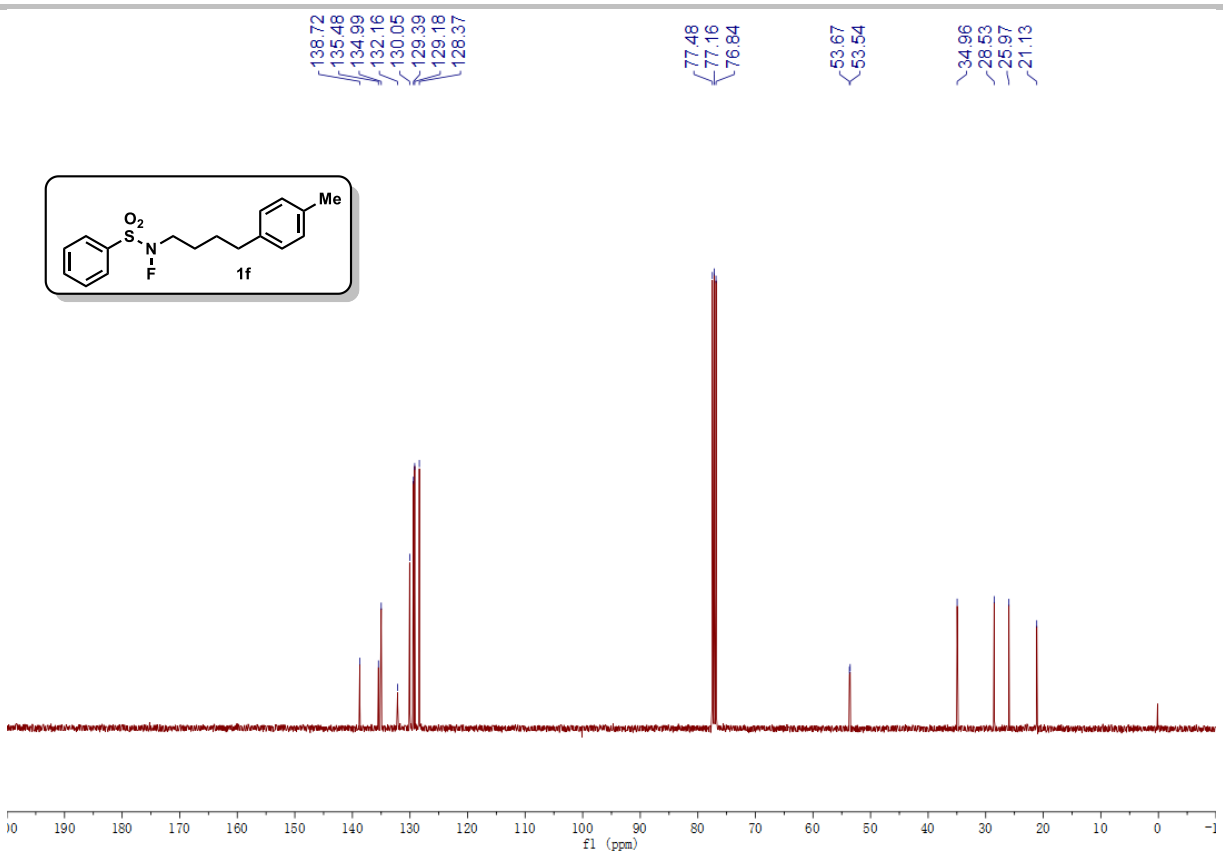

Figure S13. ^{13}C NMR of **1f**, related to Figure 2.

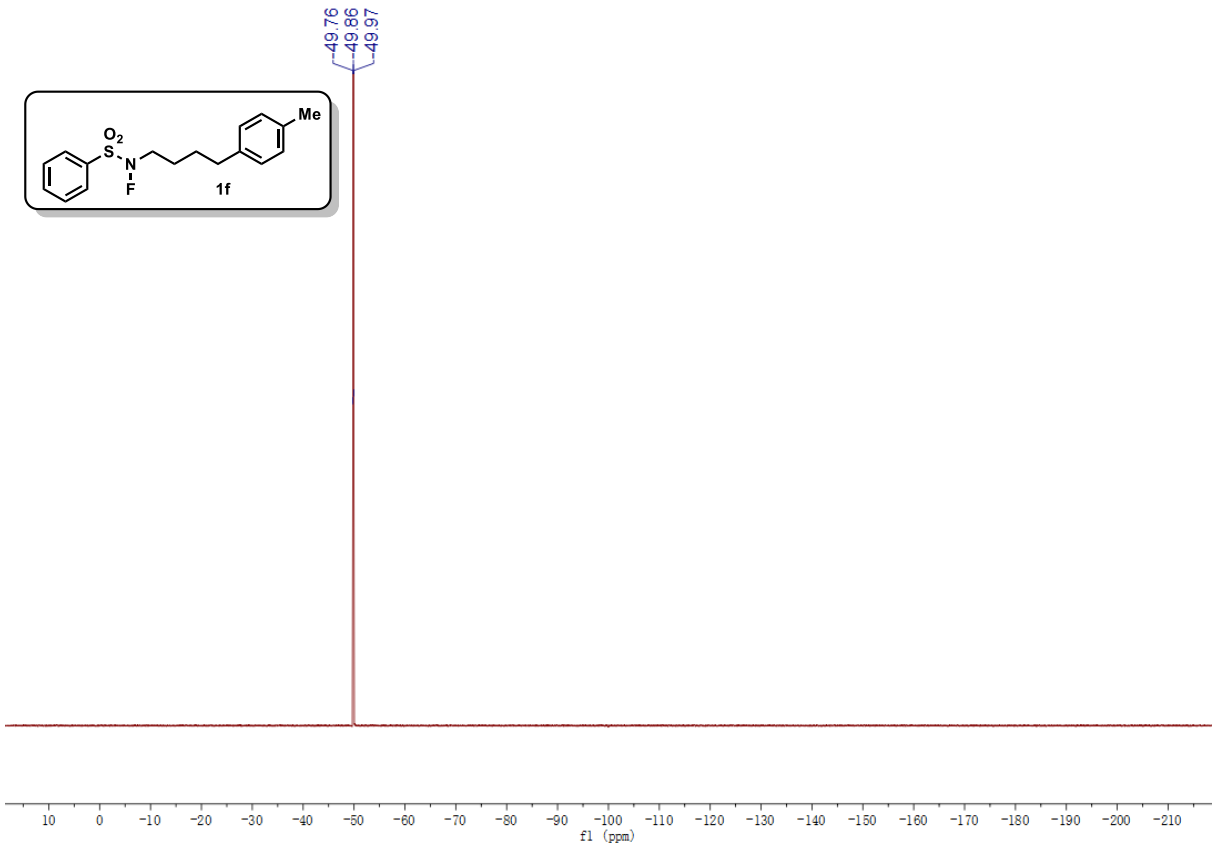

Figure S14. ^{19}F NMR of **1f**, related to Figure 2.

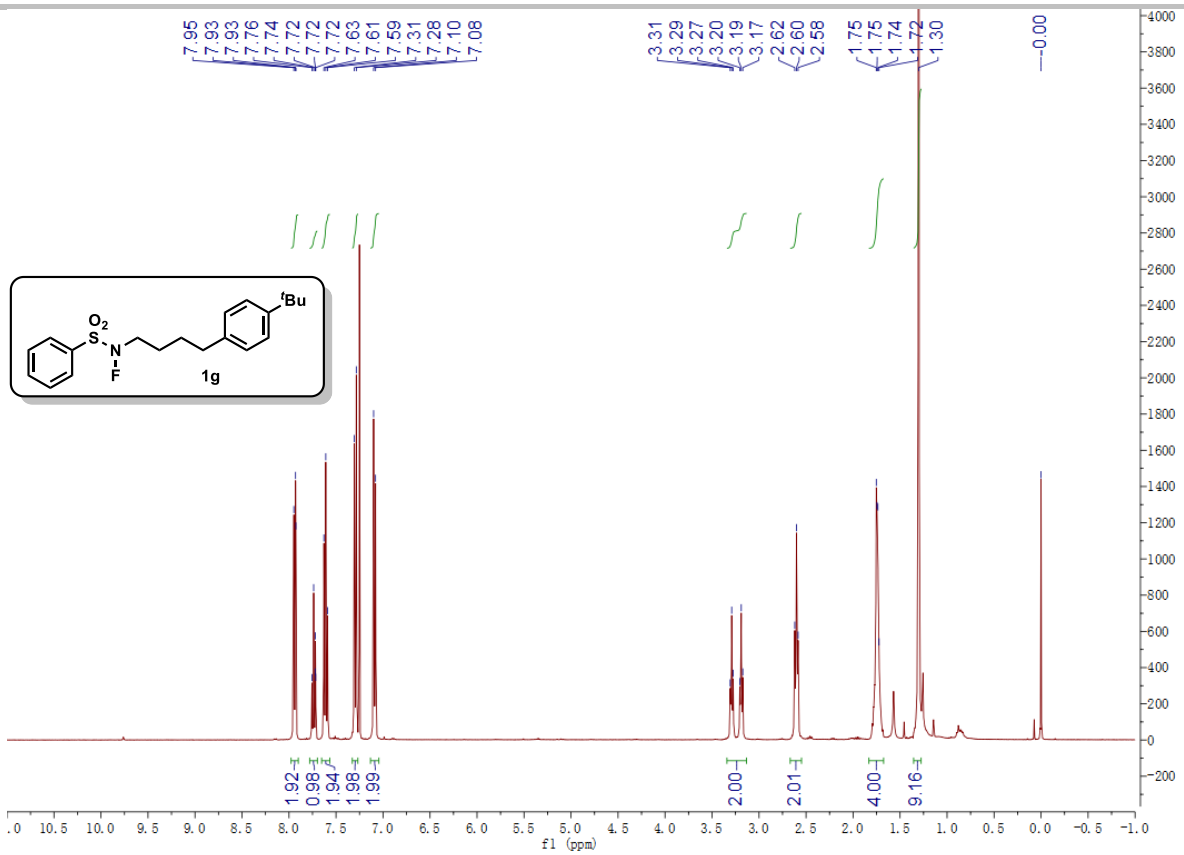

Figure S15. ^{1}H NMR of **1g**, related to Figure 2.

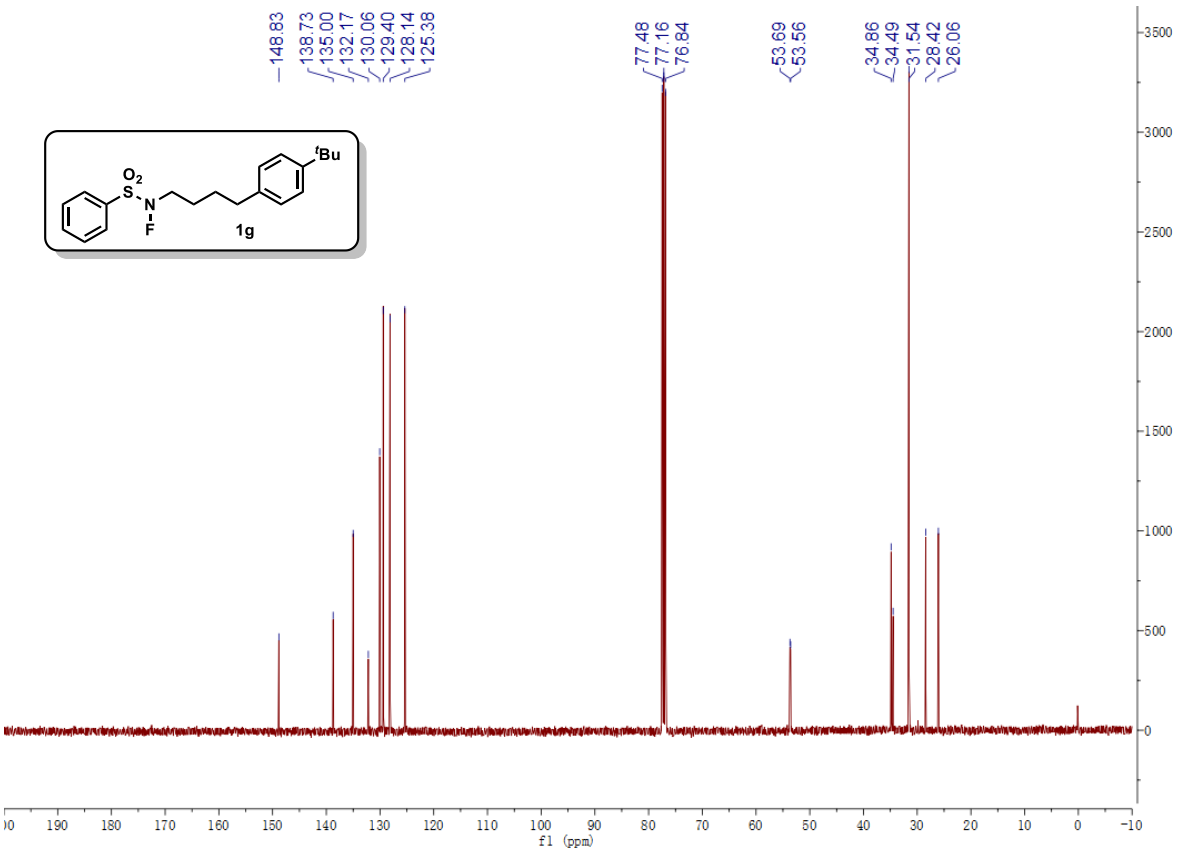

Figure S16. ^{13}C NMR of **1g**, related to Figure 2.

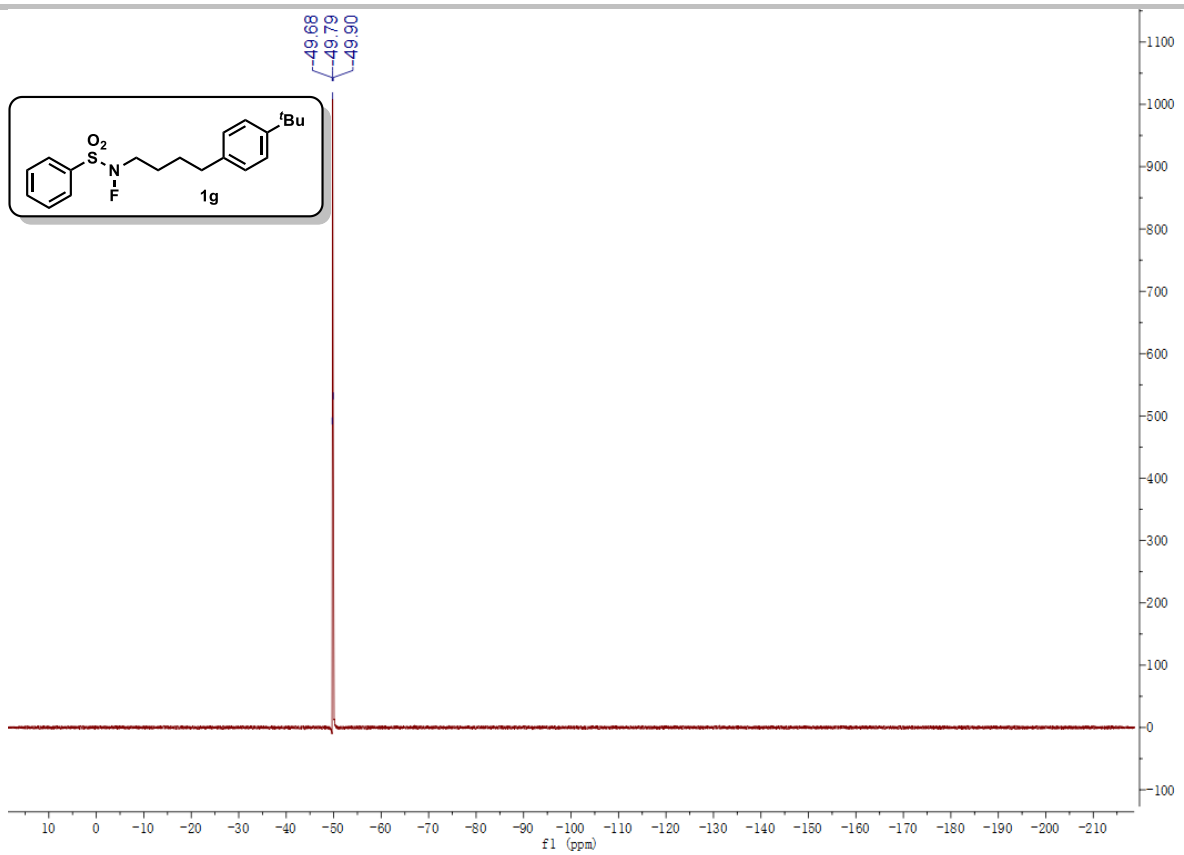

Figure S17. ^{19}C NMR of **1g**, related to Figure 2.

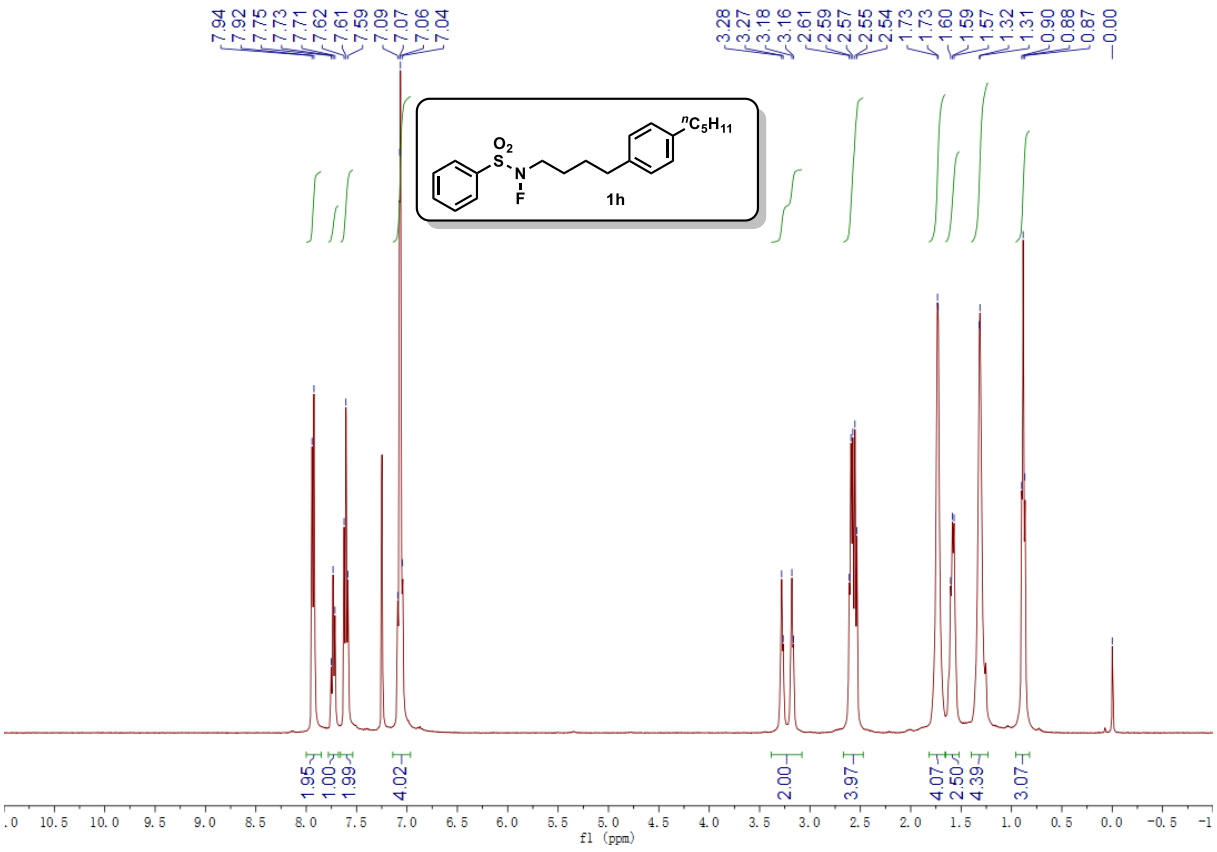

Figure S18. ^{1}H NMR of **1h**, related to Figure 2.

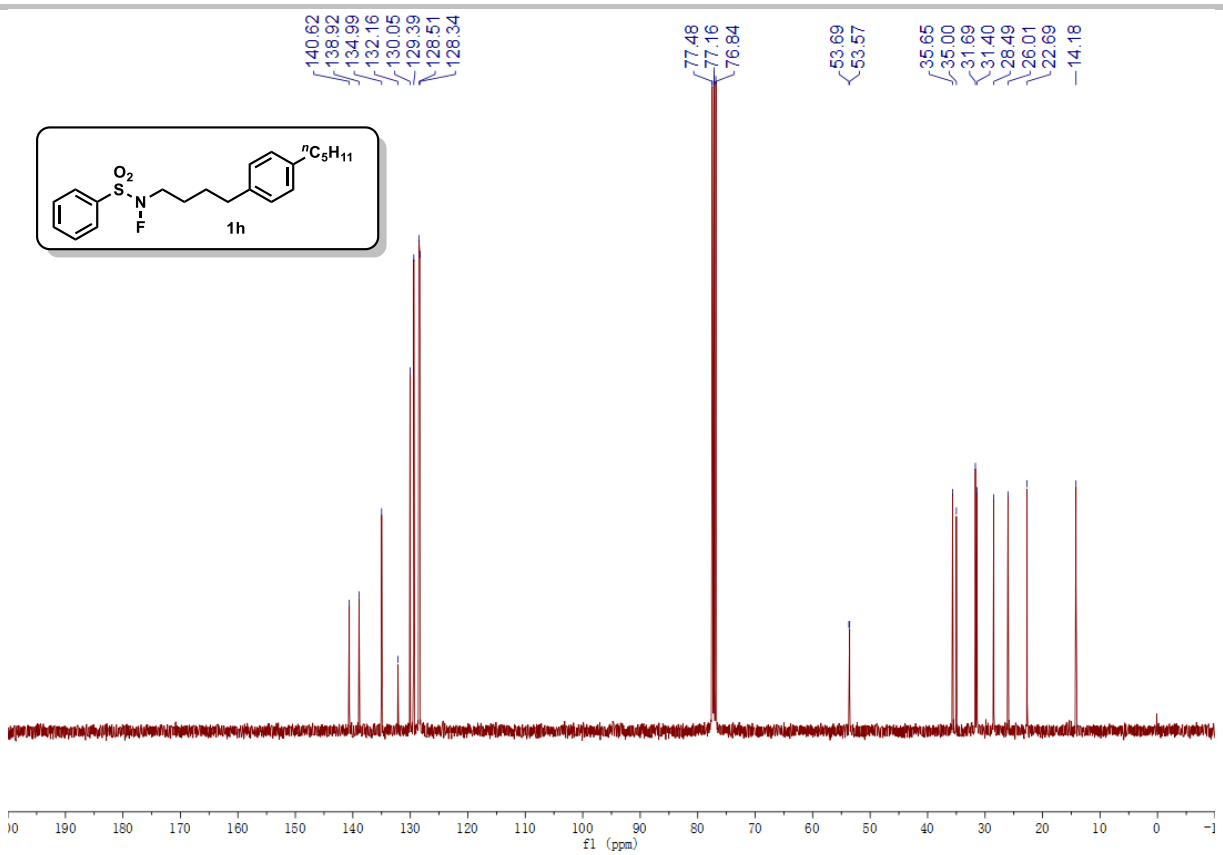

Figure S19. ^{13}C NMR of **1h**, related to Figure 2.

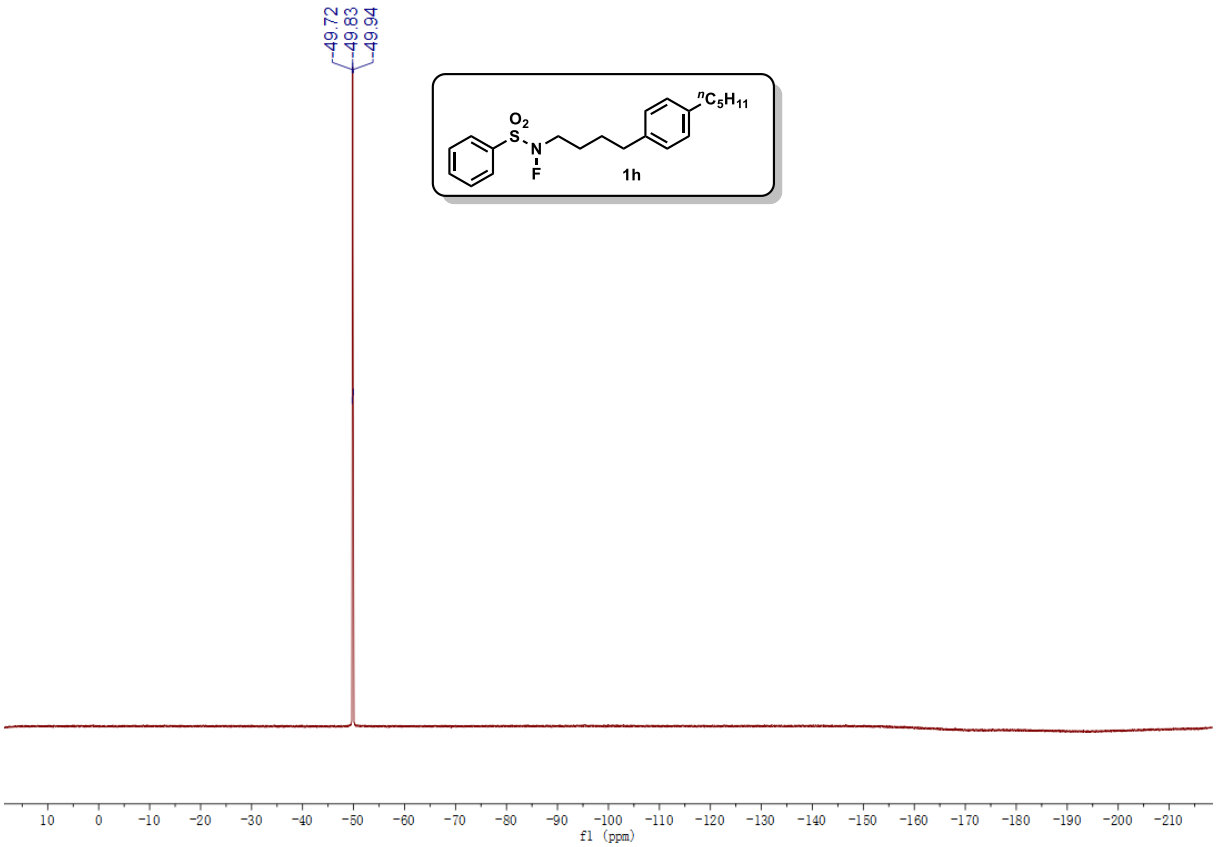

Figure S20. ^{19}H NMR of **1h**, related to Figure 2.

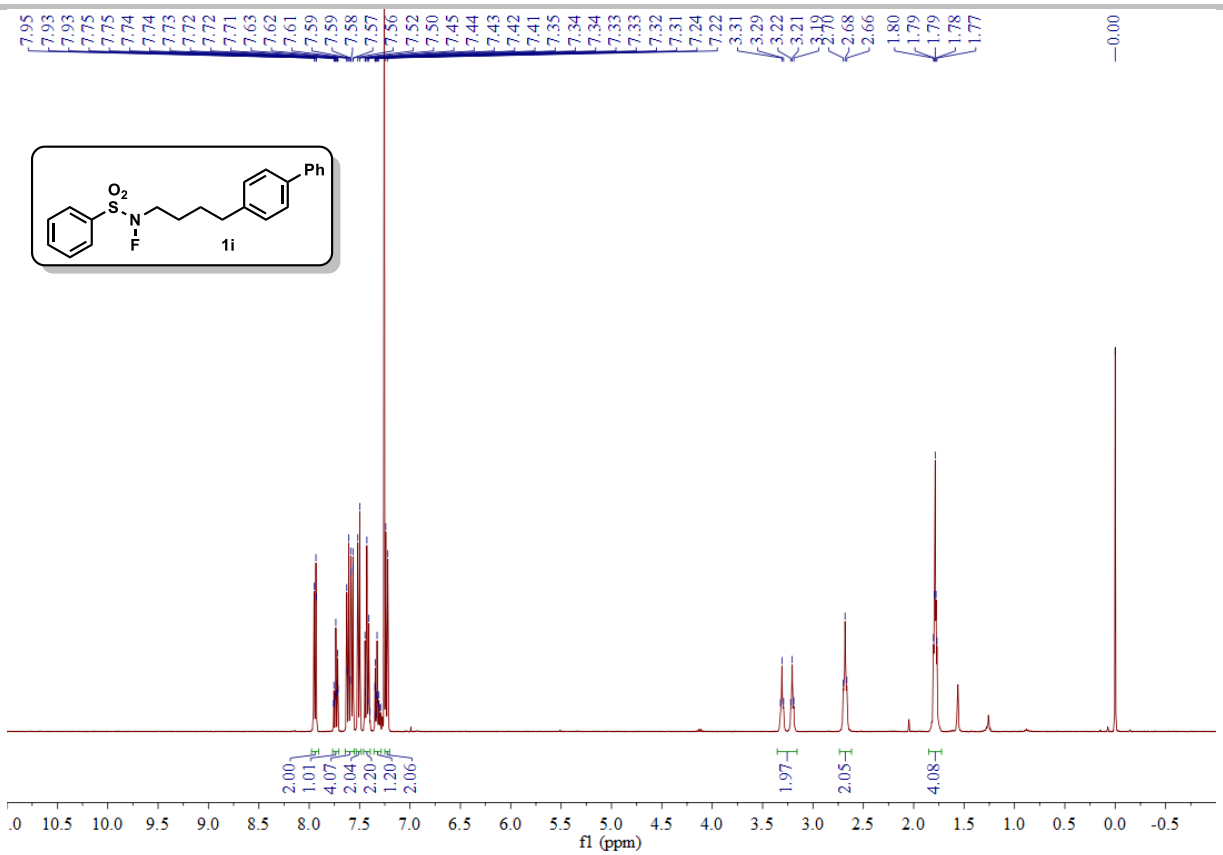

Figure S21. ^{1}H NMR of **1i**, related to Figure 2.

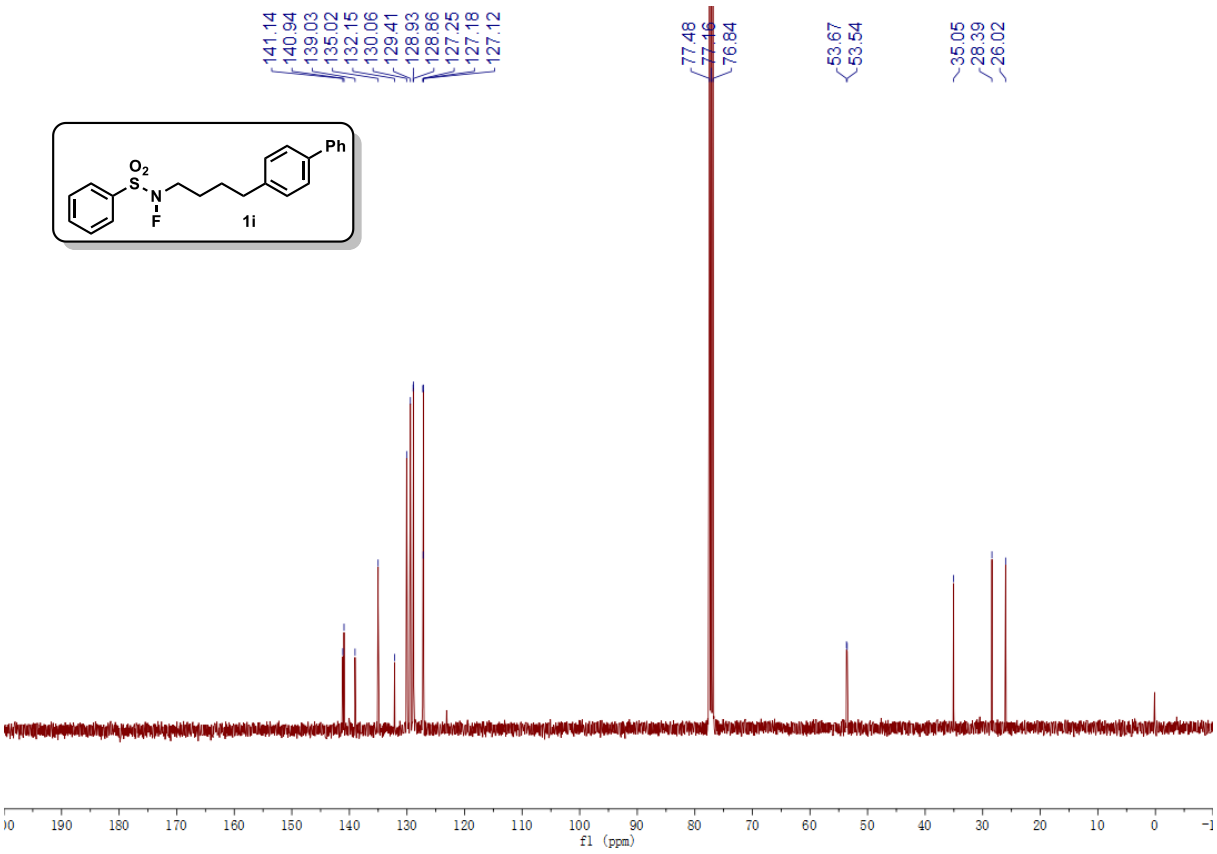

Figure S22. ^{13}C NMR of **1i**, related to Figure 2.

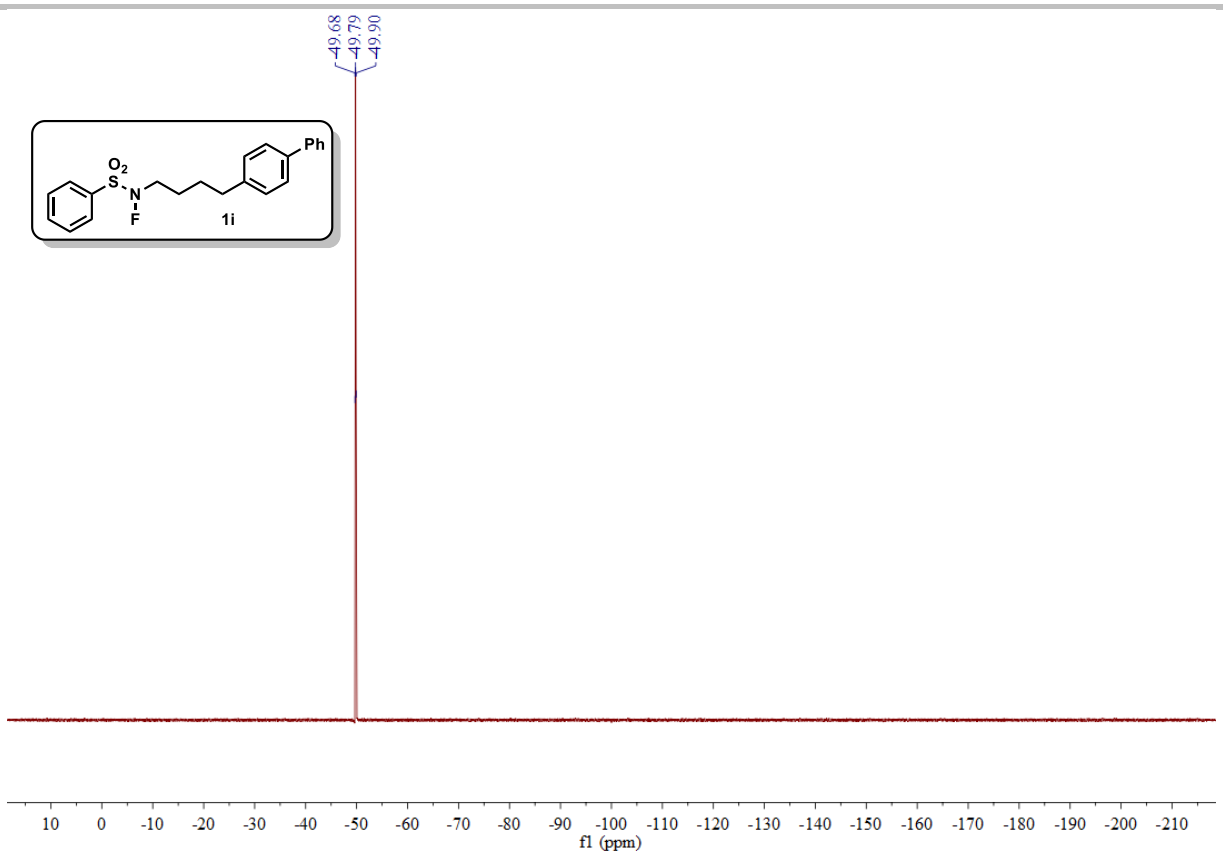

Figure S23. ^{19}F NMR of **1i**, related to Figure 2.

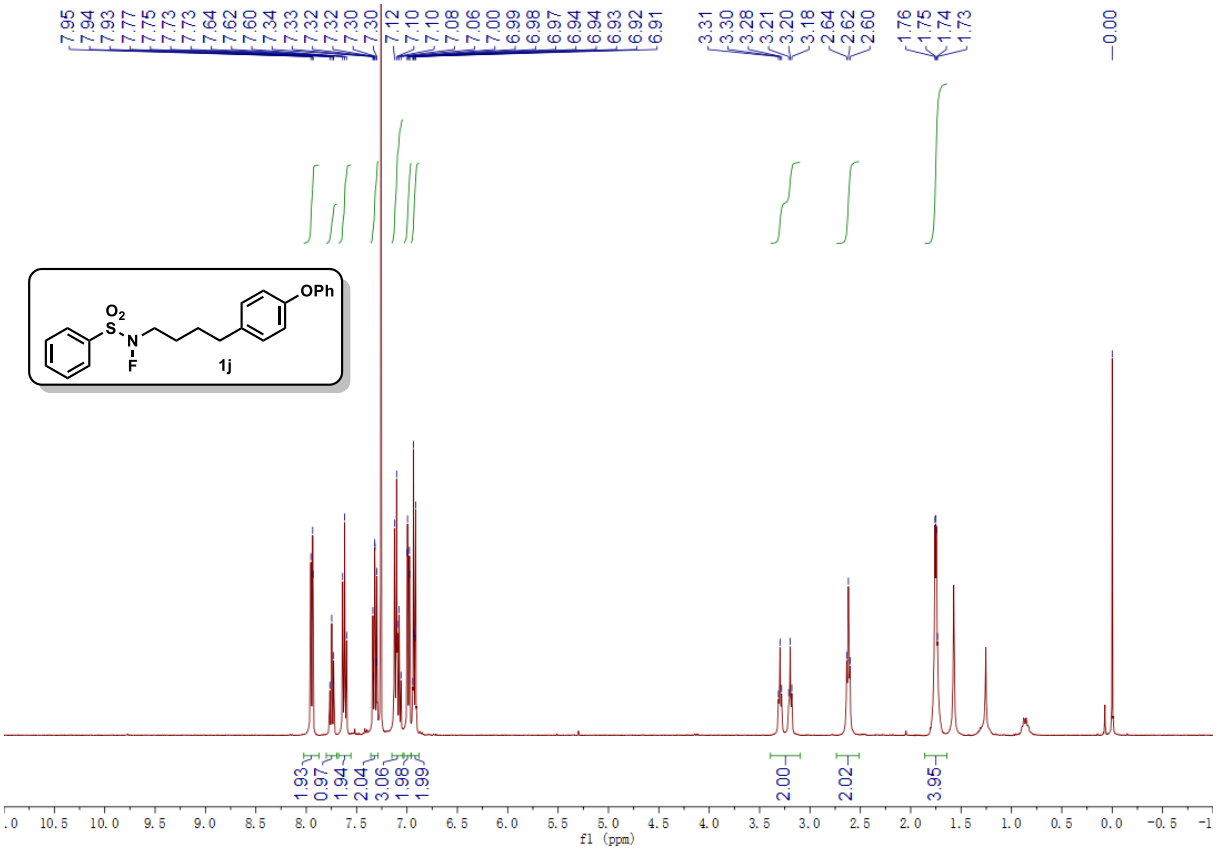

Figure S24. ^{1}H NMR of **1j**, related to Figure 2.

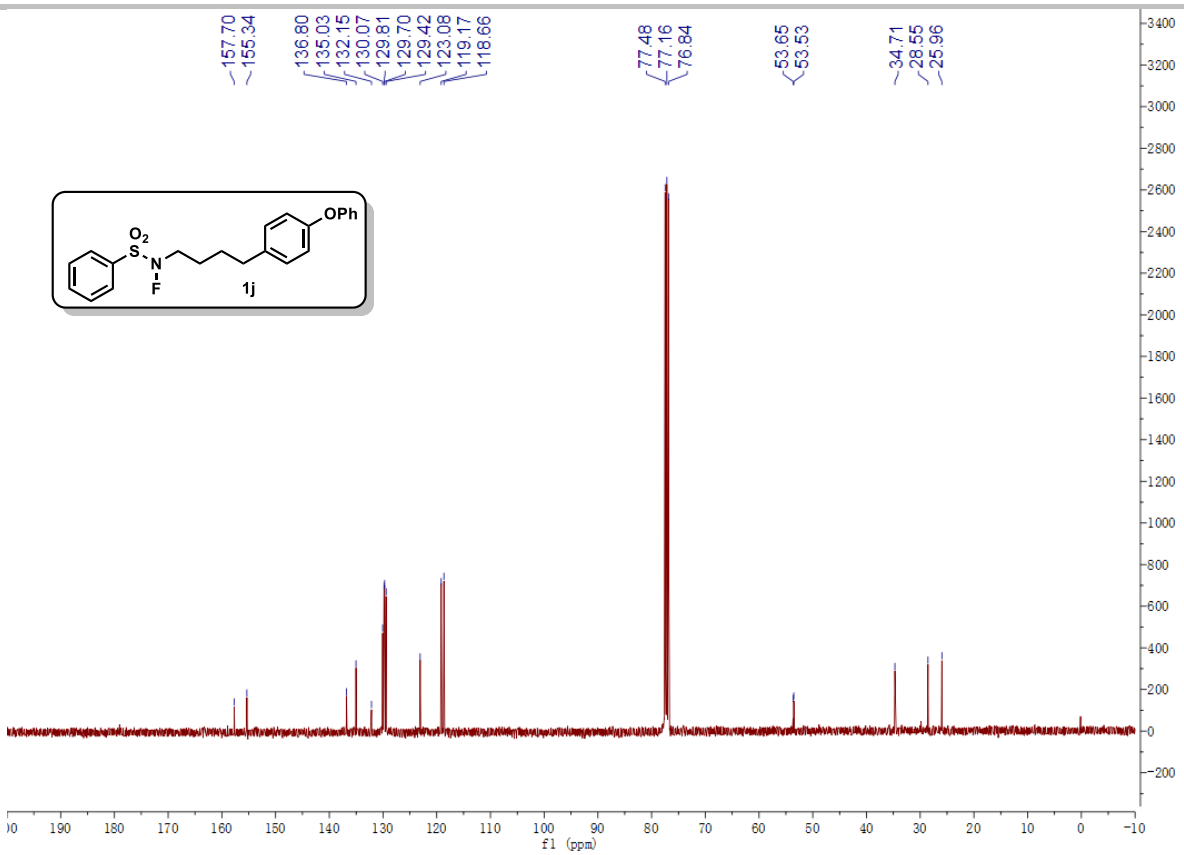

Figure S25. ^{13}C NMR of **1j**, related to Figure 2.

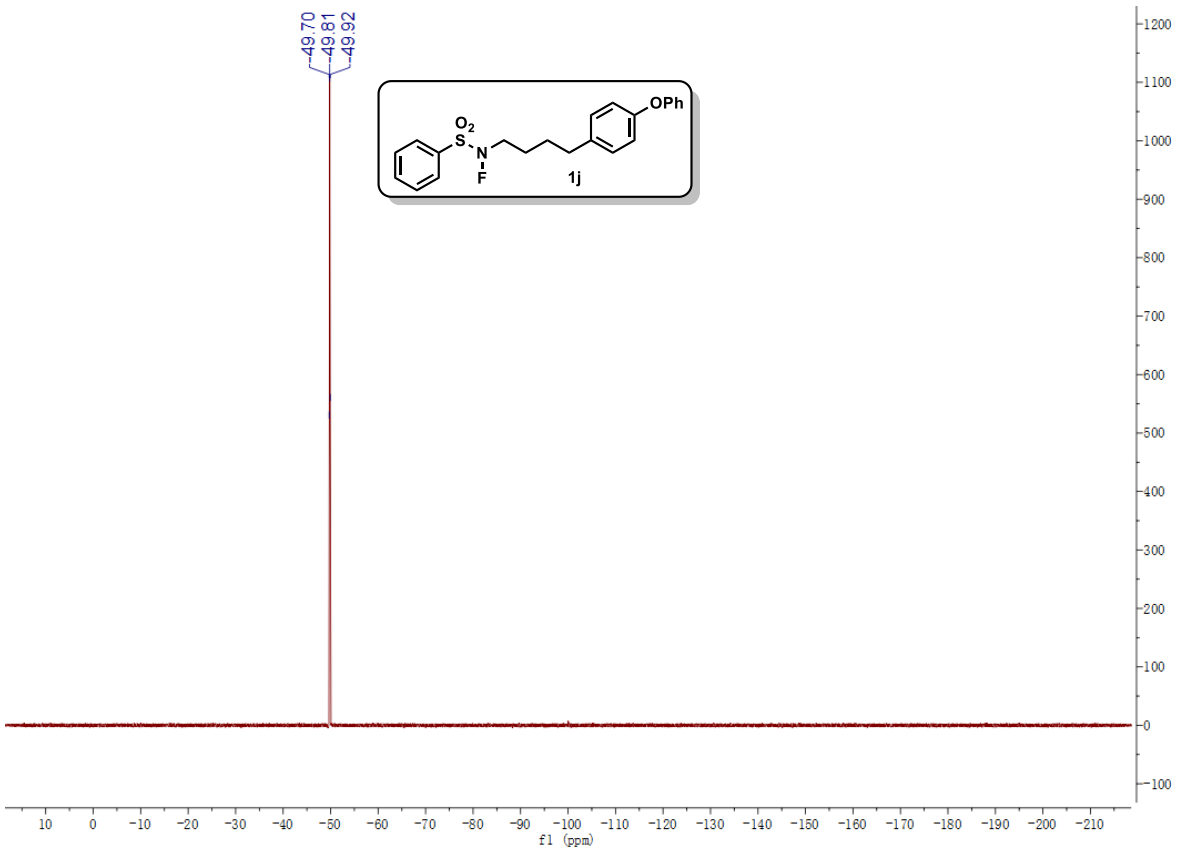

Figure S26. ^{19}F NMR of **1j**, related to Figure 2.

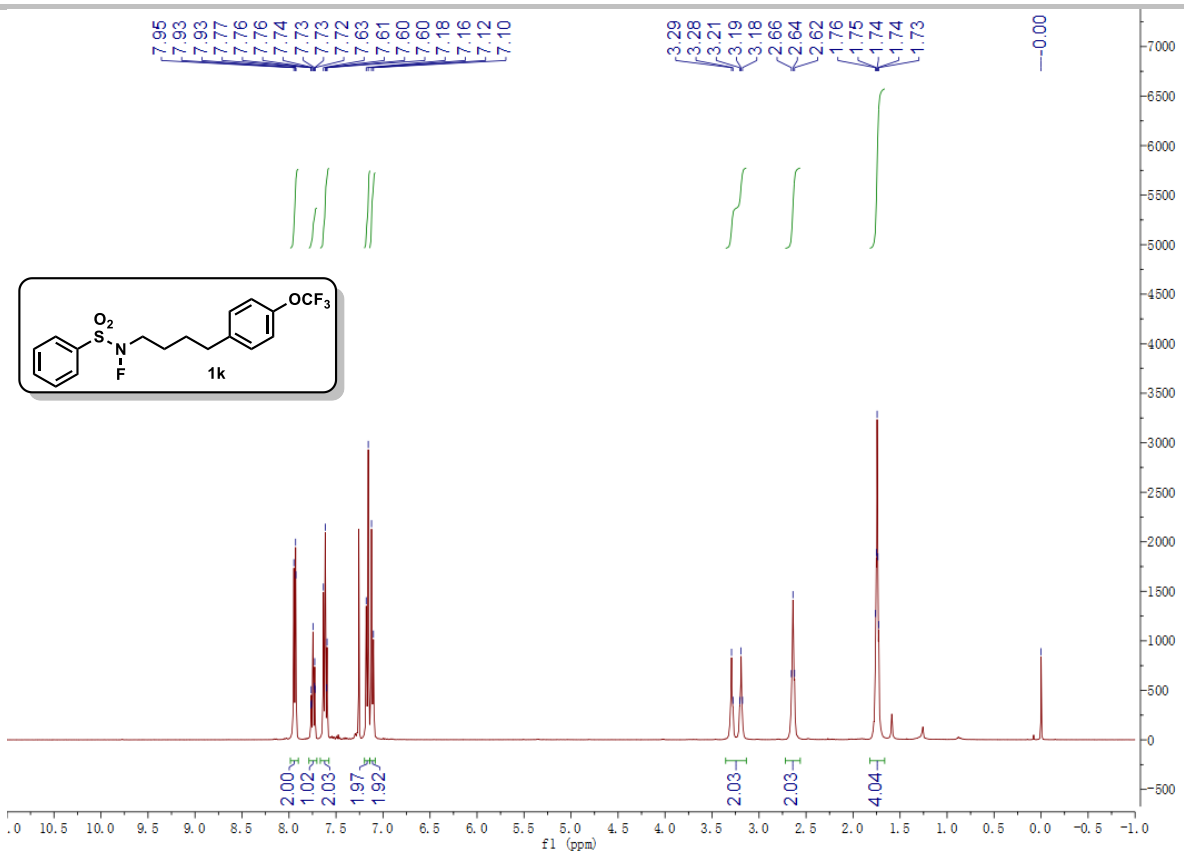

Figure S27. ^{1}H NMR of **1k**, related to Figure 2.

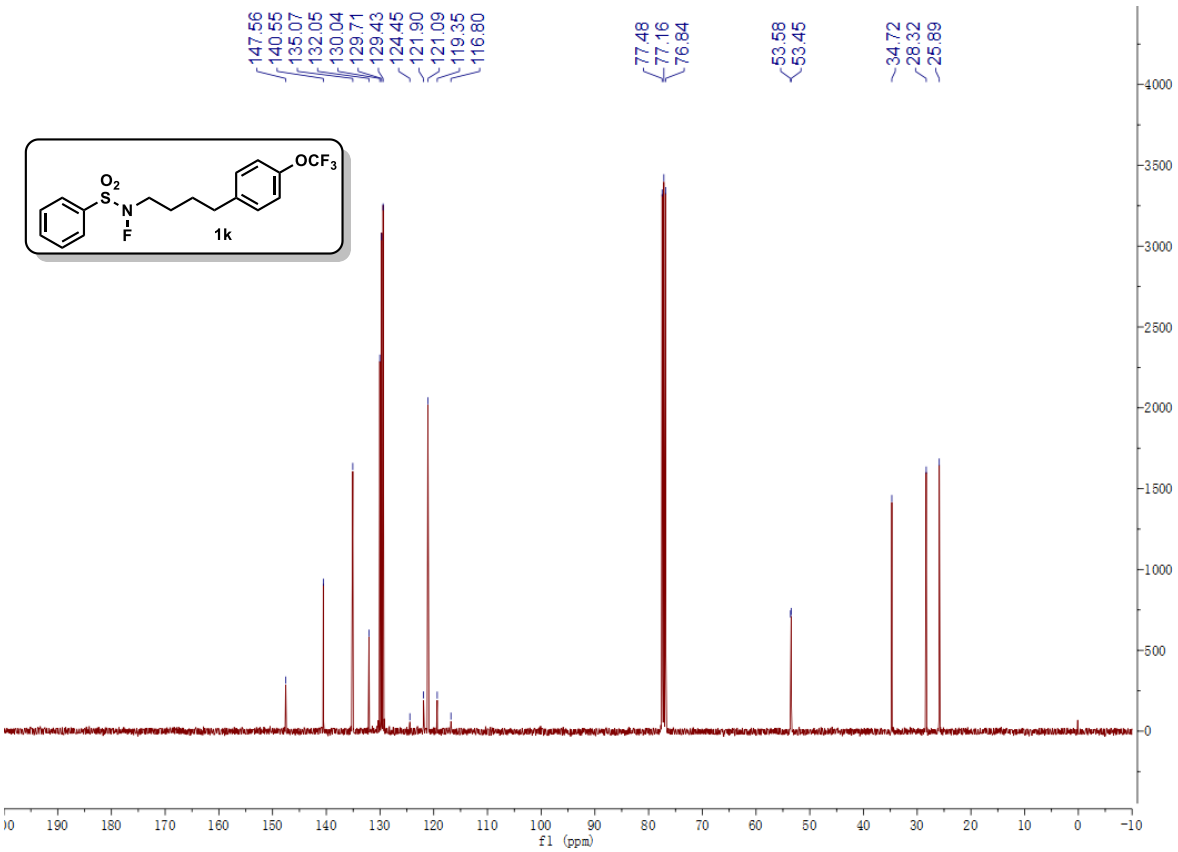

Figure S28. ^{13}C NMR of **1k**, related to Figure 2.

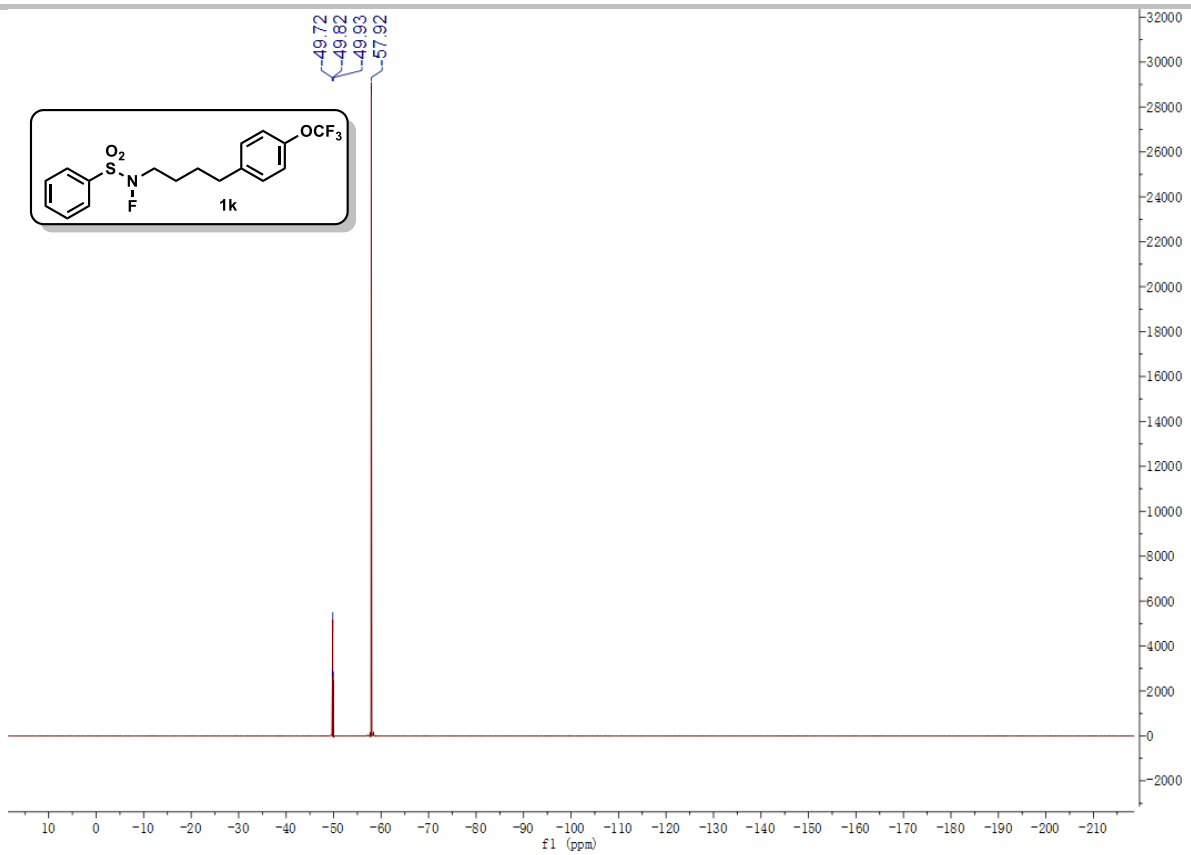

Figure S29. ^{19}F NMR of **1k**, related to Figure 2.

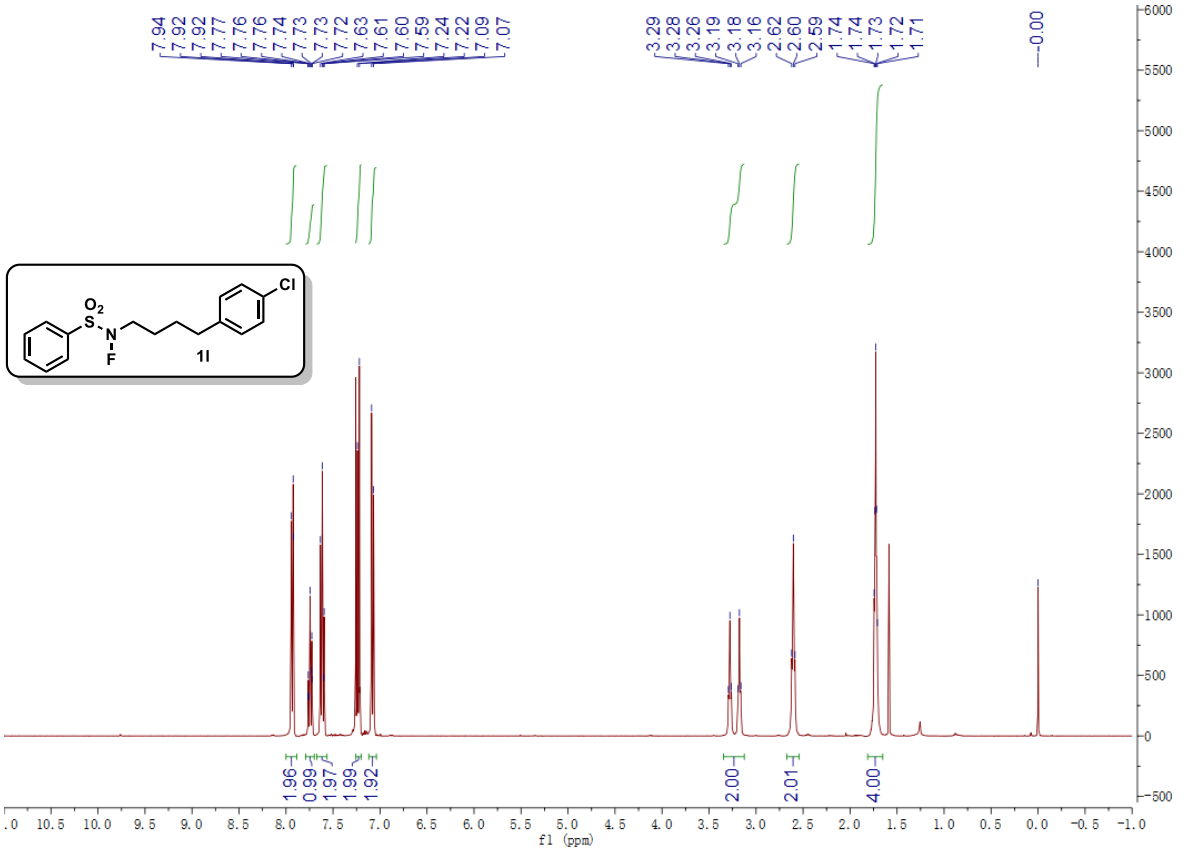

Figure S30. ^{1}H NMR of **1l**, related to Figure 2.

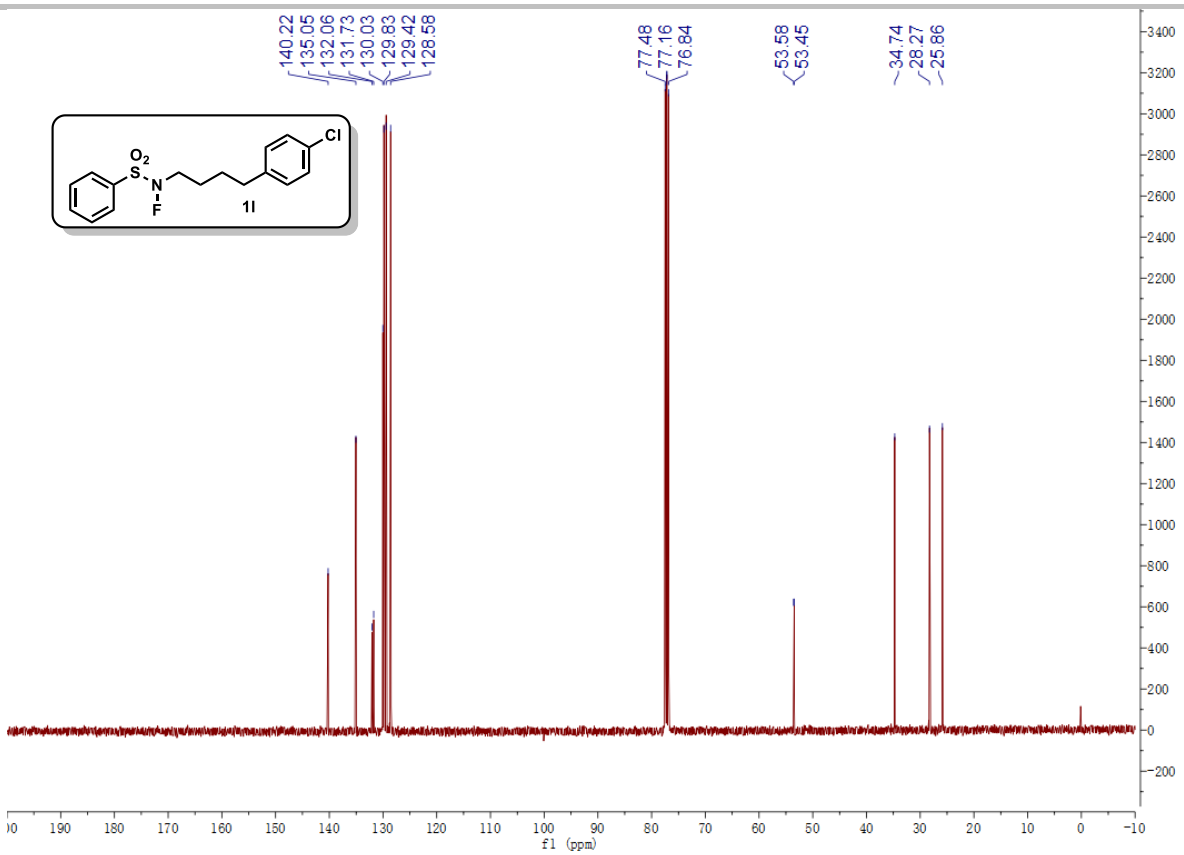

Figure S31. ^{13}C NMR of **1l**, related to Figure 2.

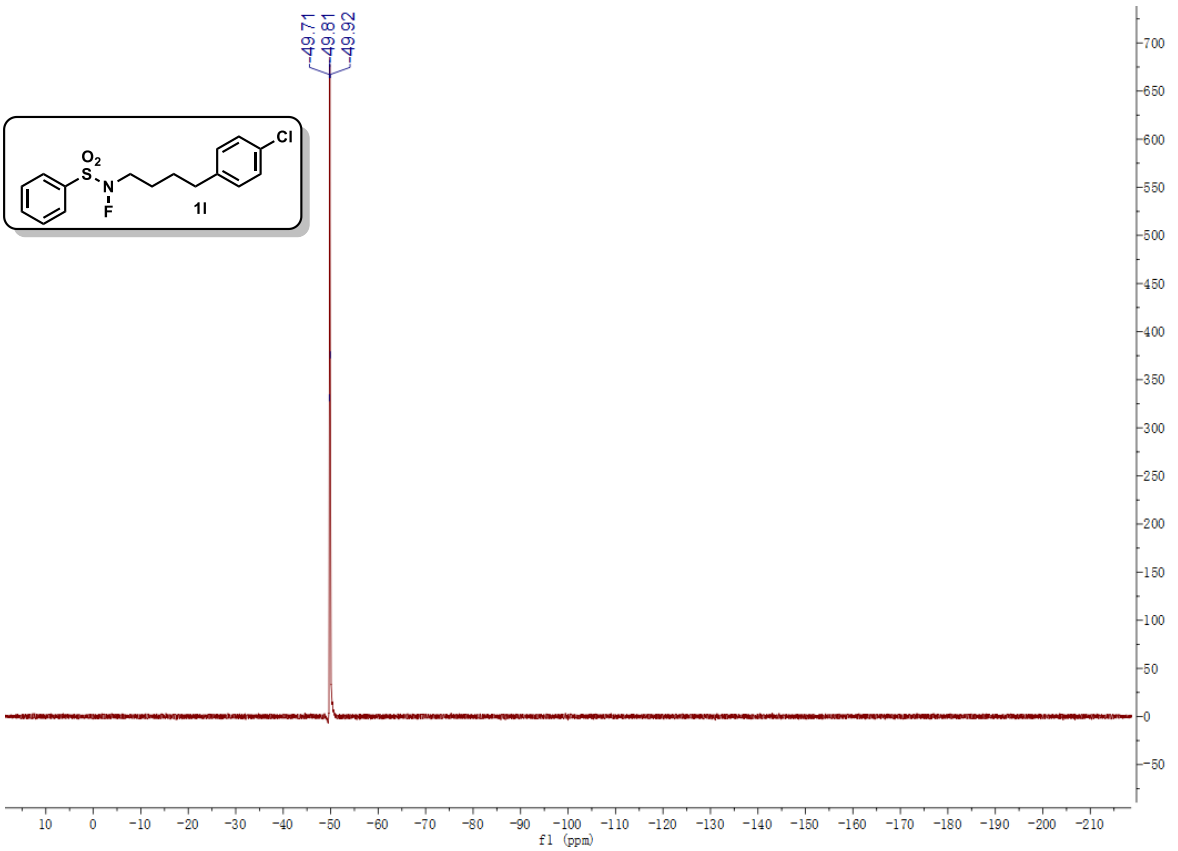

Figure S32. ^{19}F NMR of **1l**, related to Figure 2.

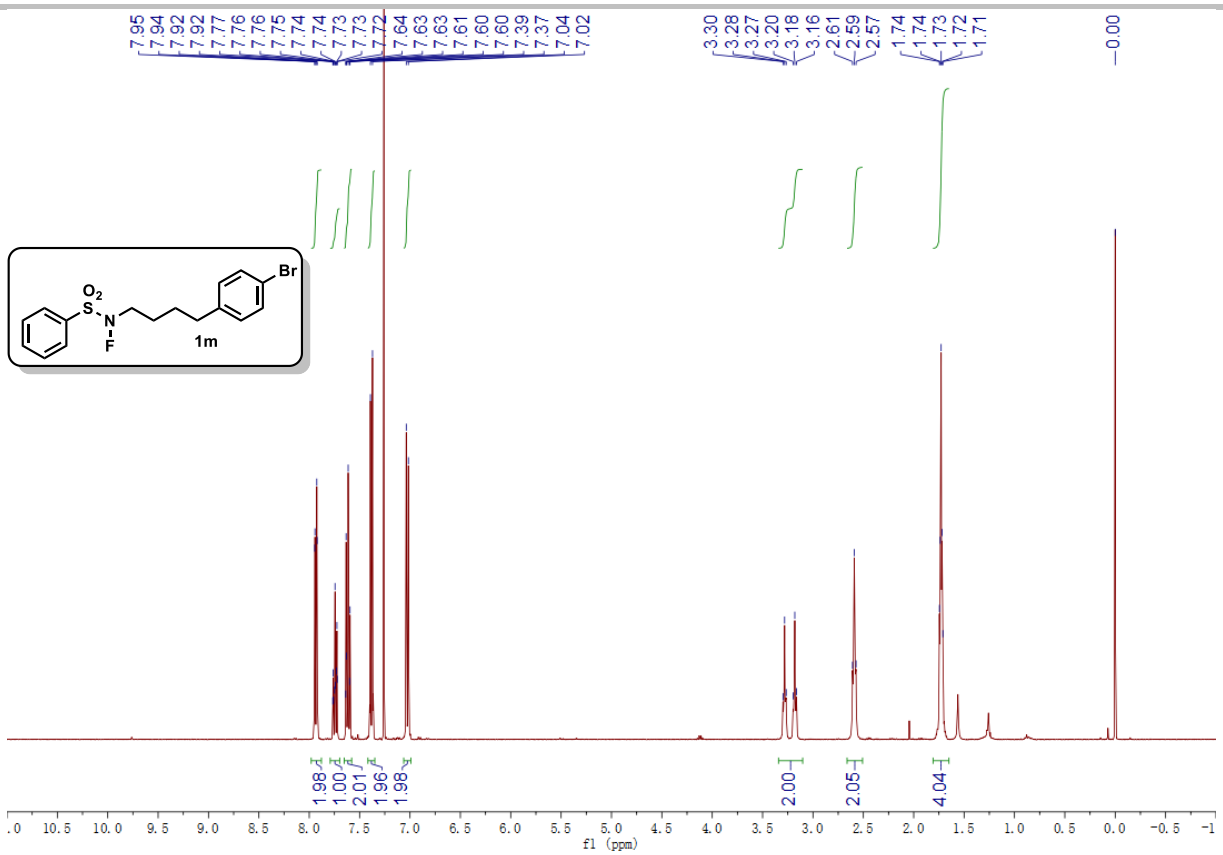

Figure S33. ^{1}H NMR of **1m**, related to Figure 2.

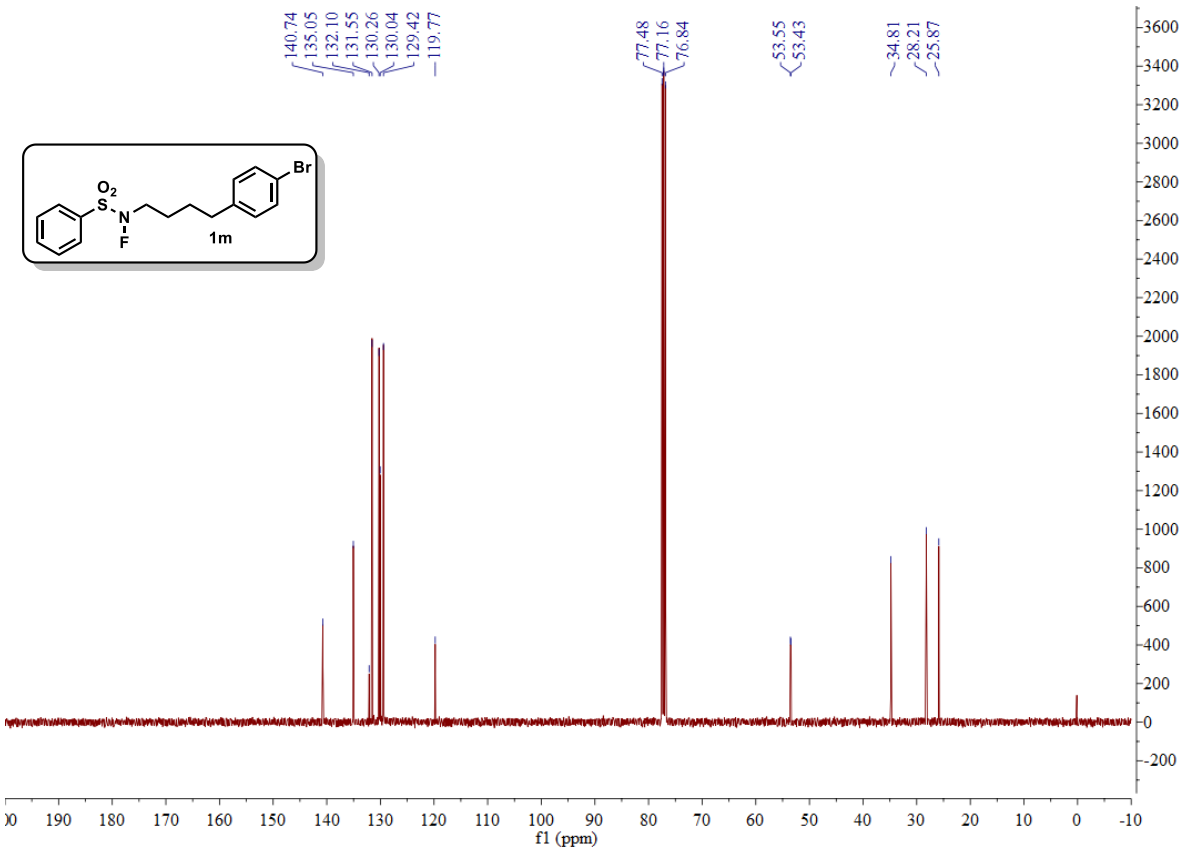

Figure S34. ^{13}C NMR of **1m**, related to Figure 2.

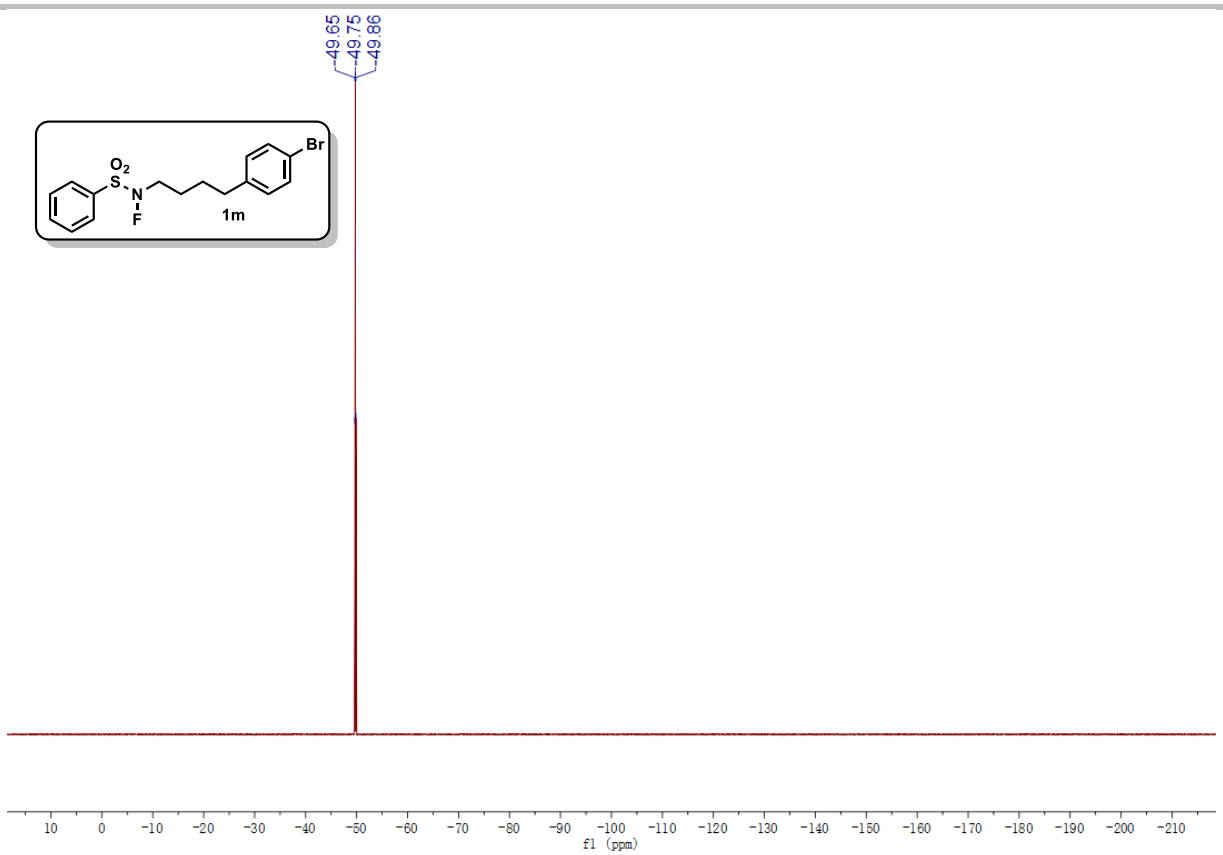

Figure S35. ^{19}F NMR of **1m**, related to Figure 2.

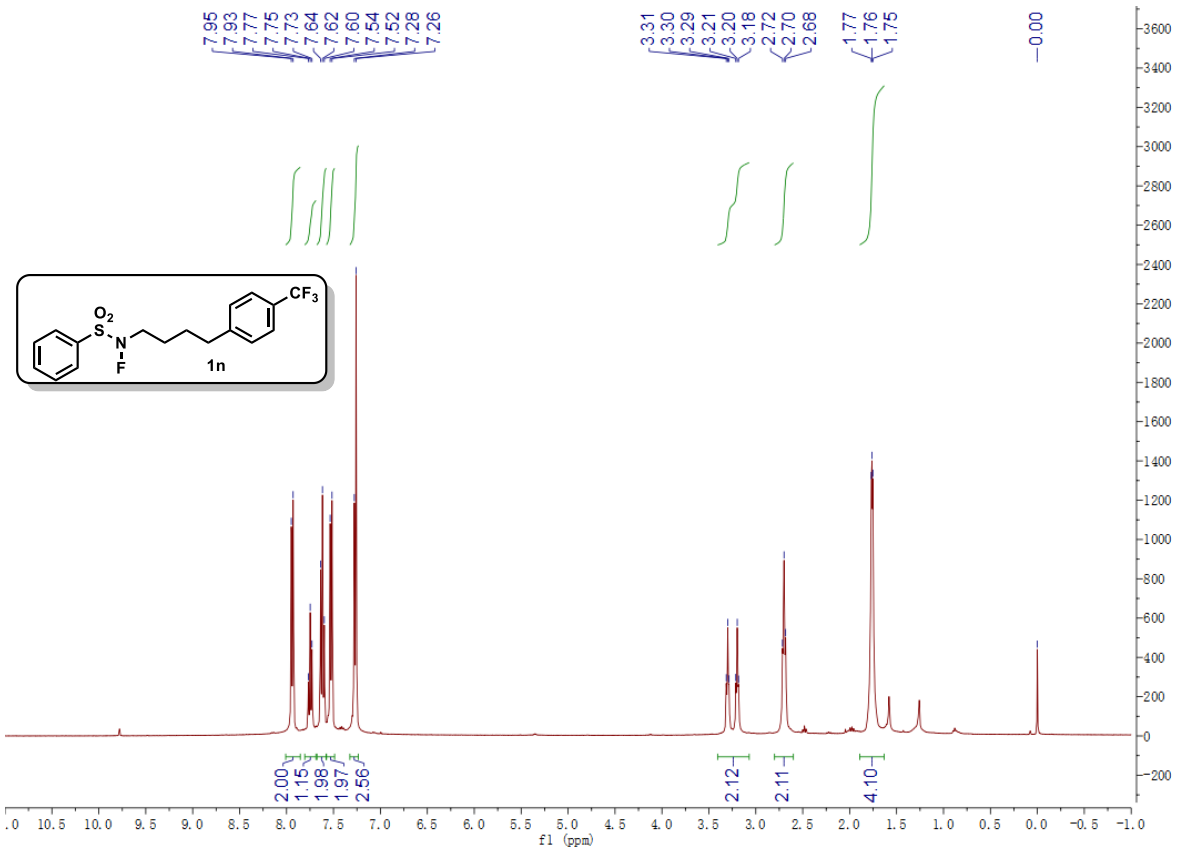

Figure S36. ^{1}H NMR of **1n**, related to Figure 2.

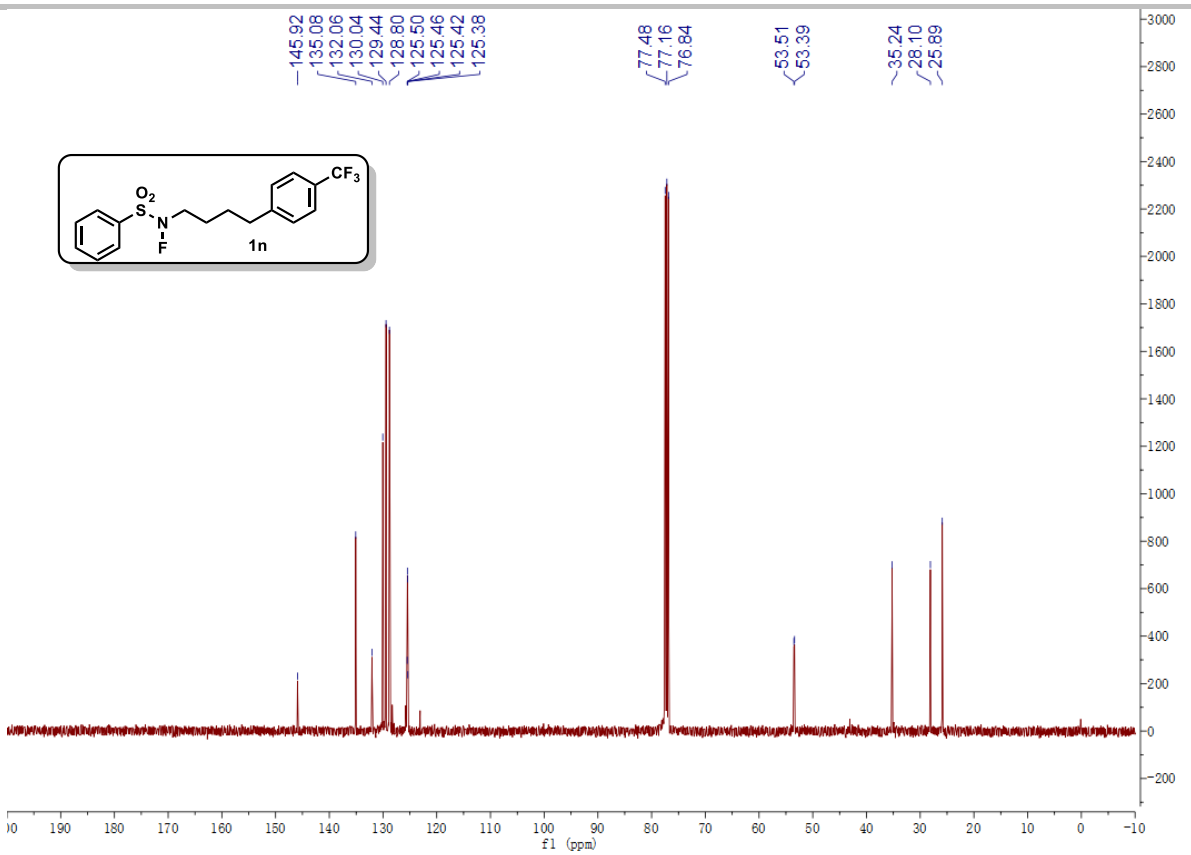

Figure S37. ^{13}C NMR of **1n**, related to Figure 2.

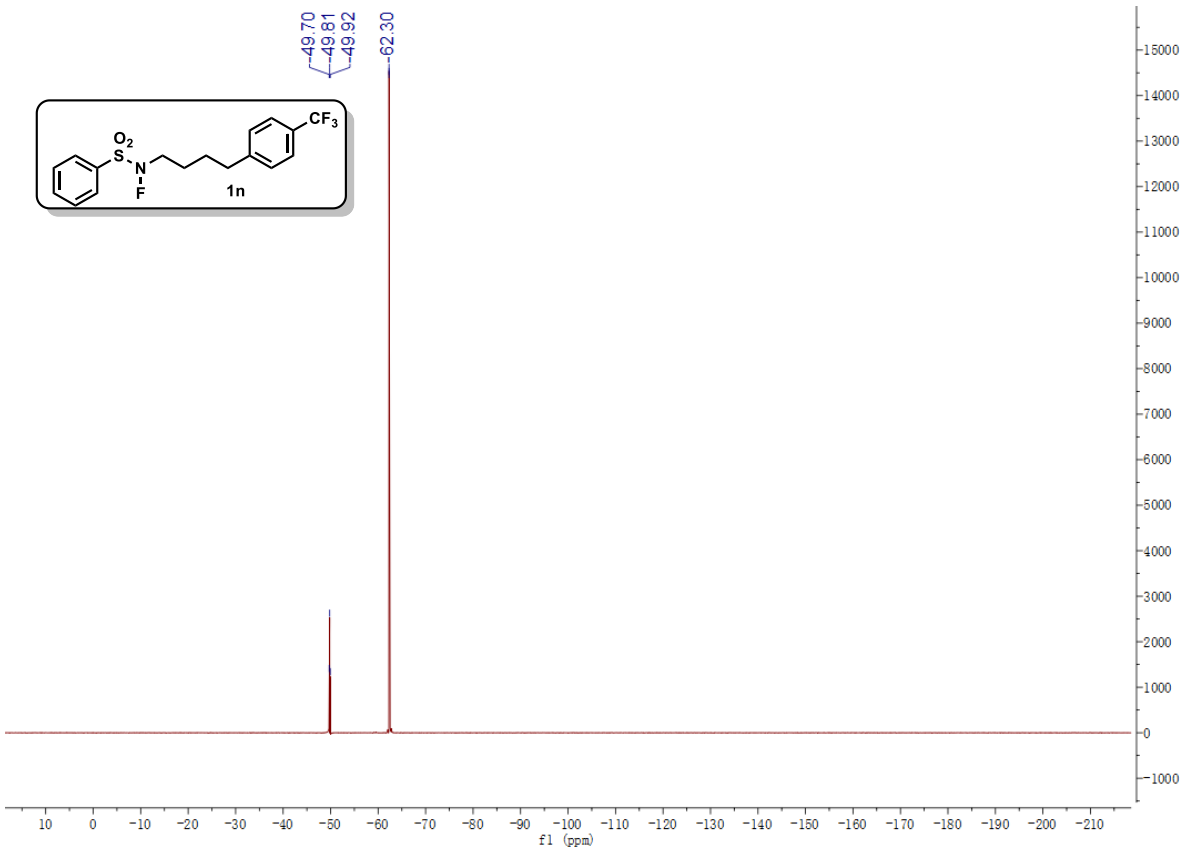

Figure S38. ^{19}F NMR of **1n**, related to Figure 2.

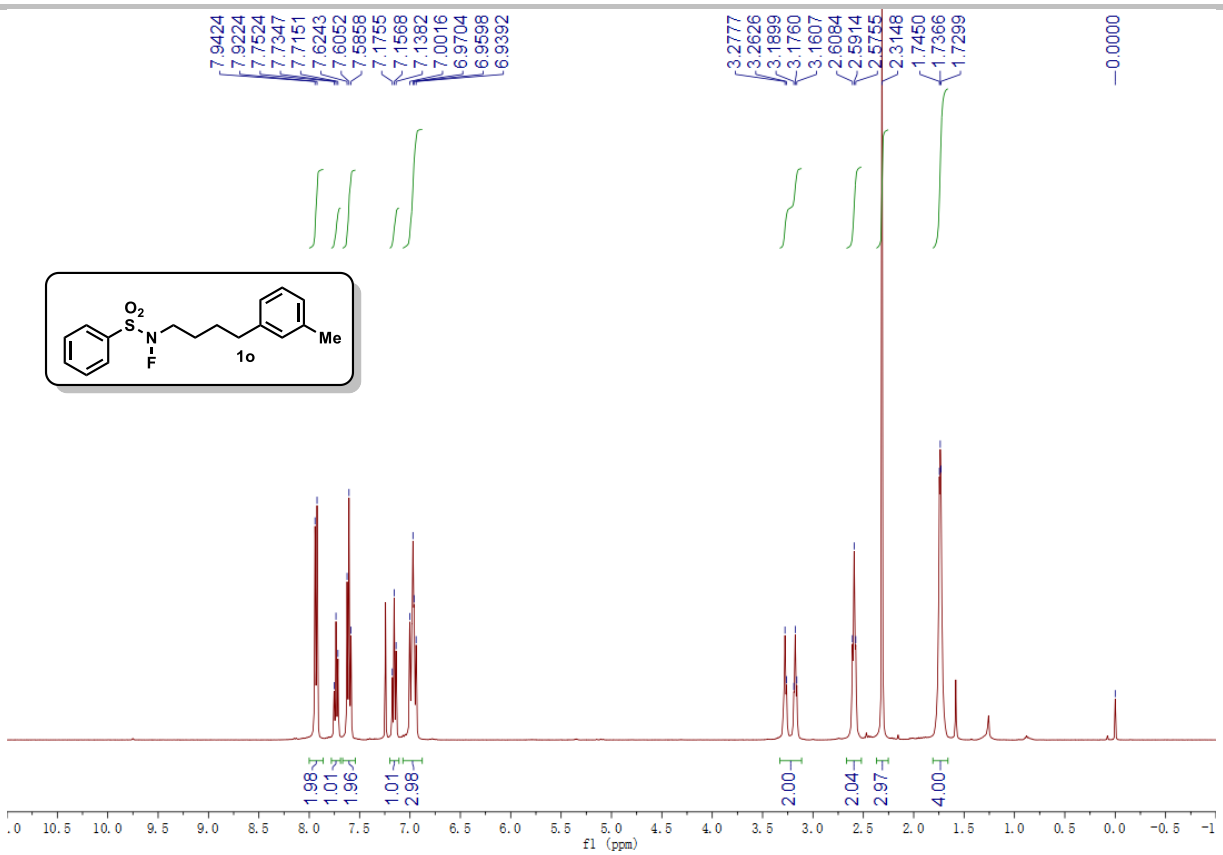

Figure S39. ^{1}H NMR of **1o**, related to Figure 2.

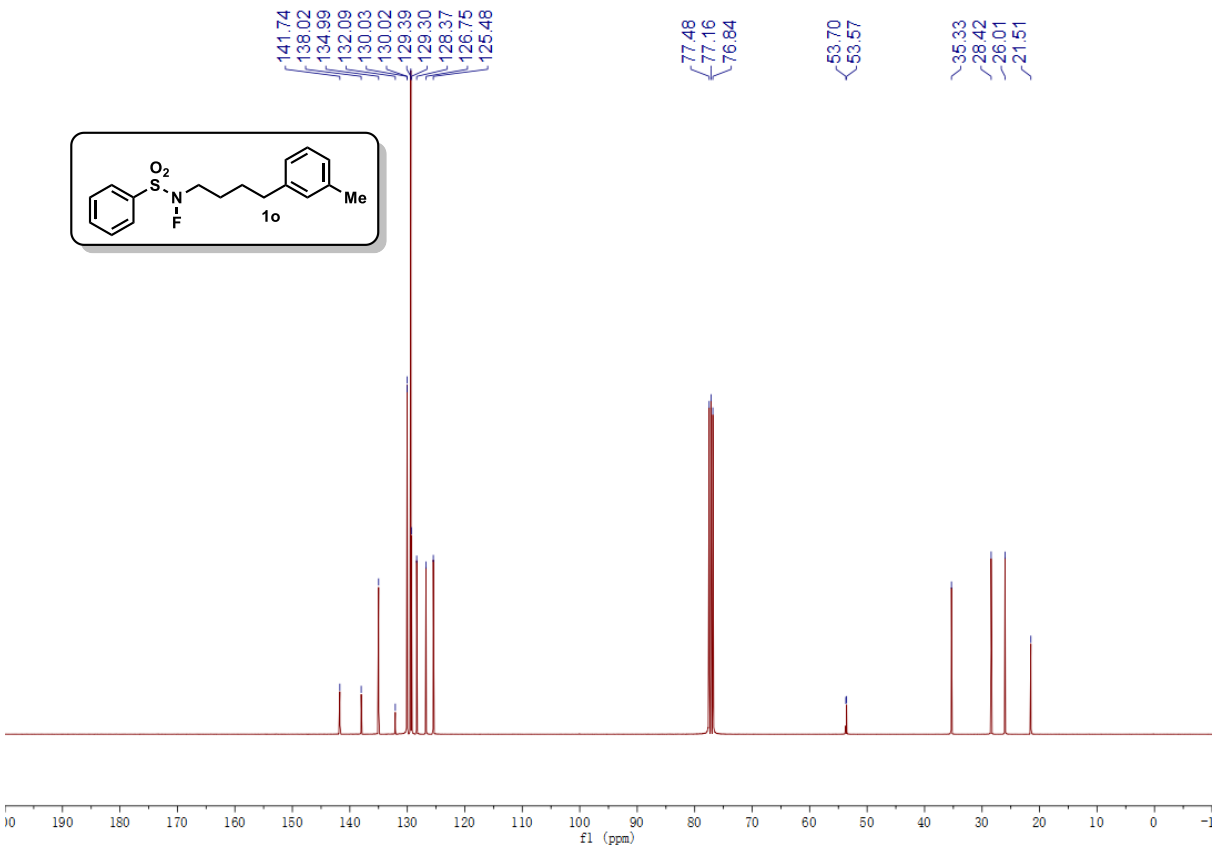

Figure S40. ^{13}C NMR of **1o**, related to Figure 2.

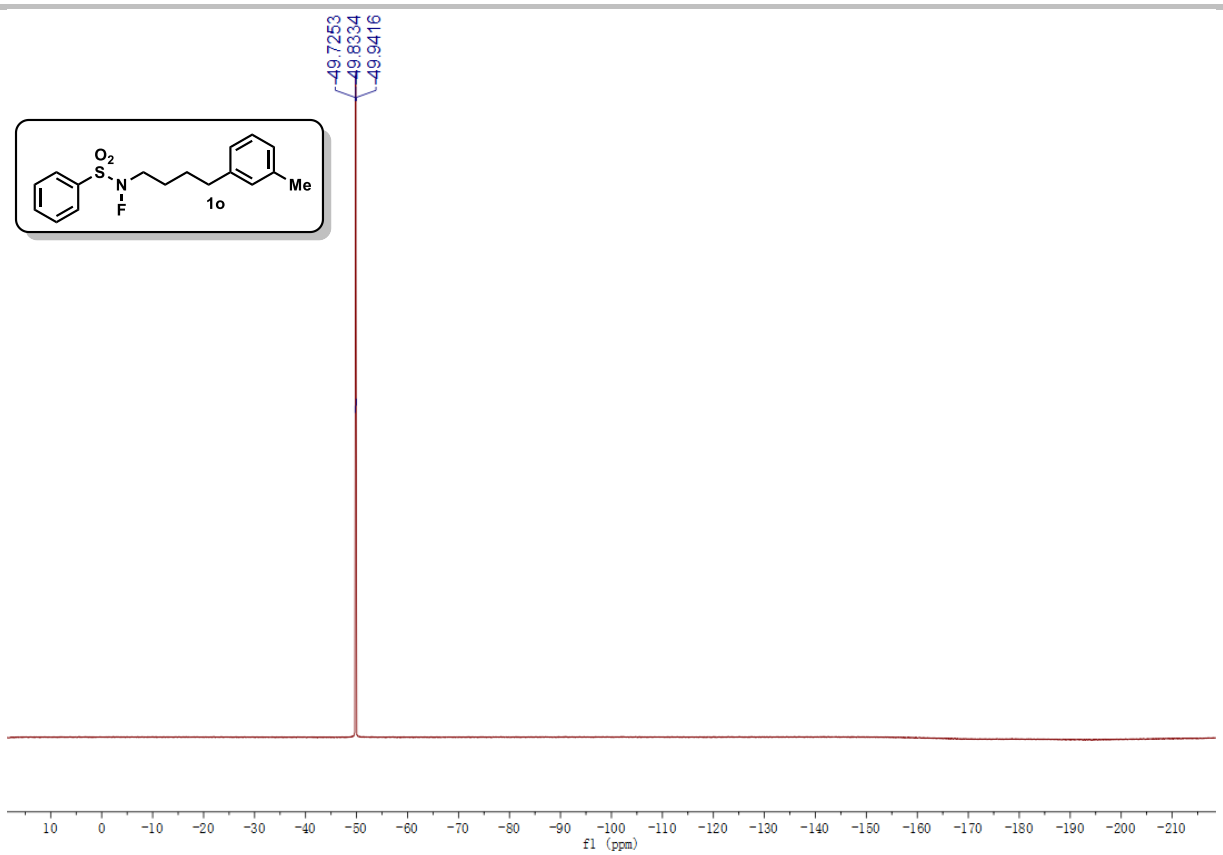

Figure S41. ^{19}F NMR of **1o**, related to Figure 2.

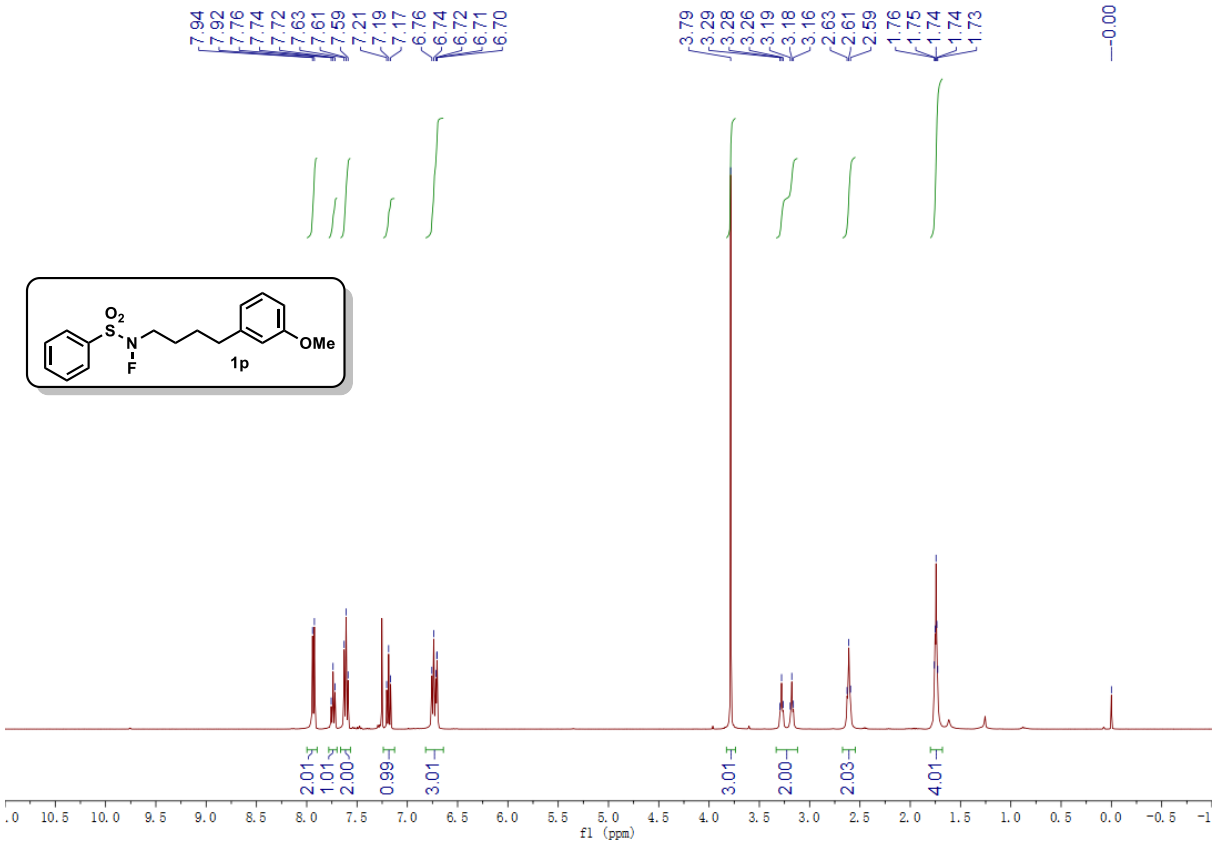

Figure S42. ^{1}H NMR of **1p**, related to Figure 2.

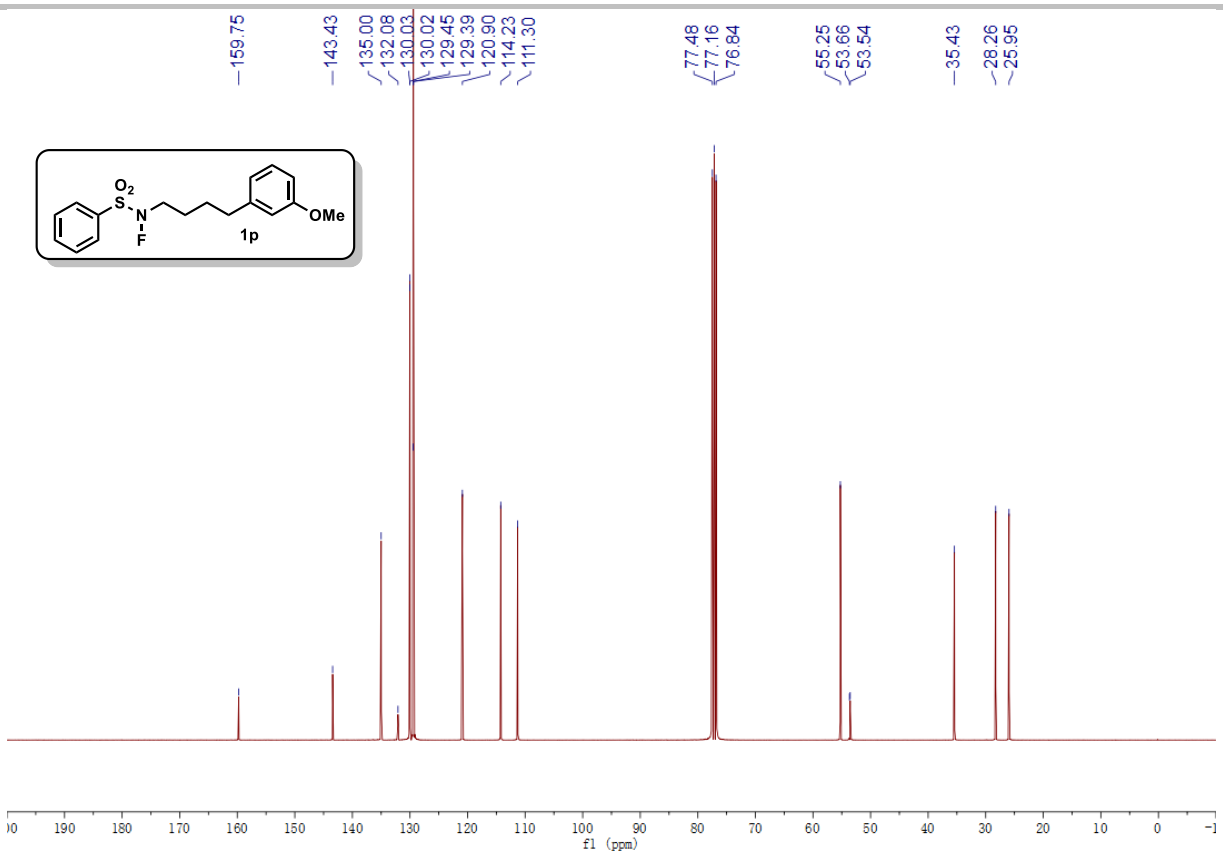

Figure S43. ^{13}C NMR of **1p**, related to Figure 2.

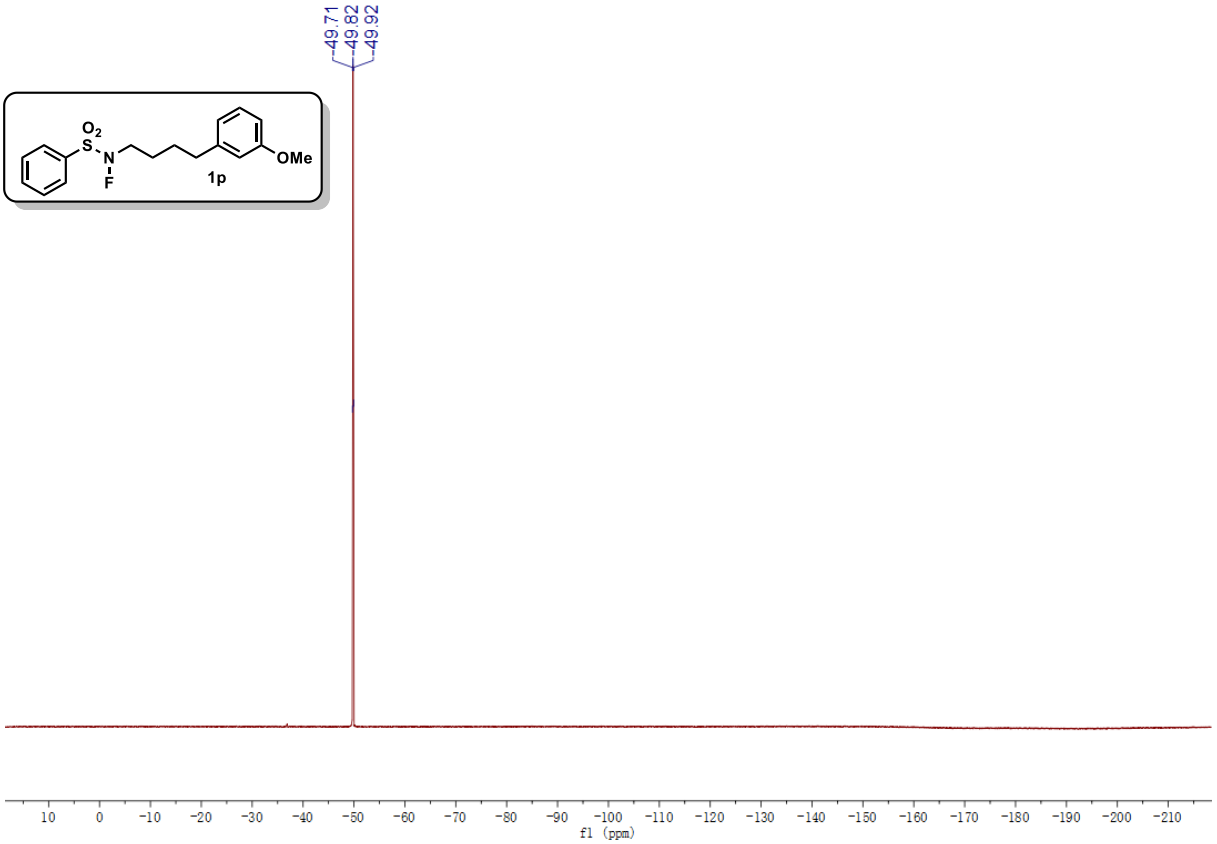

Figure S44. ^{19}F NMR of **1p**, related to Figure 2.

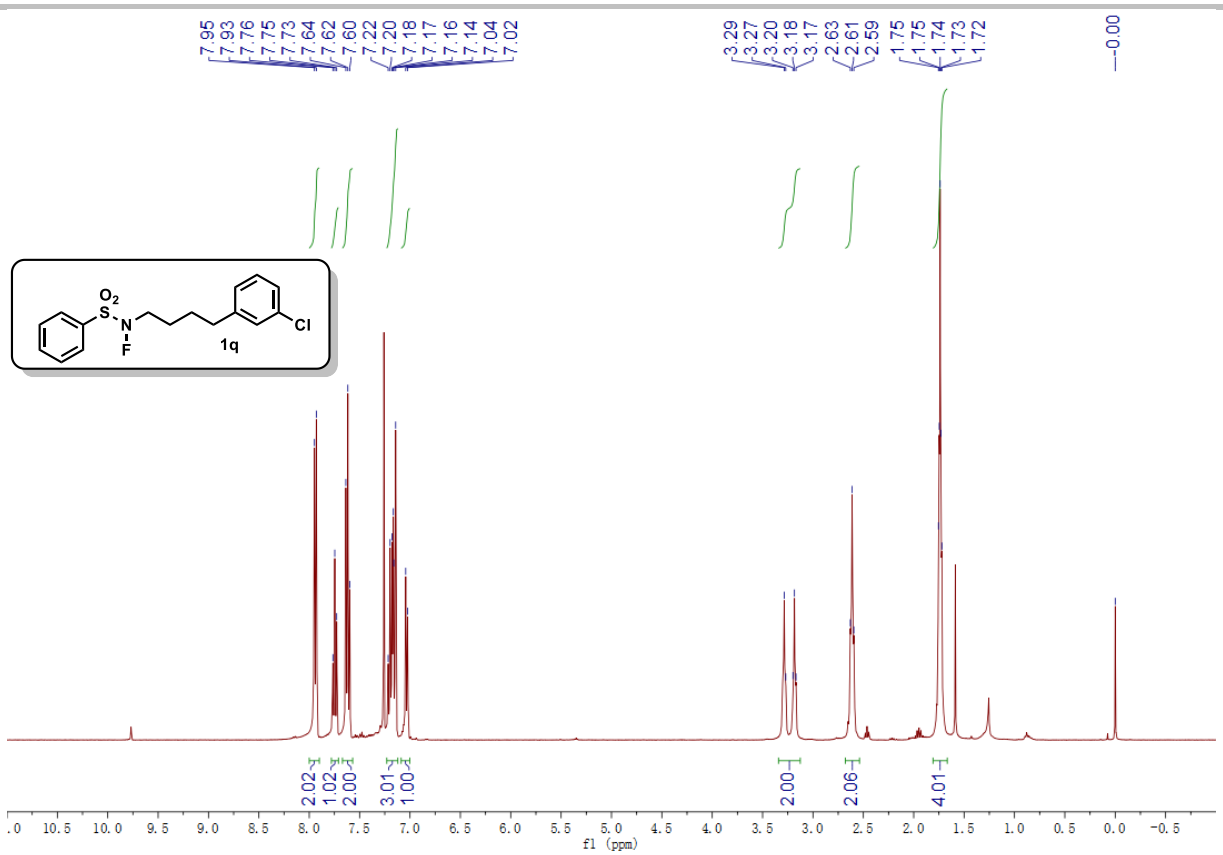

Figure S45. ^{1}H NMR of **1q**, related to Figure 2.

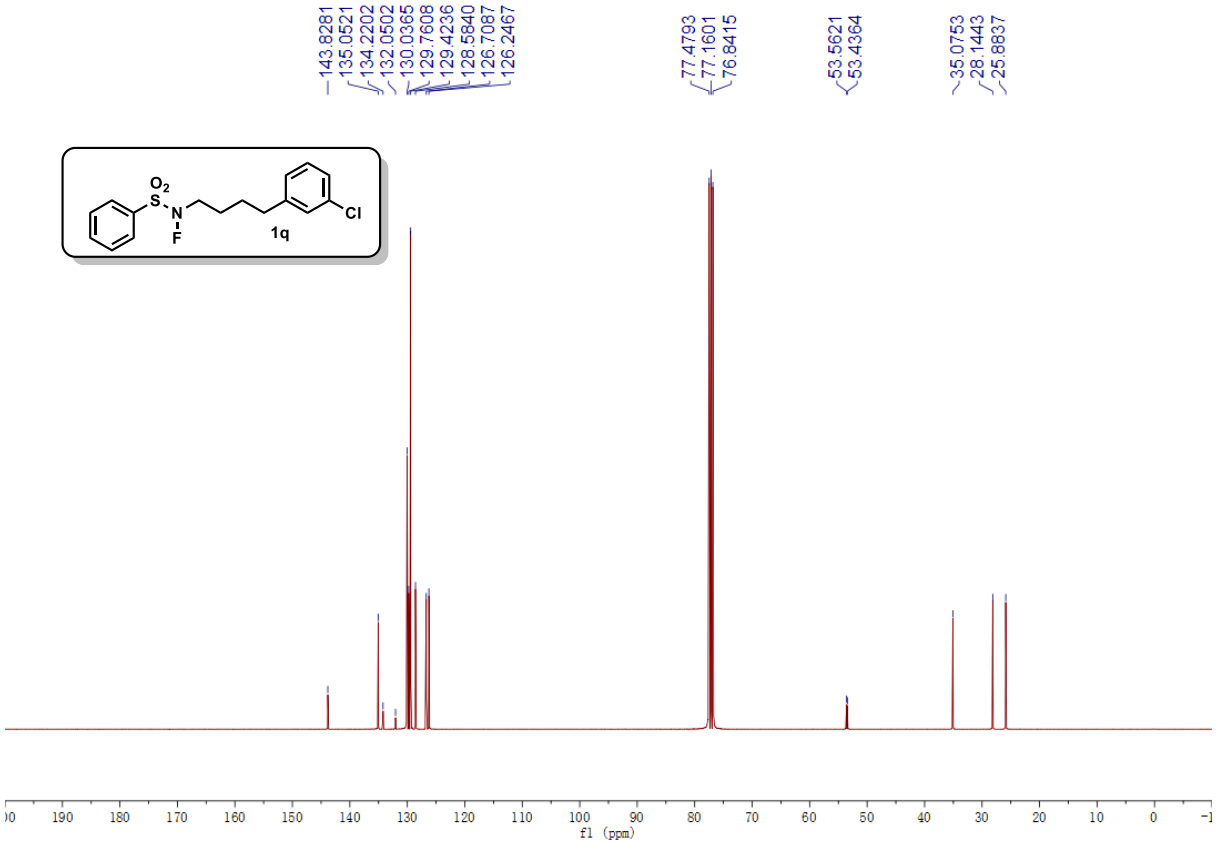

Figure S46. ^{13}C NMR of **1q**, related to Figure 2.

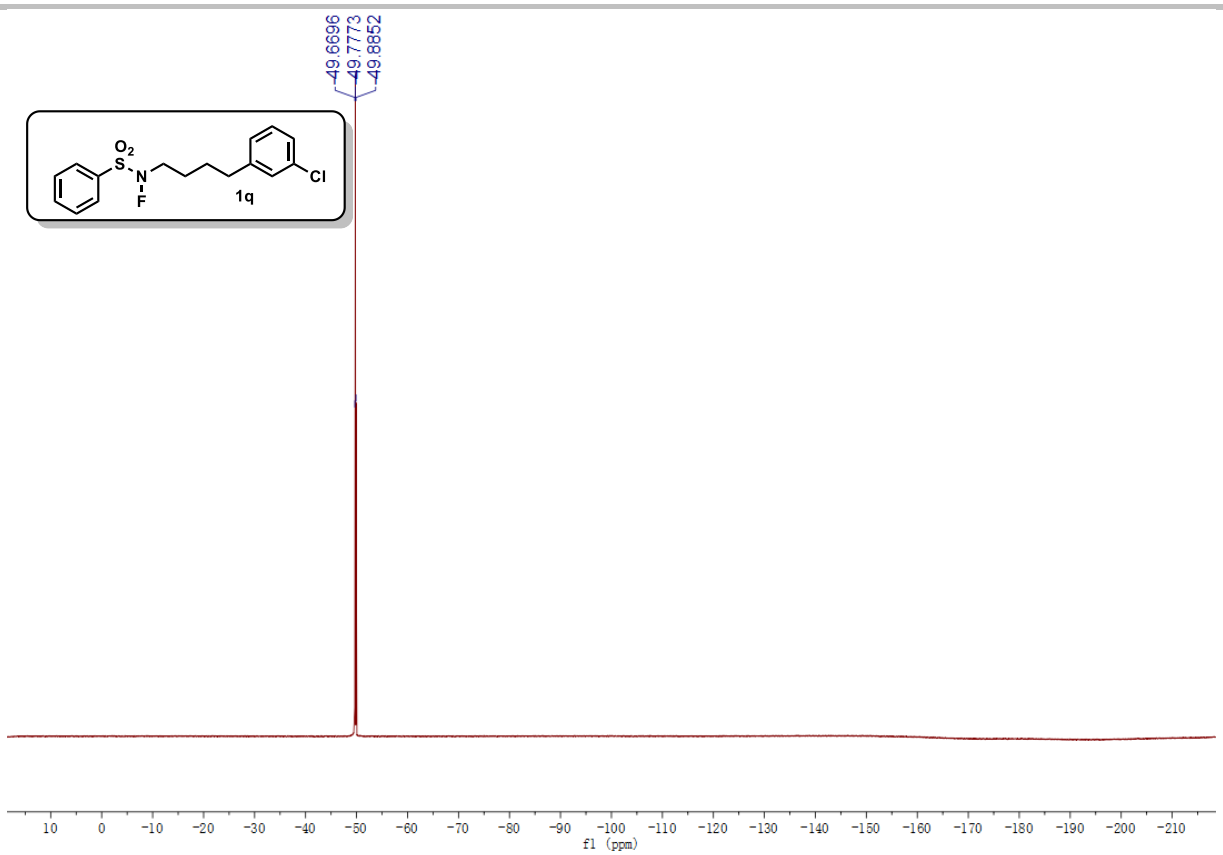

Figure S47. ^{19}F NMR of **1q**, related to Figure 2.

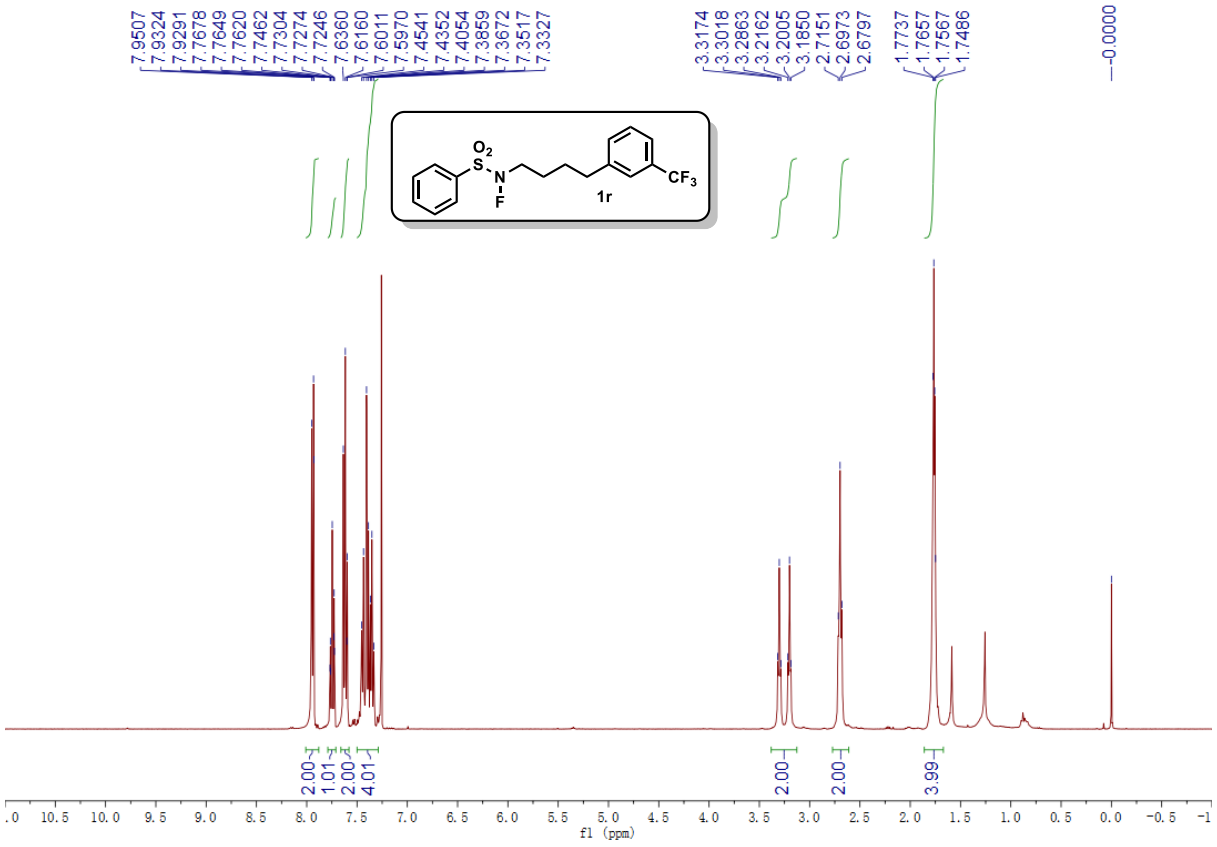

Figure S48. ^{1}H NMR of **1r**, related to Figure 2.

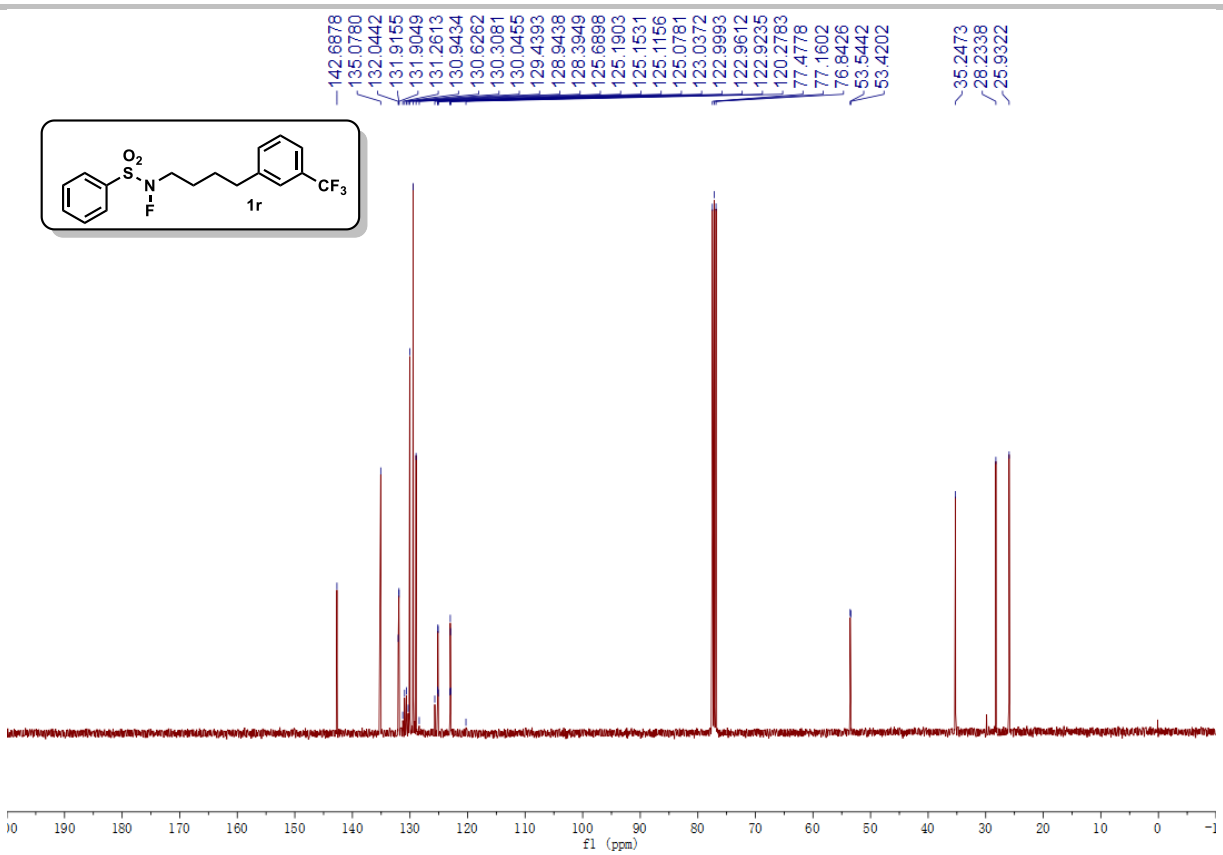

Figure S49. ^{13}C NMR of **1r**, related to Figure 2.

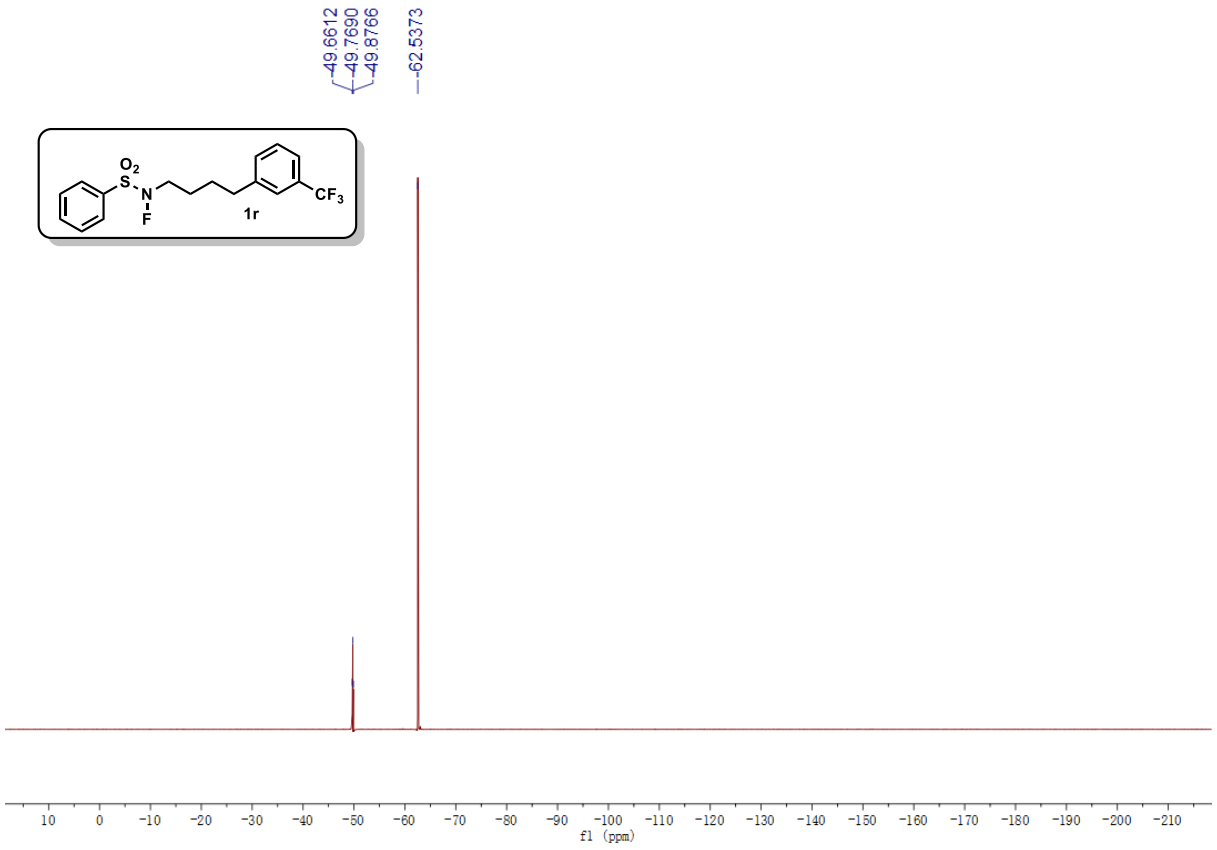

Figure S50. ^{19}F NMR of **1r**, related to Figure 2.

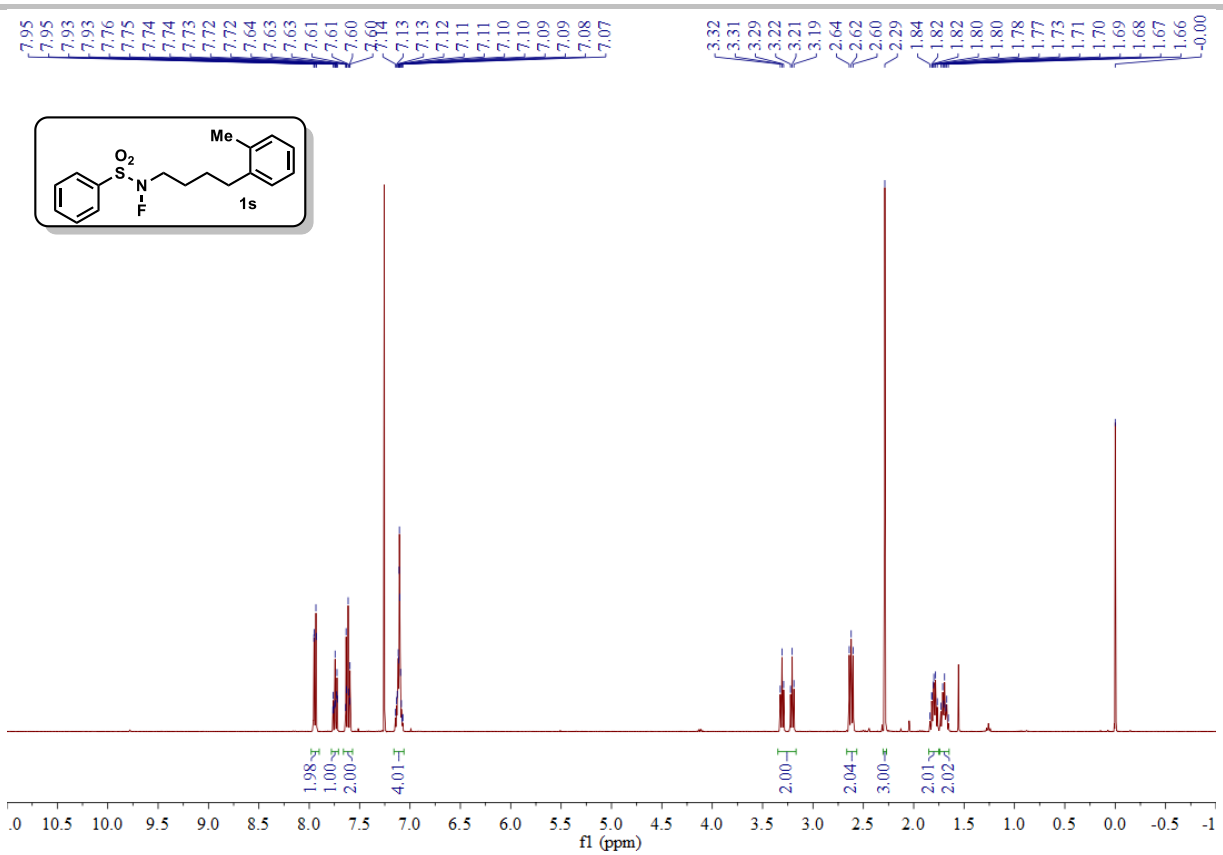

Figure S51. ^{1}H NMR of **1s**, related to Figure 2.

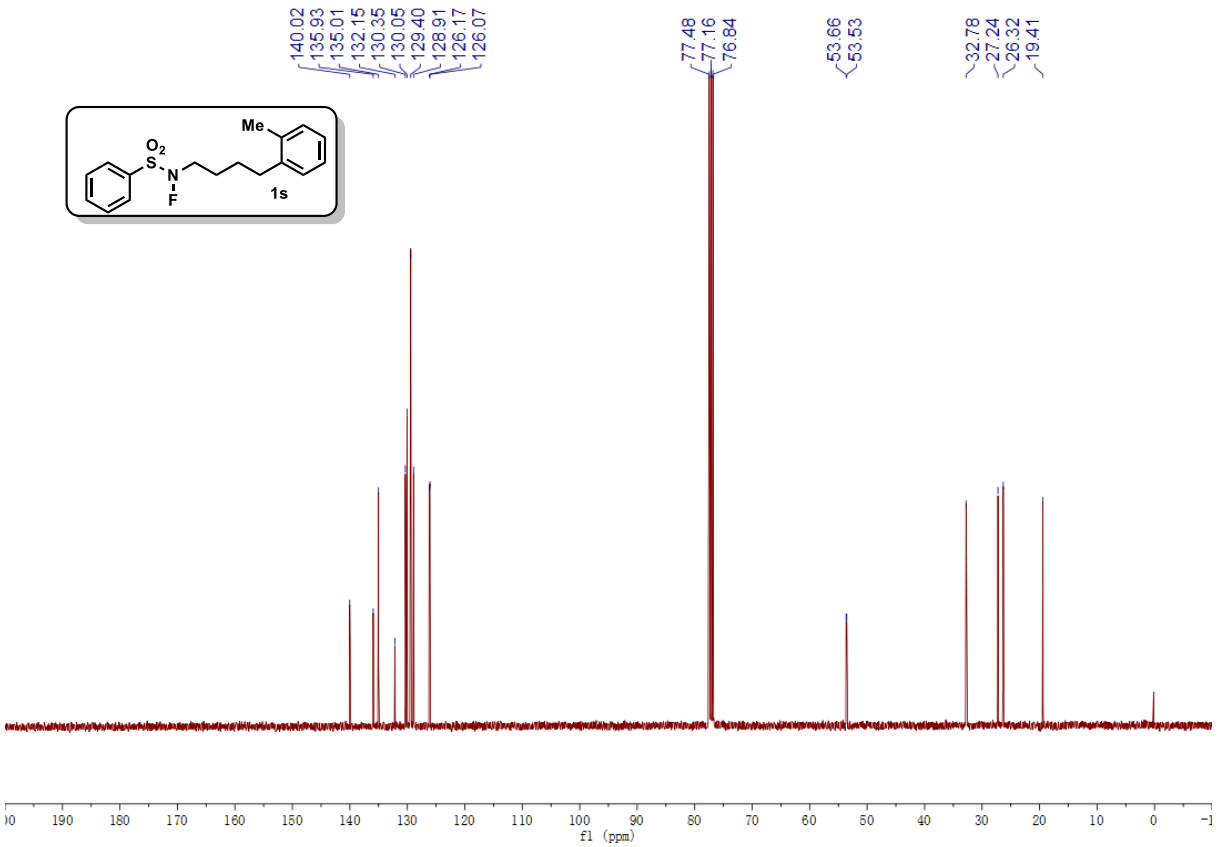

Figure S52. ^{13}C NMR of **1s**, related to Figure 2.

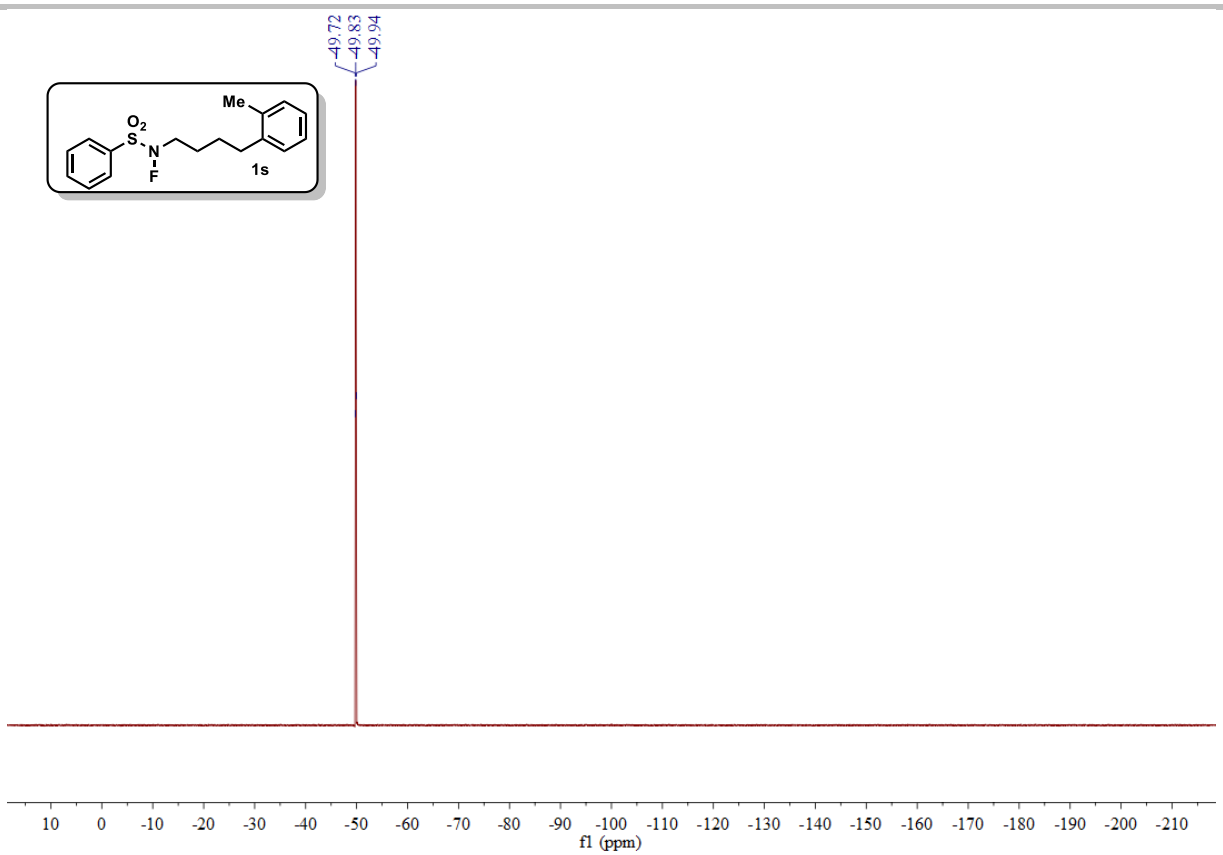

Figure S53. ^{19}F NMR of **1s**, related to Figure 2.

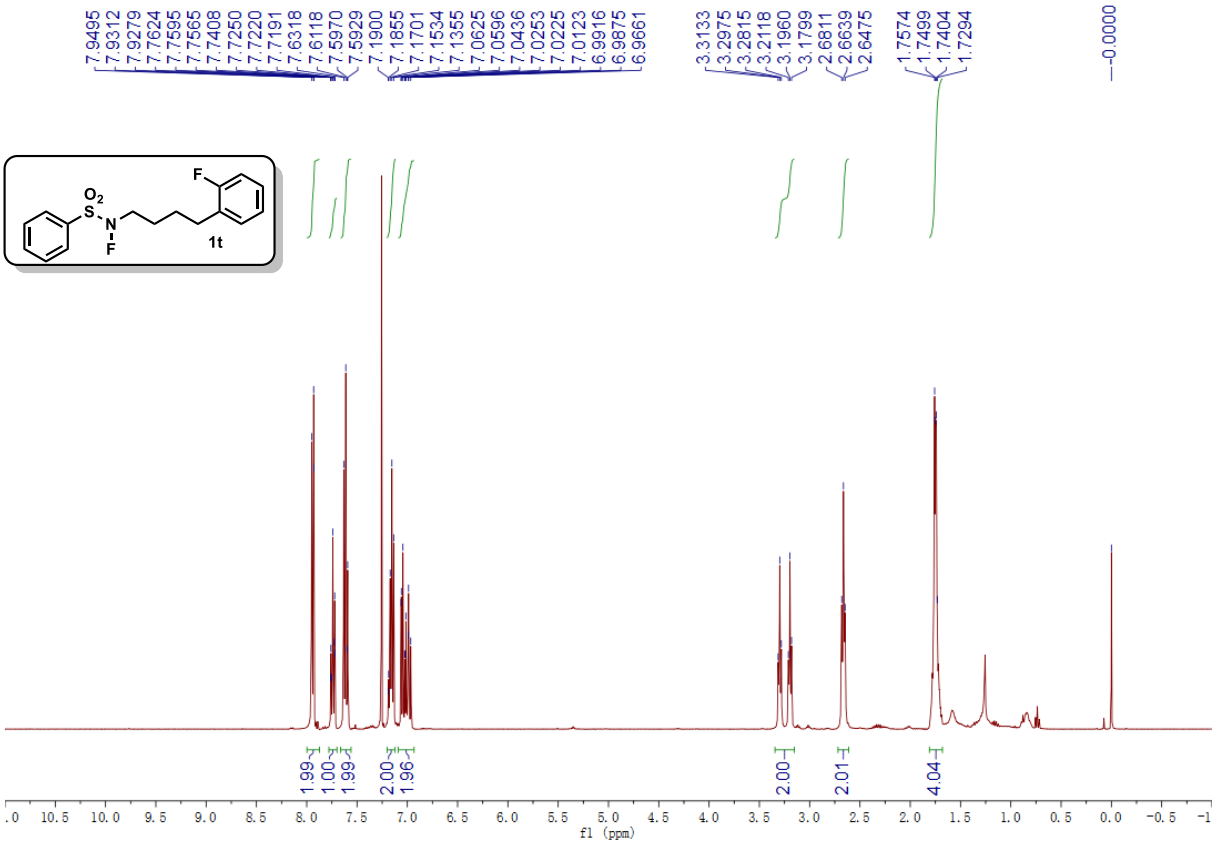

Figure S54. ^{1}H NMR of **1t**, related to Figure 2.

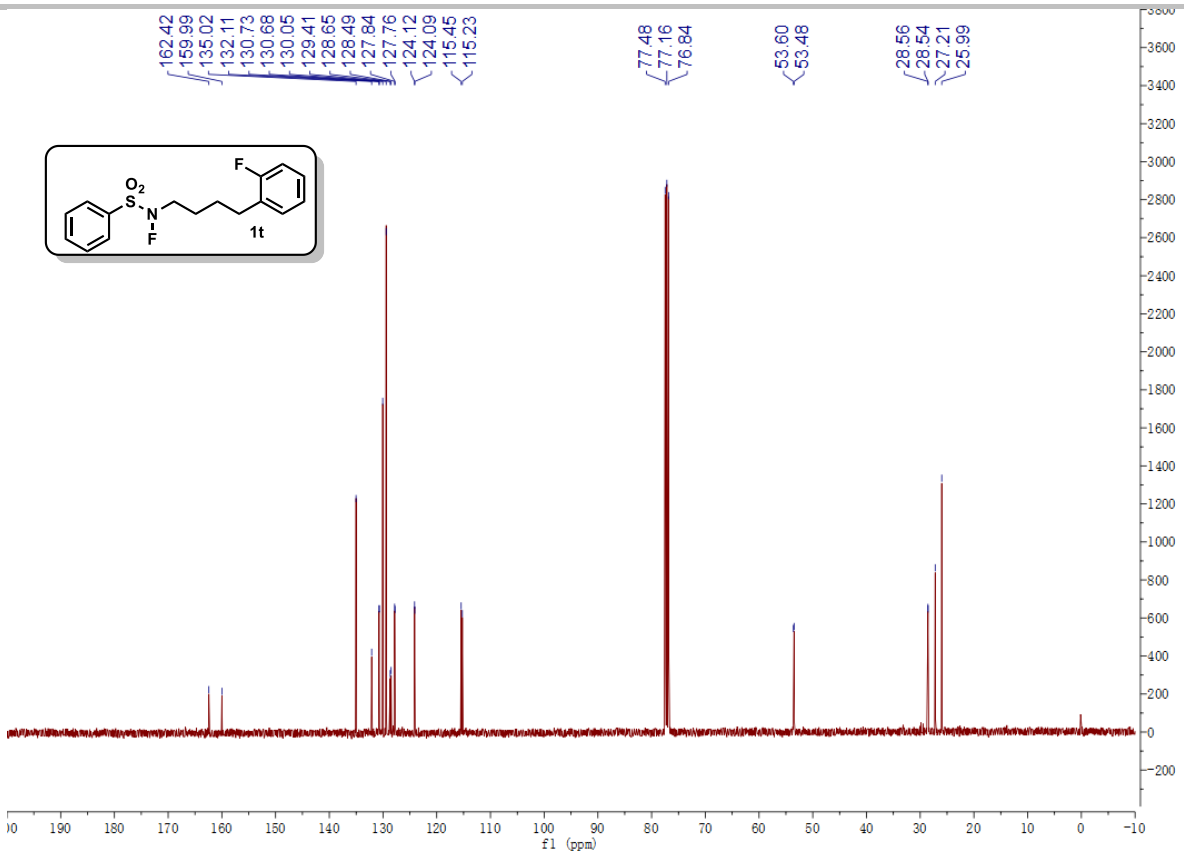

Figure S55. ^{13}C NMR of **1t**, related to Figure 2.

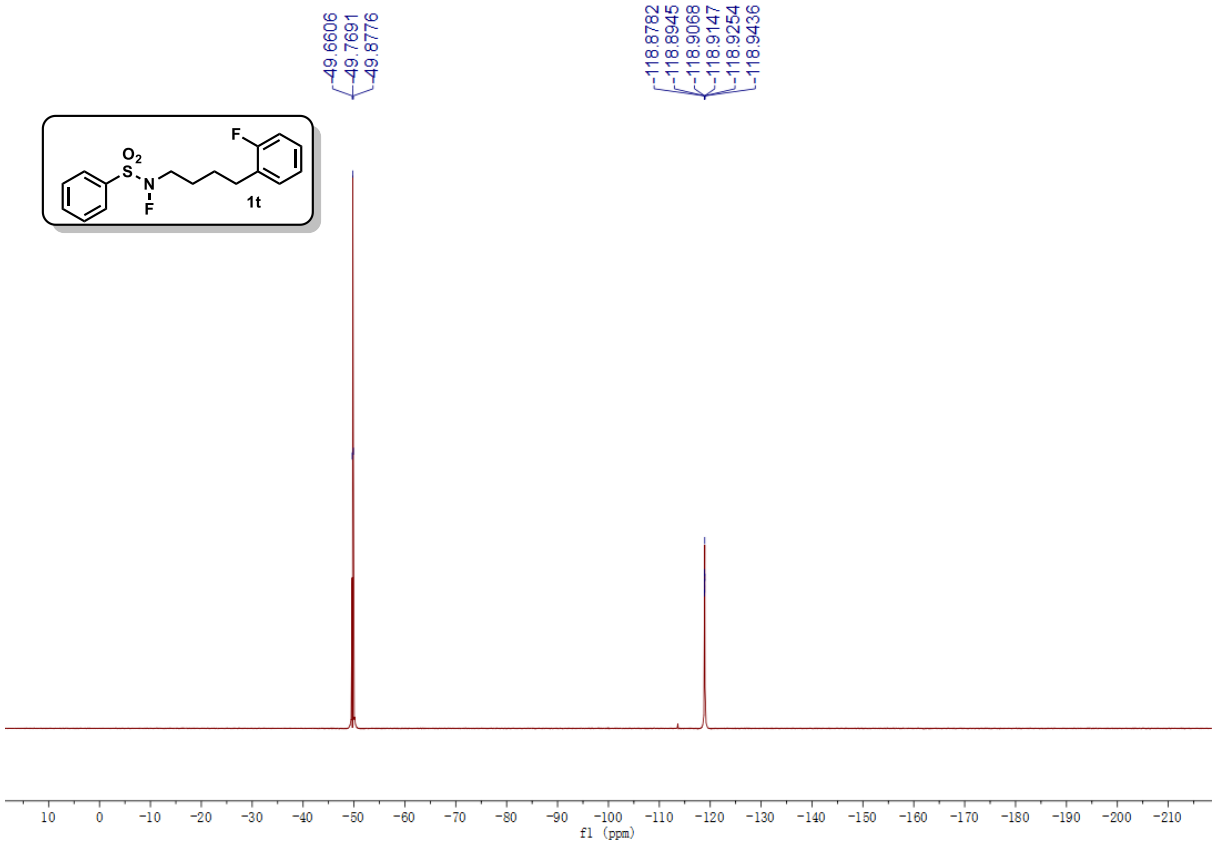

Figure S56. ^{19}F NMR of **1t**, related to Figure 2.

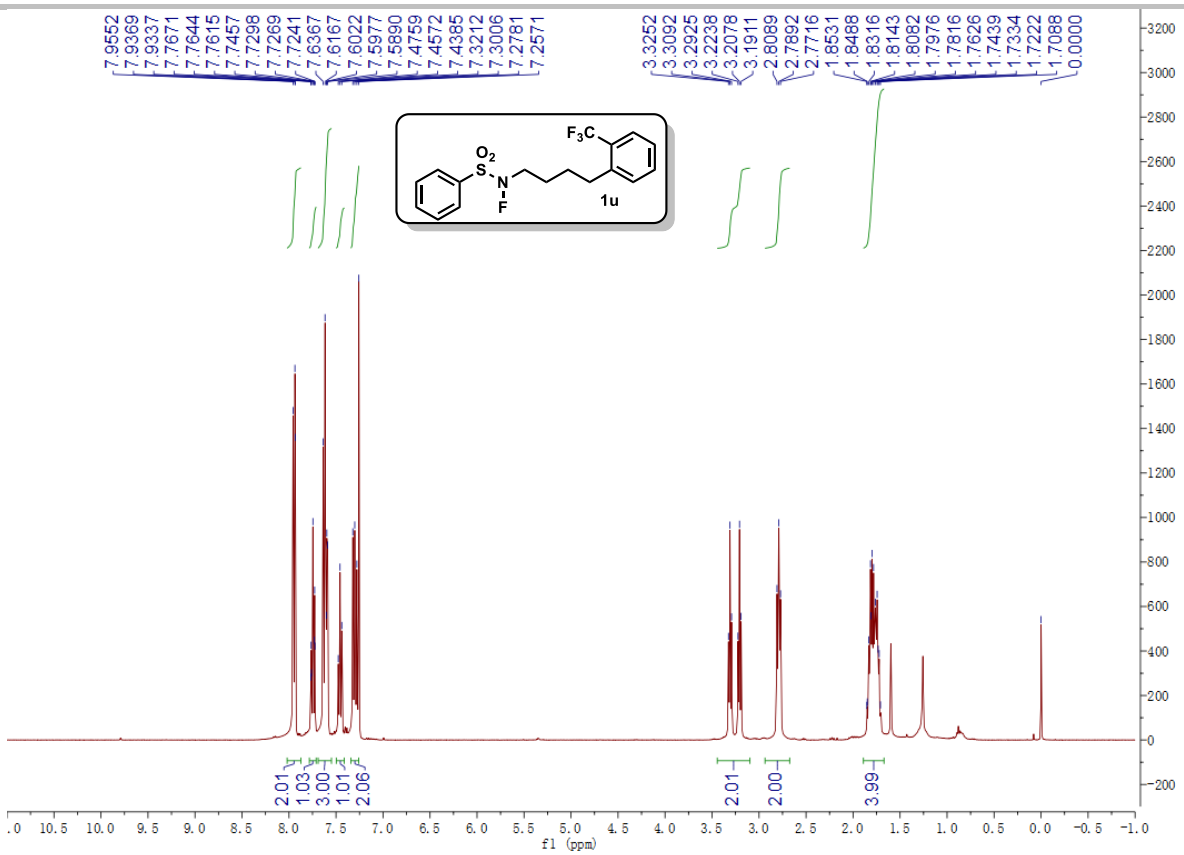

Figure S57. ^{1}H NMR of **1u**, related to Figure 2.

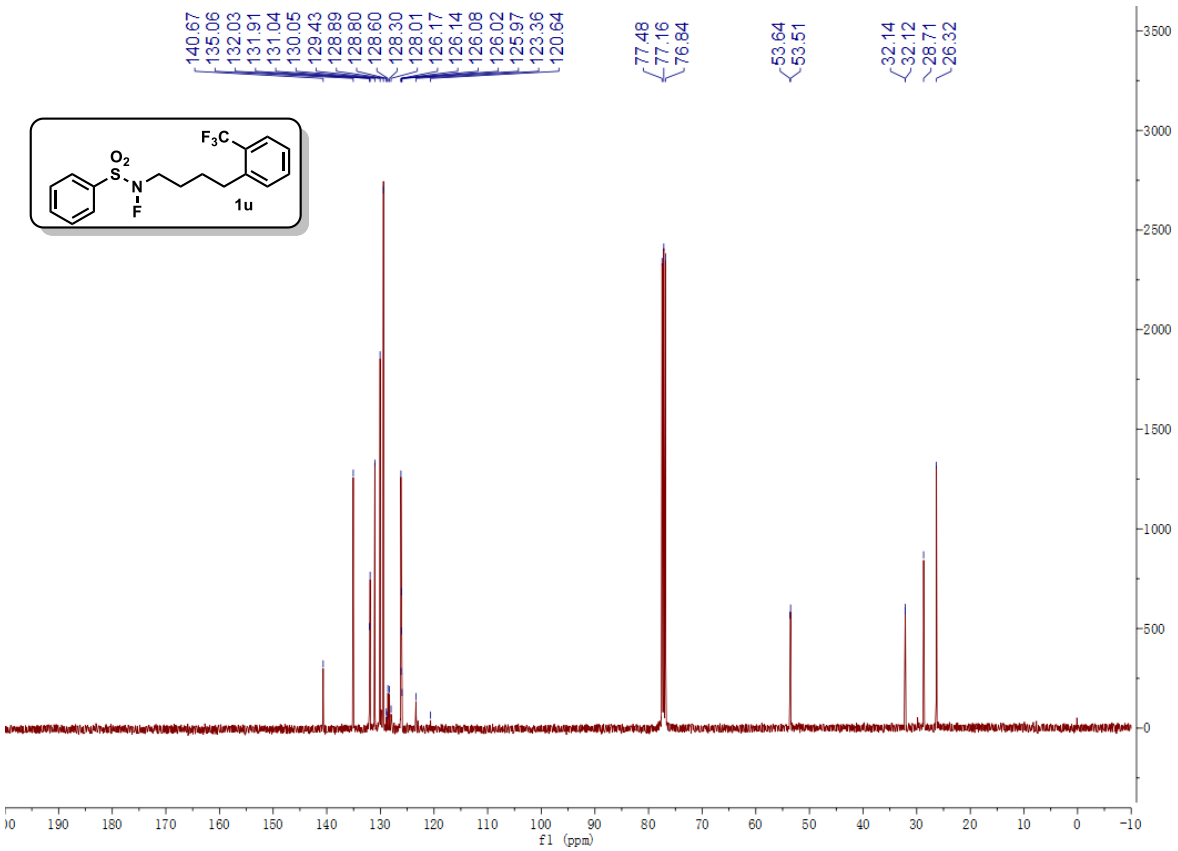

Figure S58. ^{13}C NMR of **1u**, related to Figure 2.

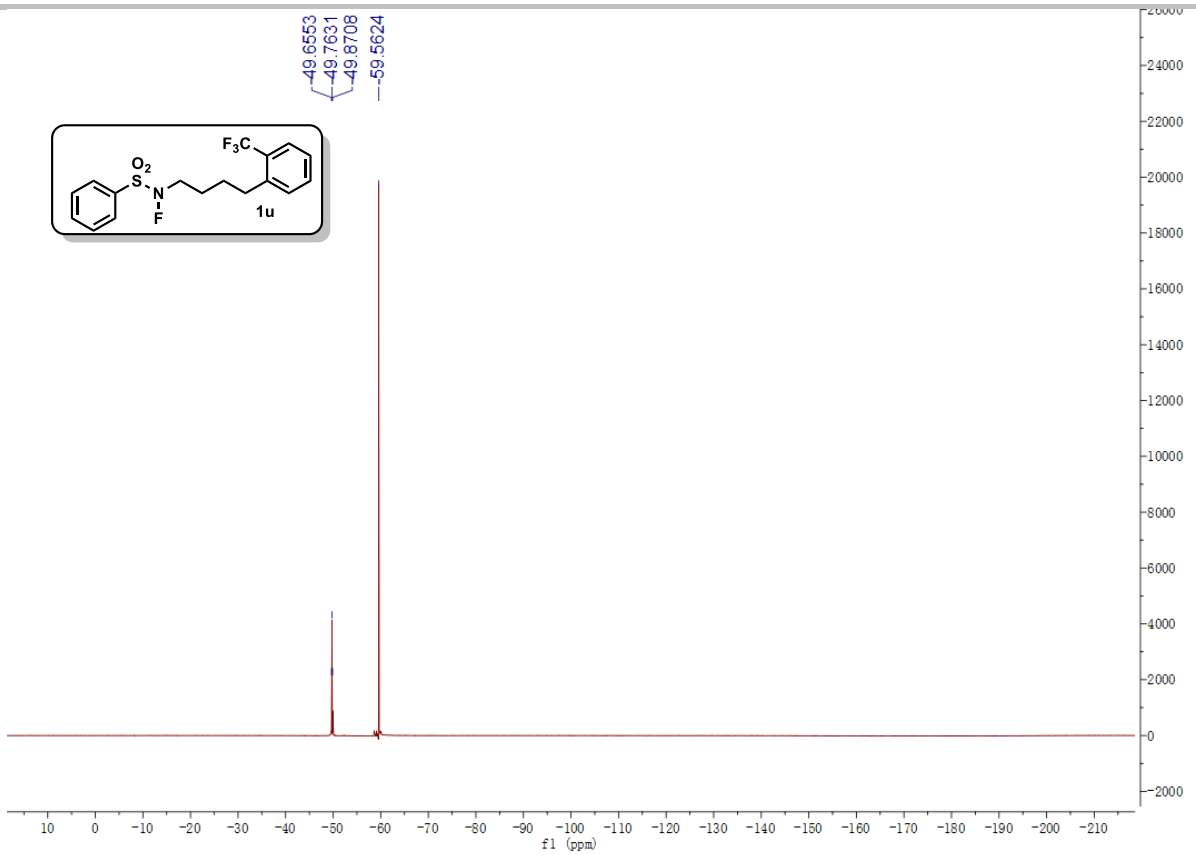

Figure S59. ^{19}F NMR of **1u**, related to Figure 2.

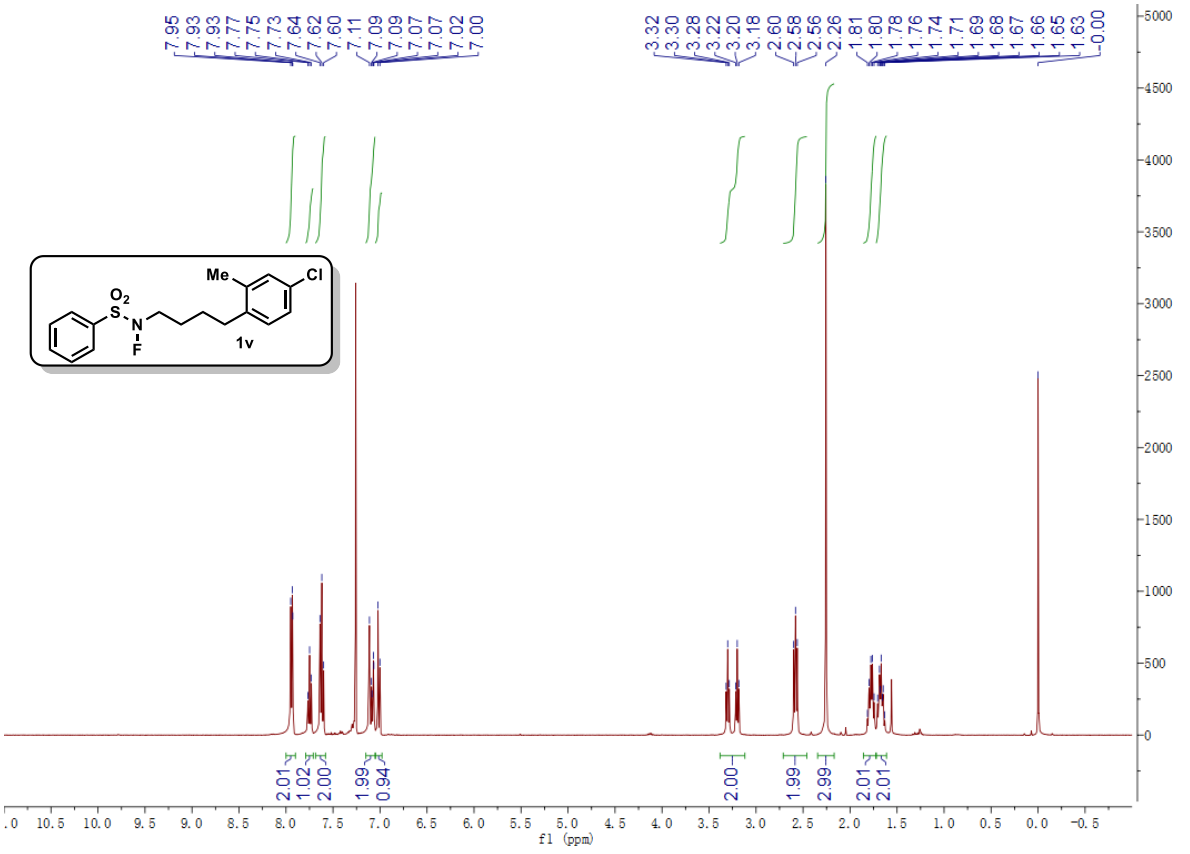

Figure S60. ^{1}H NMR of **1v**, related to Figure 2.

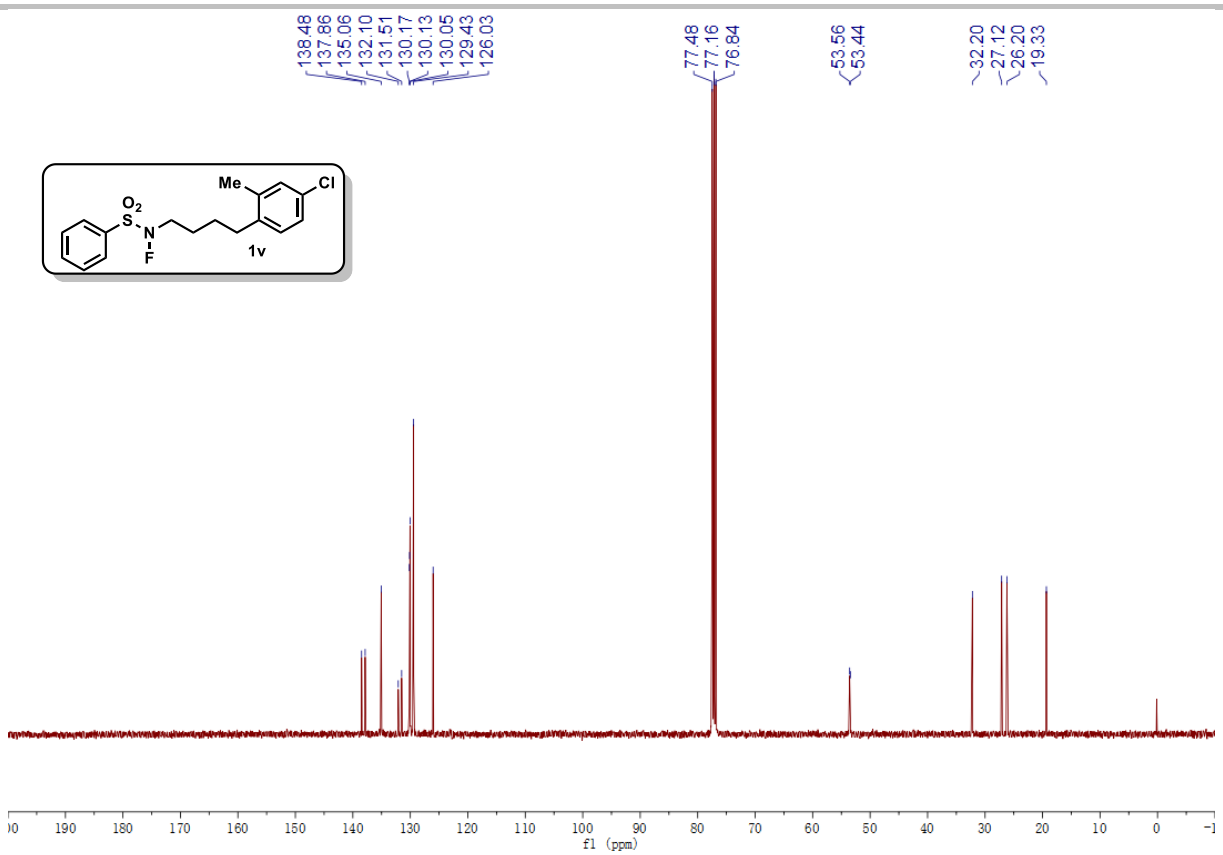

Figure S61. ^{13}C NMR of **1v**, related to Figure 2.

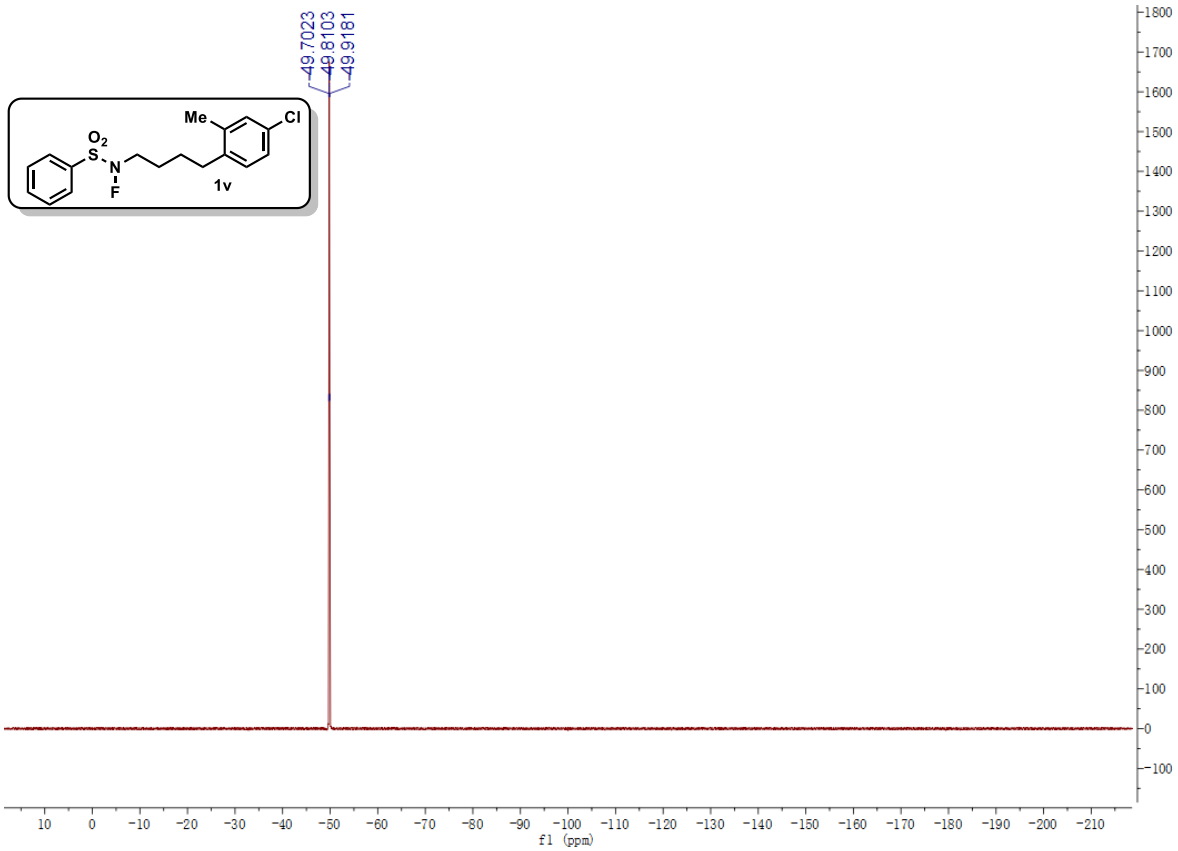

Figure S62. ^{19}F NMR of **1v**, related to Figure 2.

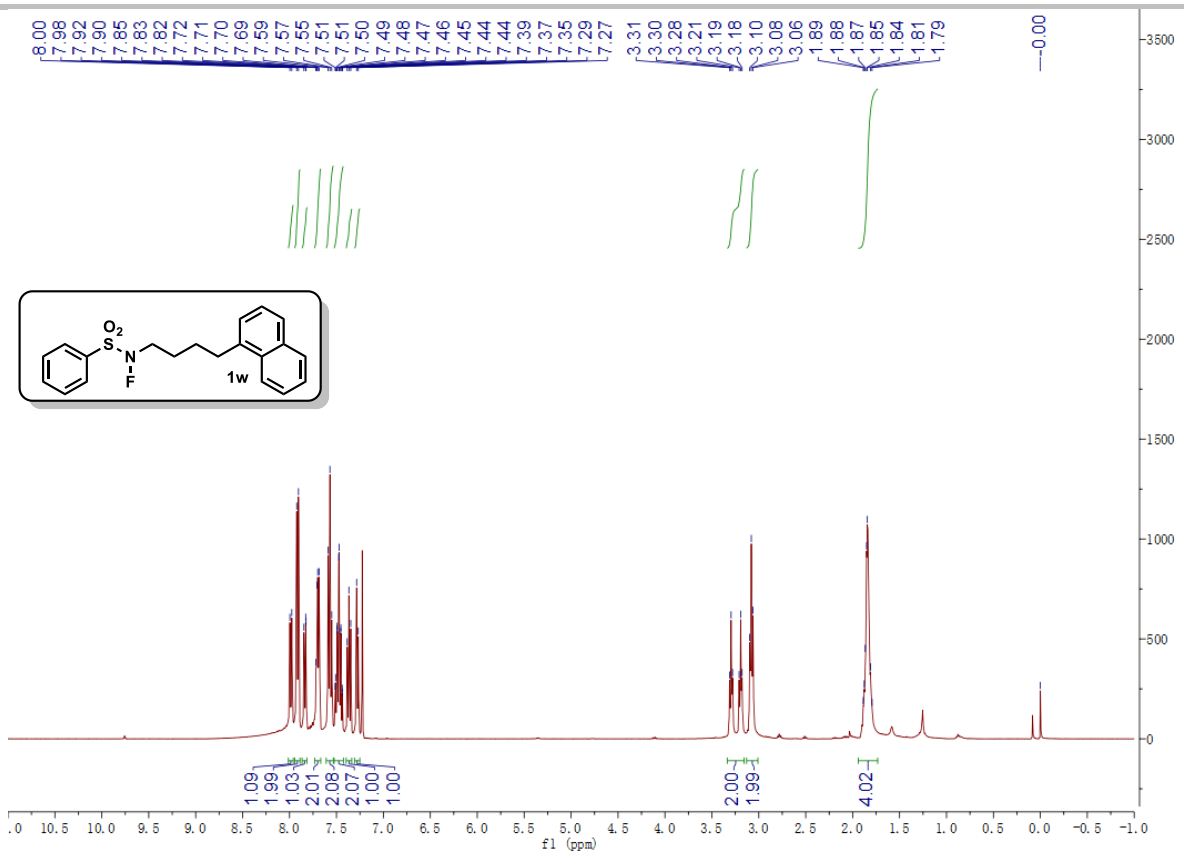

Figure S63. ^{1}H NMR of **1w**, related to Figure 2.

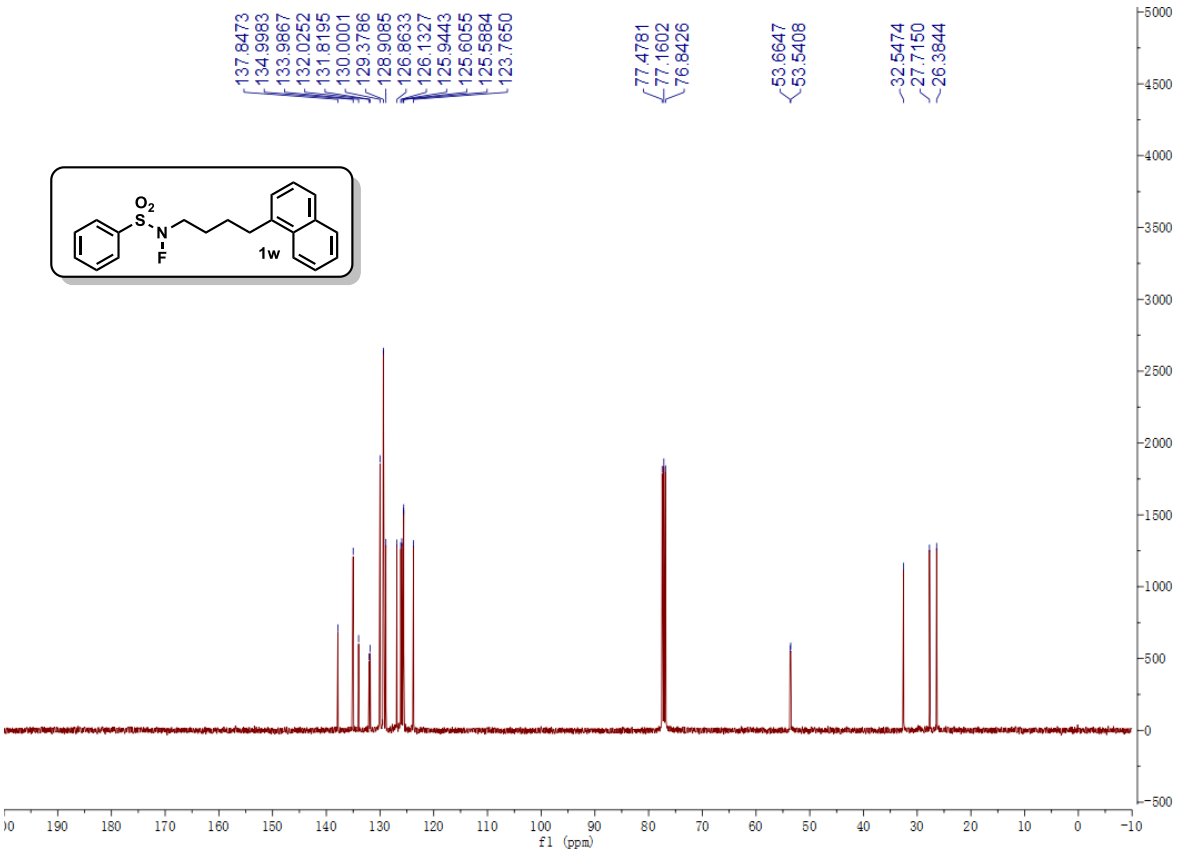

Figure S64. ^{13}C NMR of **1w**, related to Figure 2.

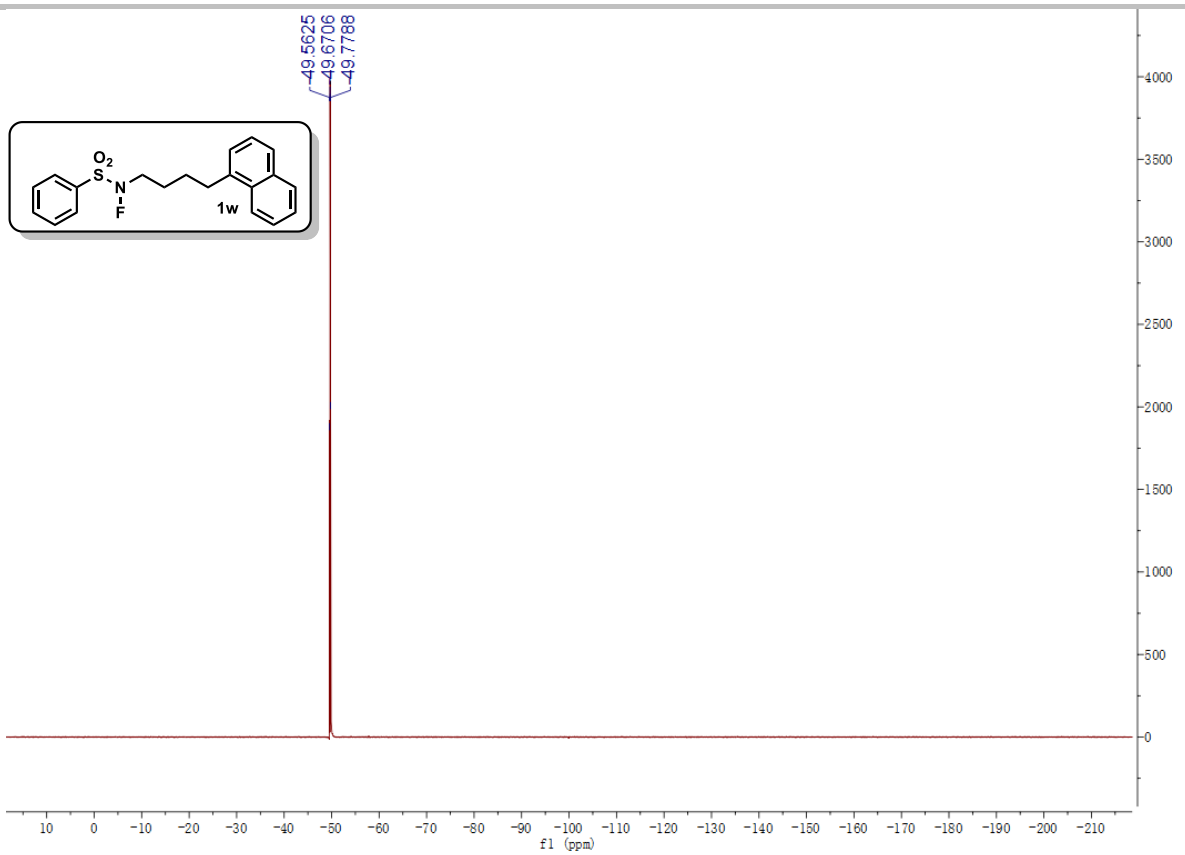

Figure S65. ^{19}F NMR of **1w**, related to Figure 2.

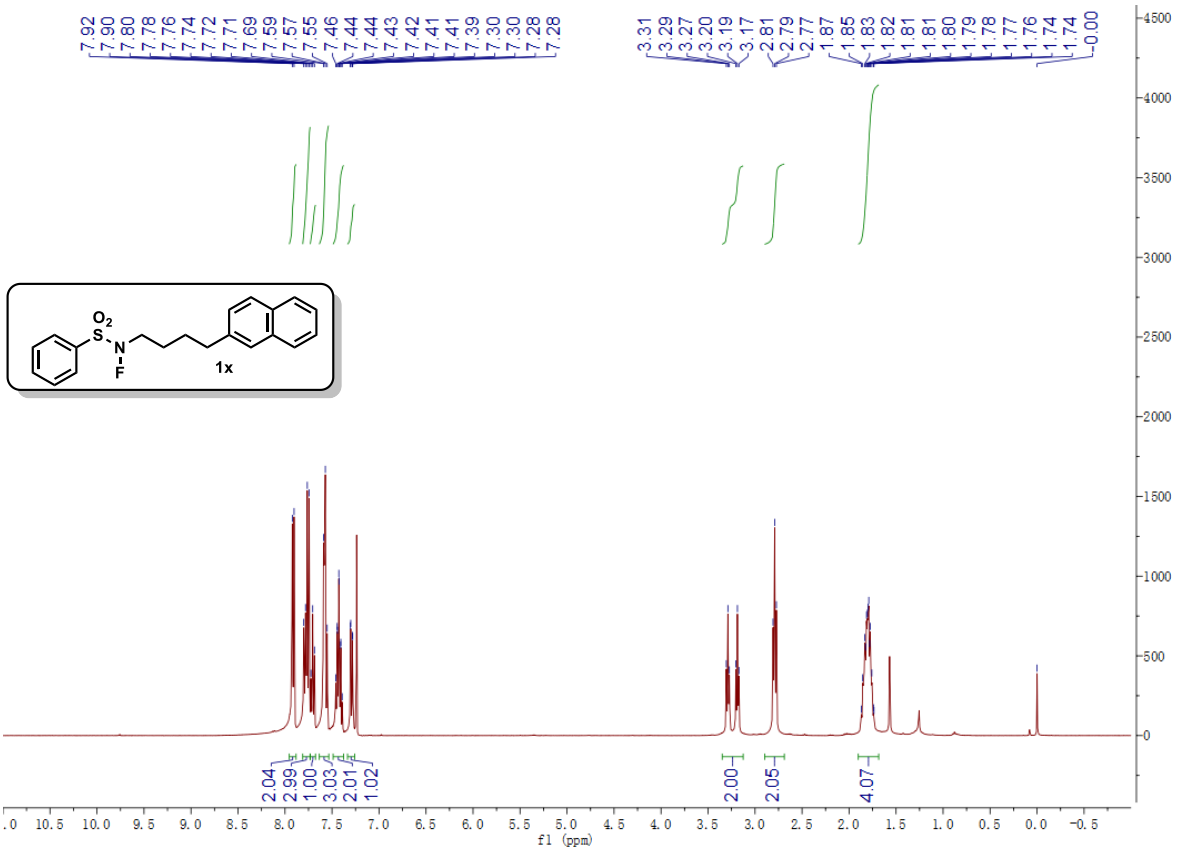

Figure S66. ^{1}H NMR of **1x**, related to Figure 2.

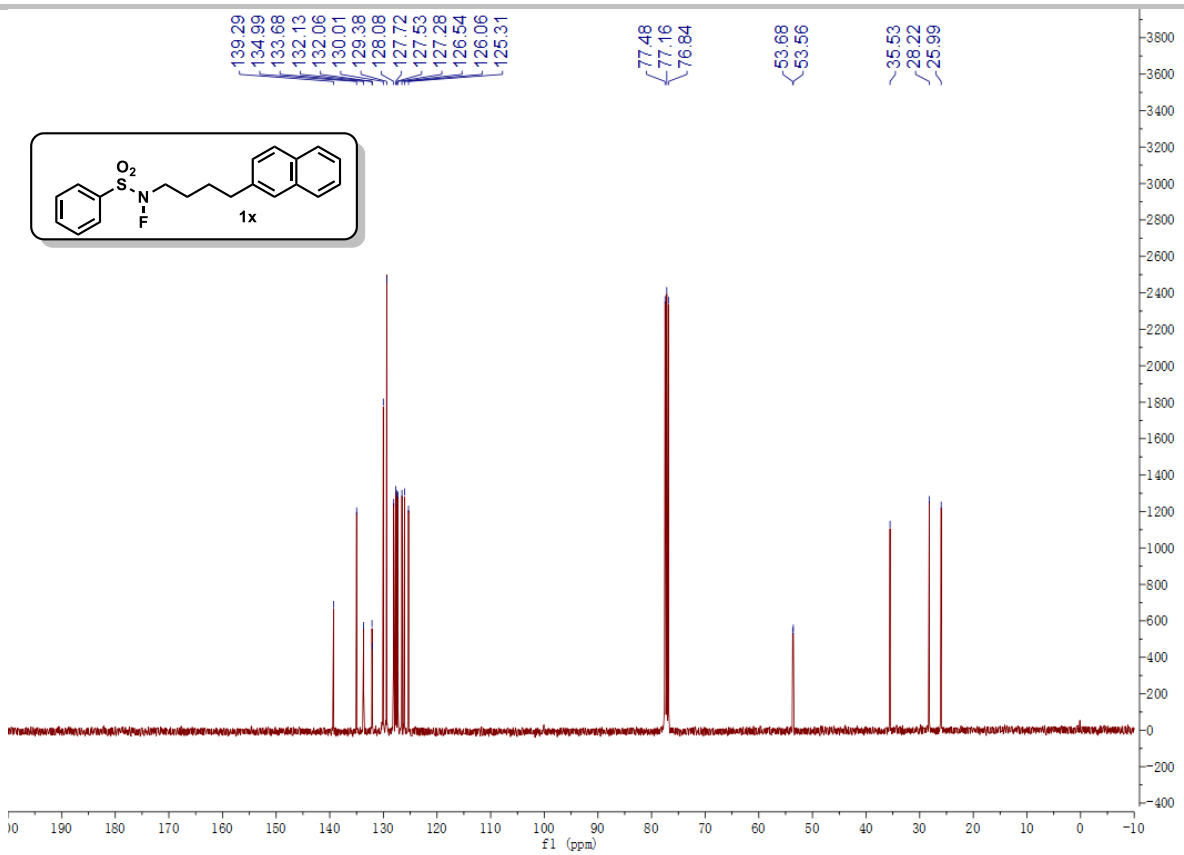

Figure S67. ^{13}C NMR of **1x**, related to Figure 2.

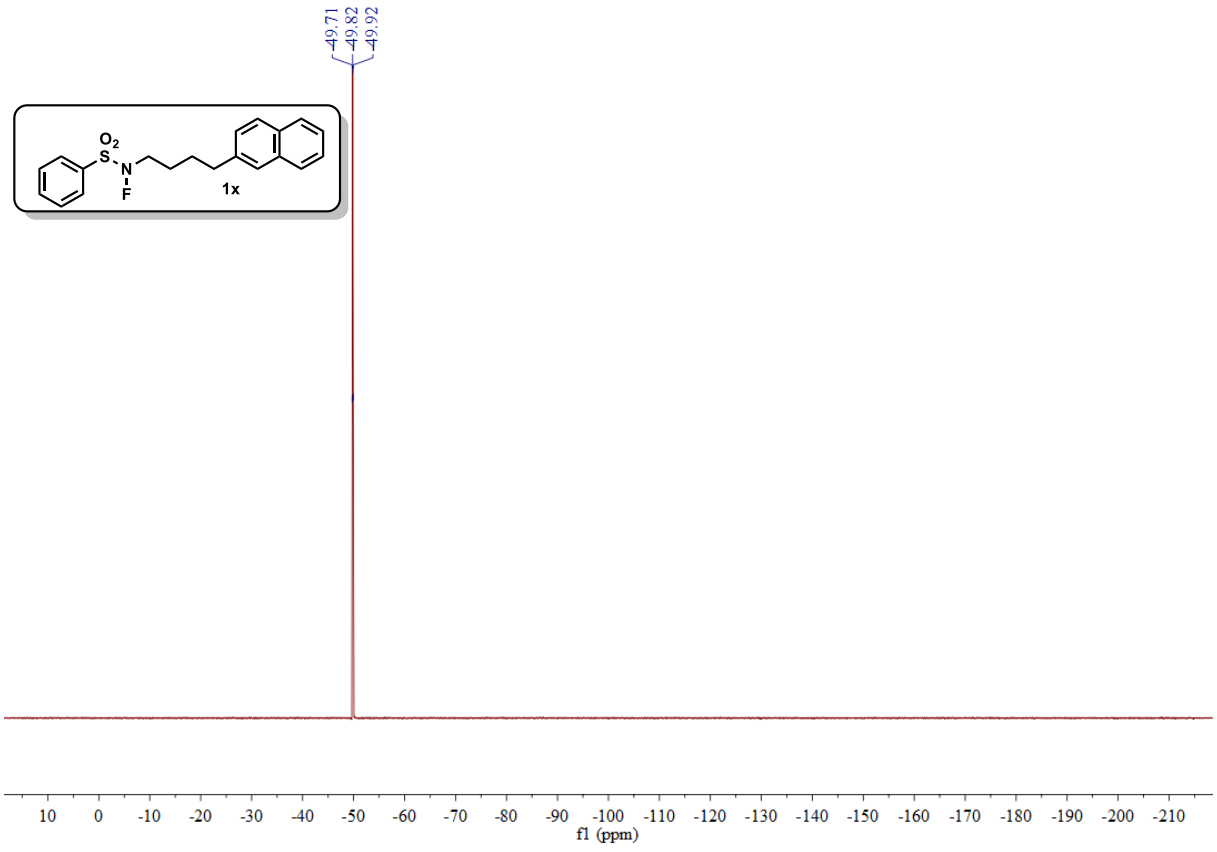

Figure S68. ^{19}F NMR of **1x**, related to Figure 2.

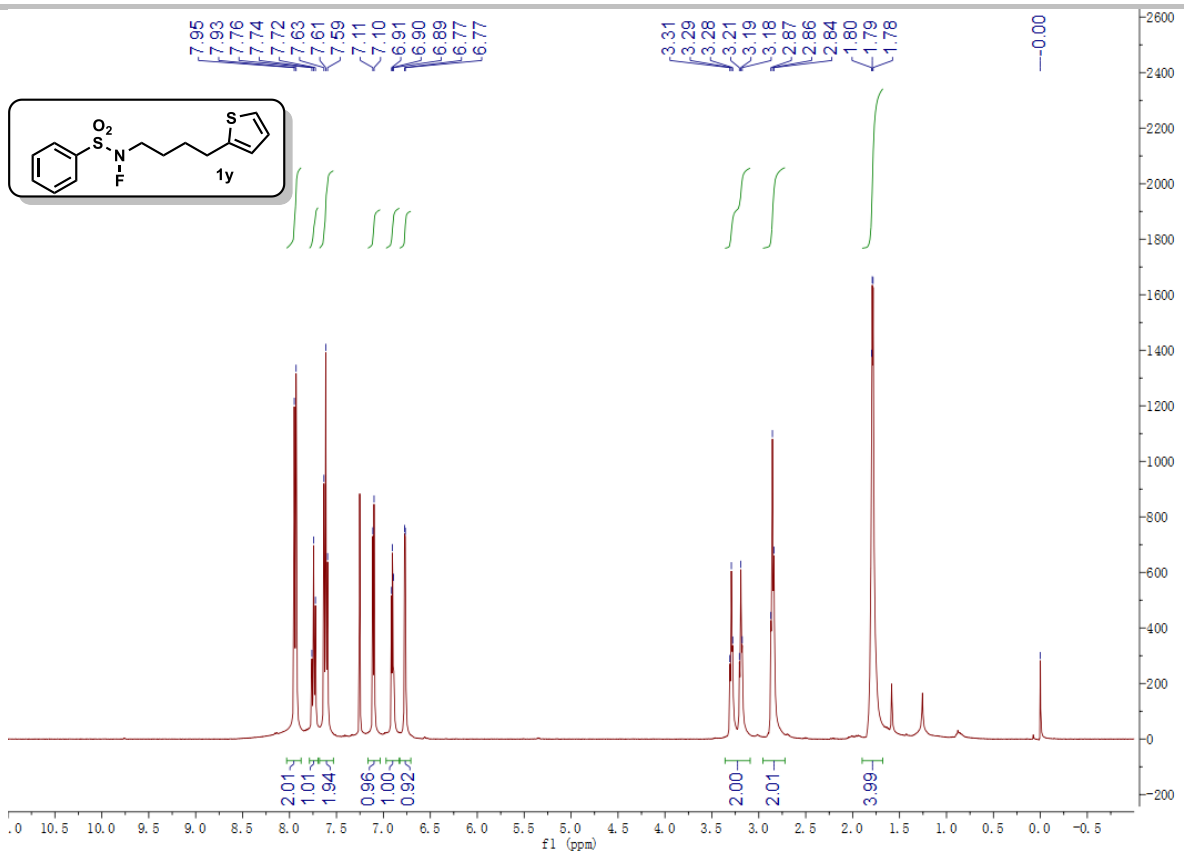

Figure S69. ^{1}H NMR of **1y**, related to Figure 2.

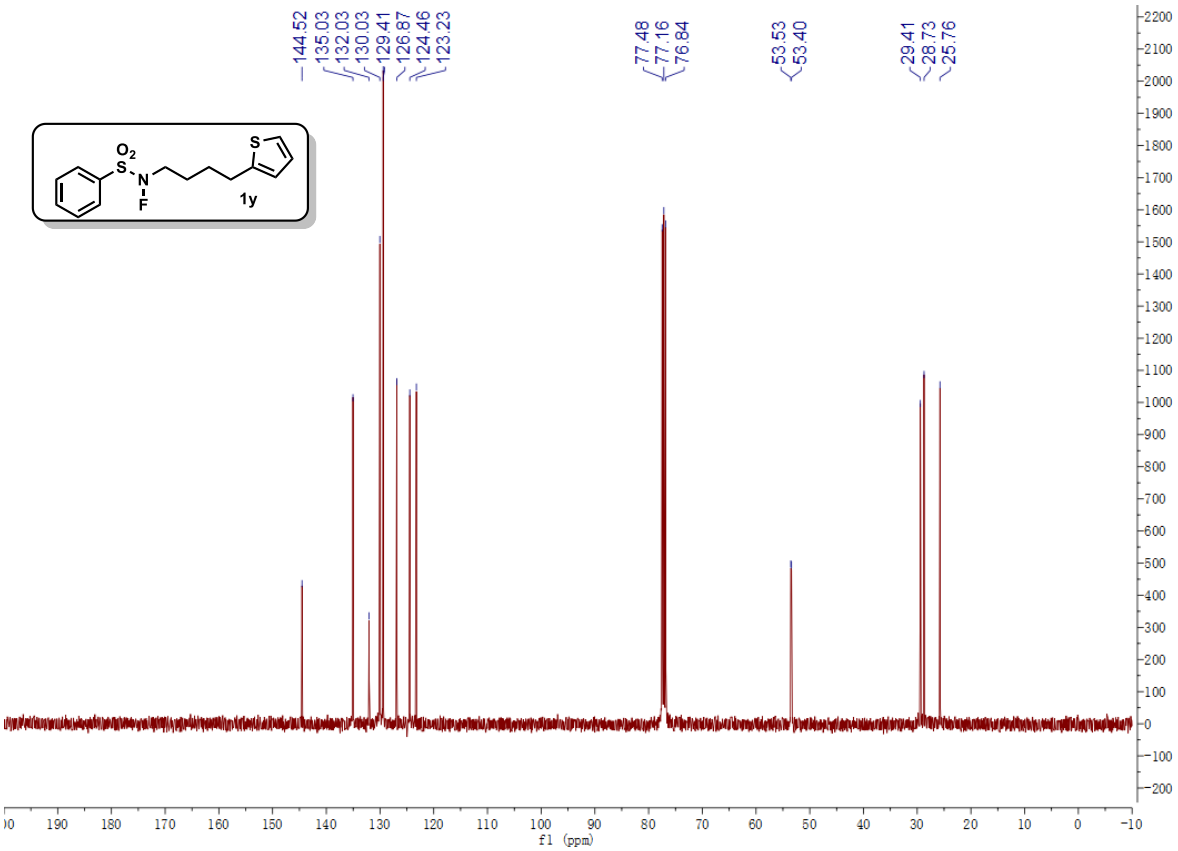

Figure S70. ^{13}C NMR of **1y**, related to Figure 2.

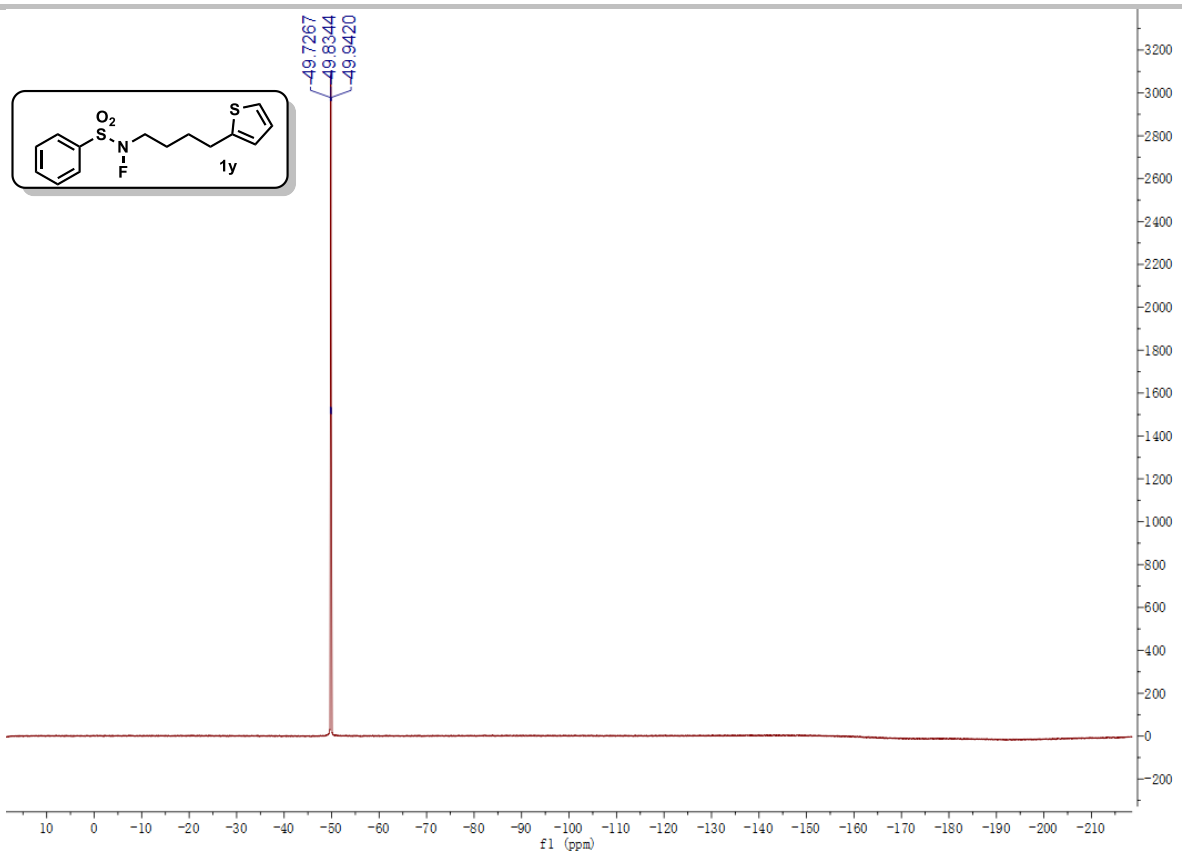

Figure S71. ^{19}F NMR of **1y**, related to Figure 2.

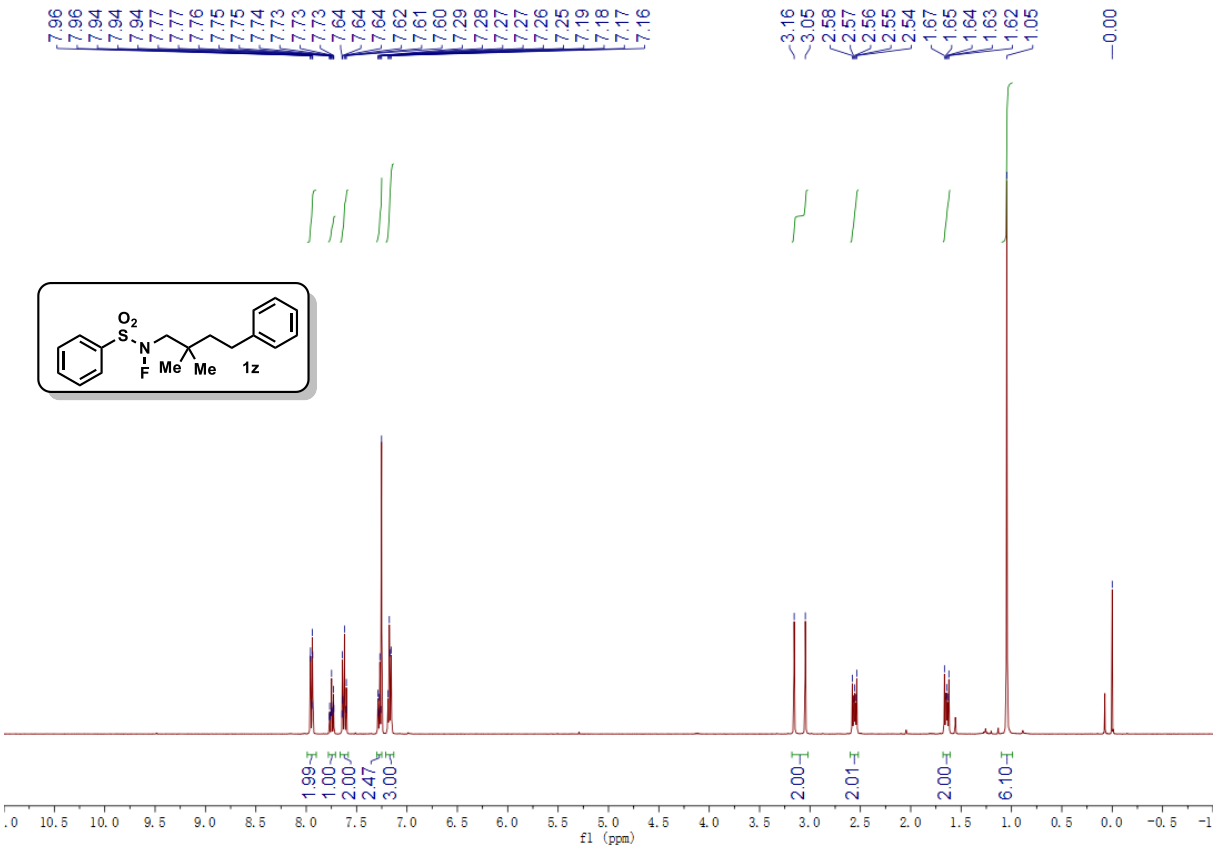

Figure S72. ^{1}H NMR of **1z**, related to Figure 2.

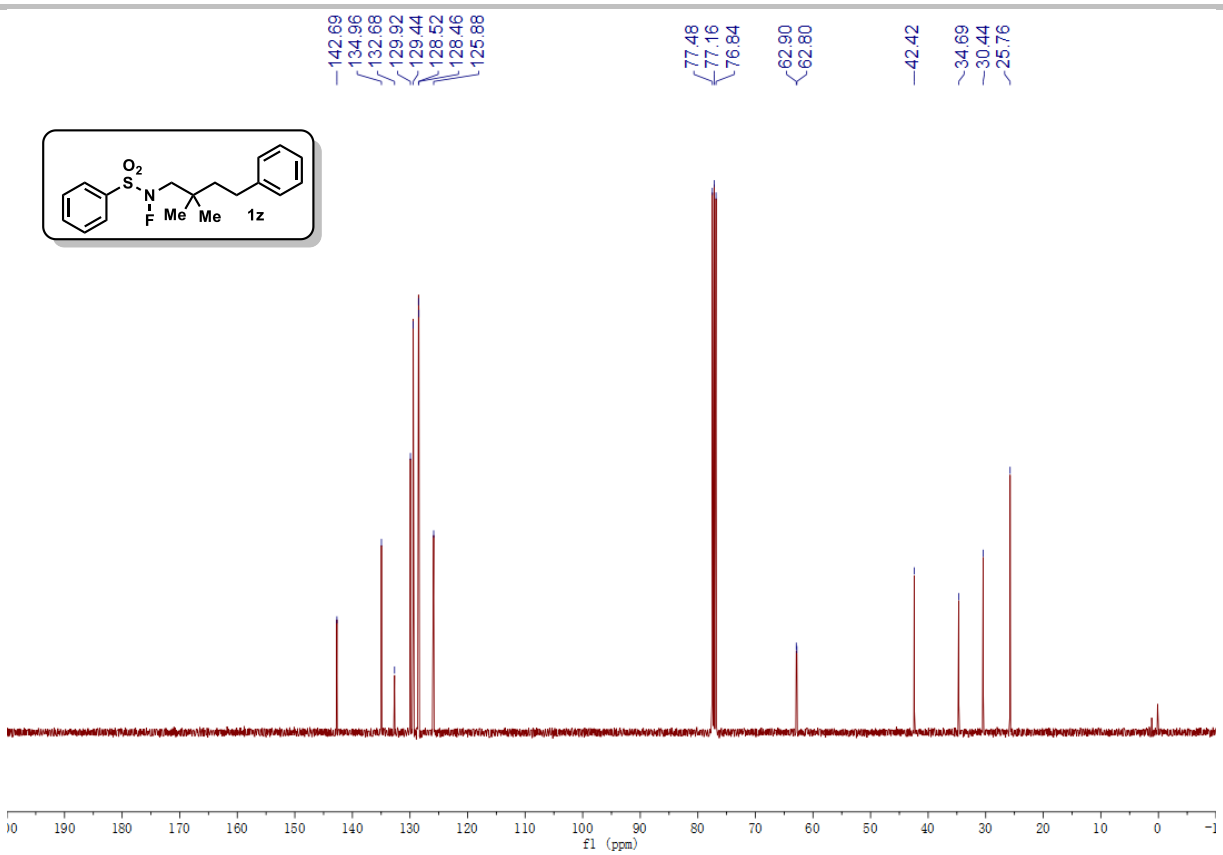

Figure S73. ^{13}C NMR of **1z**, related to Figure 2.

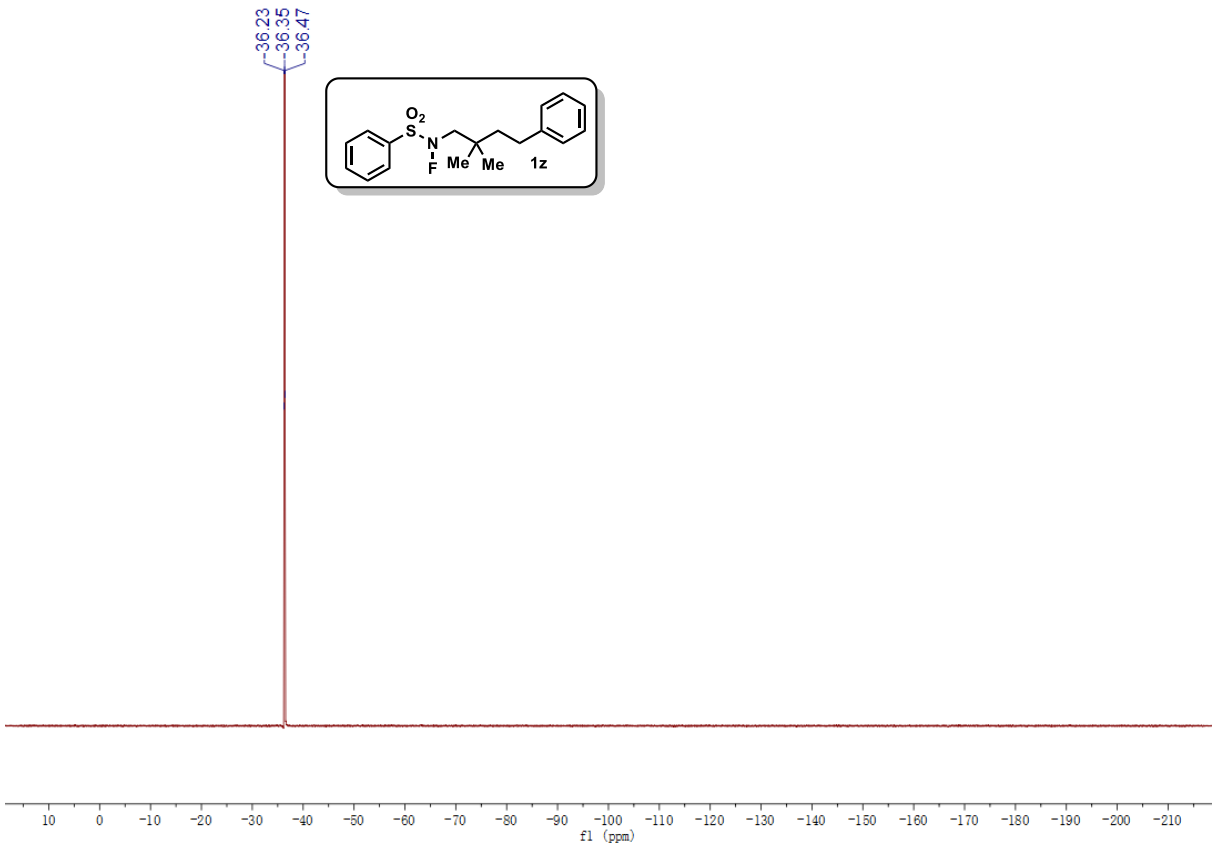

Figure S74. ^{19}F NMR of **1z**, related to Figure 2.

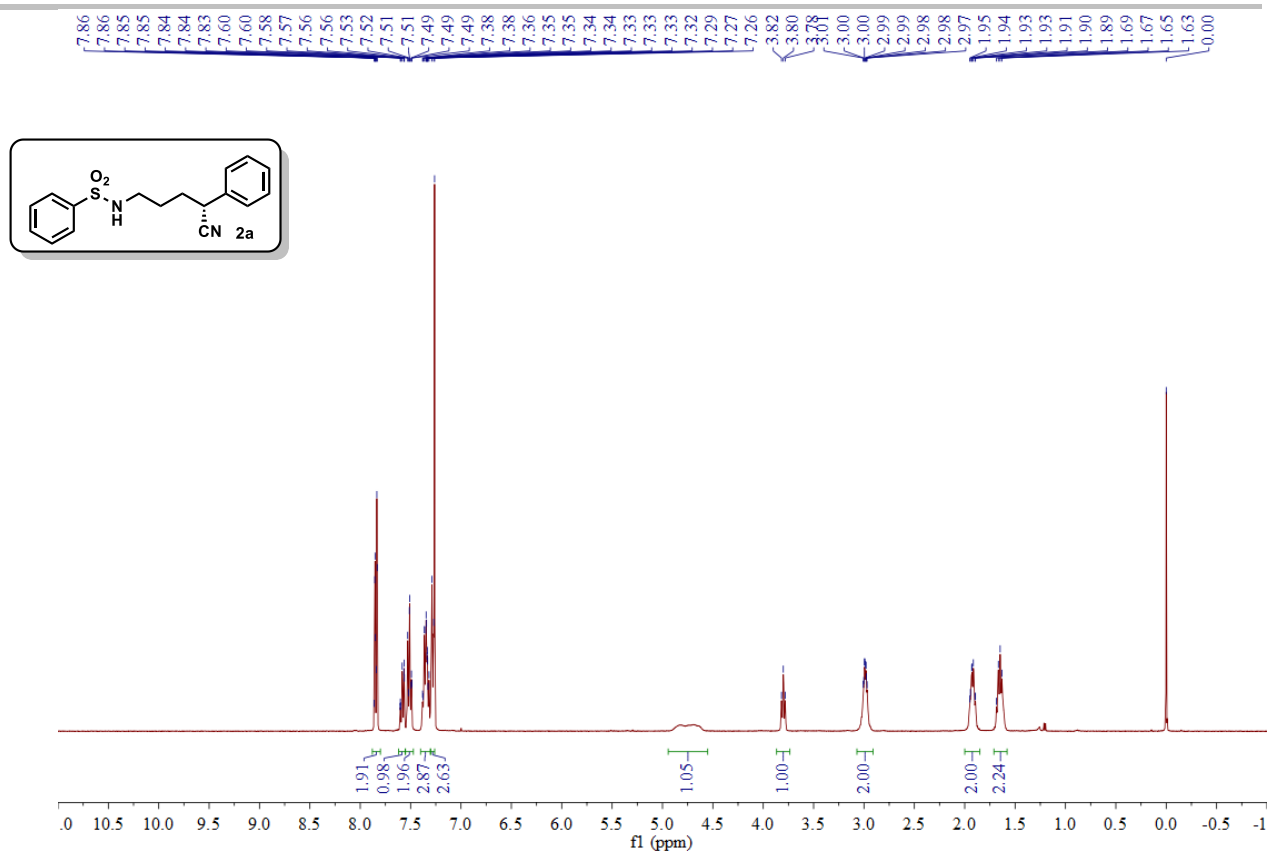

Figure S75. ^{1}H NMR of **2a**, related to Figure 2.

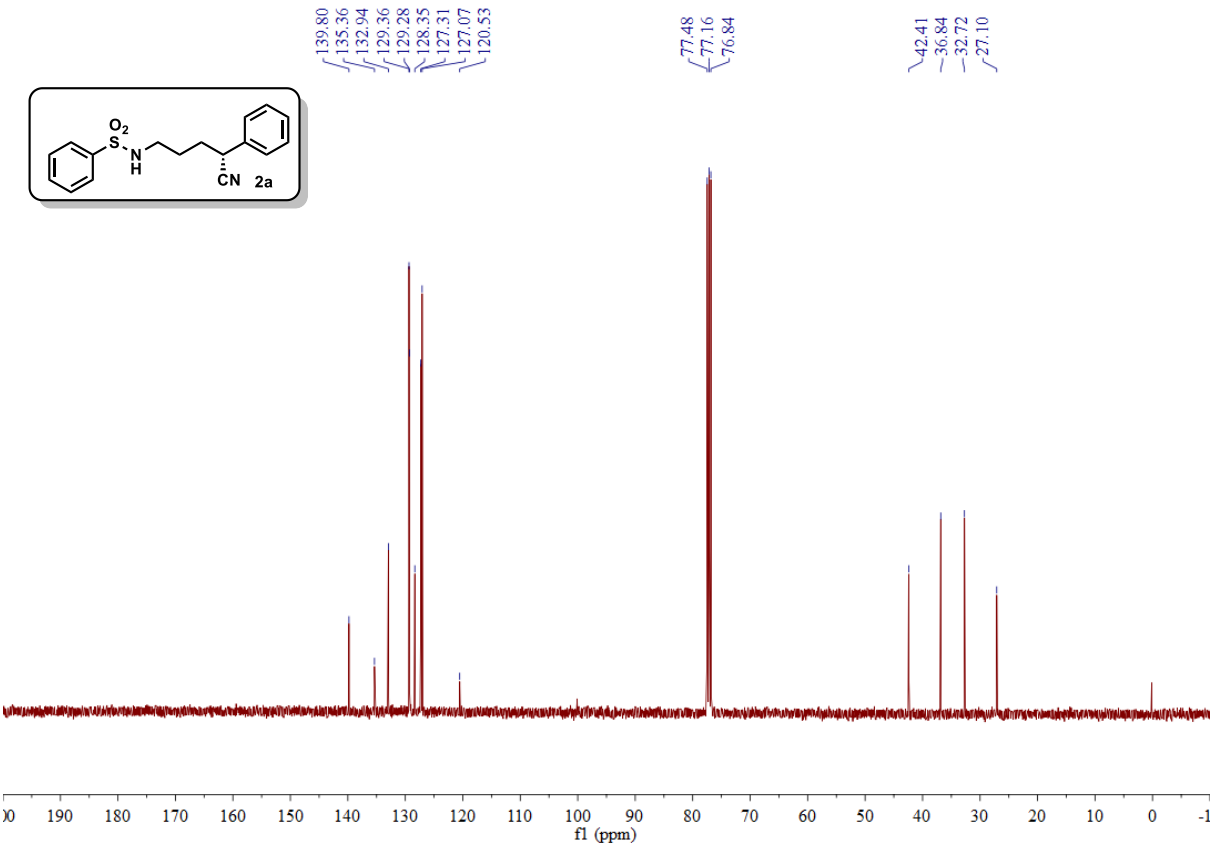

Figure S76. ^{13}C NMR of **2a**, related to Figure 2.

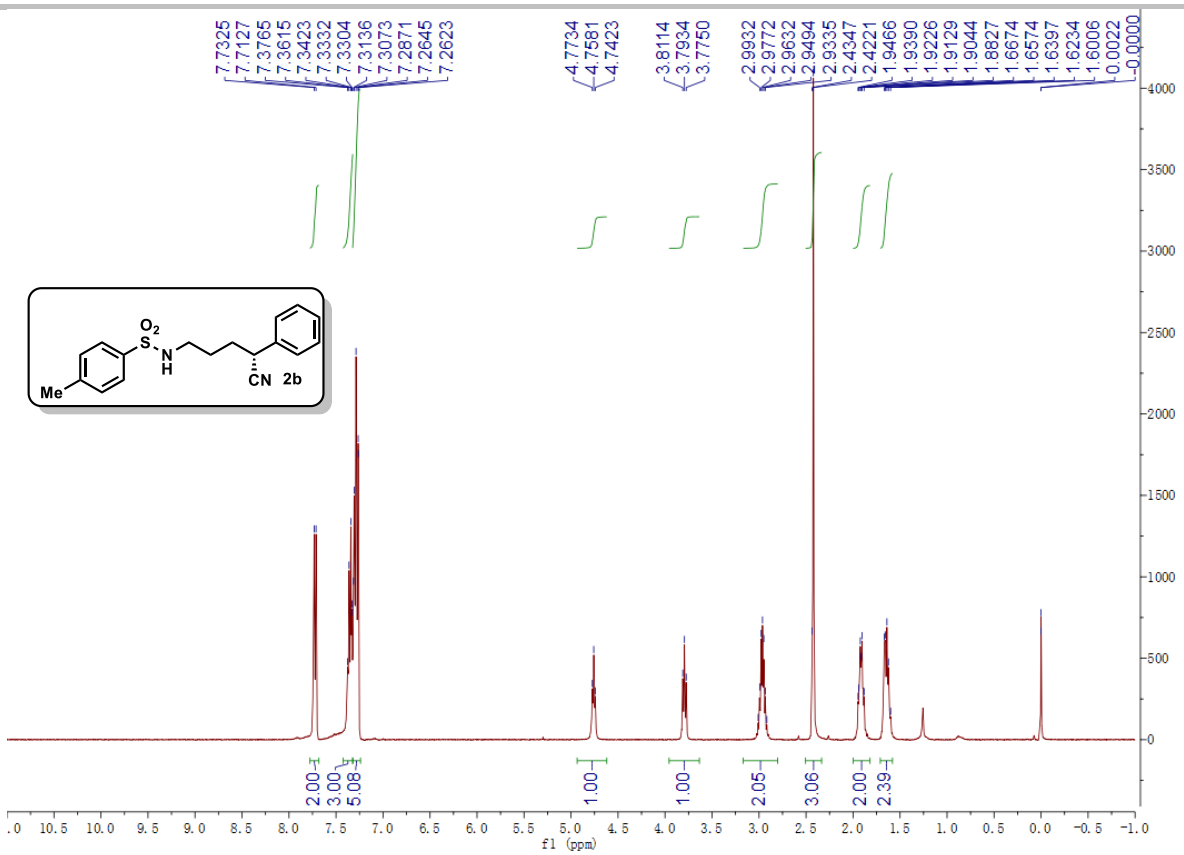

Figure S77. ^{1}H NMR of **2b**, related to Figure 2.

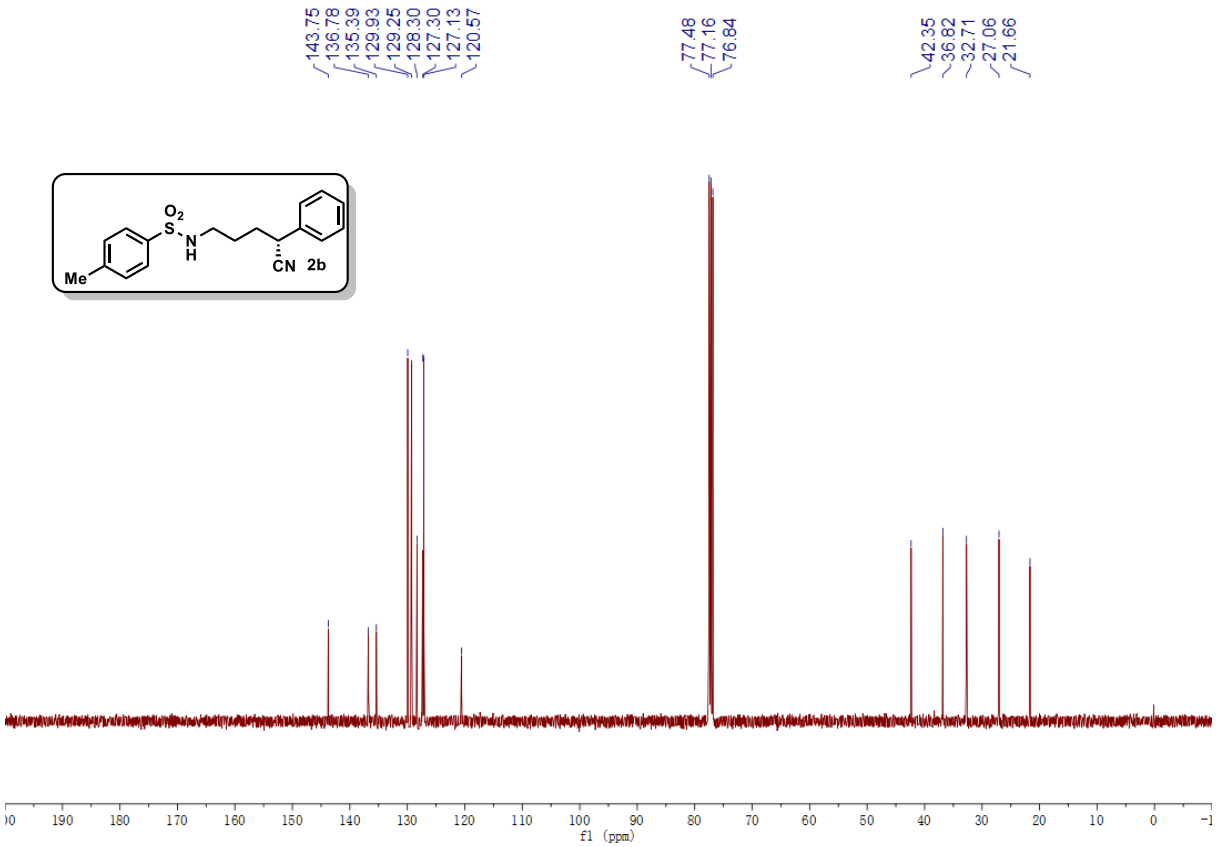

Figure S78. ^{13}C NMR of **2b**, related to Figure 2.

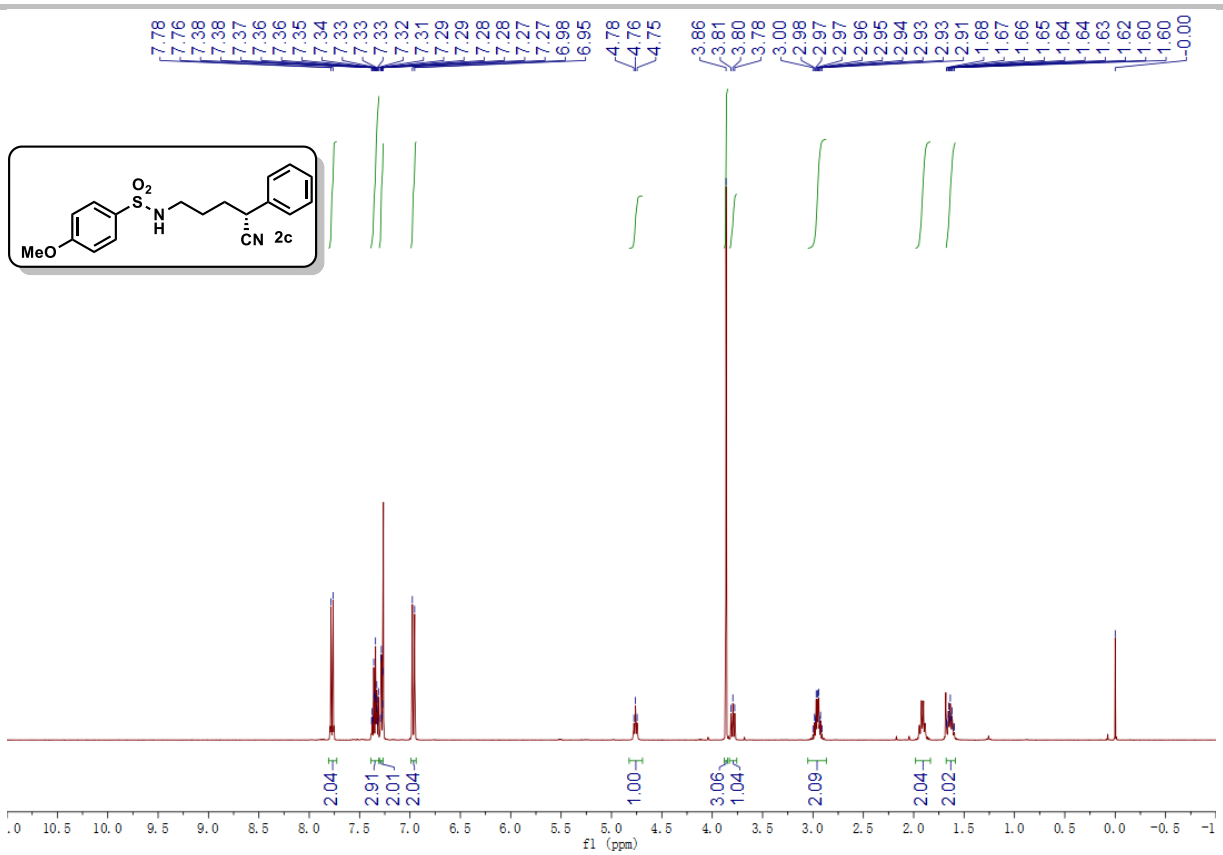

Figure S79. ^{1}H NMR of **2c**, related to Figure 2.

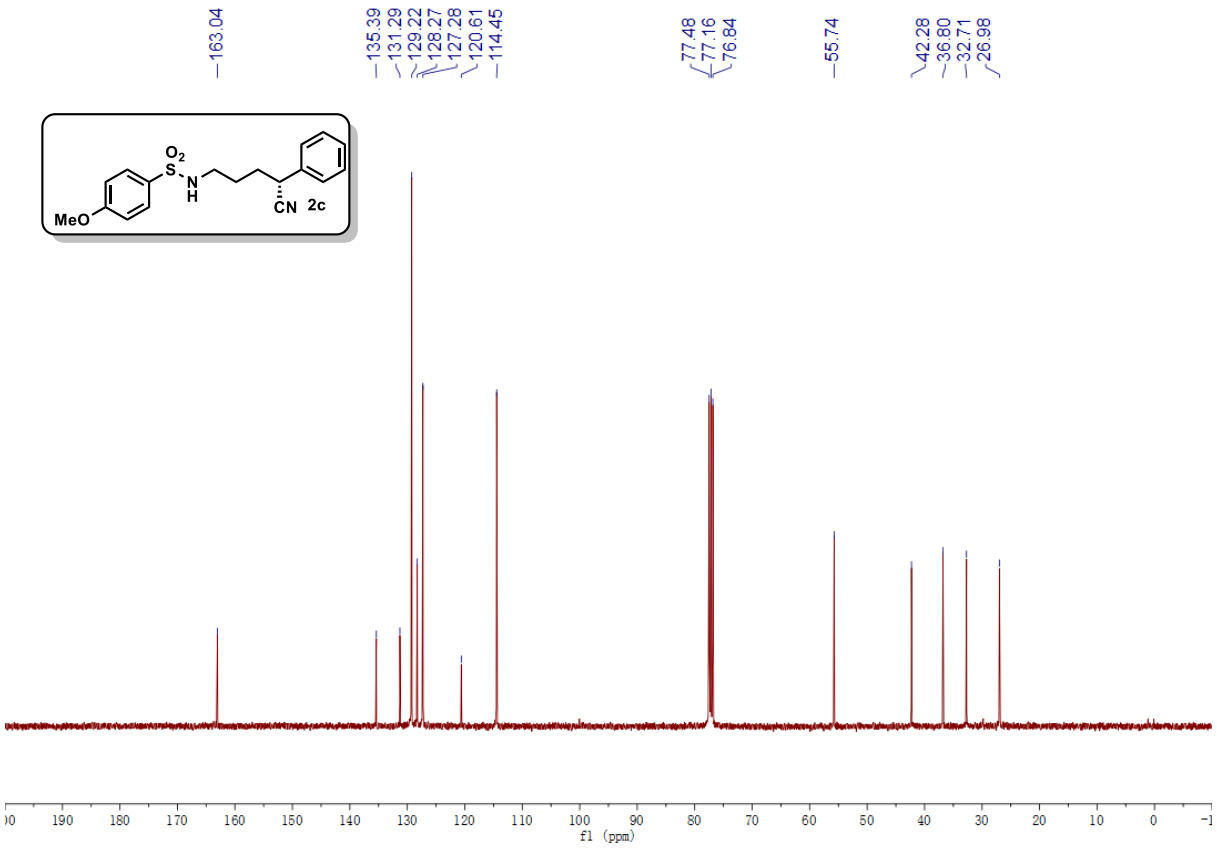

Figure S80. ^{13}C NMR of **2c**, related to Figure 2.

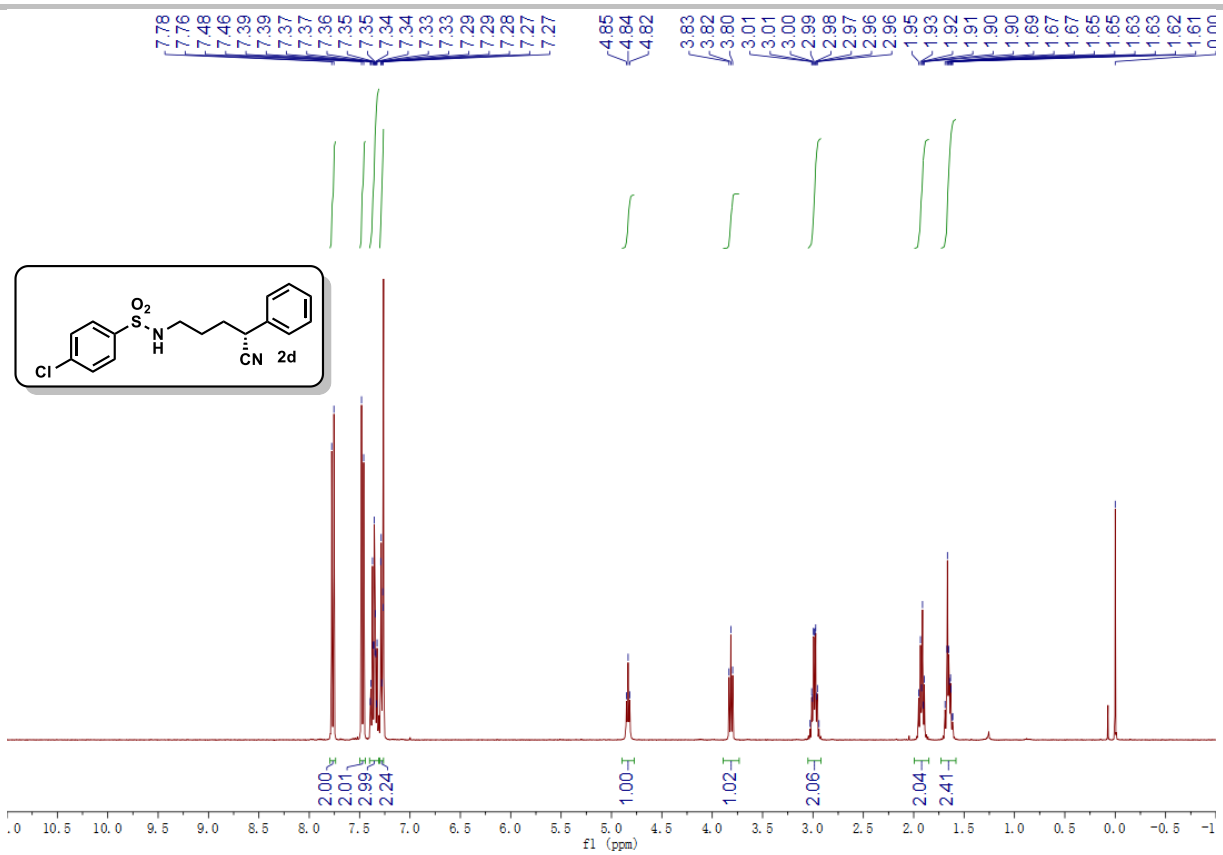

Figure S81. ^{1}H NMR of **2d**, related to Figure 2.

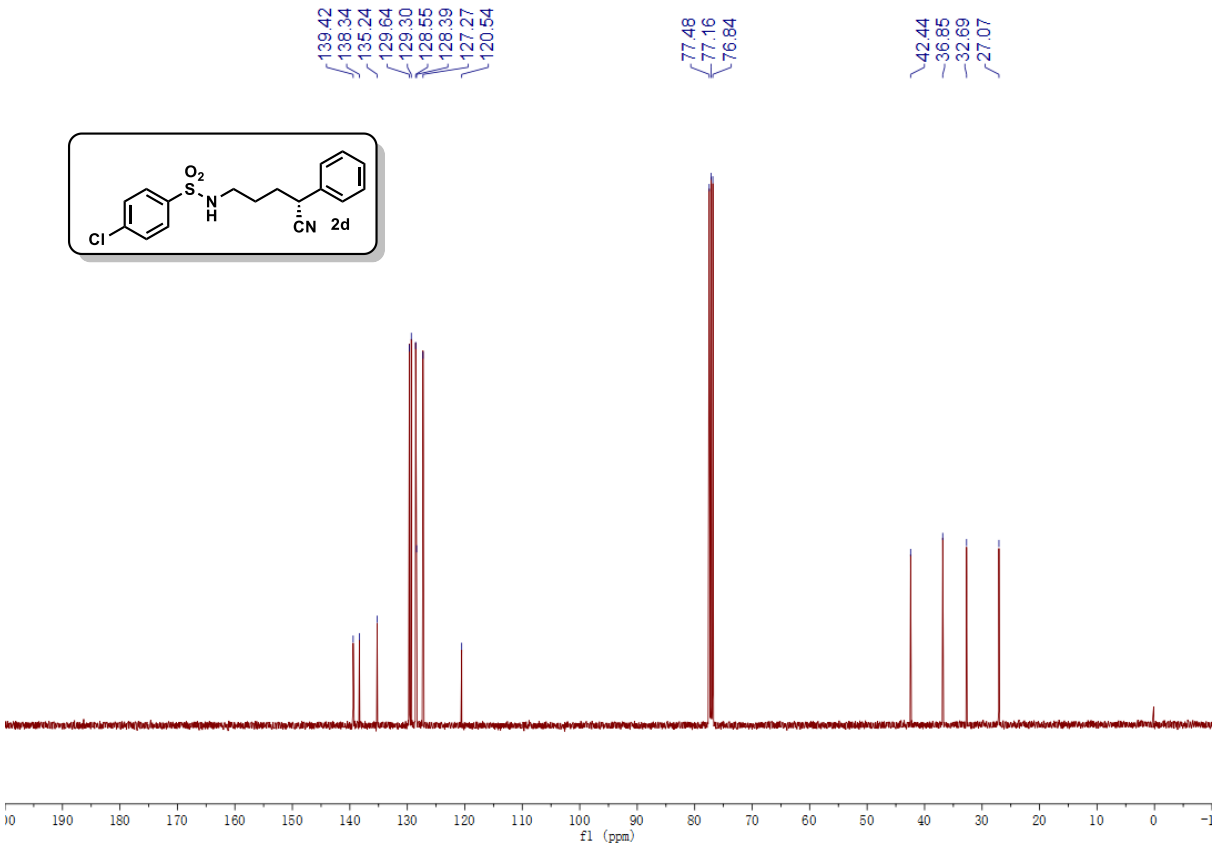

Figure S82. ^{13}C NMR of **2d**, related to Figure 2.

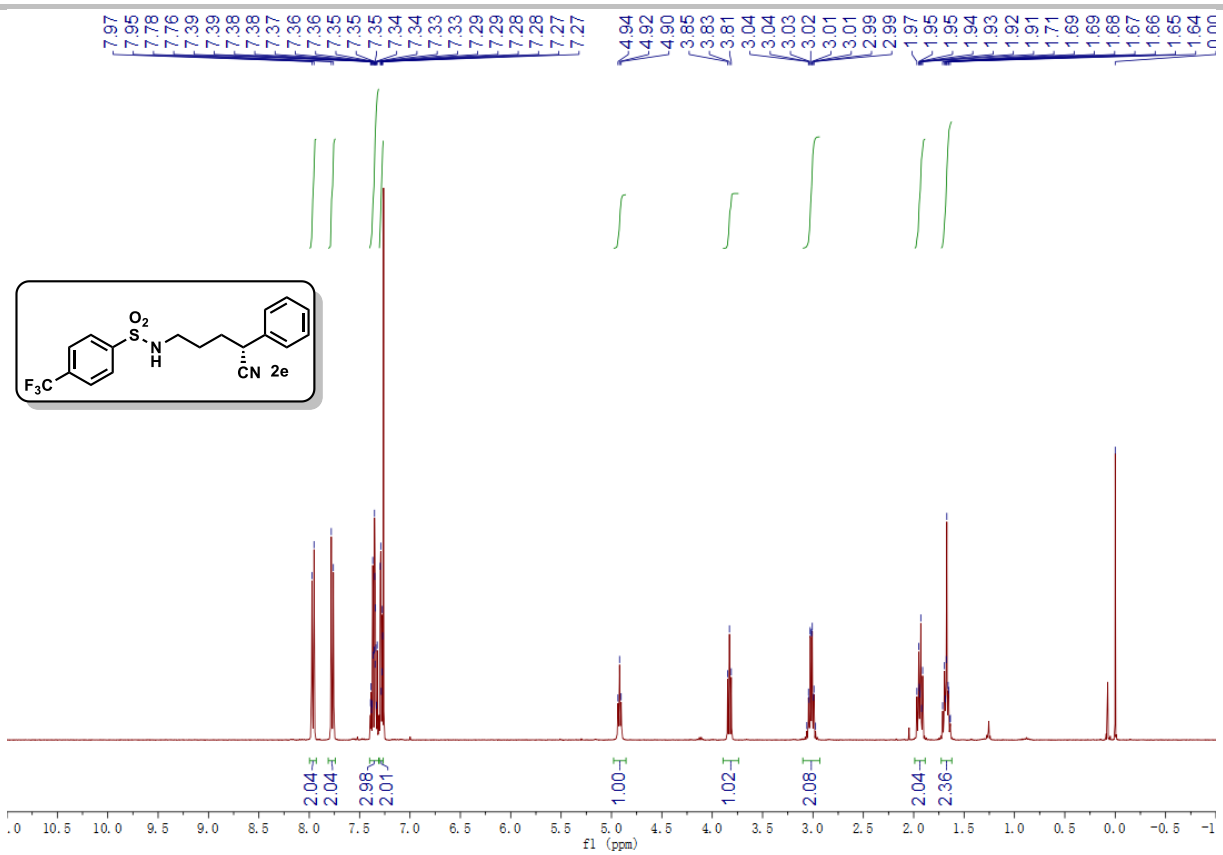

Figure S83. ^{1}H NMR of **2e**, related to Figure 2.

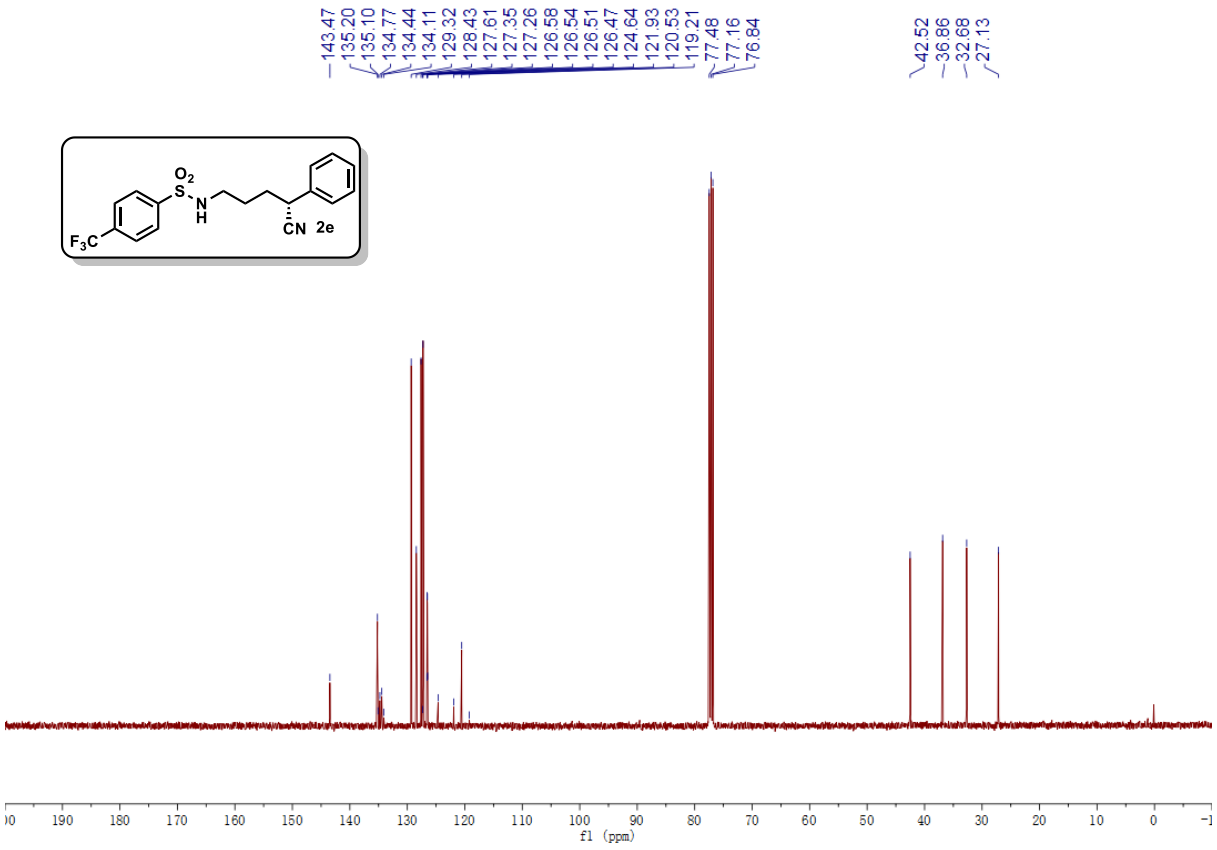

Figure S84. ^{13}C NMR of **2e**, related to Figure 2.

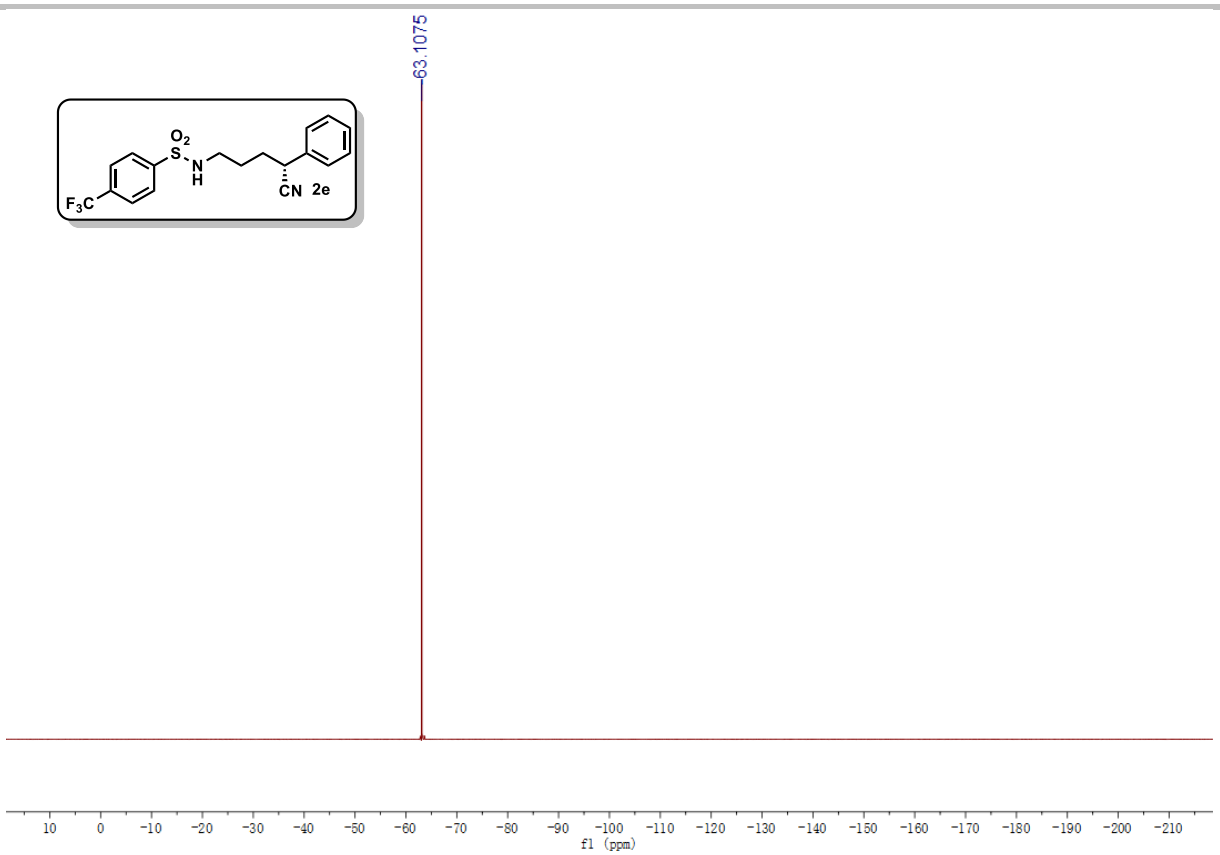

Figure S85. ^{19}F NMR of **2e**, related to Figure 2.

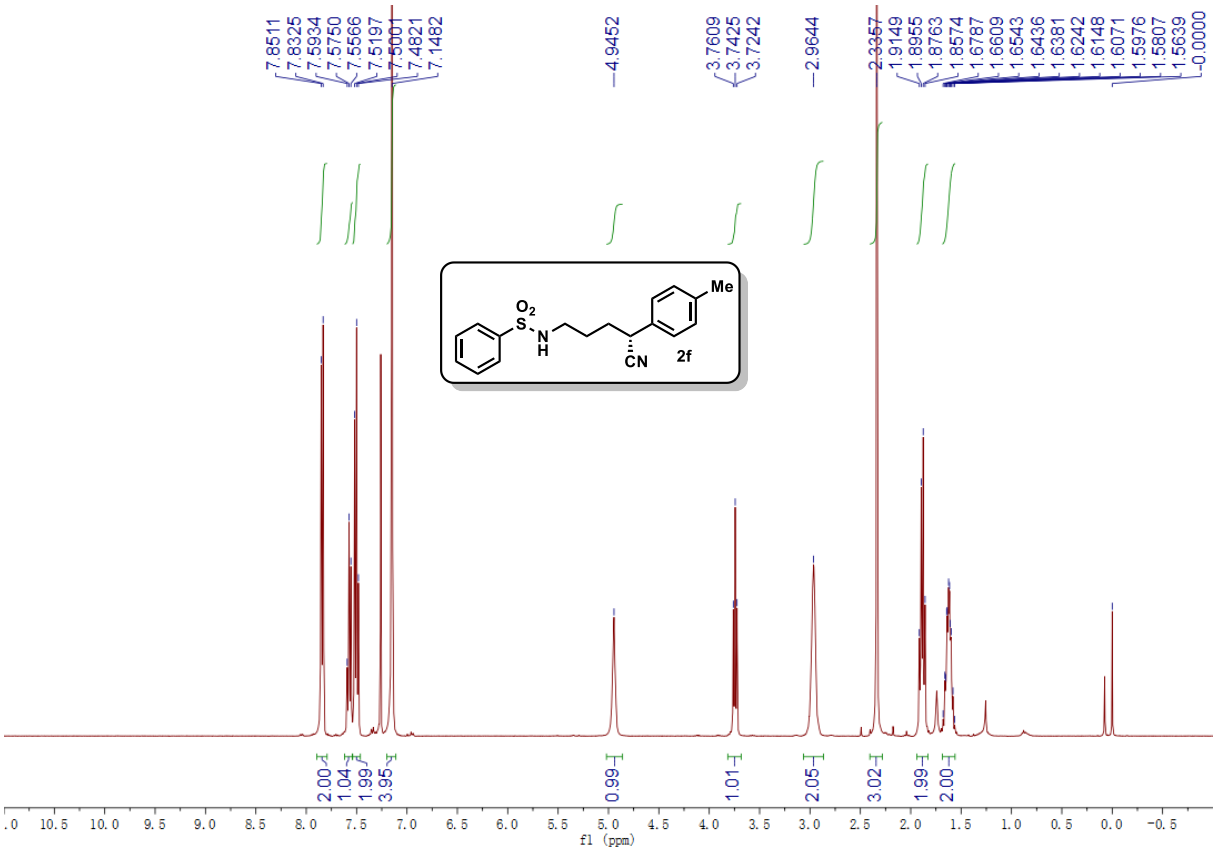

Figure S86. ^{1}H NMR of **2f**, related to Figure 2.

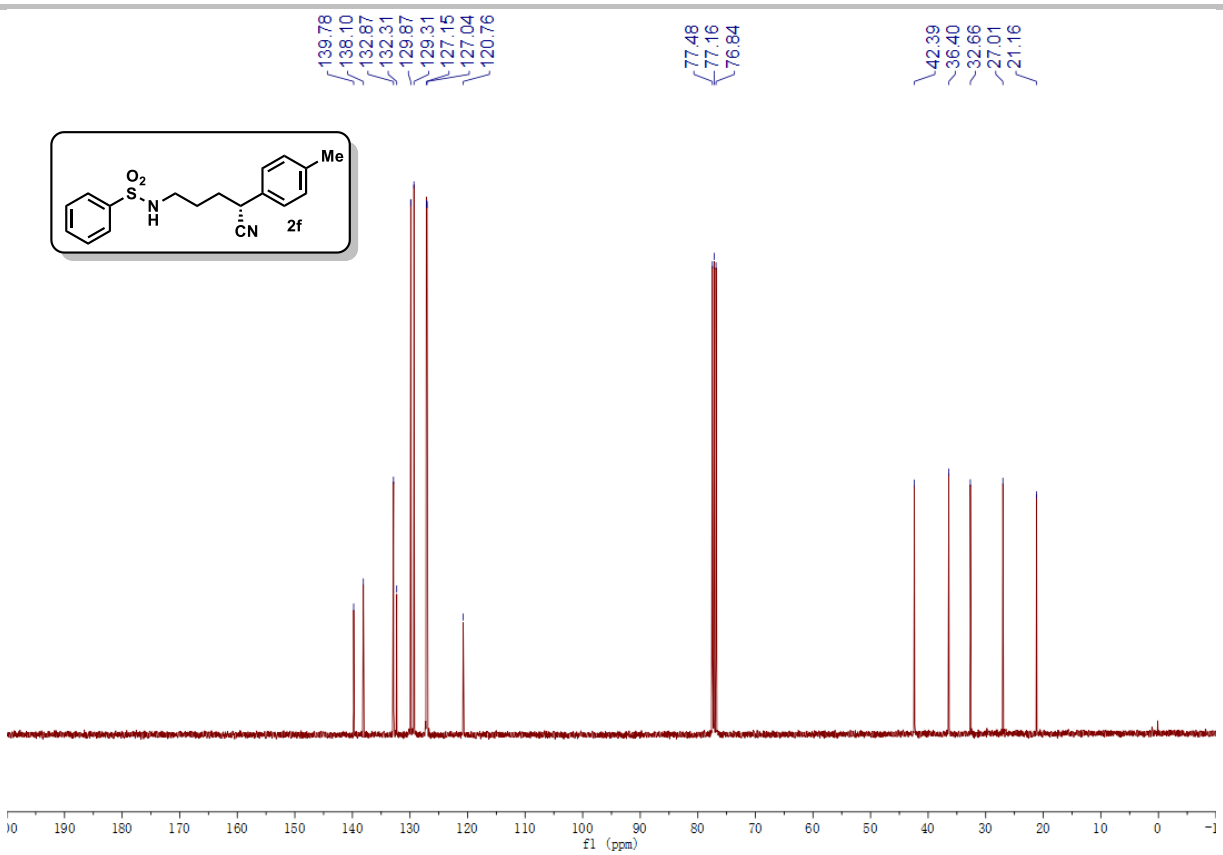

Figure S87. ^{13}C NMR of **2f**, related to Figure 2.

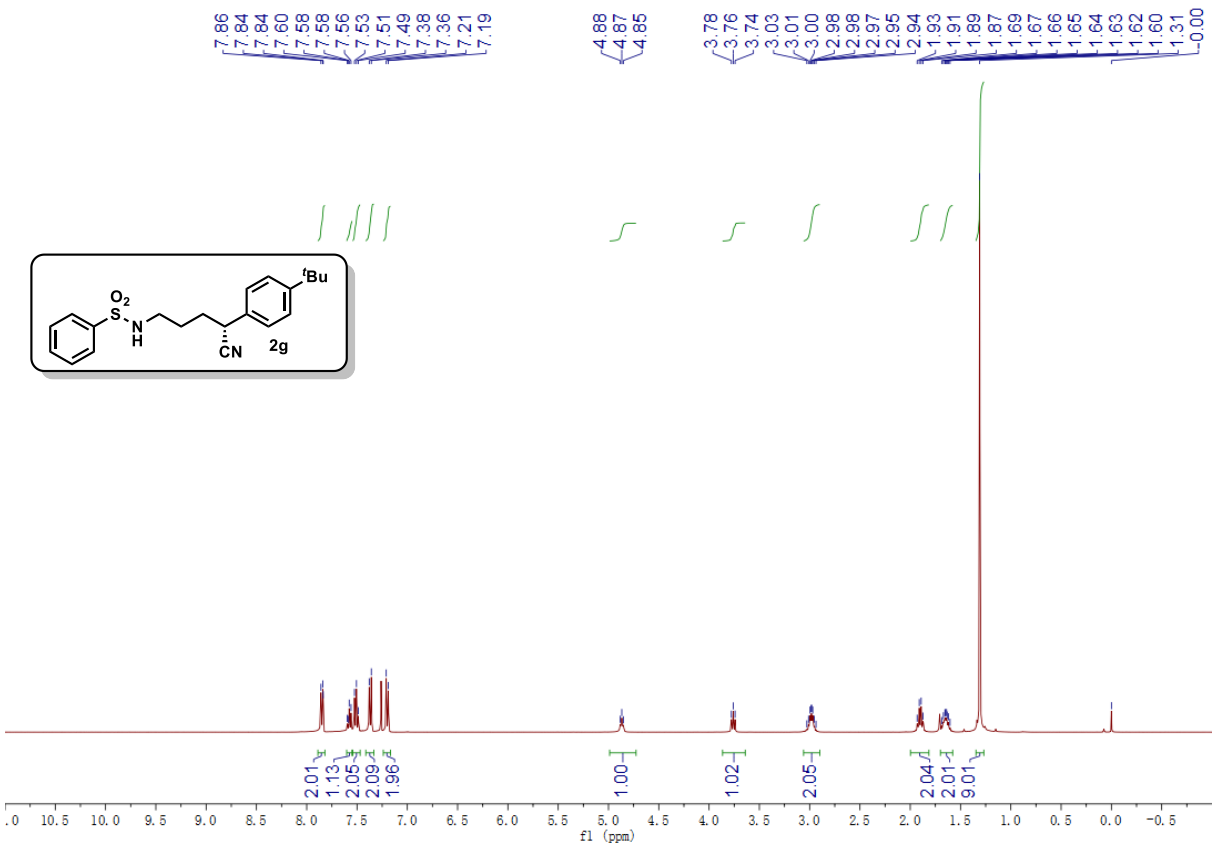

Figure S88. ^{1}H NMR of **2g**, related to Figure 2.

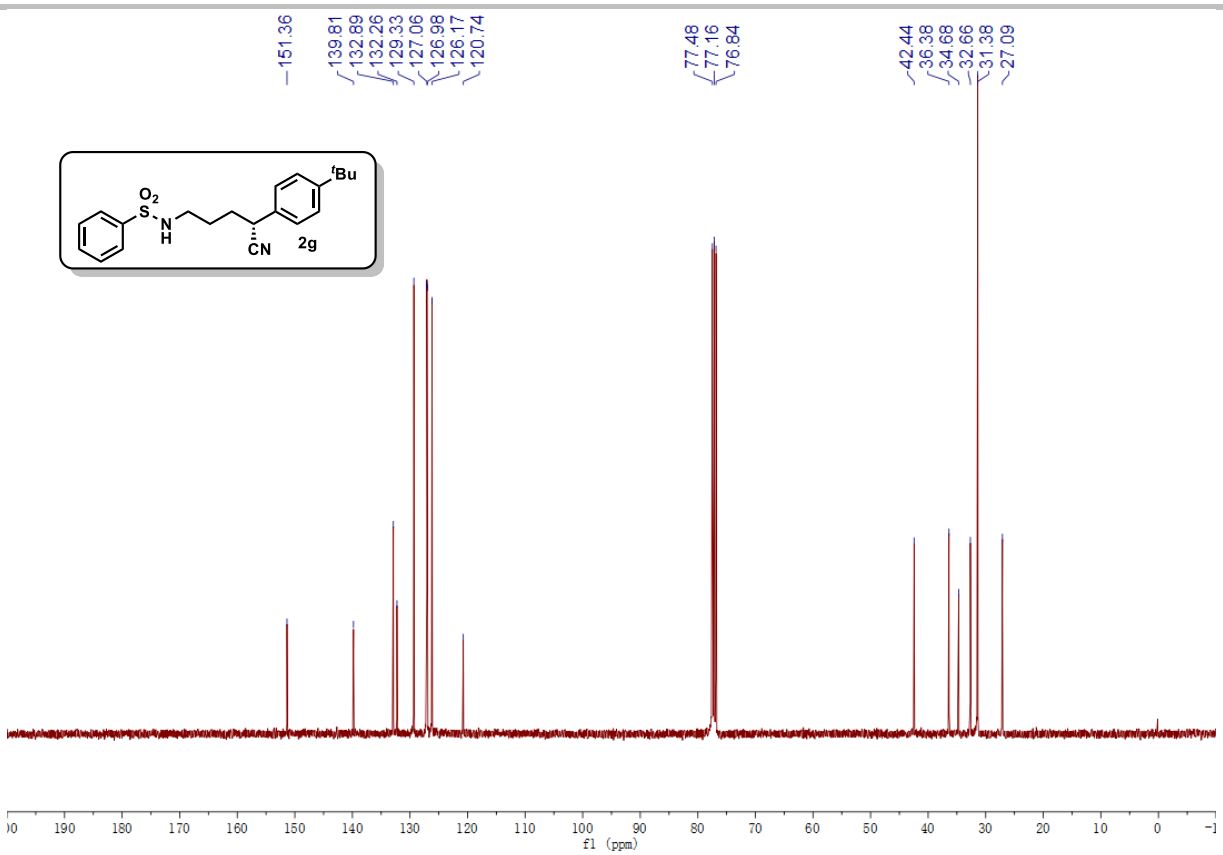

Figure S89. ^{13}C NMR of **2g**, related to Figure 2.

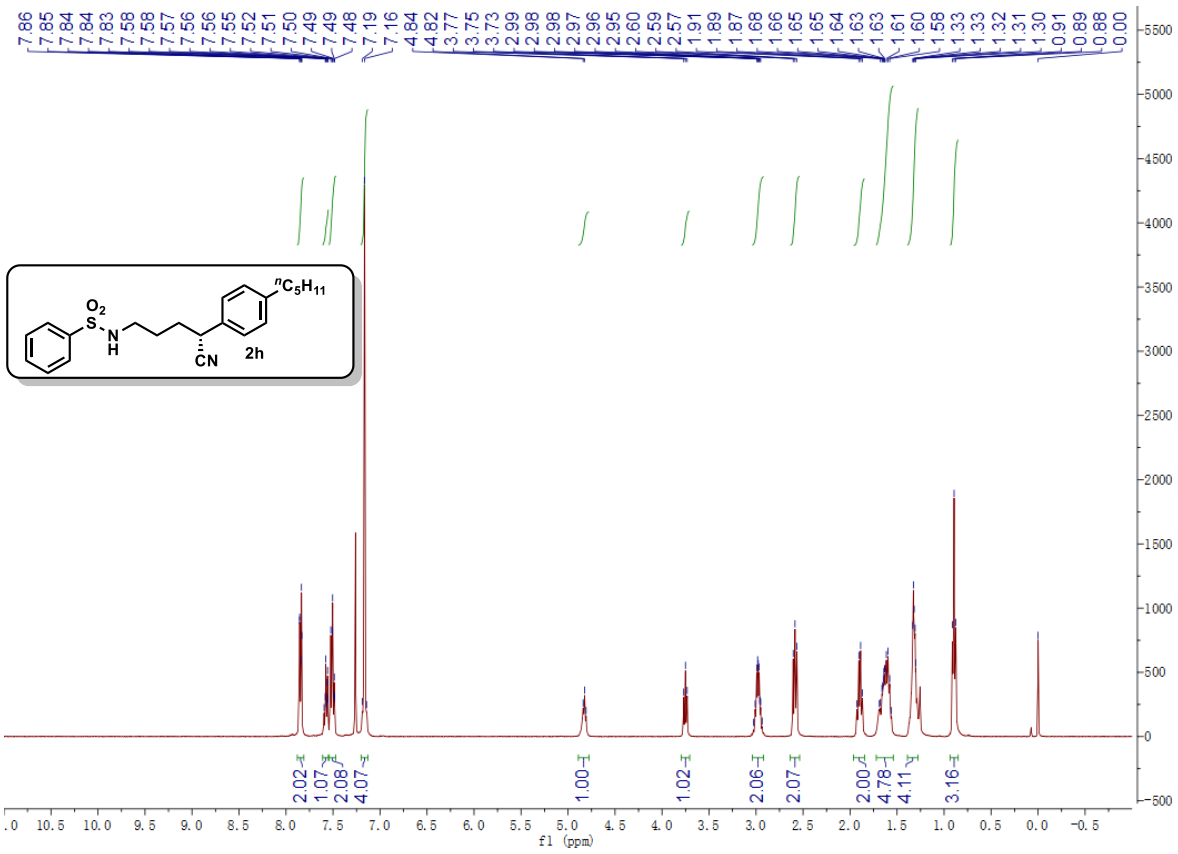

Figure S90. ^{1}H NMR of **2h**, related to Figure 2.

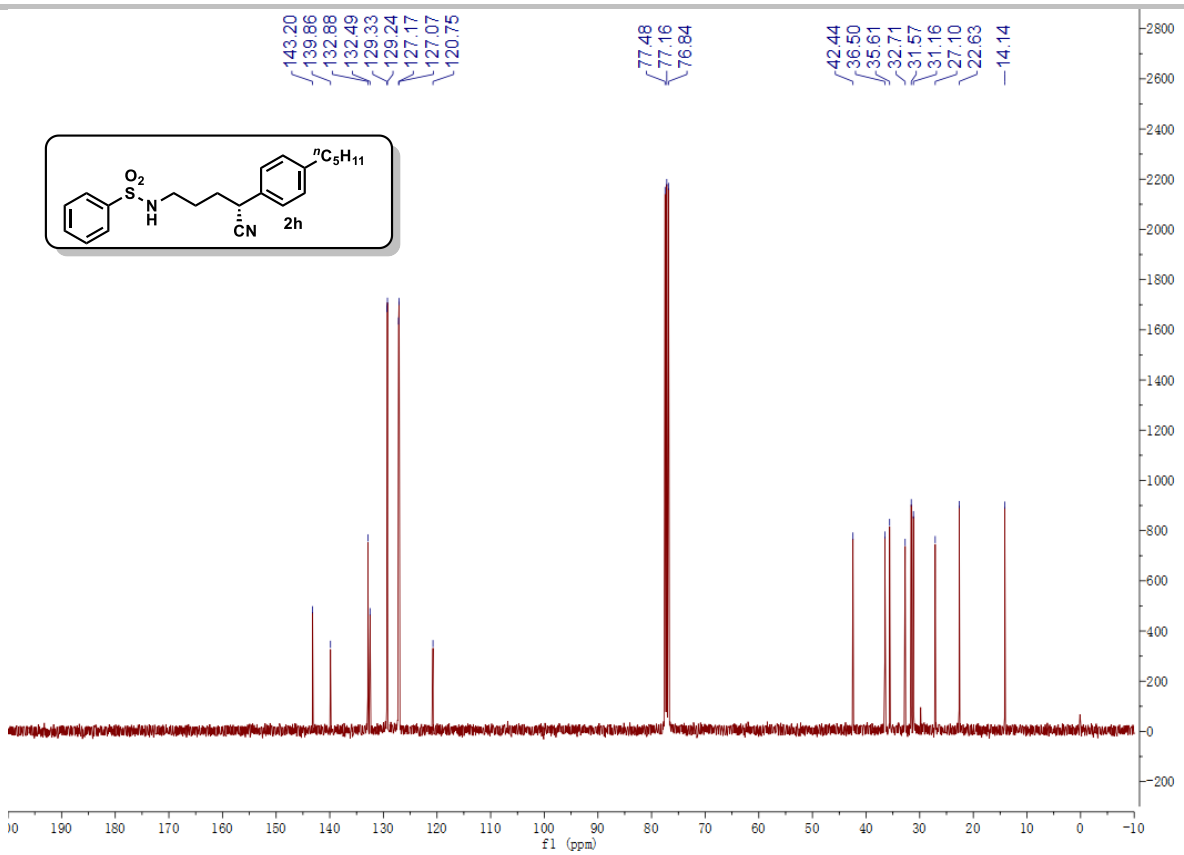

Figure S91. ^{13}C NMR of **2h**, related to Figure 2.

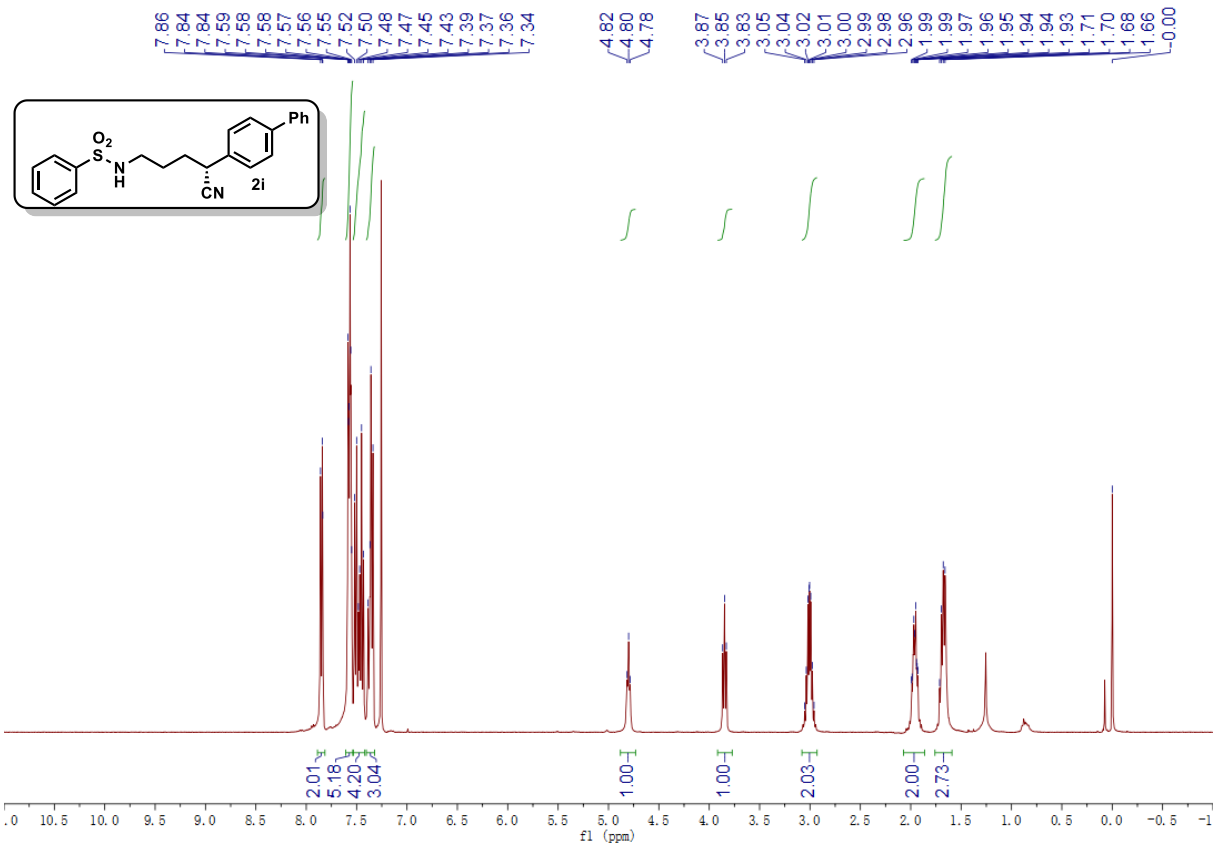

Figure S92. ^{1}H NMR of **2i**, related to Figure 2.

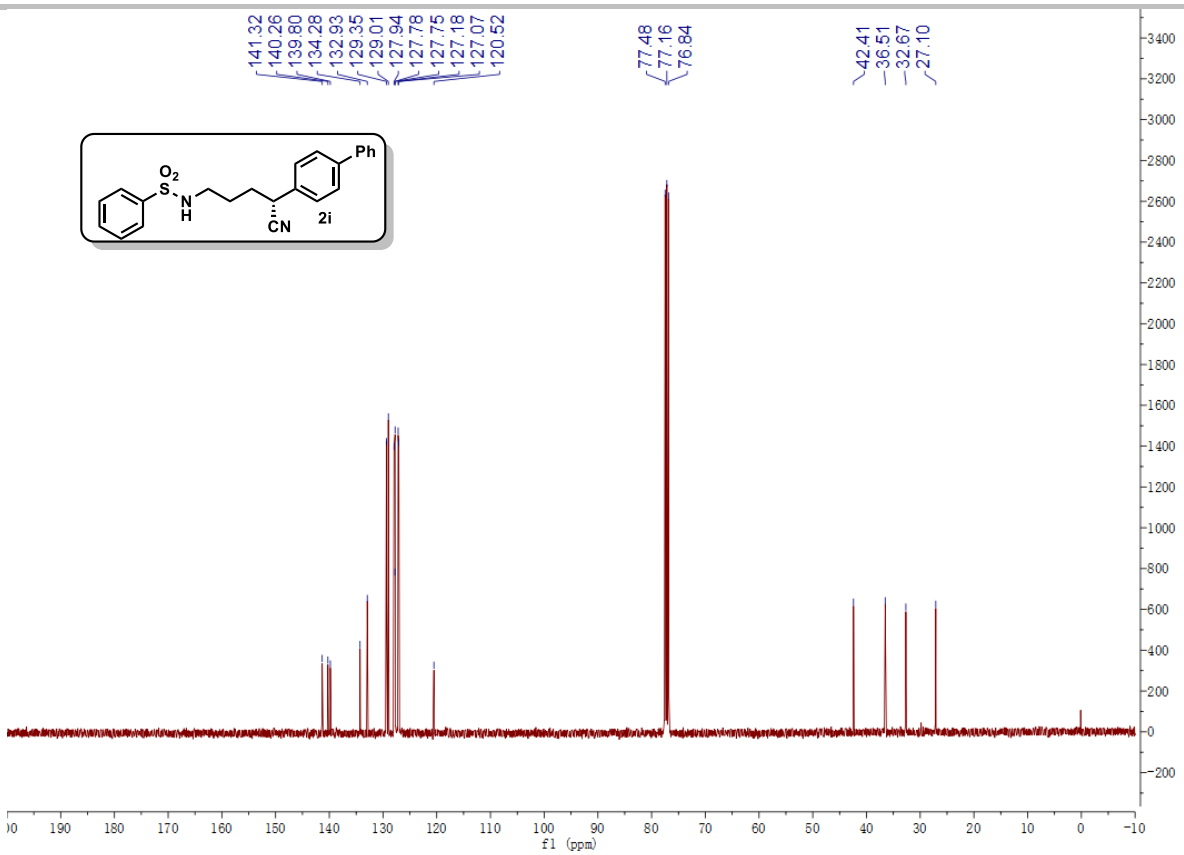

Figure S93. ^{13}C NMR of **2i**, related to Figure 2.

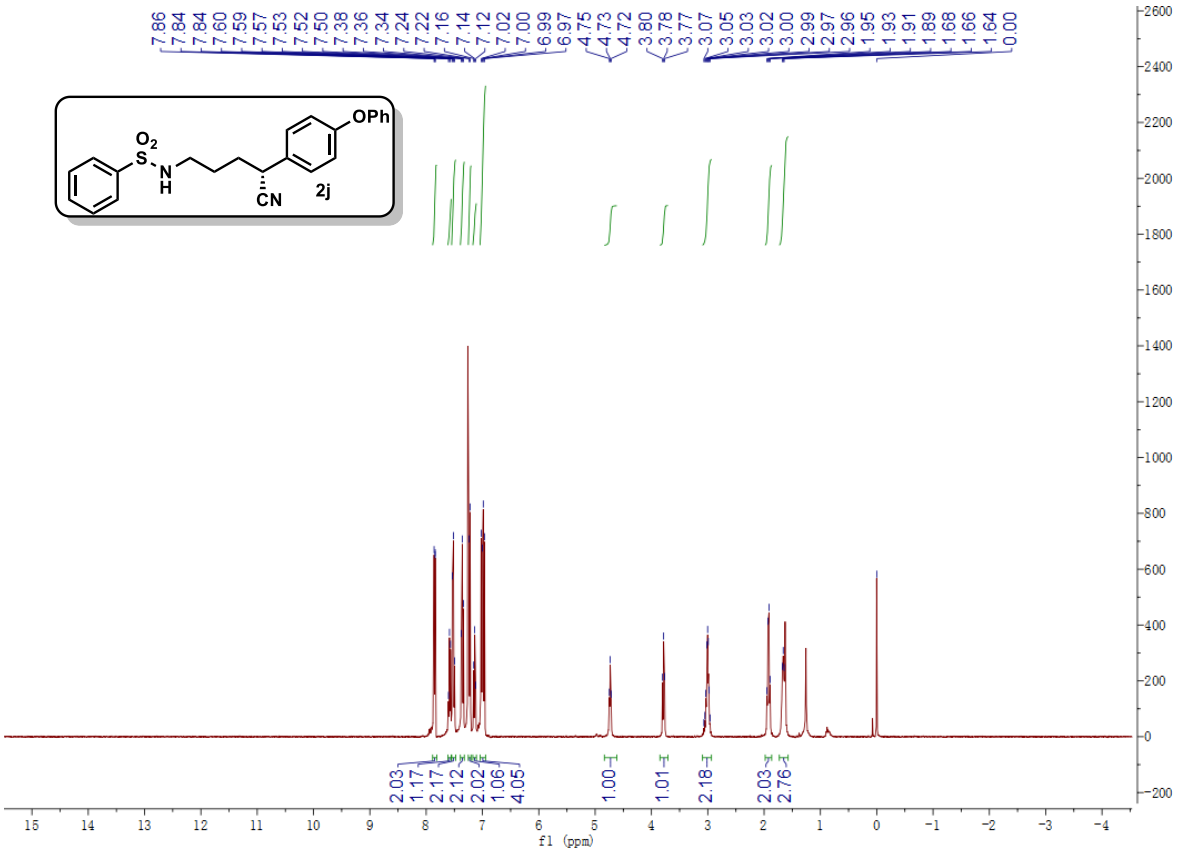

Figure S94. ^{1}H NMR of **2j**, related to Figure 2.

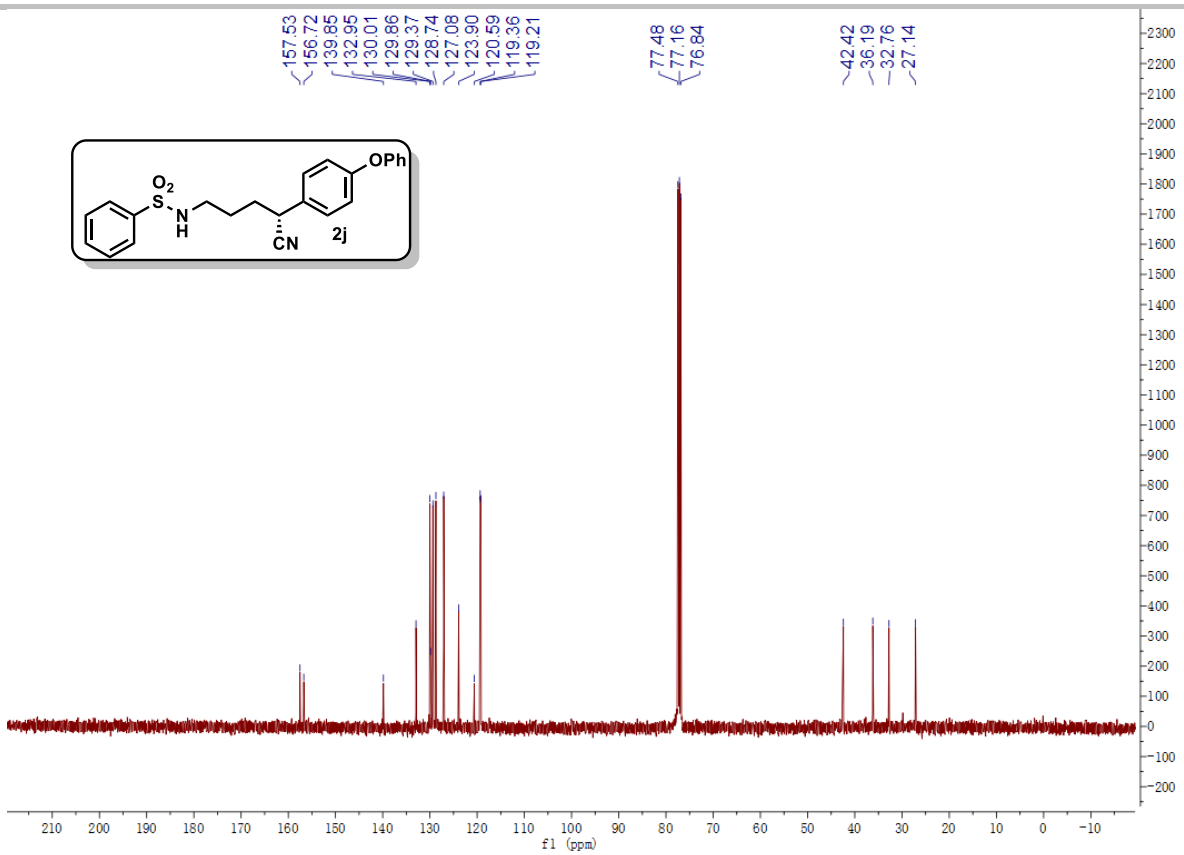

Figure S95. ^{13}C NMR of **2j**, related to Figure 2.

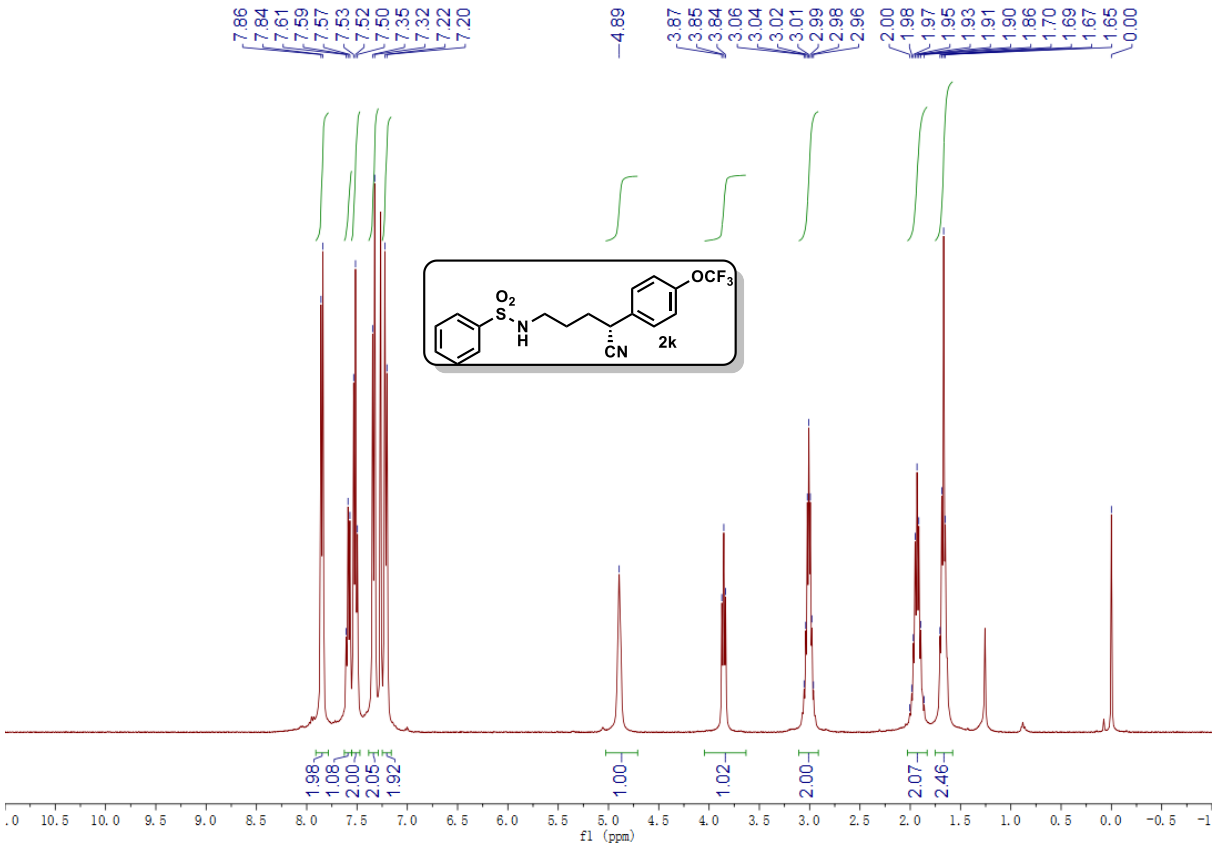

Figure S96. ^{1}H NMR of **2k**, related to Figure 2.

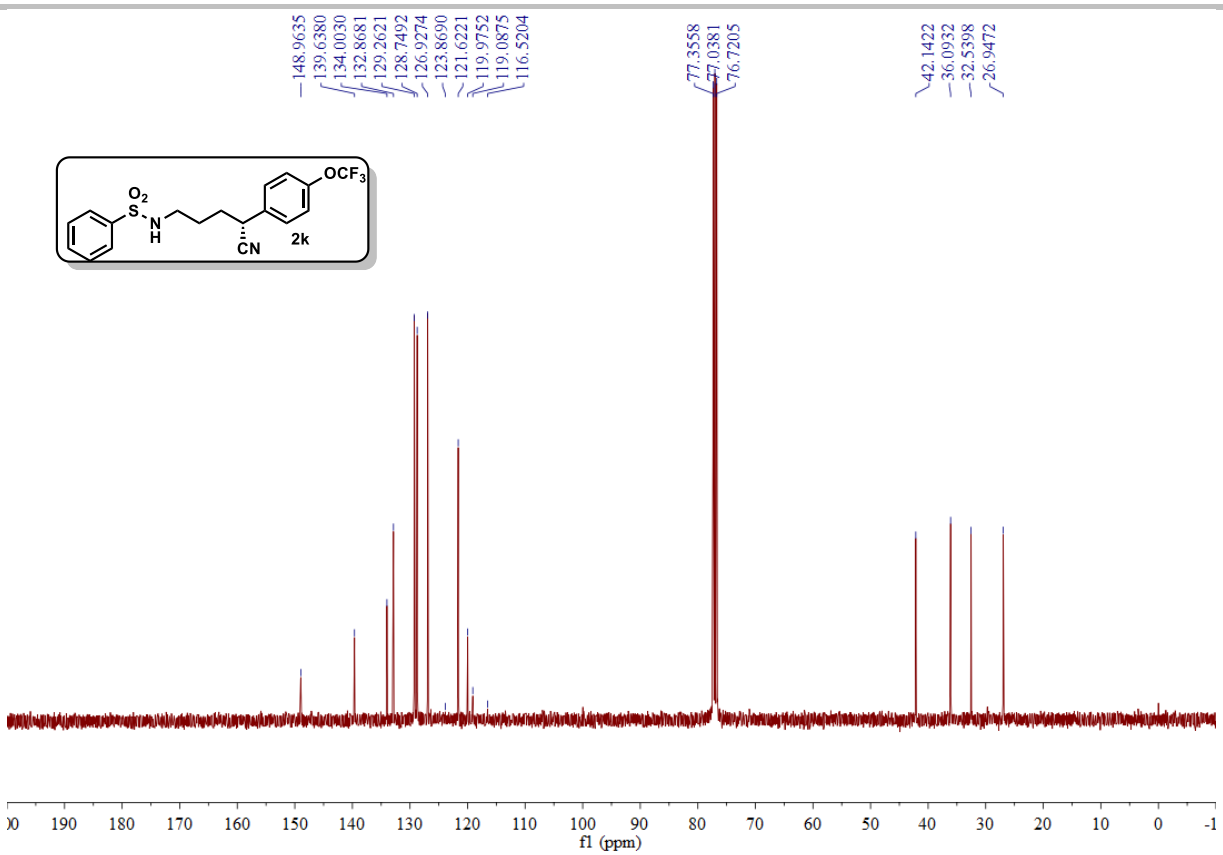

Figure S97. ^{13}C NMR of **2k**, related to Figure 2.

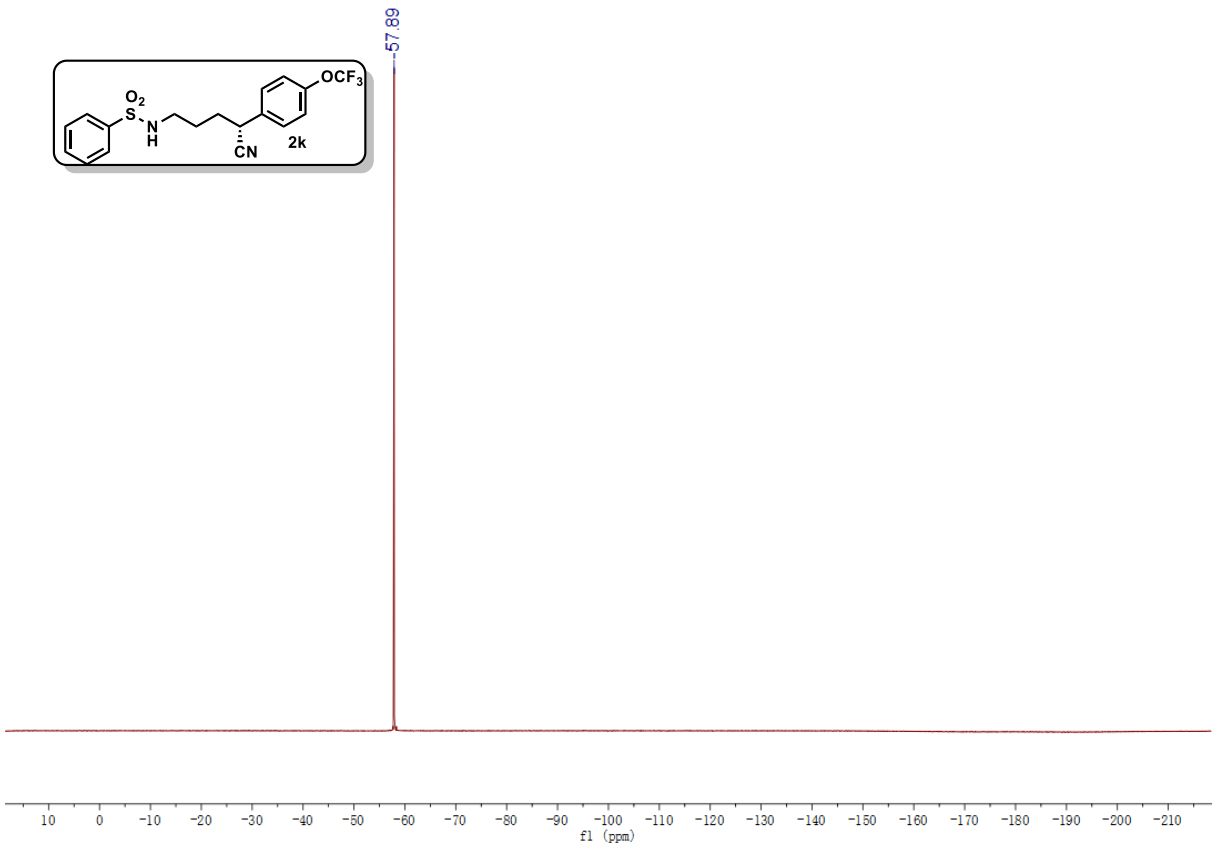

Figure S98. ^{19}F NMR of **2k**, related to Figure 2.

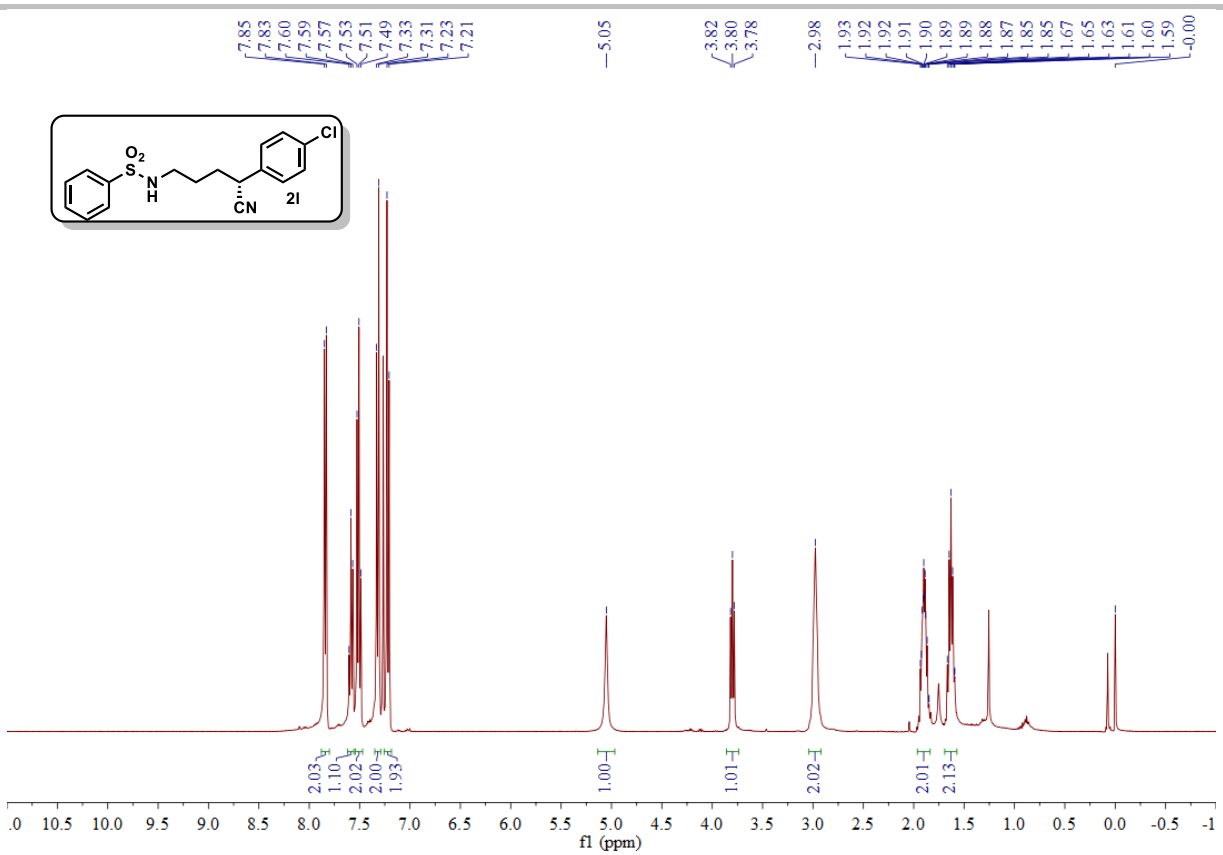

Figure S99. ^{1}H NMR of **2l**, related to Figure 2.

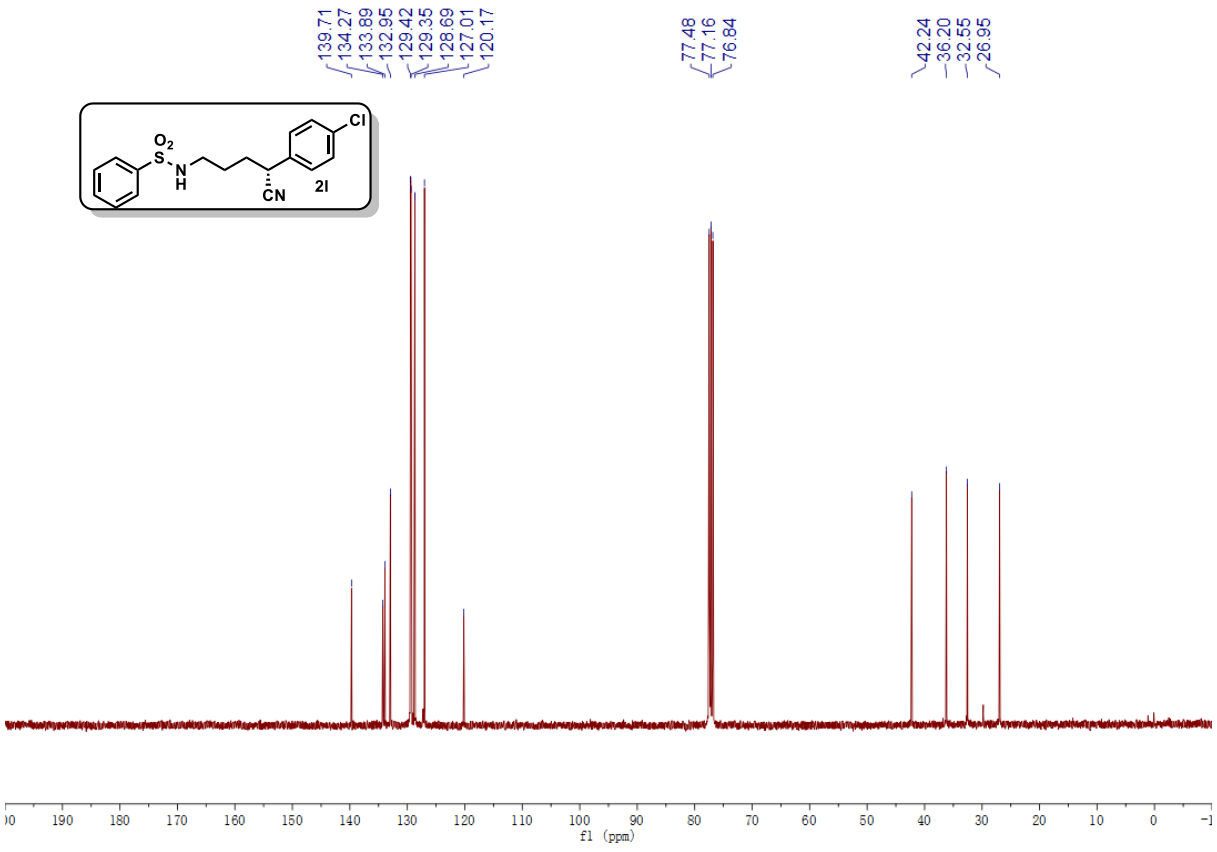

Figure S100. ^{13}C NMR of **2l**, related to Figure 2.

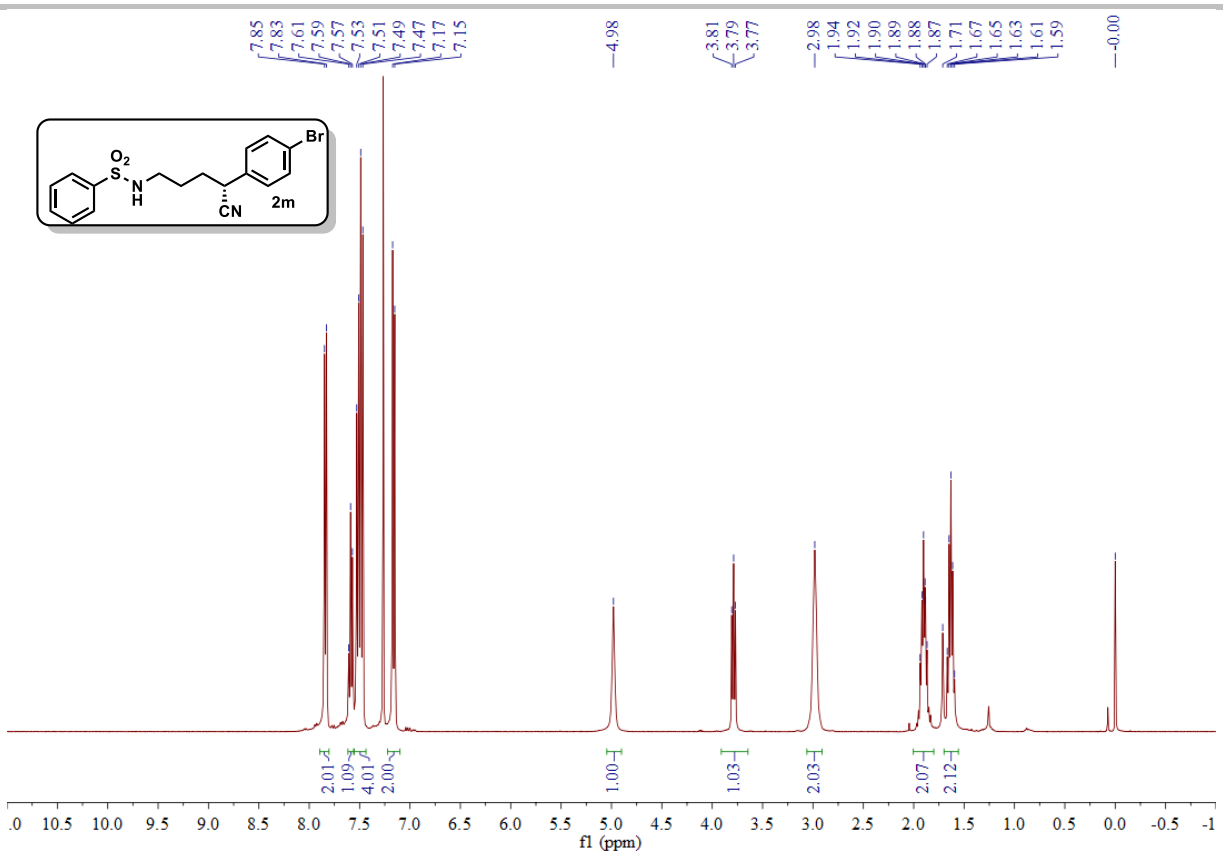

Figure S101. ^{1}H NMR of **2m**, related to Figure 2.

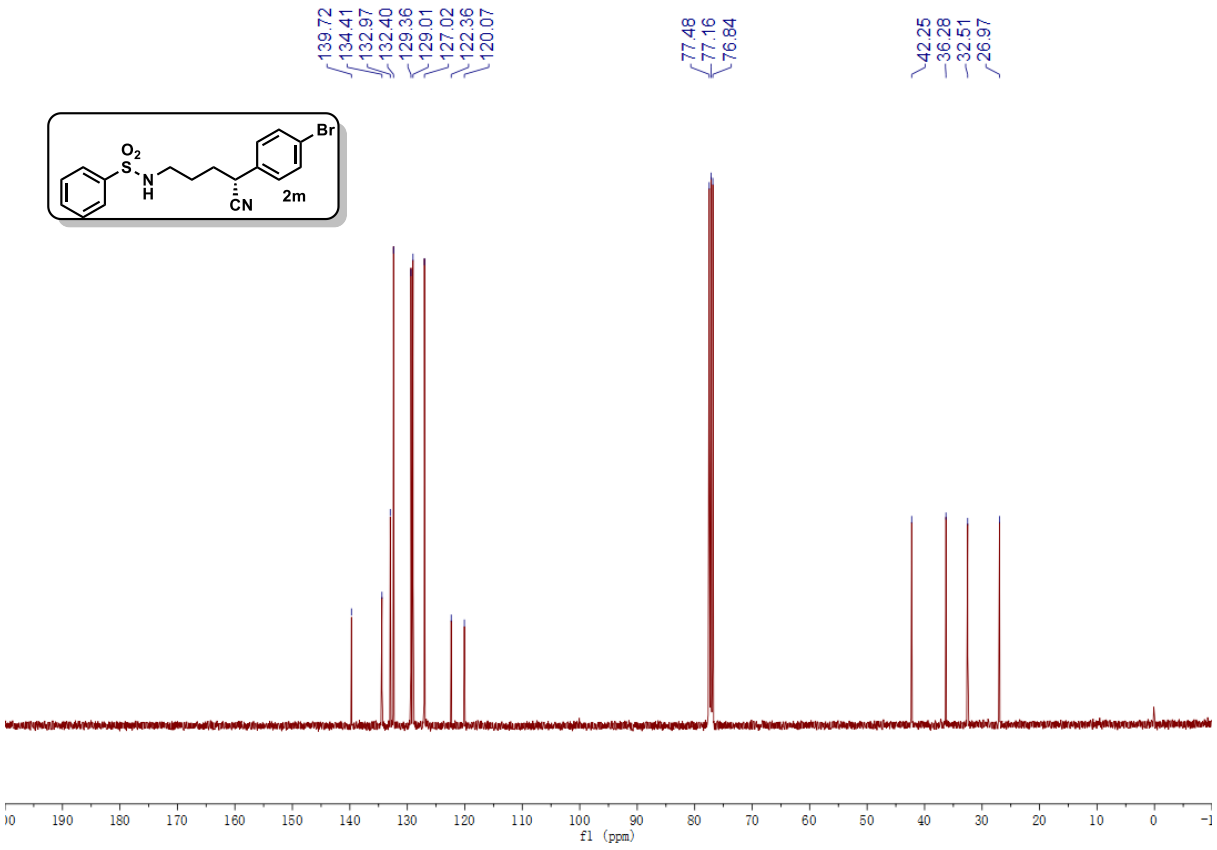

Figure S102. ^{13}C NMR of **2m**, related to Figure 2.

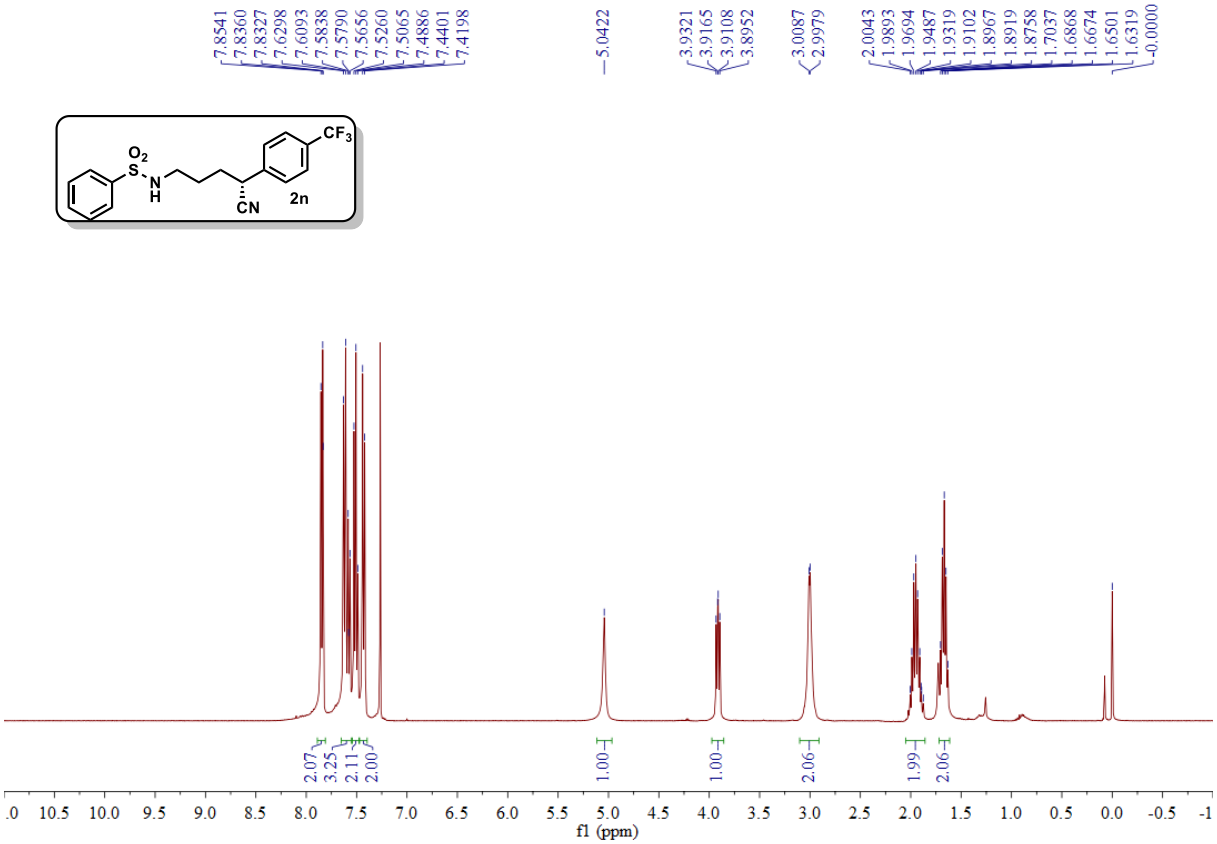

Figure S103. ^{1}H NMR of **2n**, related to Figure 2.

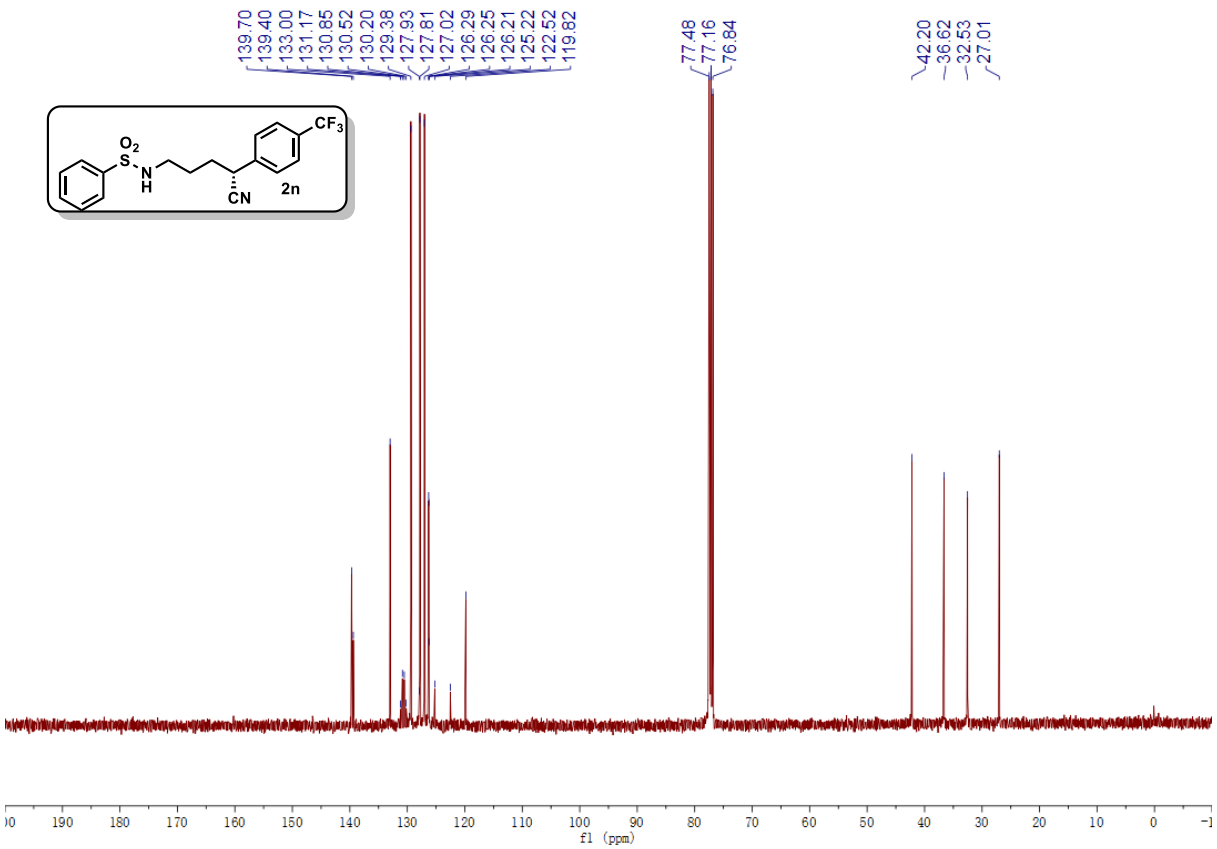

Figure S104. ^{13}C NMR of **2n**, related to Figure 2.

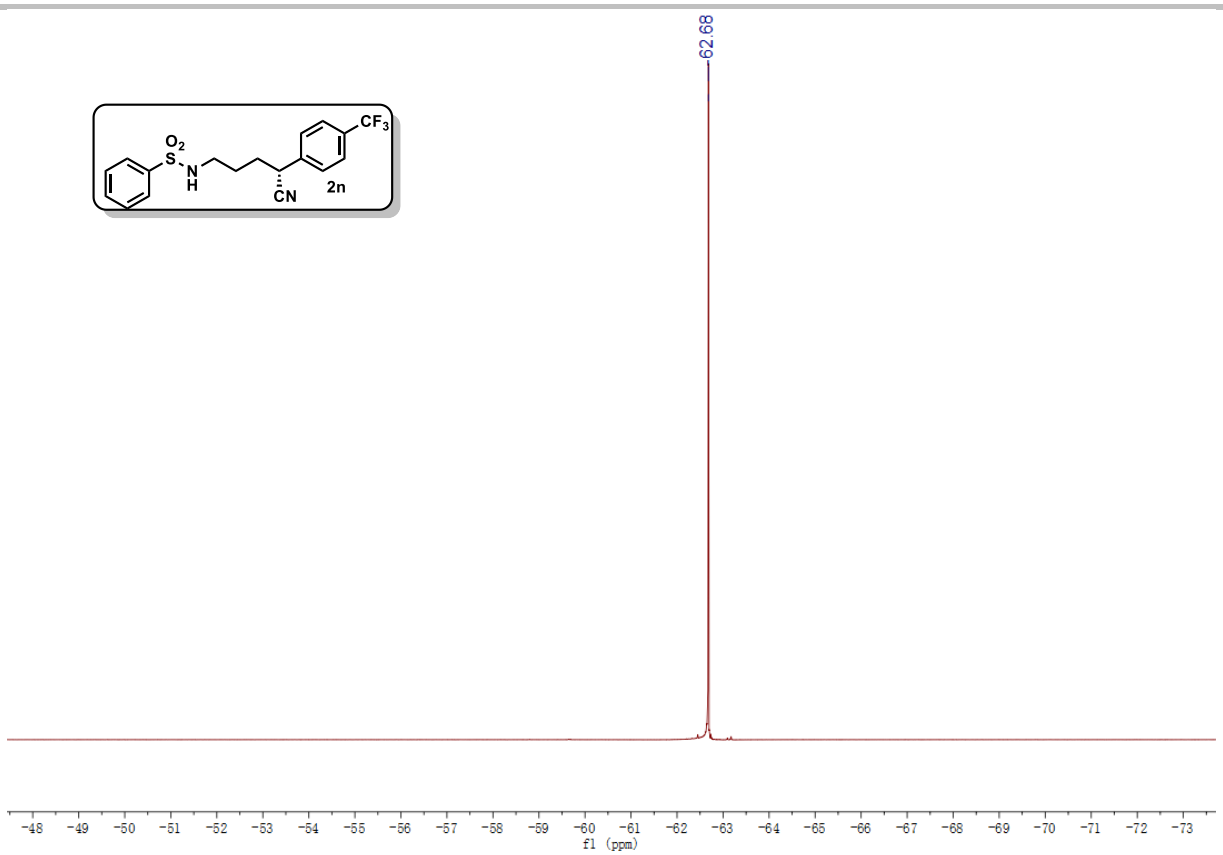

Figure S105. ^{19}F NMR of **2n**, related to Figure 2.

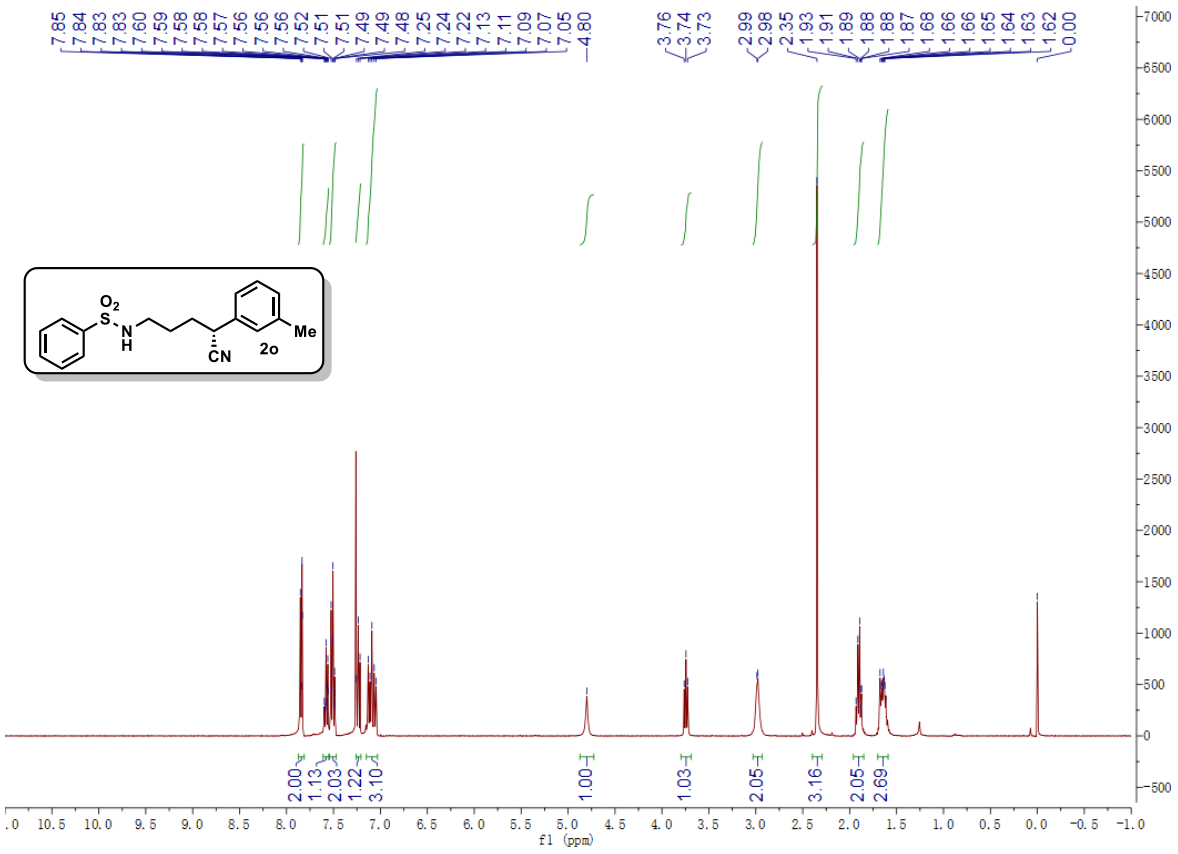

Figure S106. ^{1}H NMR of **2o**, related to Figure 2.

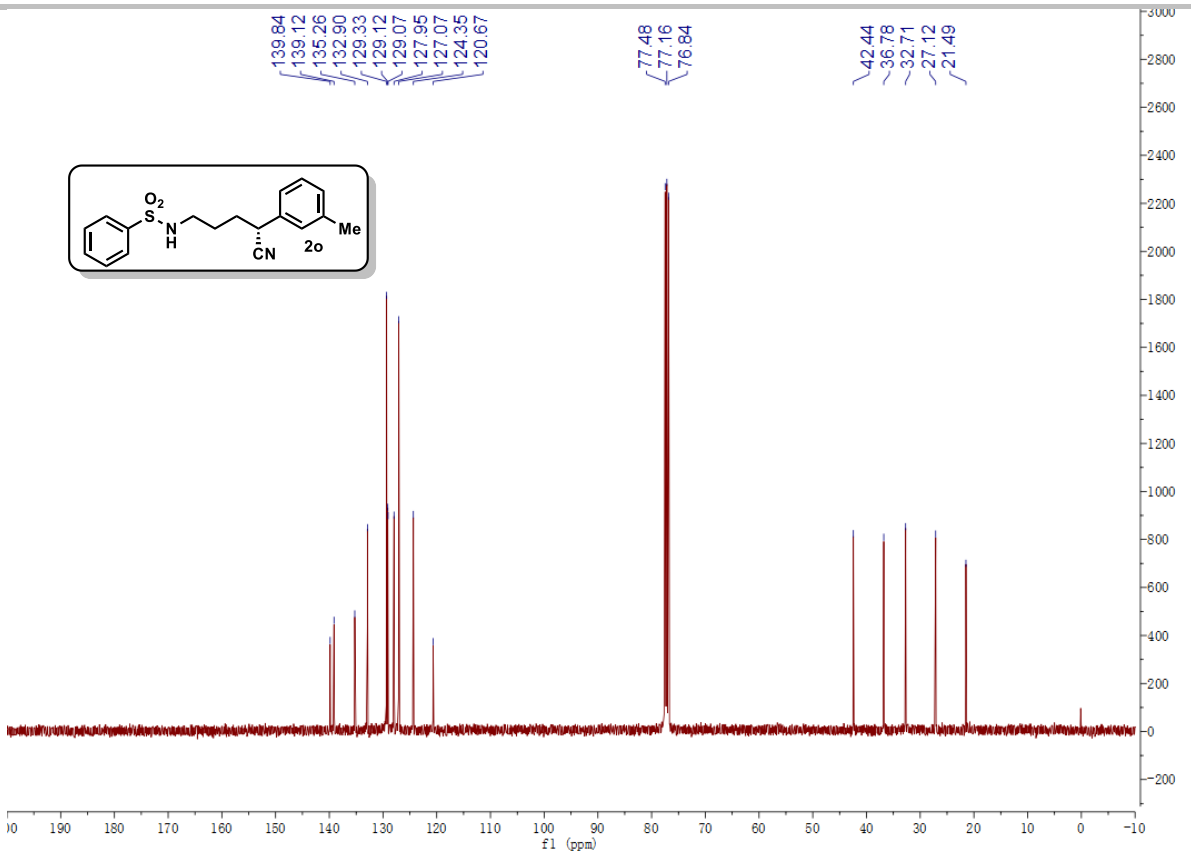

Figure S107. ^{13}C NMR of **2o**, related to Figure 2.

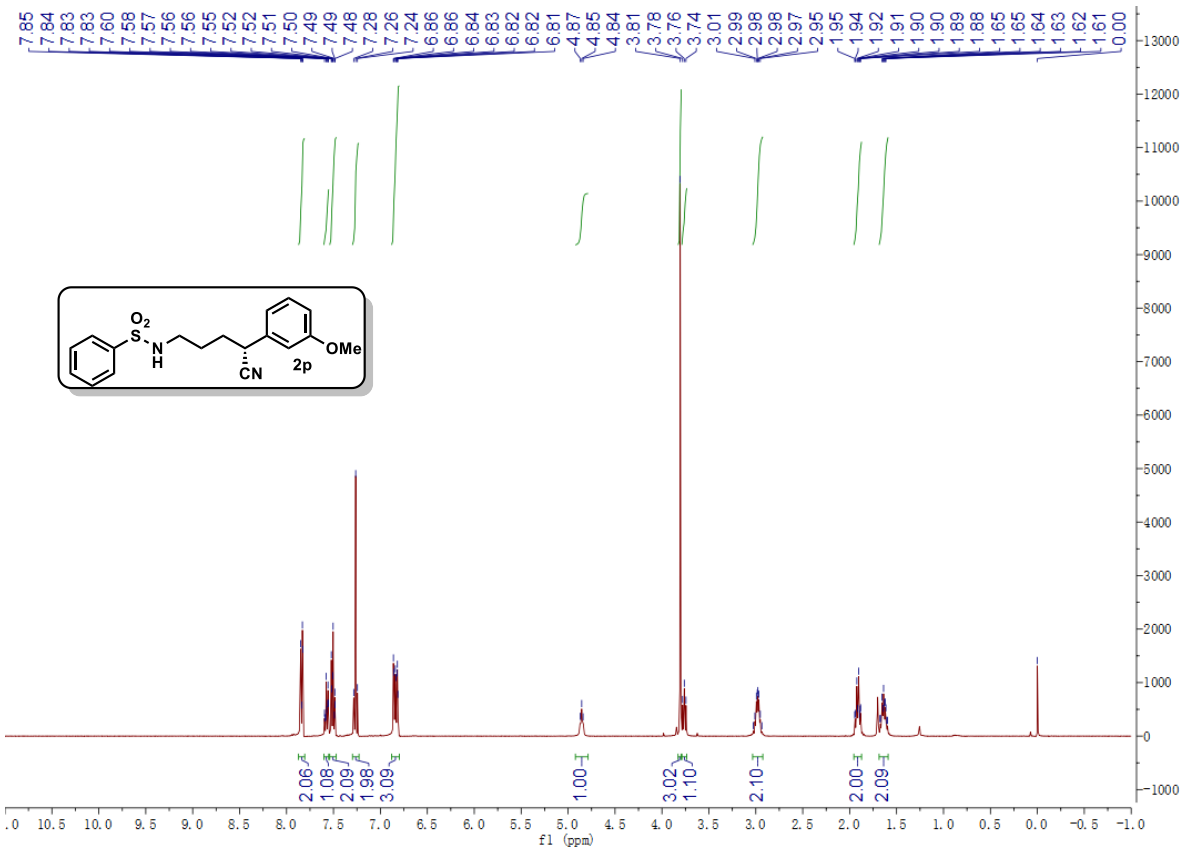

Figure S108. ^{1}H NMR of **2p**, related to Figure 2.

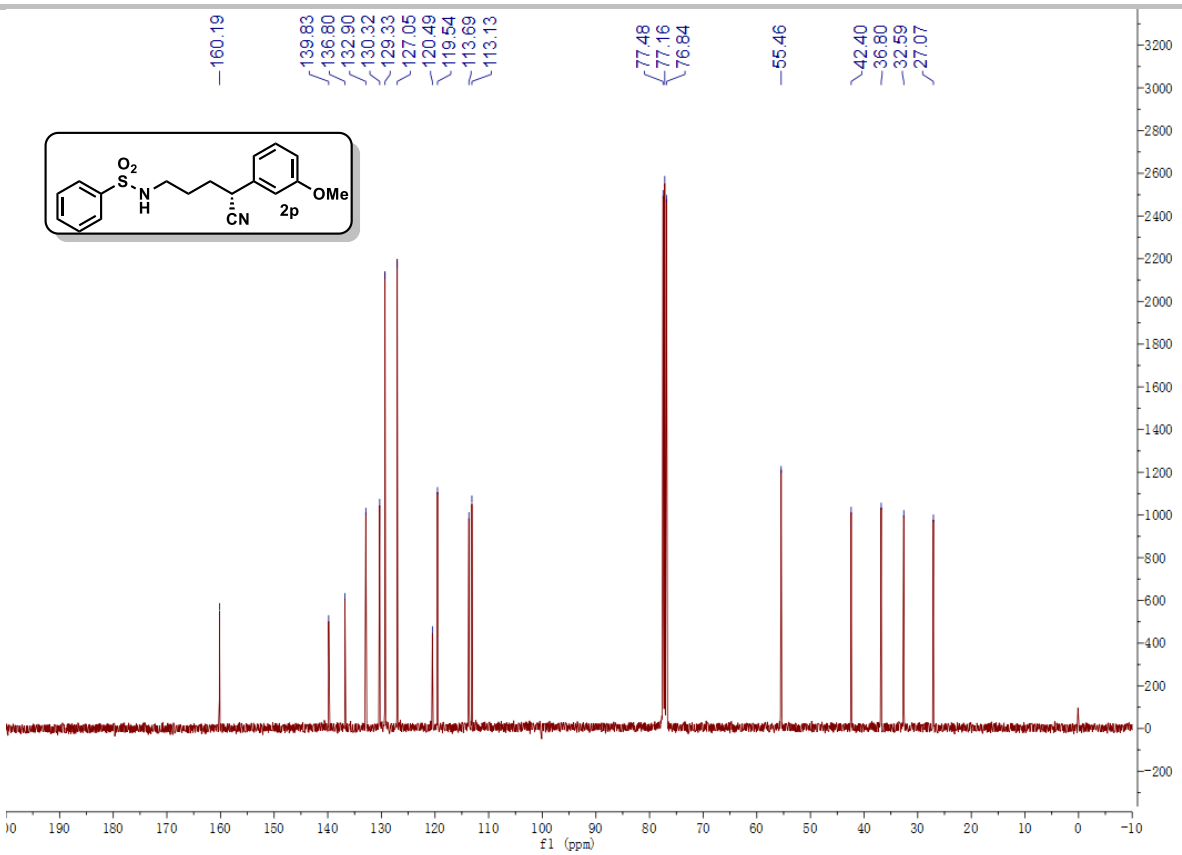

Figure S109. ^{13}C NMR of **2p**, related to Figure 2.

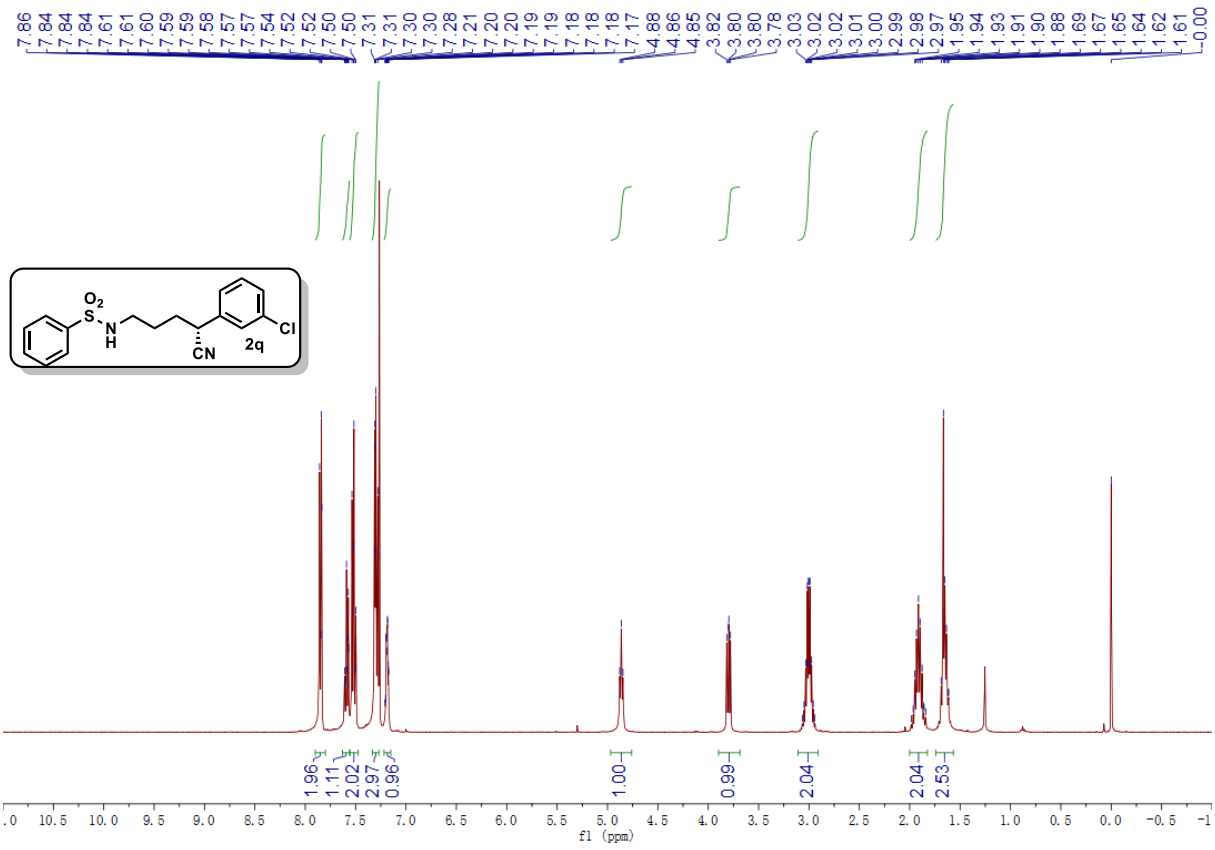

Figure S110. ^{1}H NMR of **2q**, related to Figure 2.

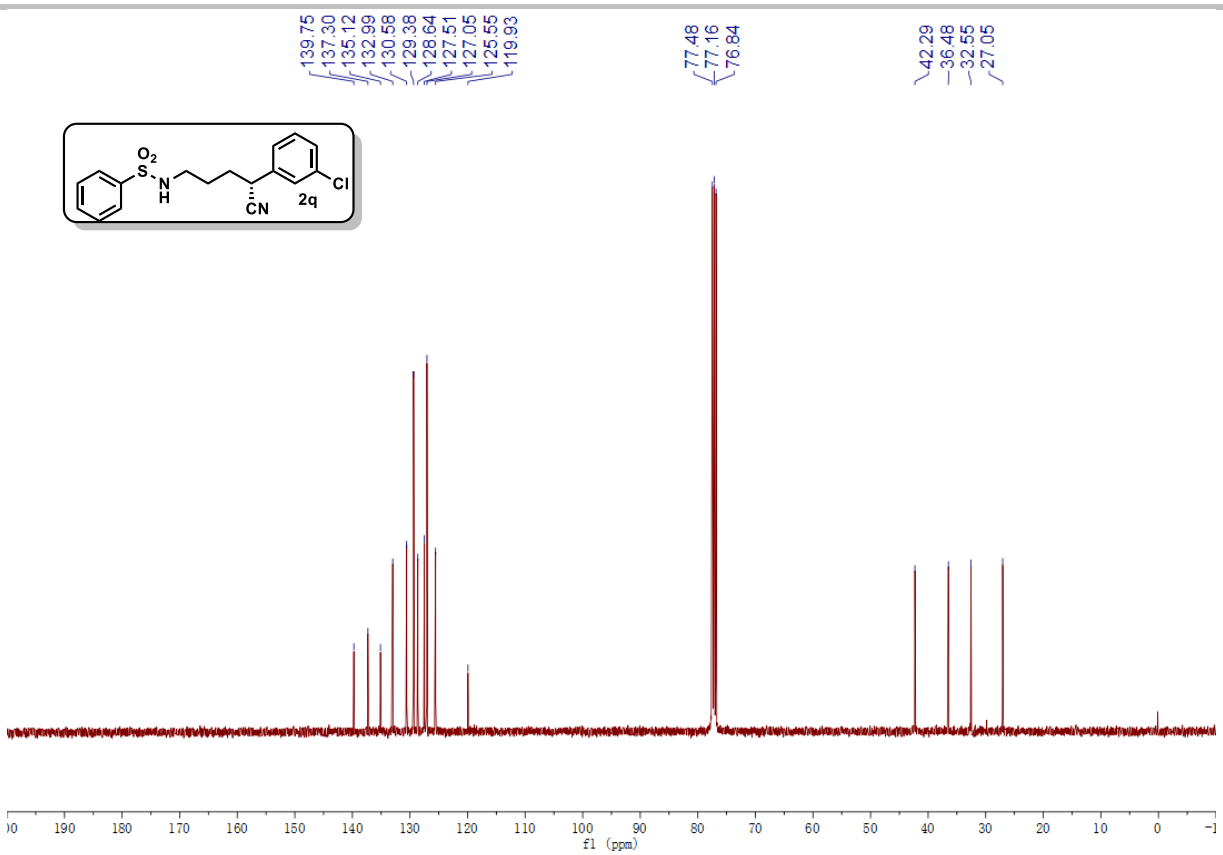

Figure S111. ^{13}C NMR of **2q**, related to Figure 2.

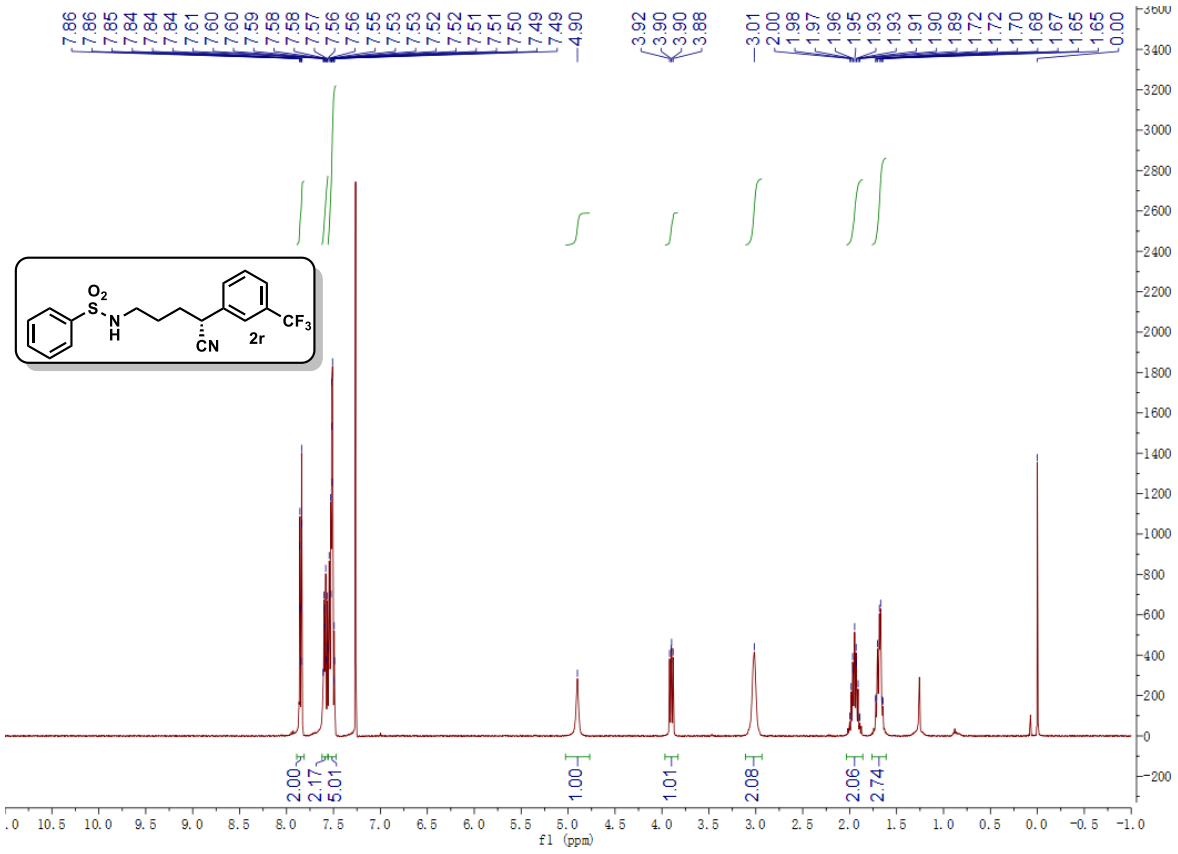

Figure S112. ^{1}H NMR of **2r**, related to Figure 2.

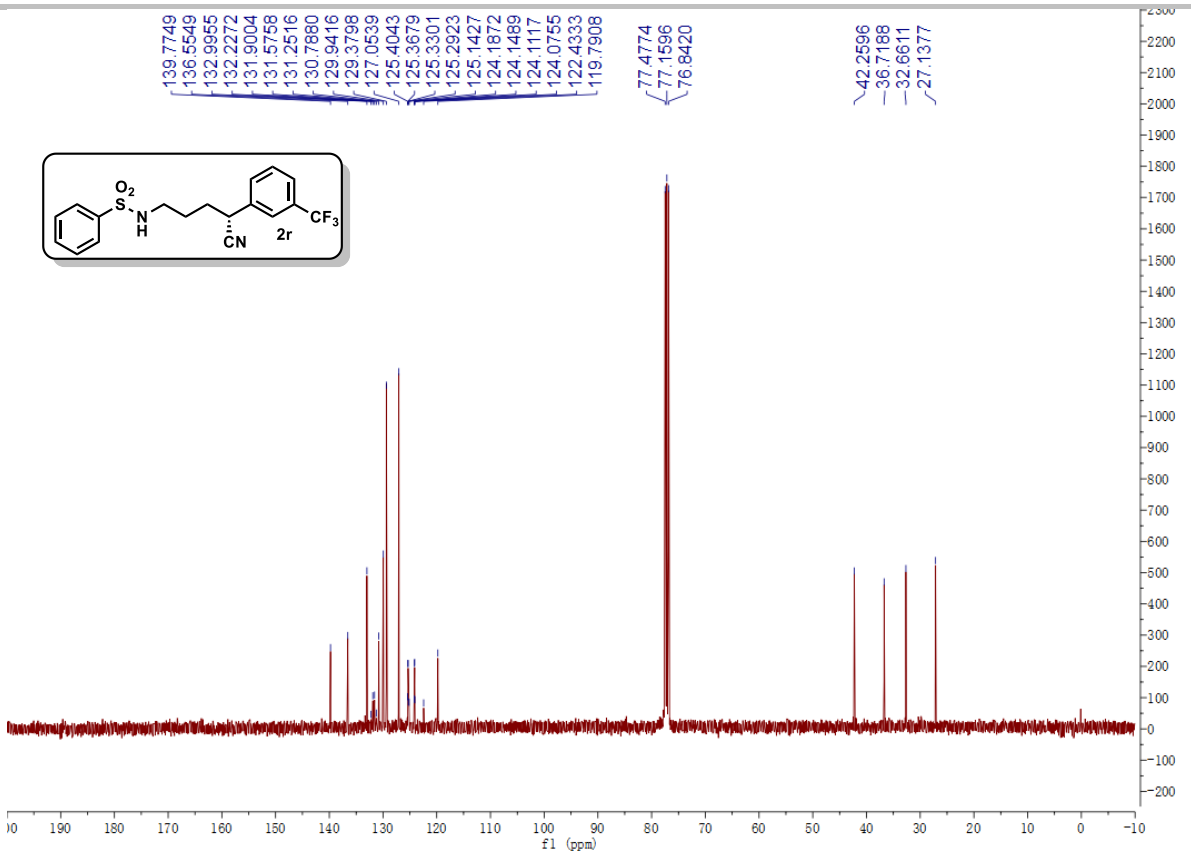

Figure S113. ^{13}C NMR of **2r**, related to Figure 2.

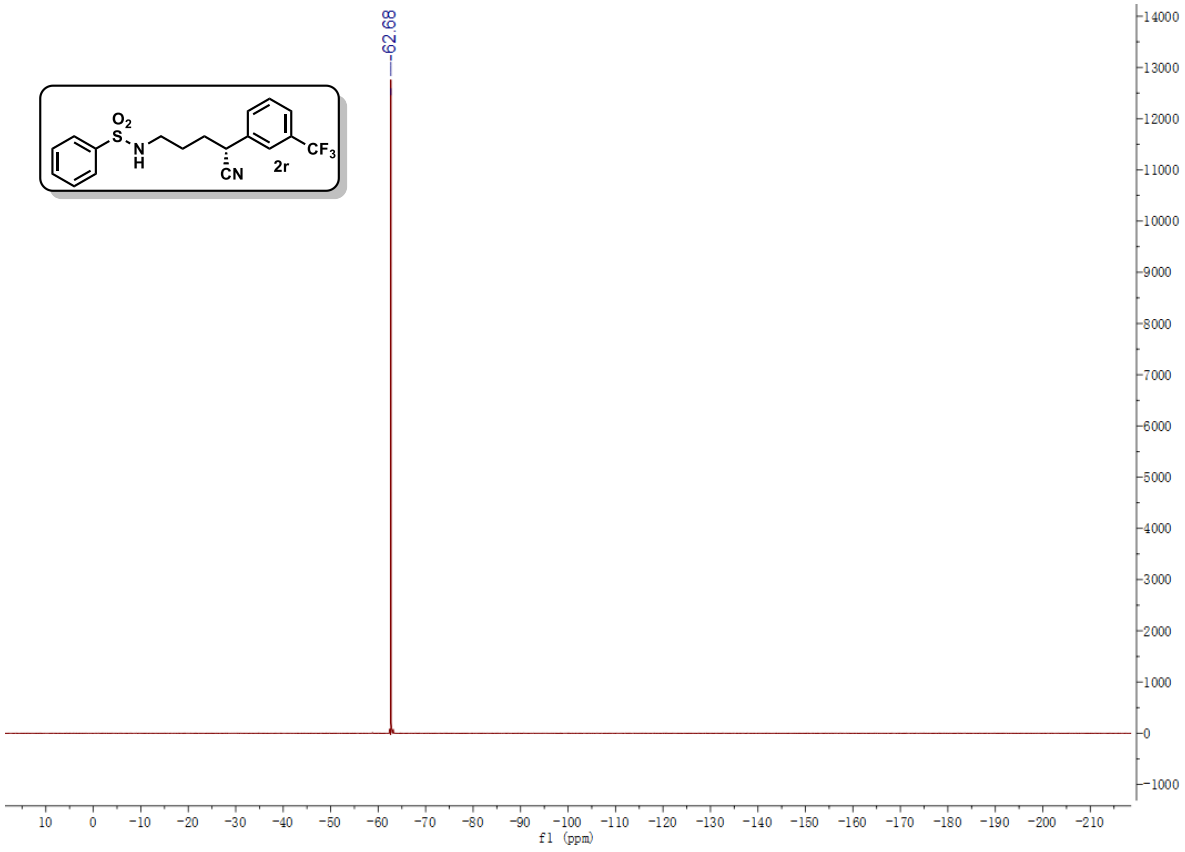

Figure S114. ^{19}F NMR of **2r**, related to Figure 2.

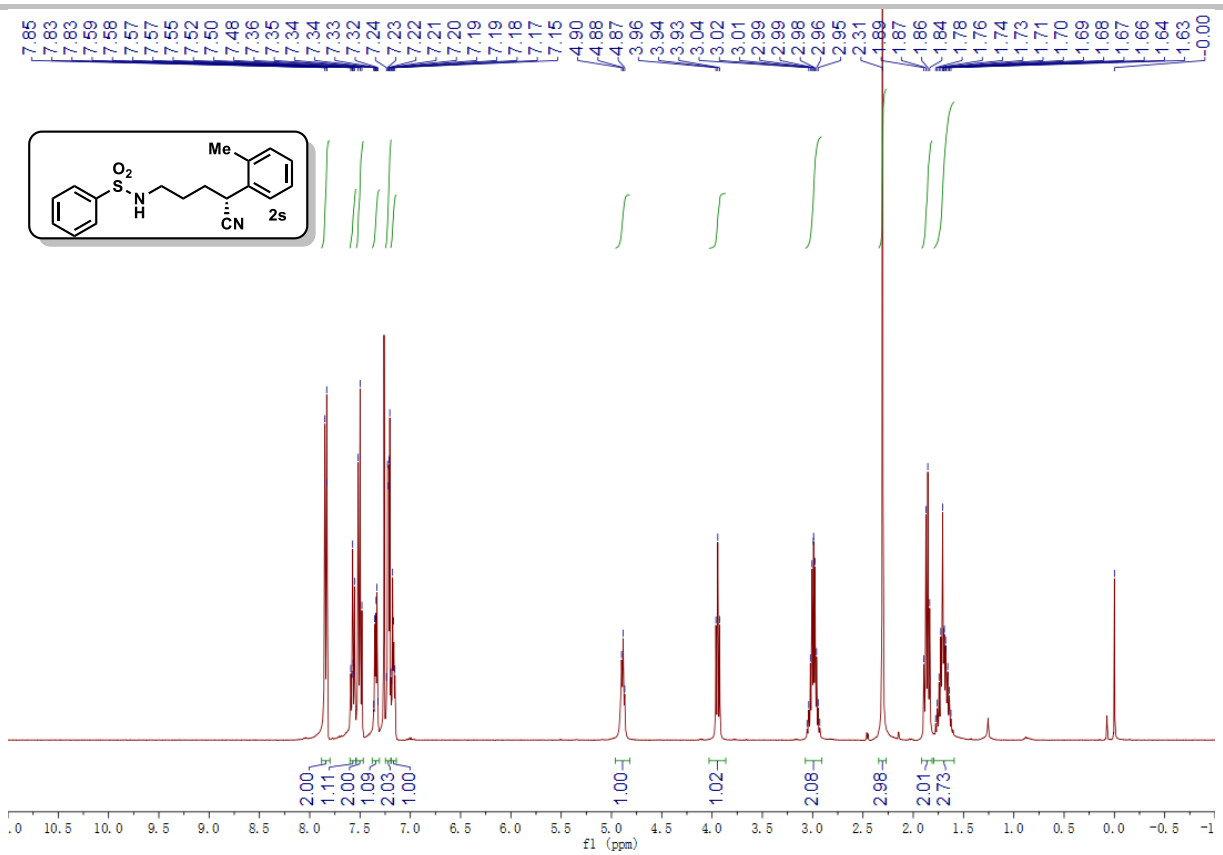

Figure S115. ^{1}H NMR of **2s**, related to Figure 2.

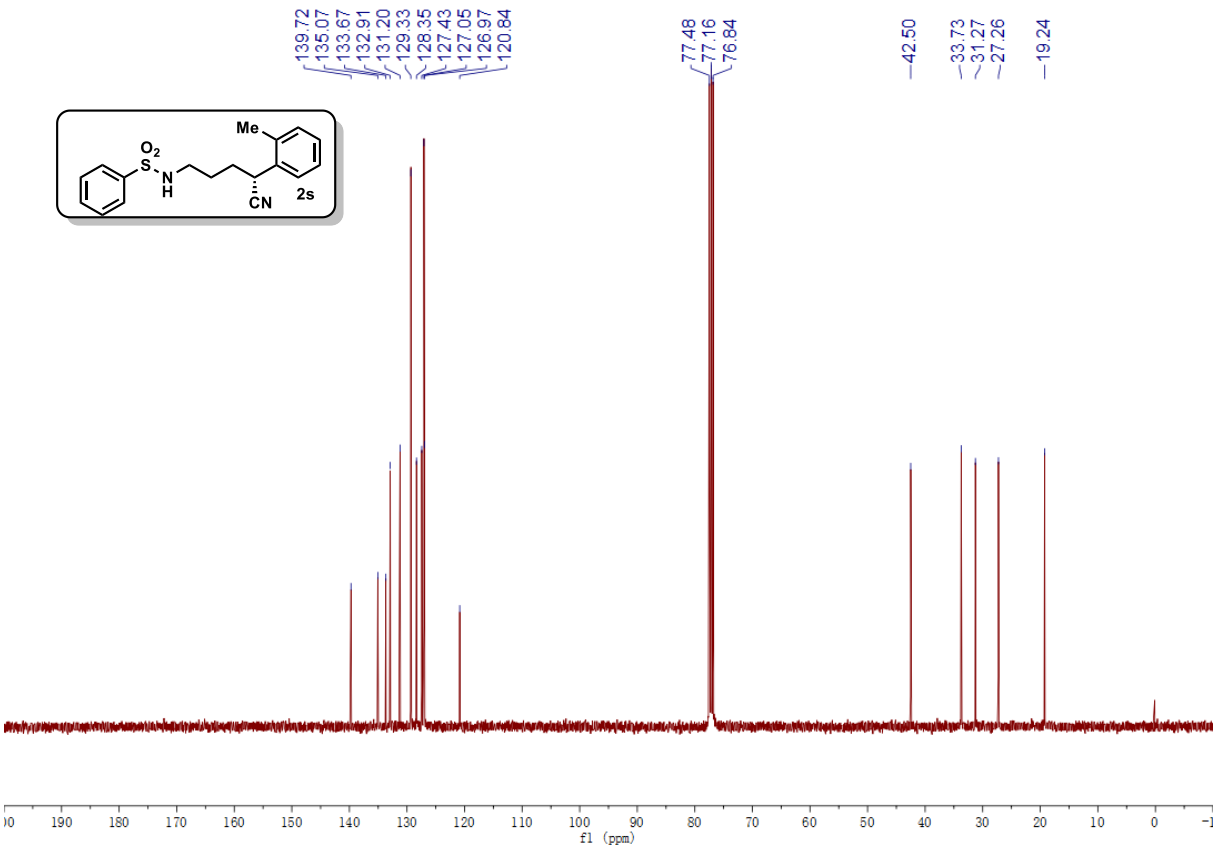

Figure S116. ^{13}C NMR of **2s**, related to Figure 2.

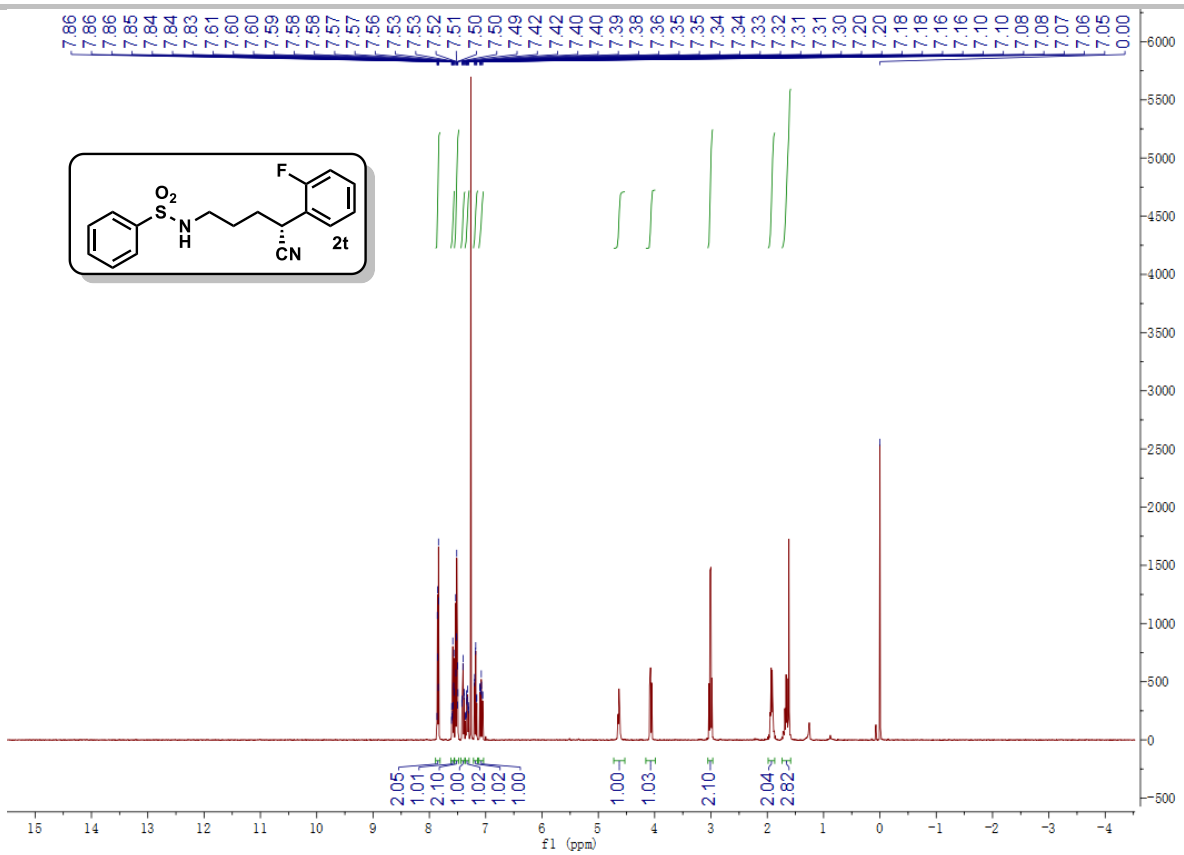

Figure S117. ^{1}H NMR of **2t**, related to Figure 2.

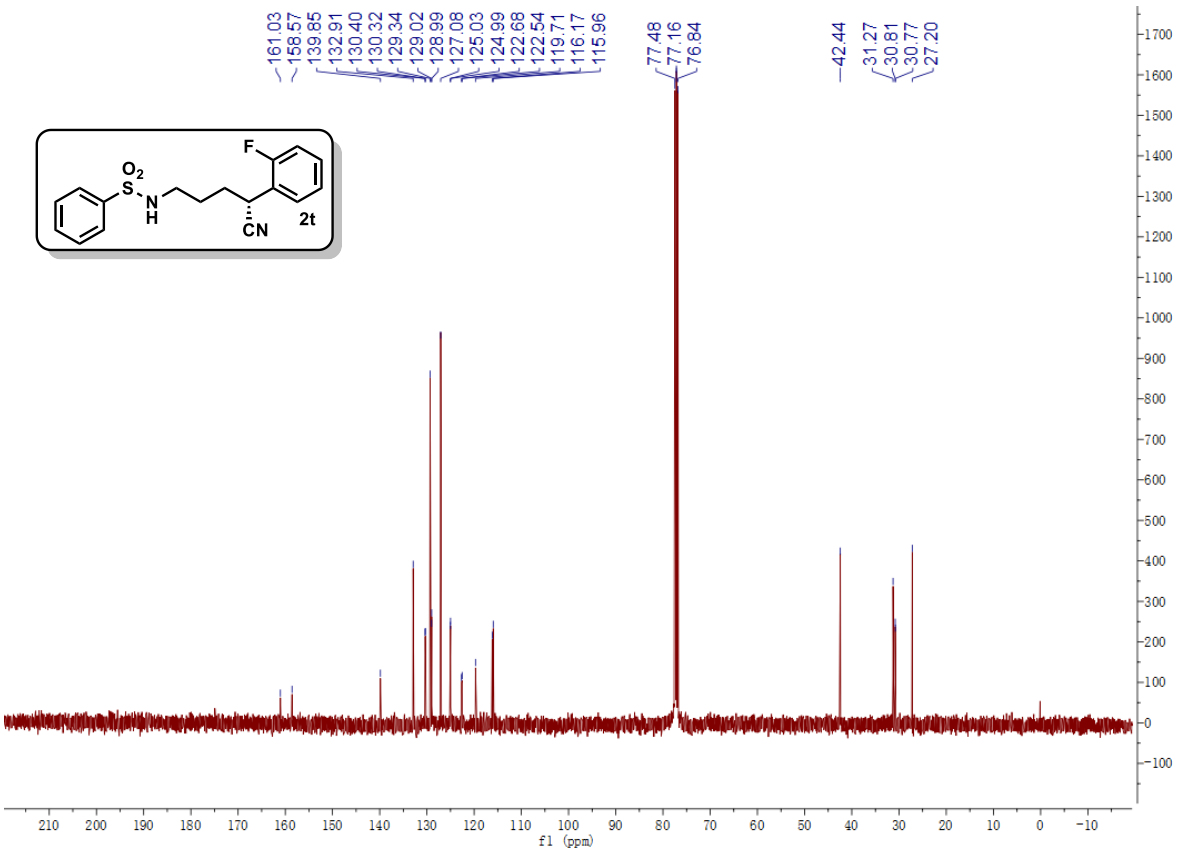

Figure S118. ^{13}C NMR of **2t**, related to Figure 2.

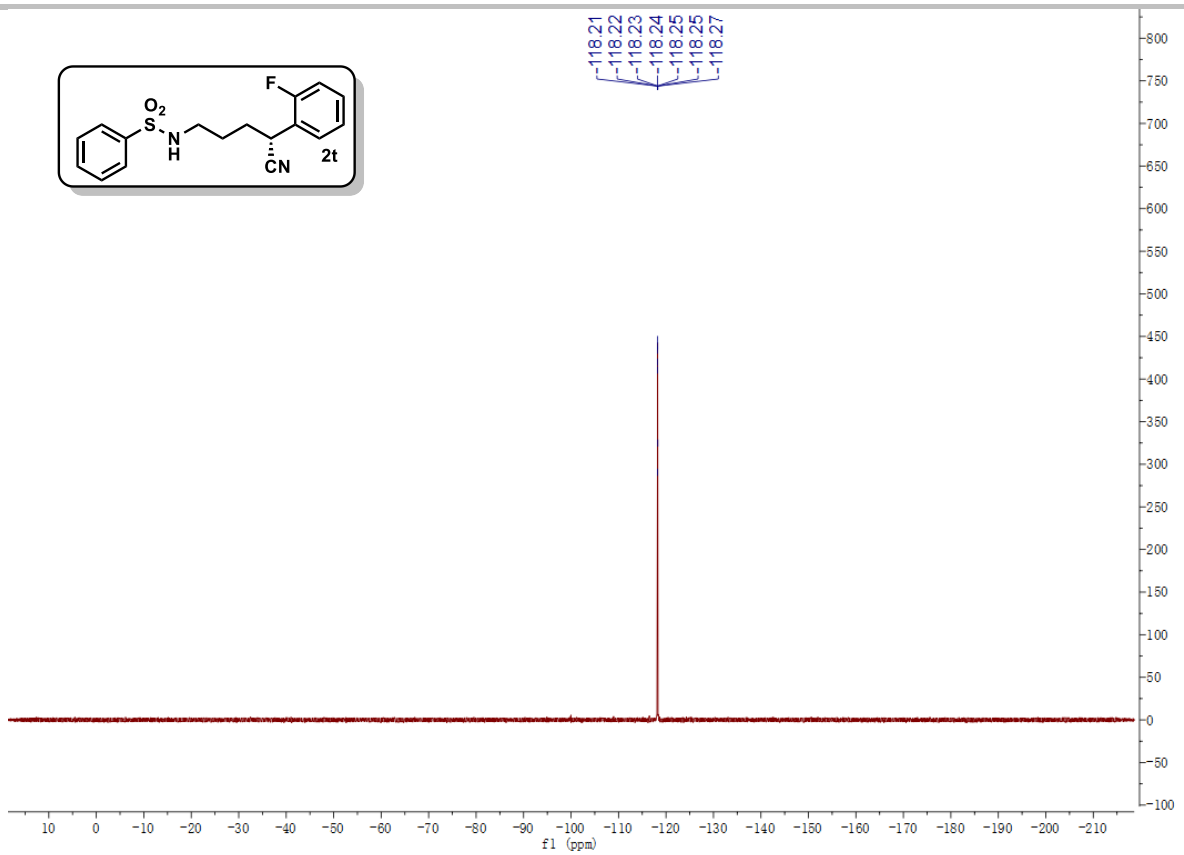

Figure S119. ^{19}F NMR of **2t**, related to Figure 2.

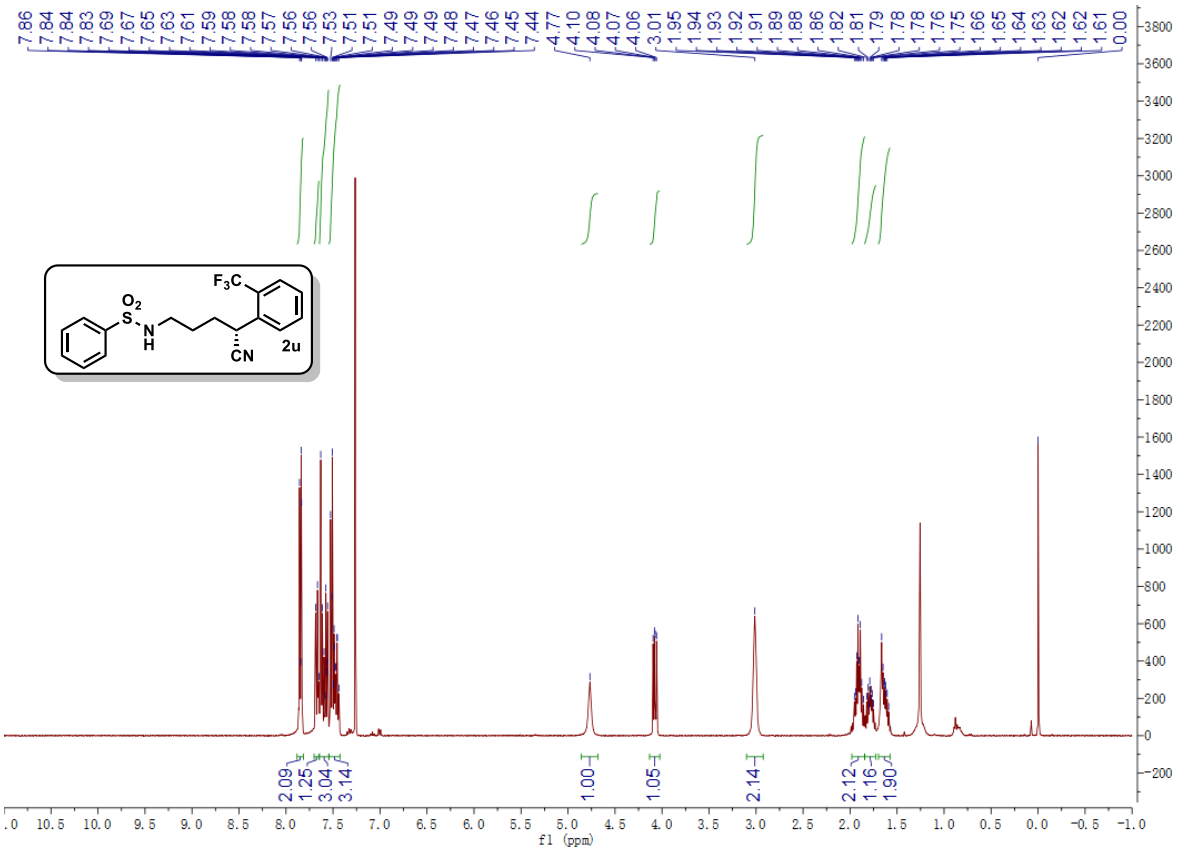

Figure S120. ^{1}H NMR of **2u**, related to Figure 2.

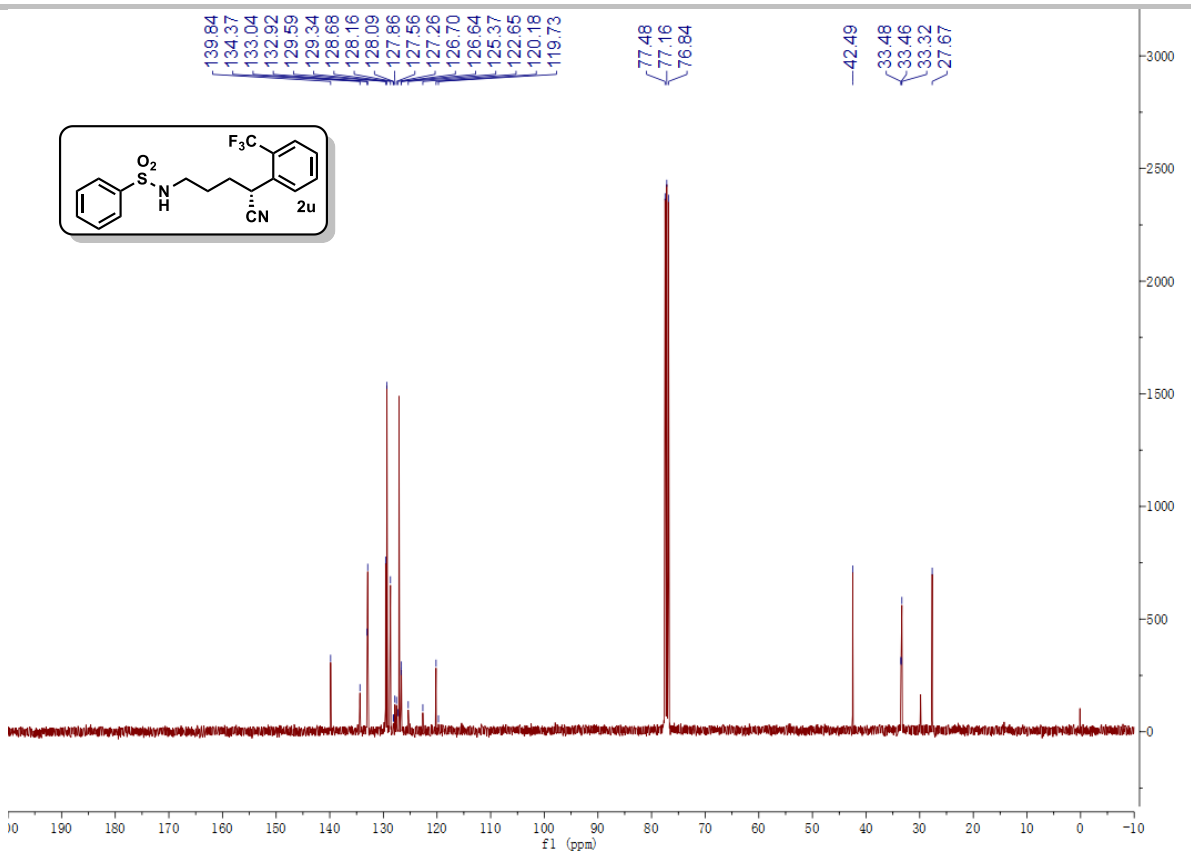

Figure S121. ^{13}C NMR of **2u**, related to Figure 2.

Figure S122. ^{19}F NMR of **2u**, related to Figure 2.

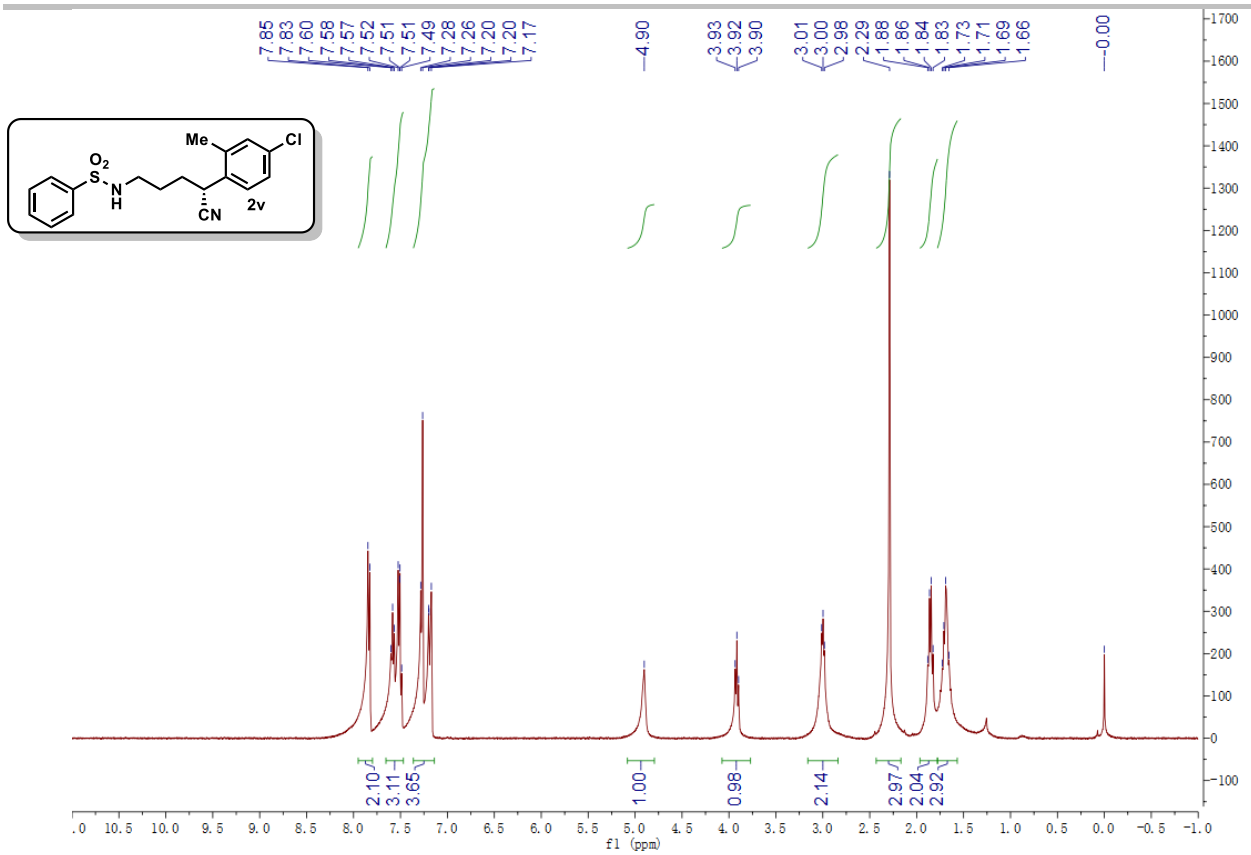

Figure S123. ^{1}H NMR of **2v**, related to Figure 2.

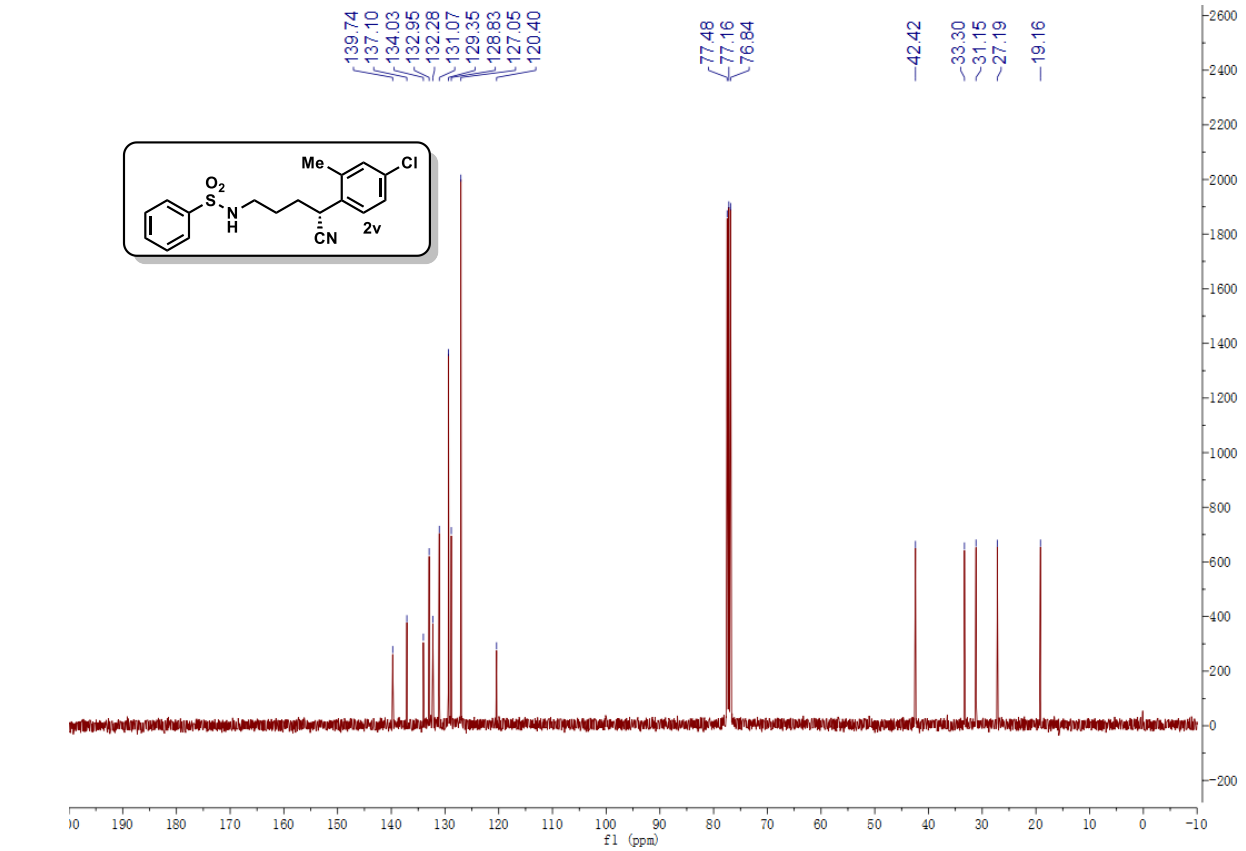

Figure S124. ^{13}C NMR of **2v**, related to Figure 2.

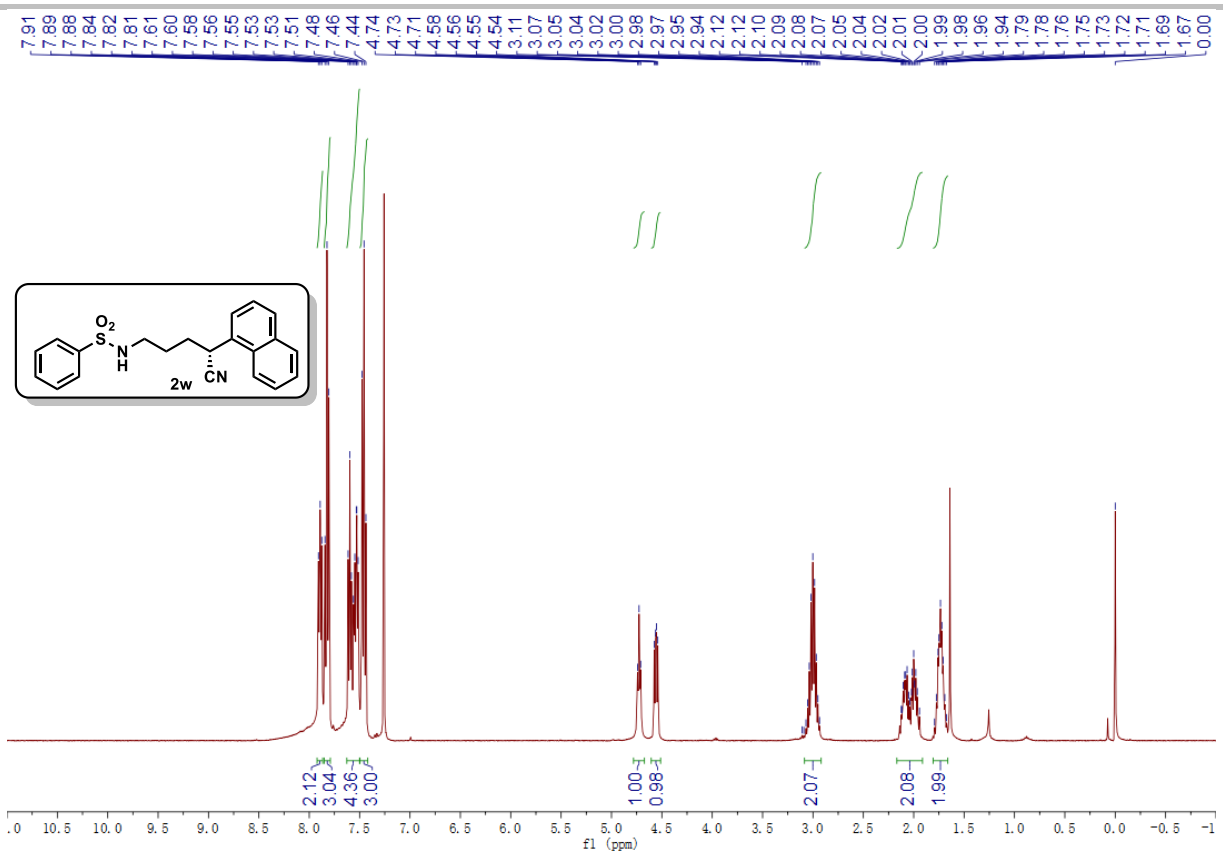

Figure S125. ^{1}H NMR of **2w**, related to Figure 2.

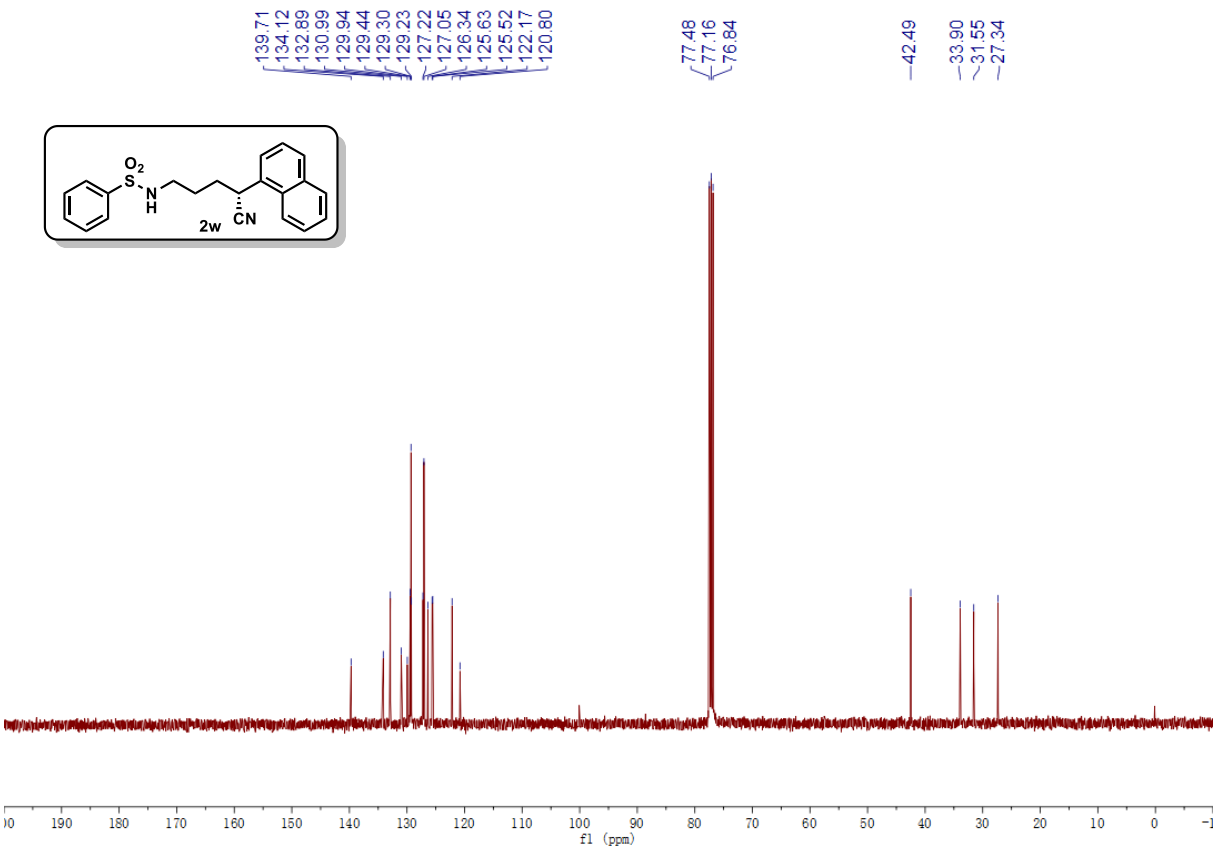

Figure S126. ^{13}C NMR of **2w**, related to Figure 2.

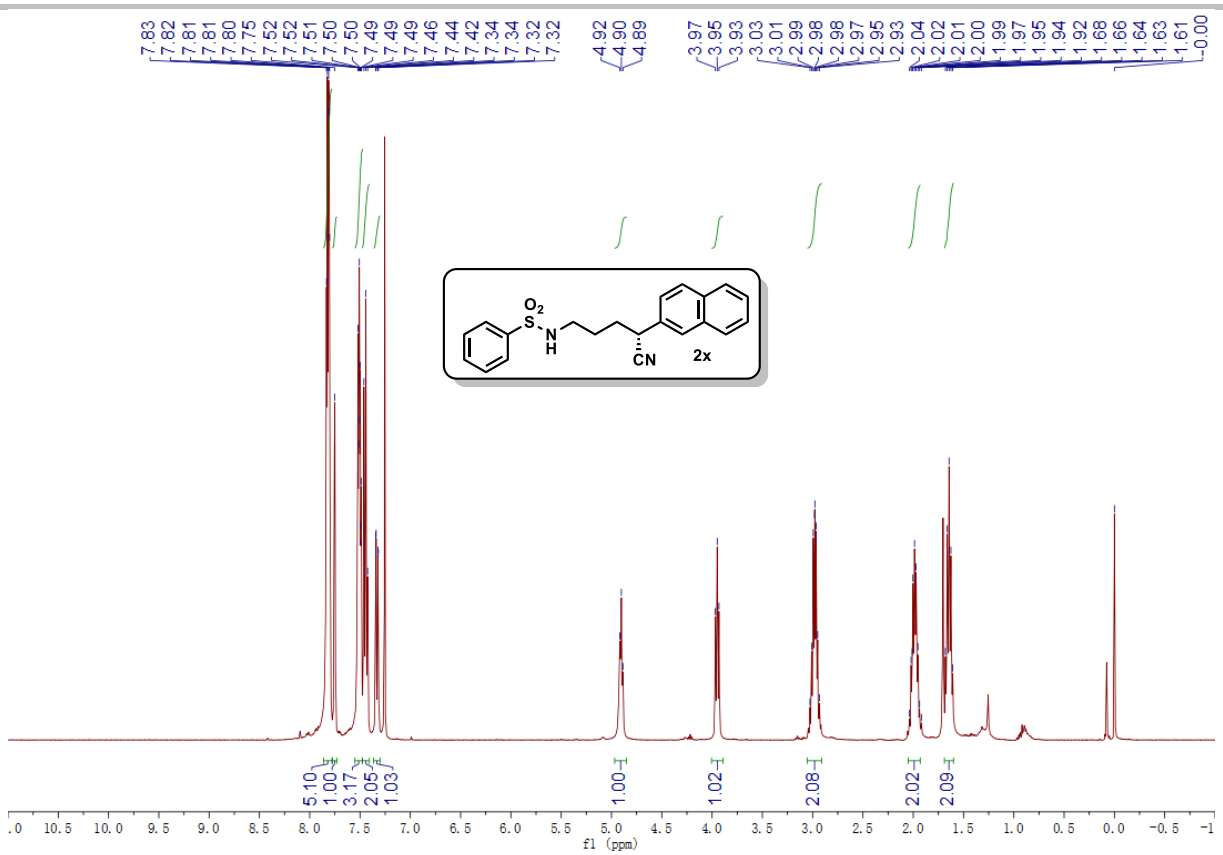

Figure S127. ^{1}H NMR of **2x**, related to Figure 2.

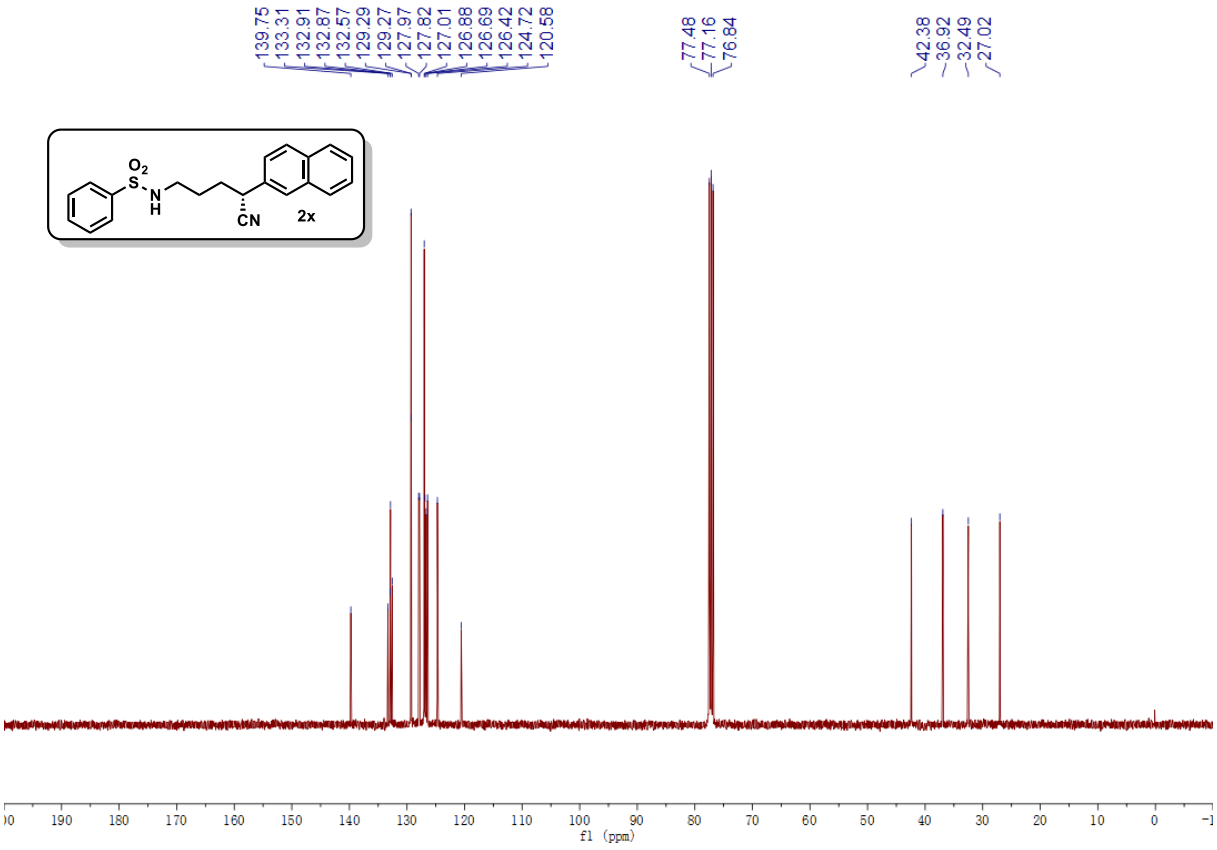

Figure S128. ^{13}C NMR of **2x**, related to Figure 2.

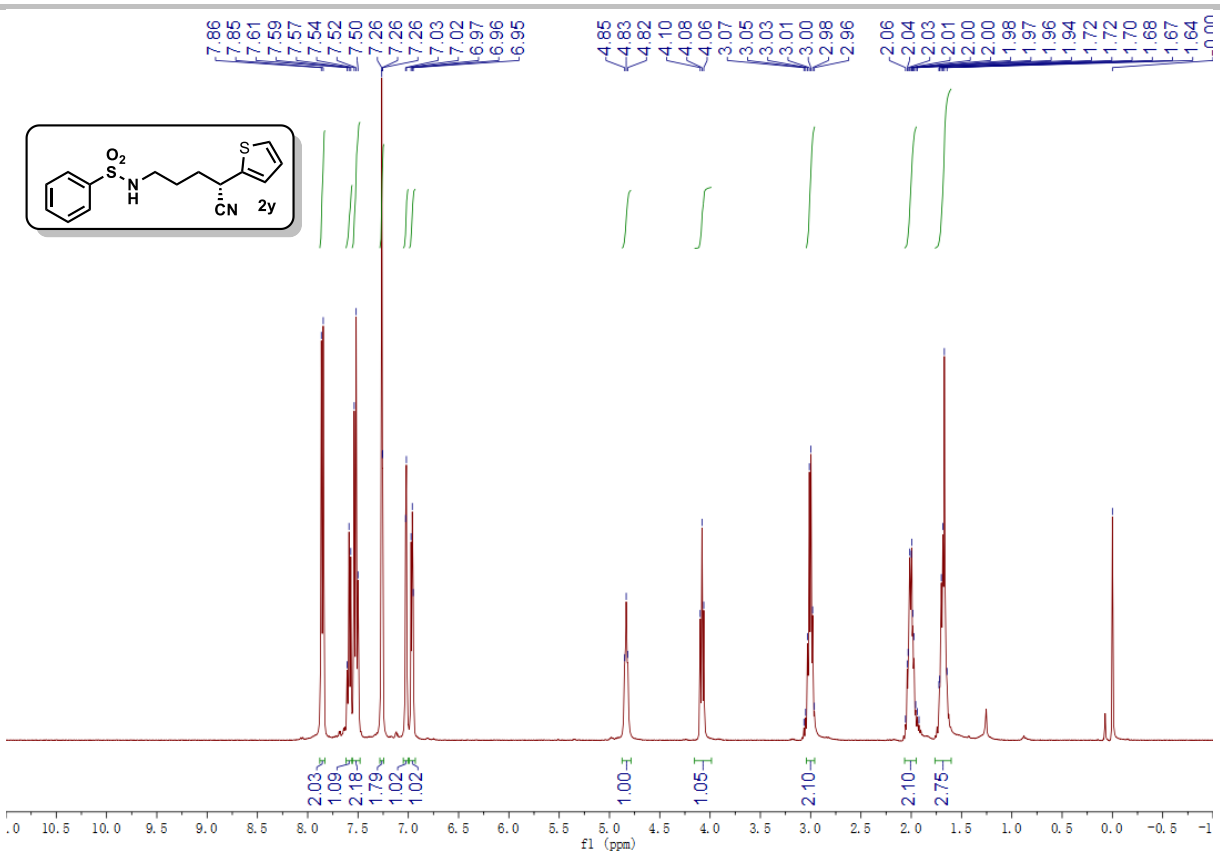

Figure S129. ^{1}H NMR of **2y**, related to Figure 2.

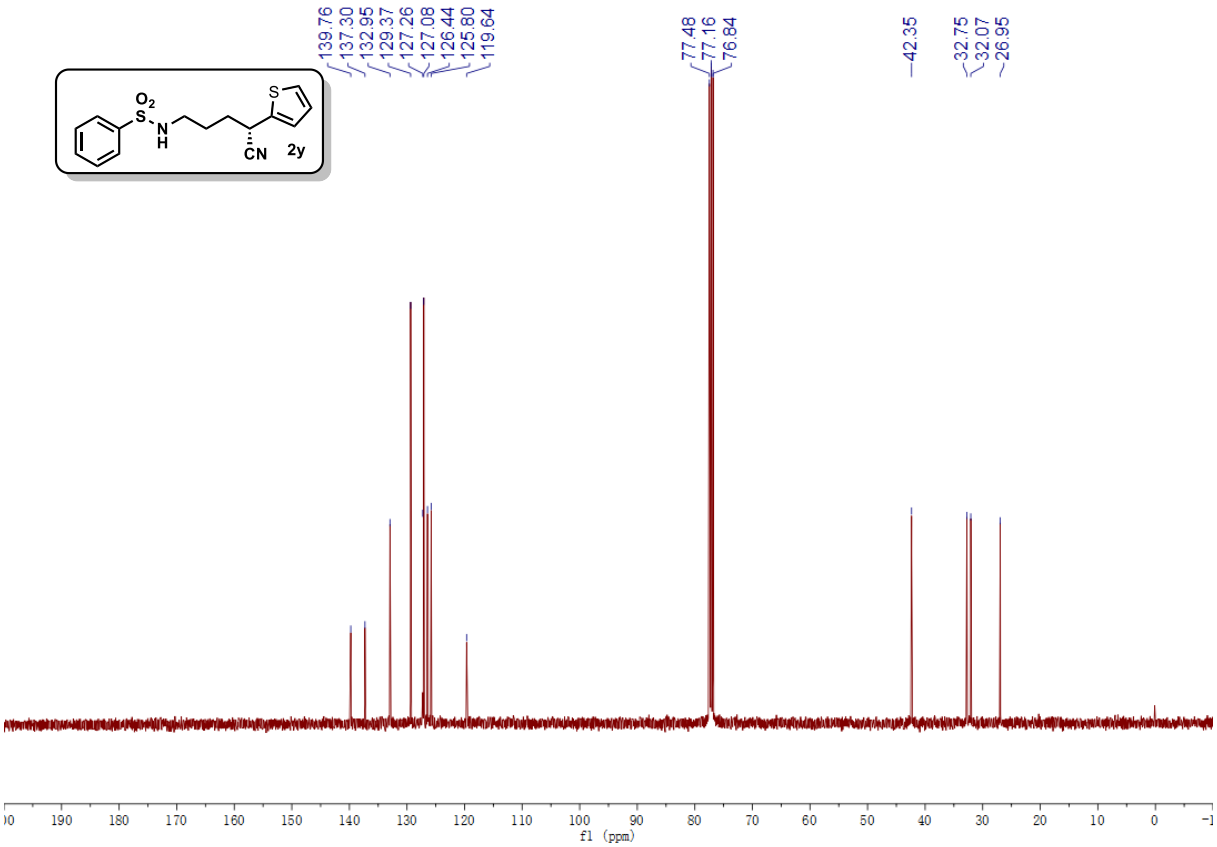

Figure S130. ^{13}C NMR of **2y**, related to Figure 2.

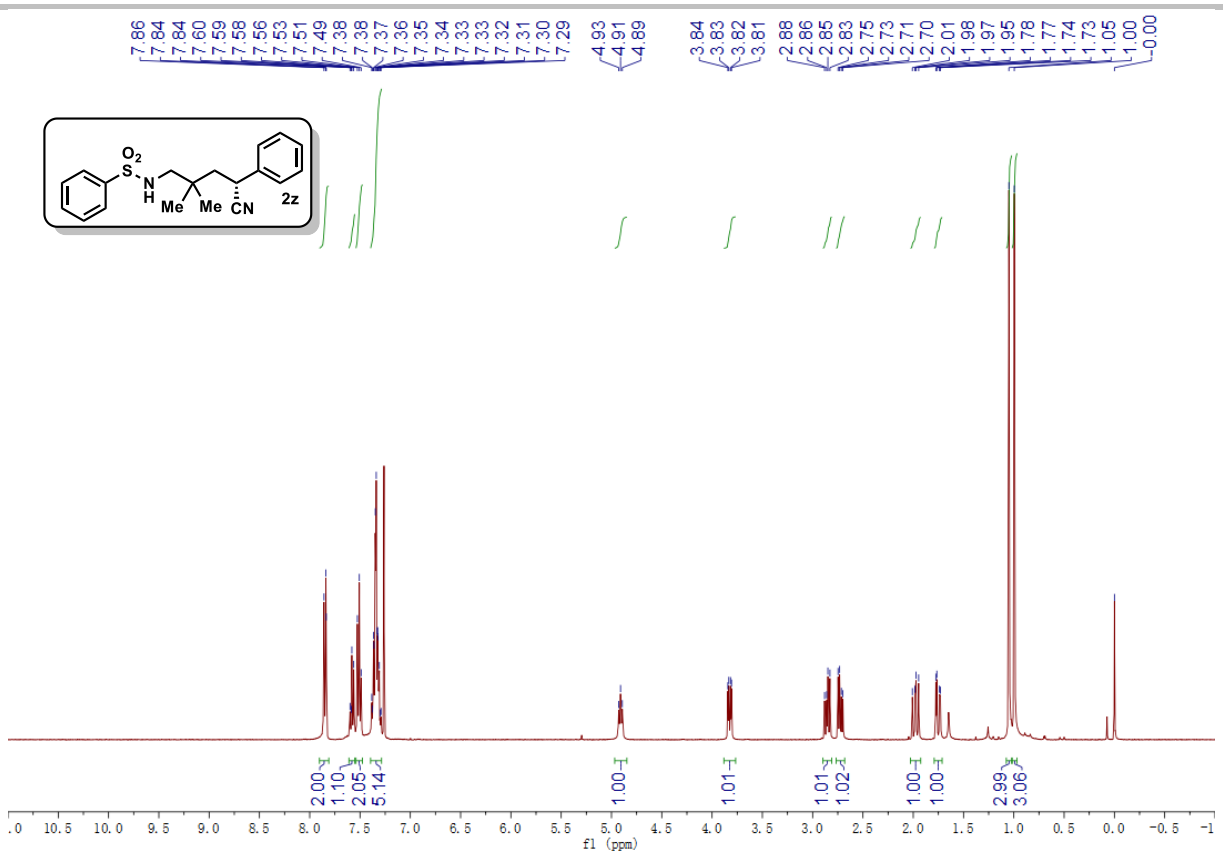

Figure S131. ^{1}H NMR of **2z**, related to Figure 2.

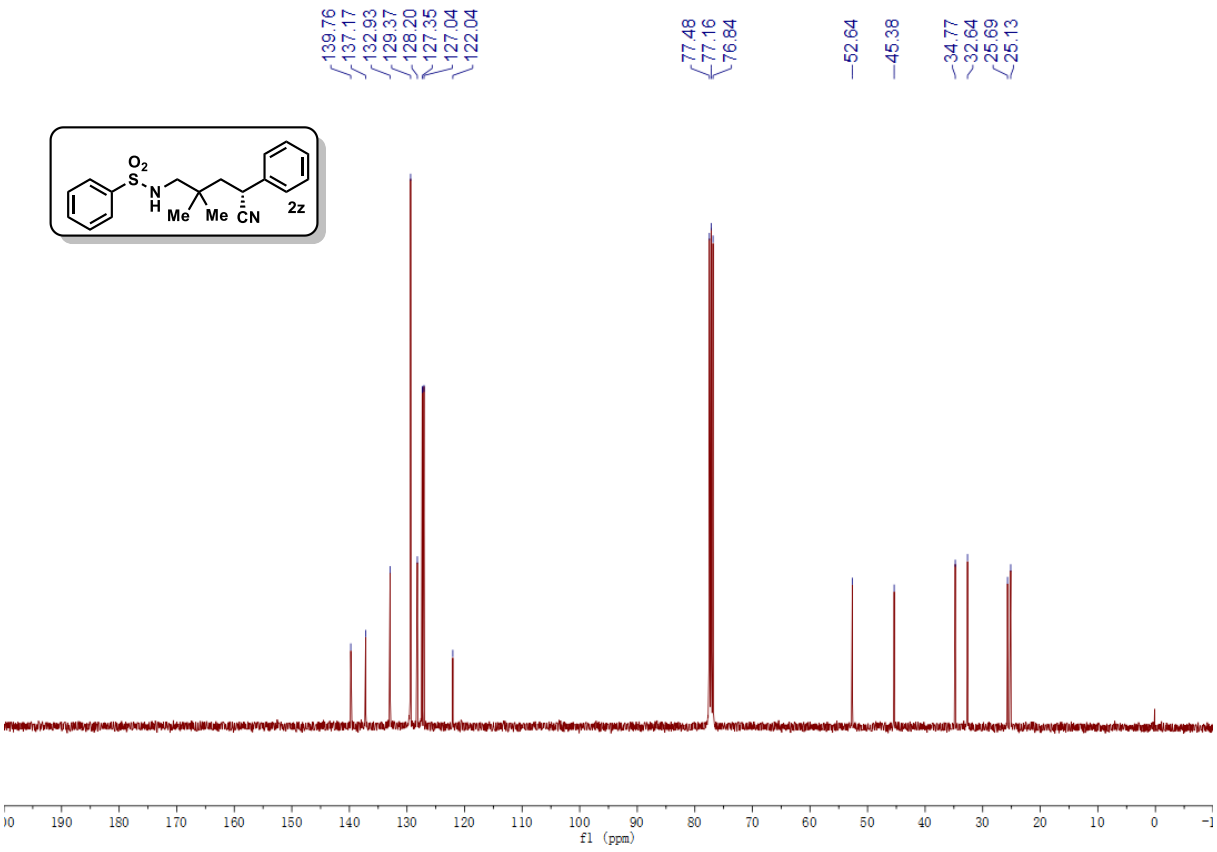

Figure S132. ^{13}C NMR of **2z**, related to Figure 2.

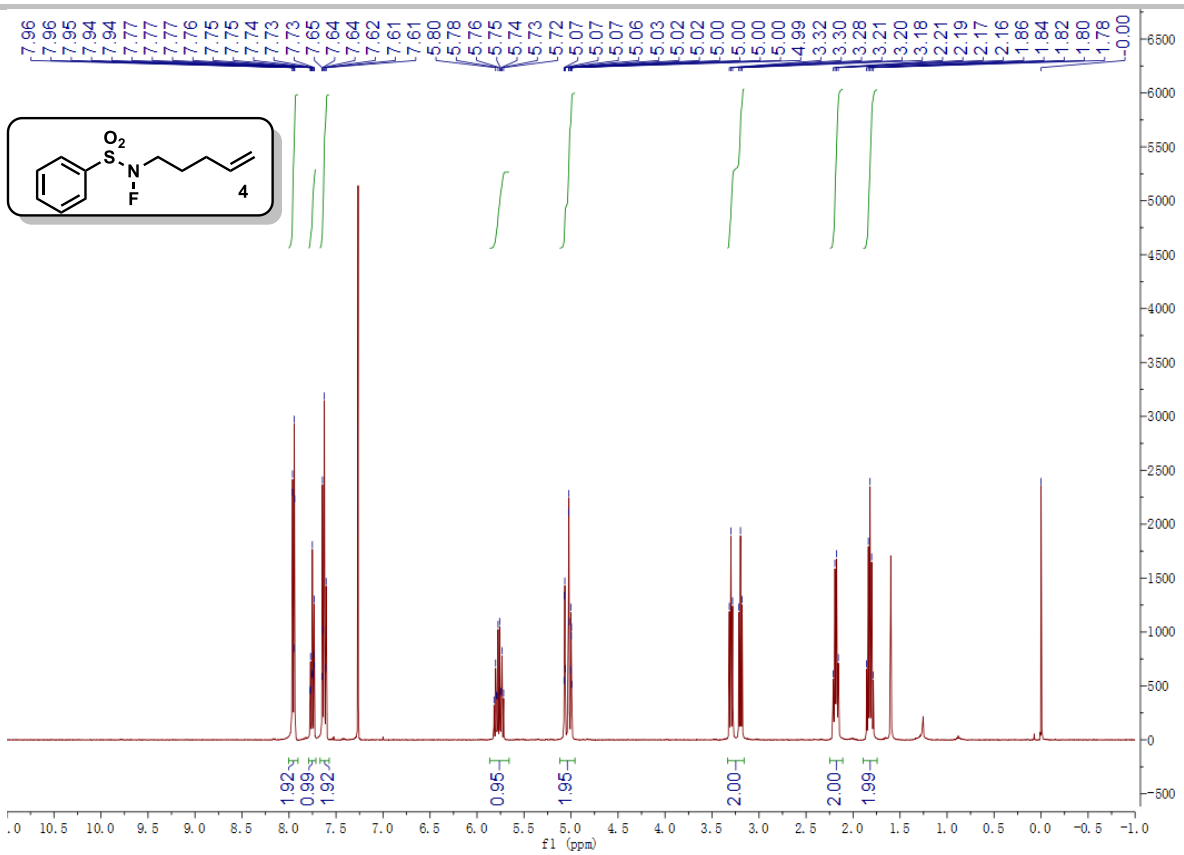

Figure S133. ^{1}H NMR of **4**, related to Scheme 2.

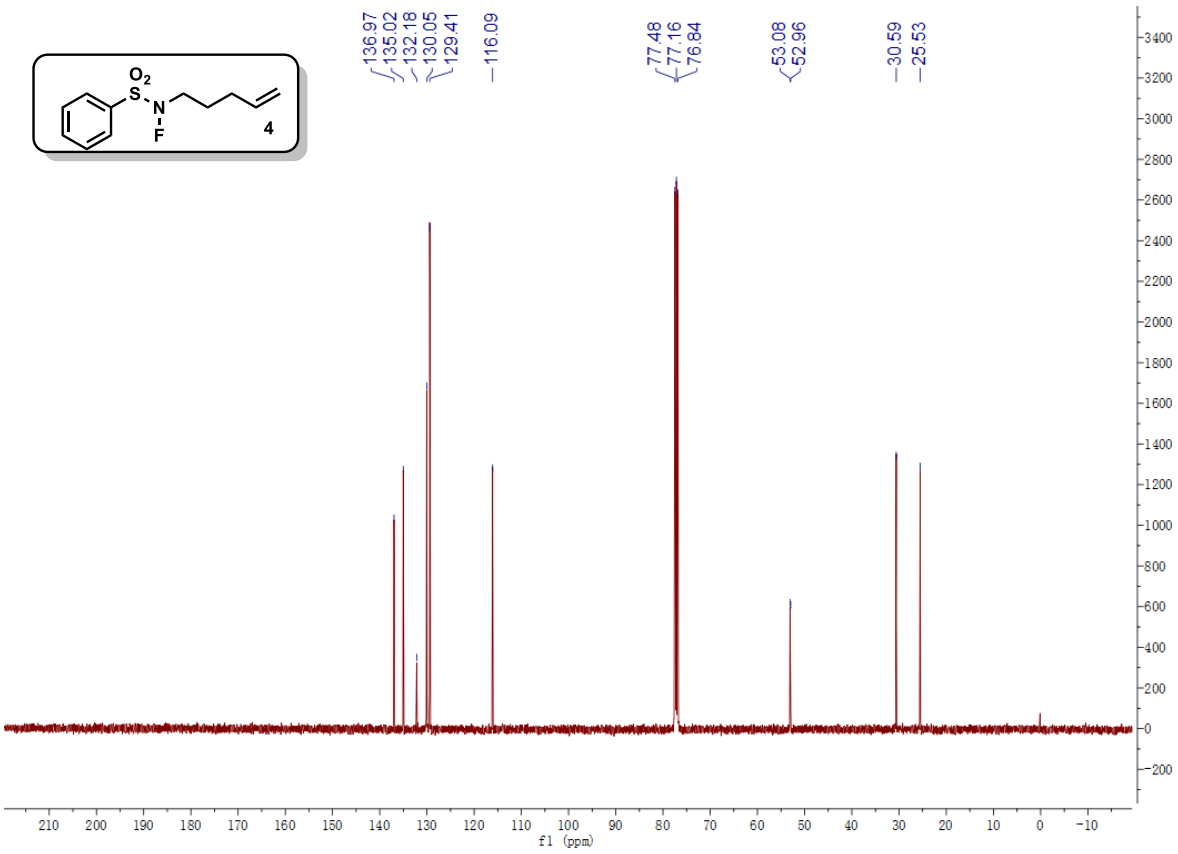

Figure S134. ^{13}C NMR of **4**, related to Scheme 2.

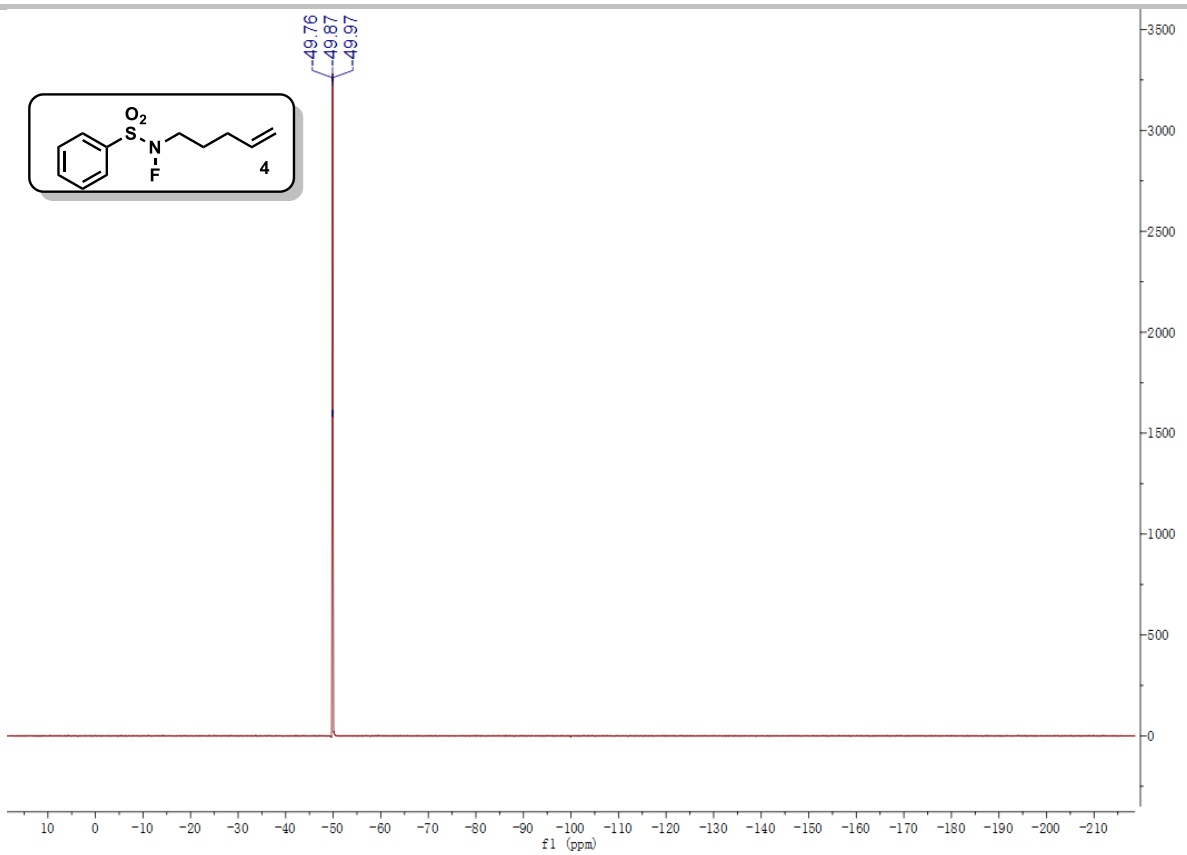

Figure S135. ^{19}F NMR of **4**, related to Scheme 2.

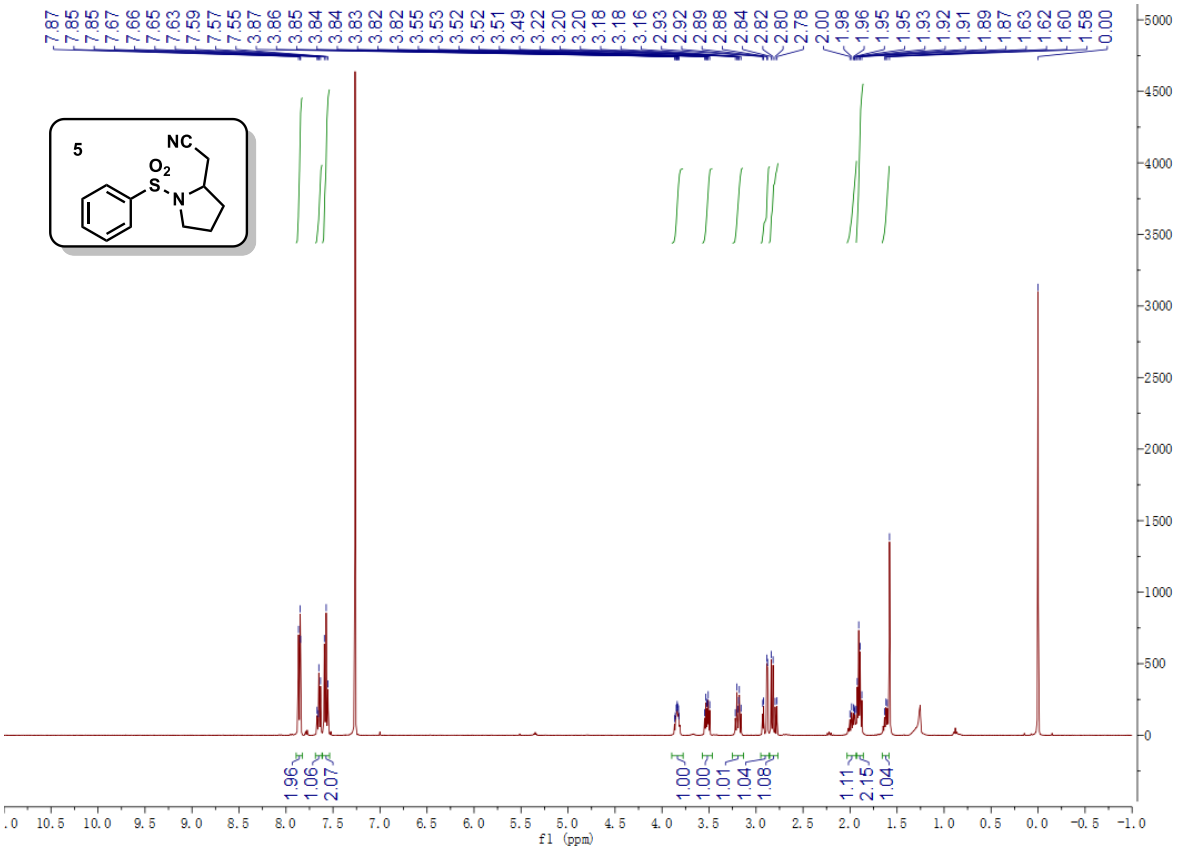

Figure S136. ^{1}H NMR of **5**, related to Scheme 2.

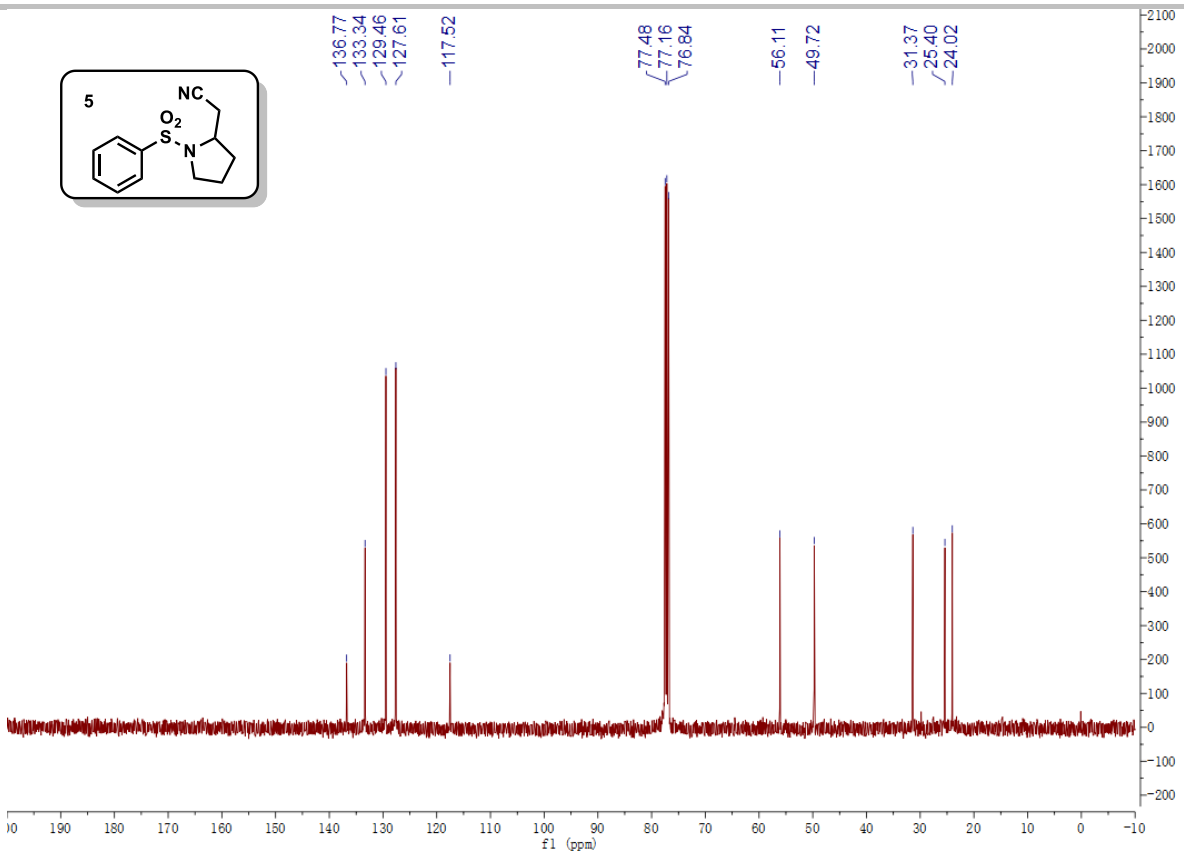

Figure S137. ^{13}C NMR of **5**, related to Scheme 2.

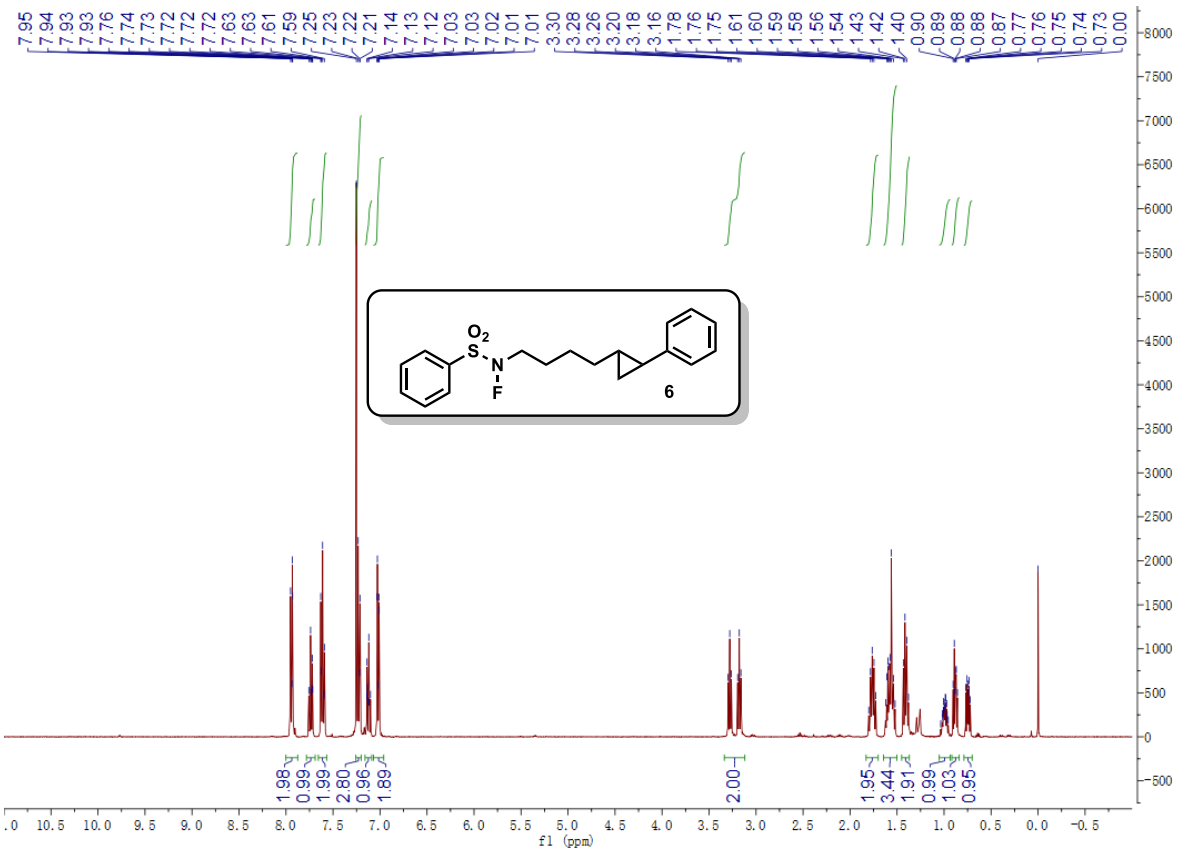

Figure S138. ^{1}H NMR of **6**, related to Scheme 2.

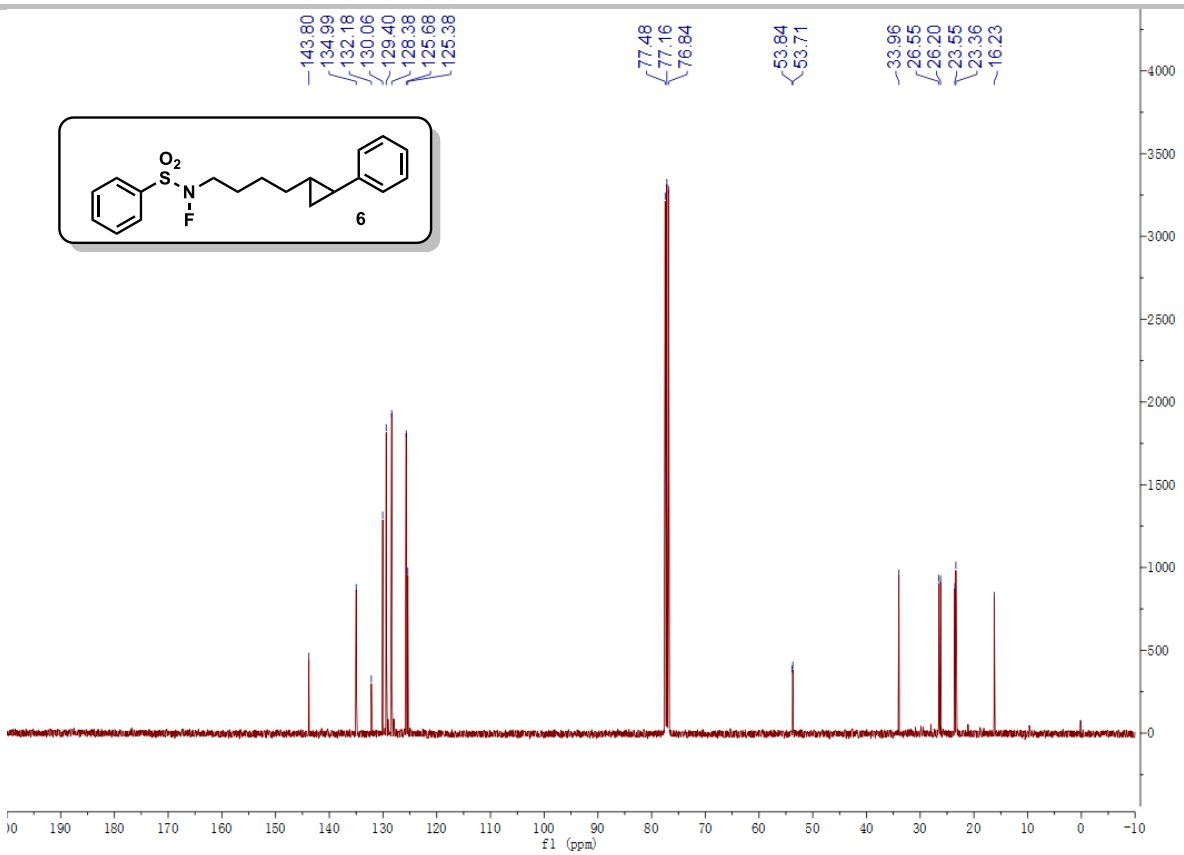

Figure S139. ^{13}C NMR of **6**, related to Scheme 2.

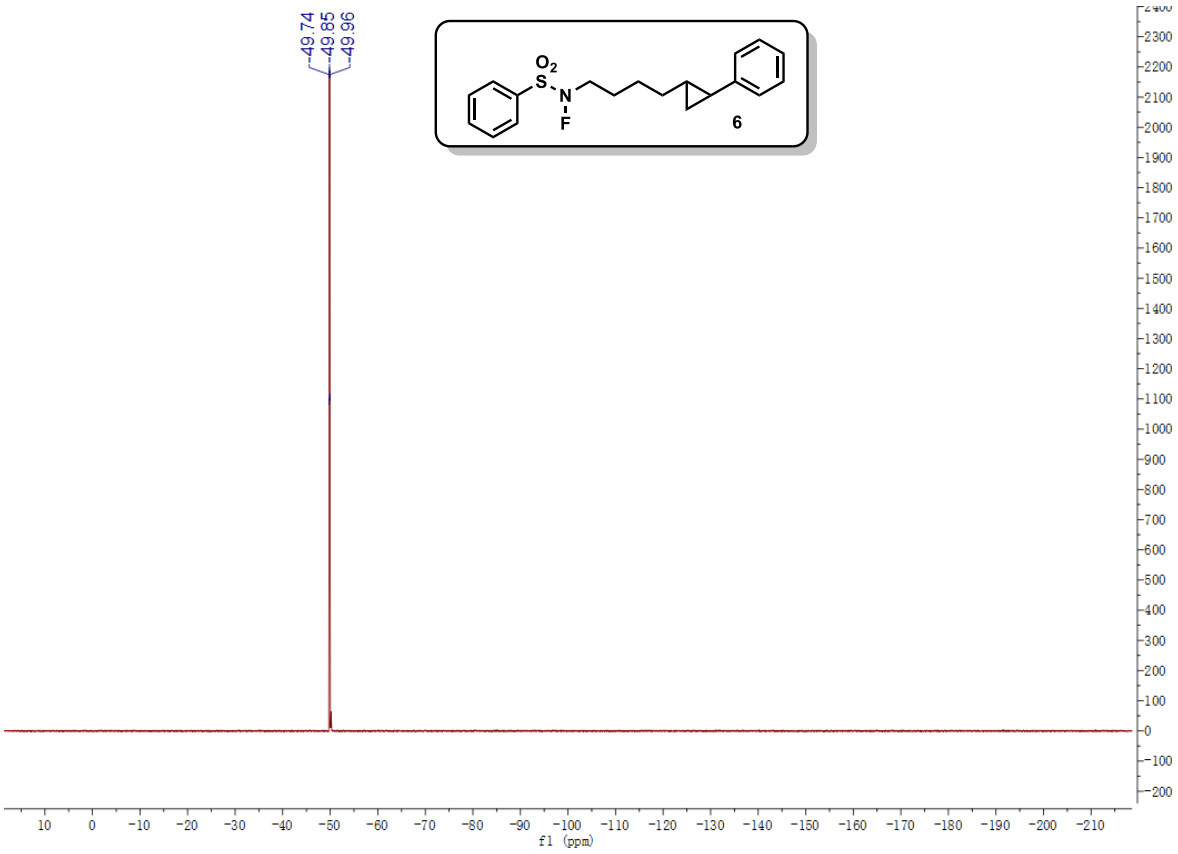

Figure S140. ^{19}F NMR of **6**, related to Scheme 2.

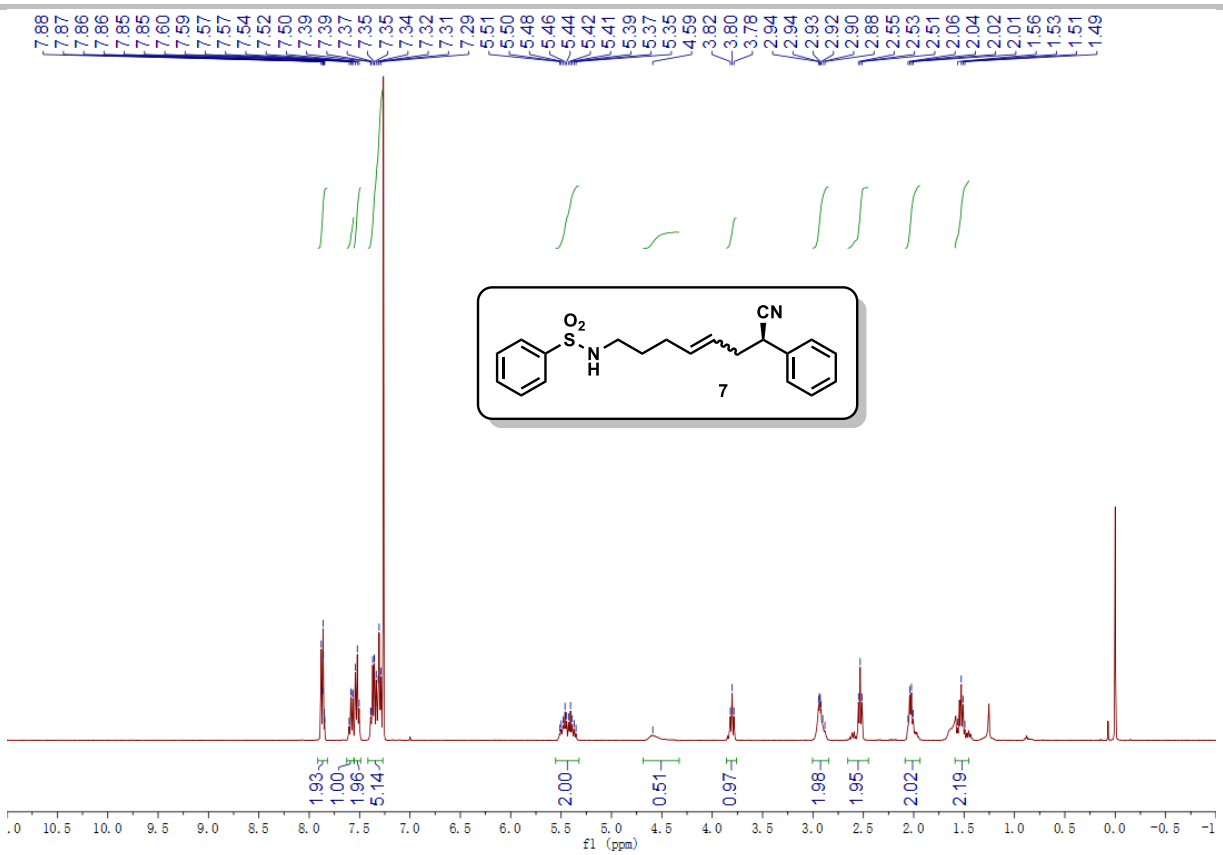

Figure S141. ^{1}H NMR of **7**, related to Scheme 2.

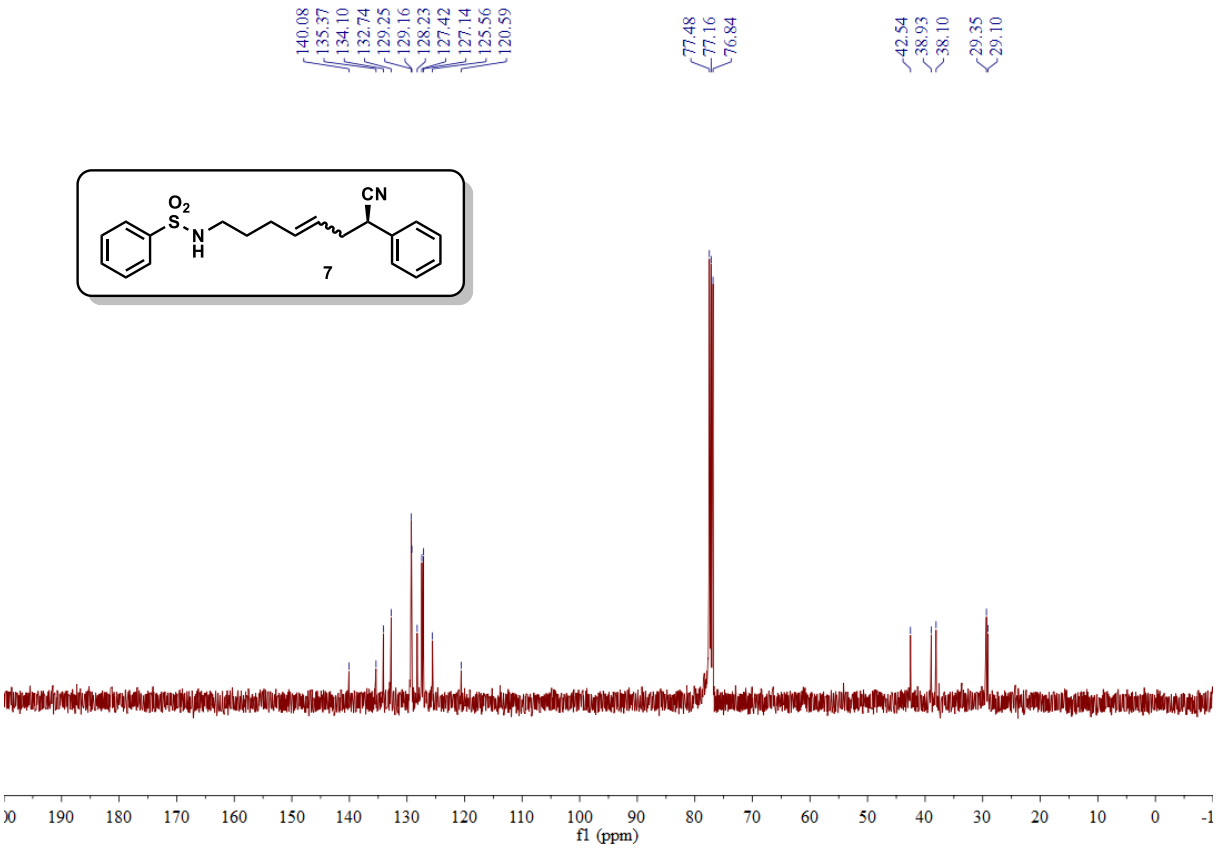

Figure S142. ^{13}C NMR of **7**, related to Scheme 2.

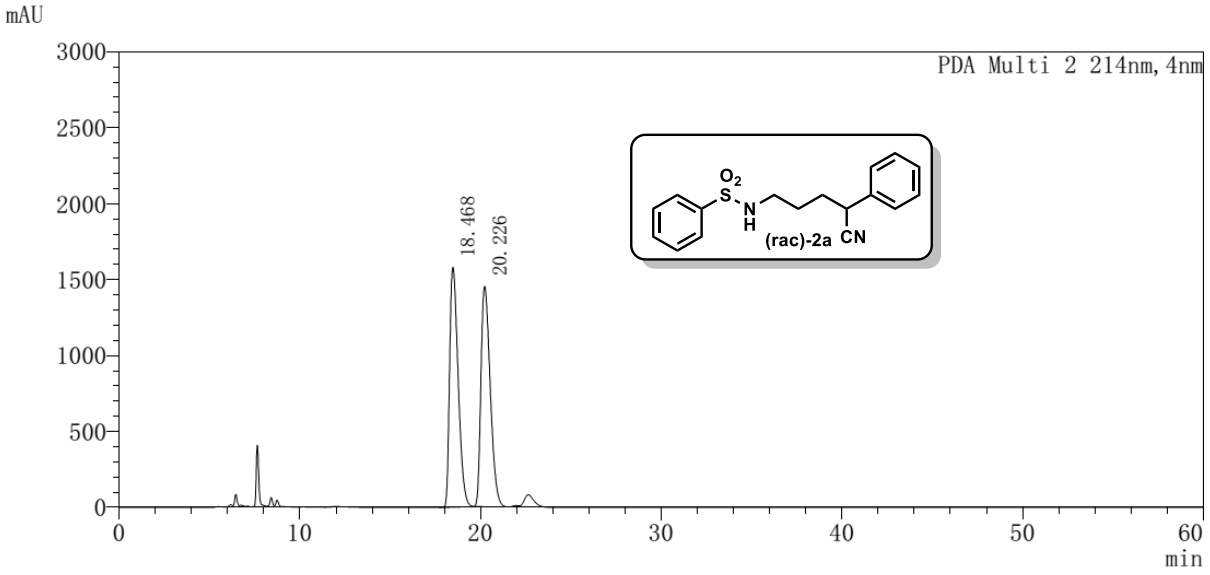

〈峰表〉

PDA Ch2 214nm

峰号	保留时间	面积%	面积	高度	标记
1	18.468	49.840	51634016	1578336	M
2	20.226	50.160	51965091	1450311	M
总计		100.000	103599107	3028647	

Figure S143. HPLC data of rac-**2a**, related to Figure 2**.**

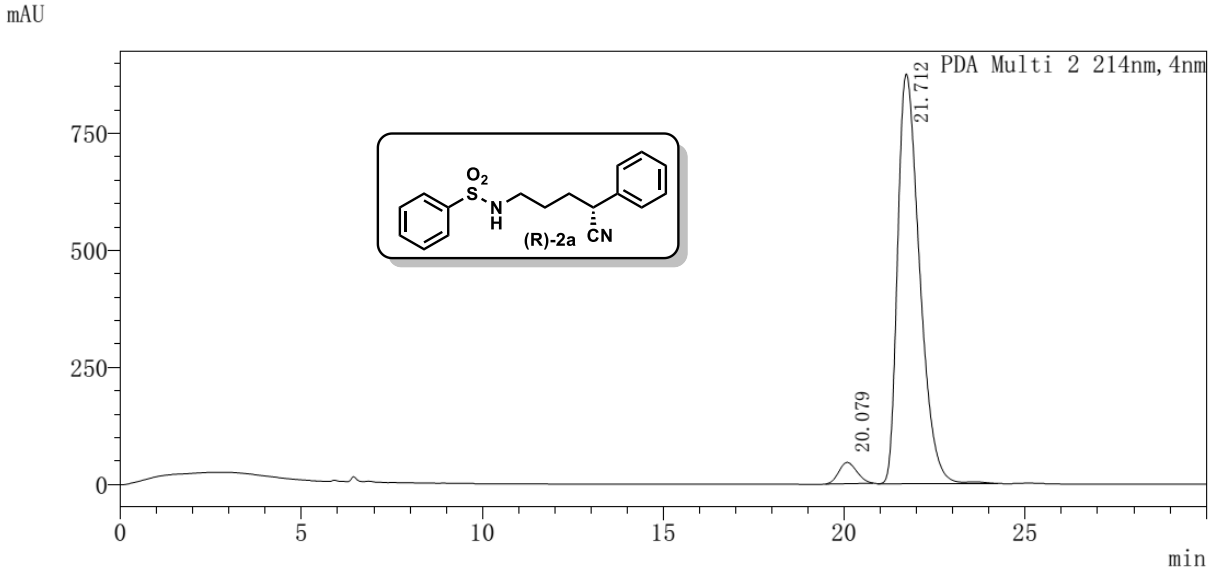

〈峰表〉

PDA Ch2 214nm

Peak#	Time	area%	area	Hight	Mark
1	20.079	4.053	1557621	44962	M
2	21.712	95.947	36876595	874883	M
总计		100.000	38434217	919844	

Figure S144. HPLC data of **2a**, related to Figure 2**.**

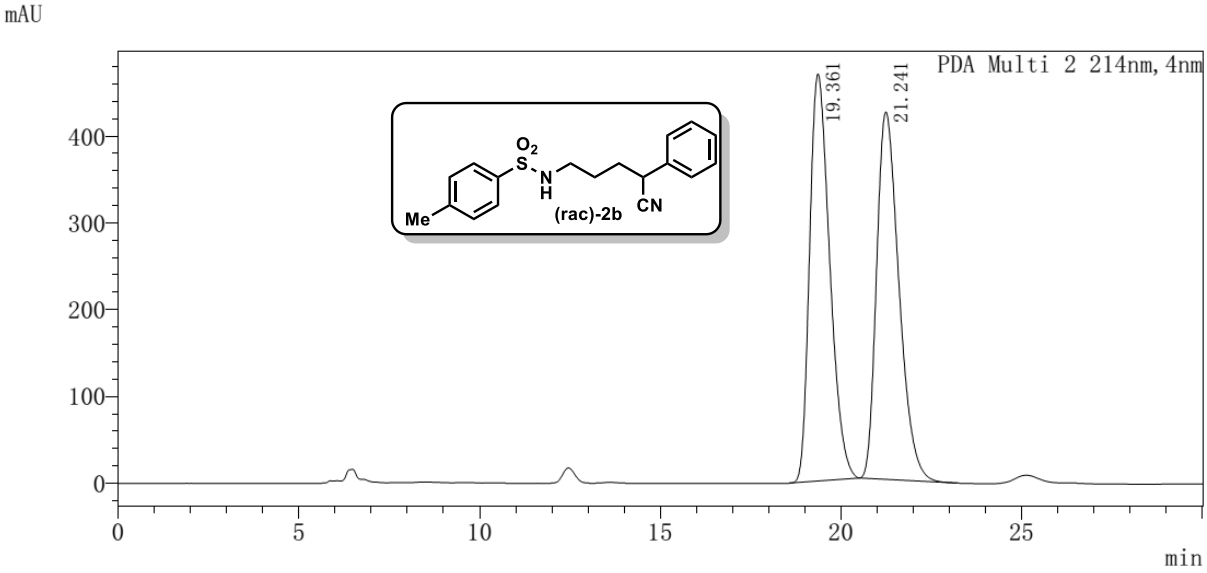

〈峰表〉

PDA Ch2 214nm

Peak#	Time	Area%	Area	Hight	Mark
1	19.361	49.923	18168735	469313	M
2	21.241	50.077	18225044	423638	M
总计		100.000	36393778	892951	

Figure S145. HPLC data of rac-**2b**, related to Figure 2.

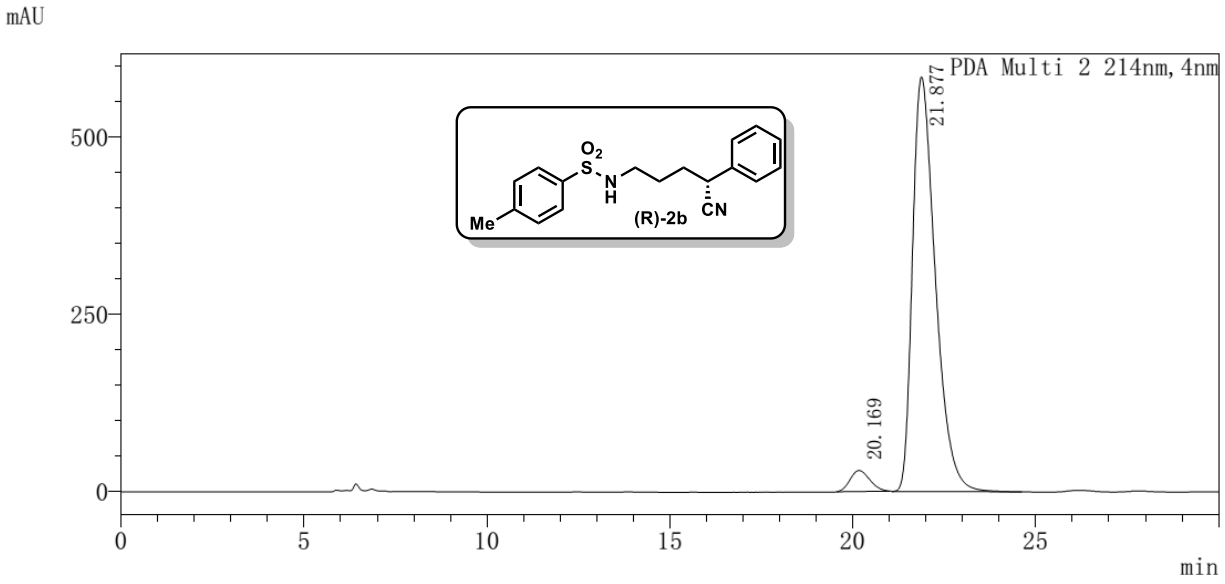

〈峰表〉

PDA Ch2 214nm

Peak#	保留时间	面积%	面积	高度	标记
1	20.169	4.189	1110061	29648	M
2	21.877	95.811	25388185	584640	M
总计		100.000	26498246	614288	

Figure S146. HPLC data of **2b**, related to Figure 2.

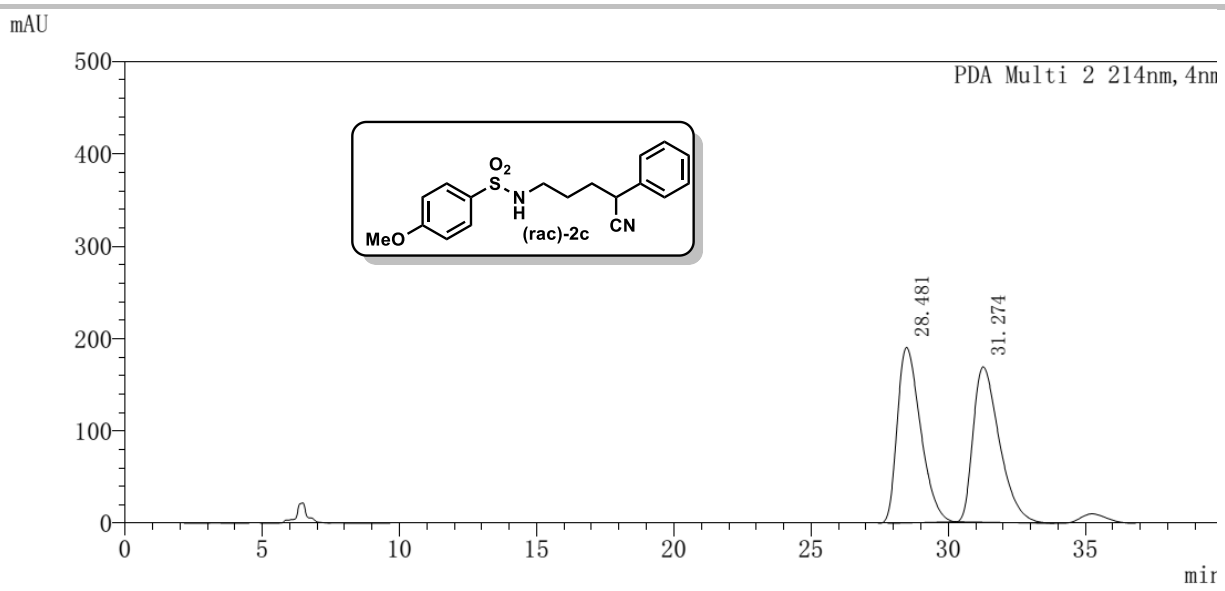

〈峰表〉

PDA Ch2 214nm

峰号	保留时间	面积%	面积	高度	标记
1	28.481	50.055	11278576	190303	M
2	31.274	49.945	11253992	168234	M
总计		100.000	22532568	358537	

Figure S147. HPLC data of rac-**2c**, related to Figure 2.

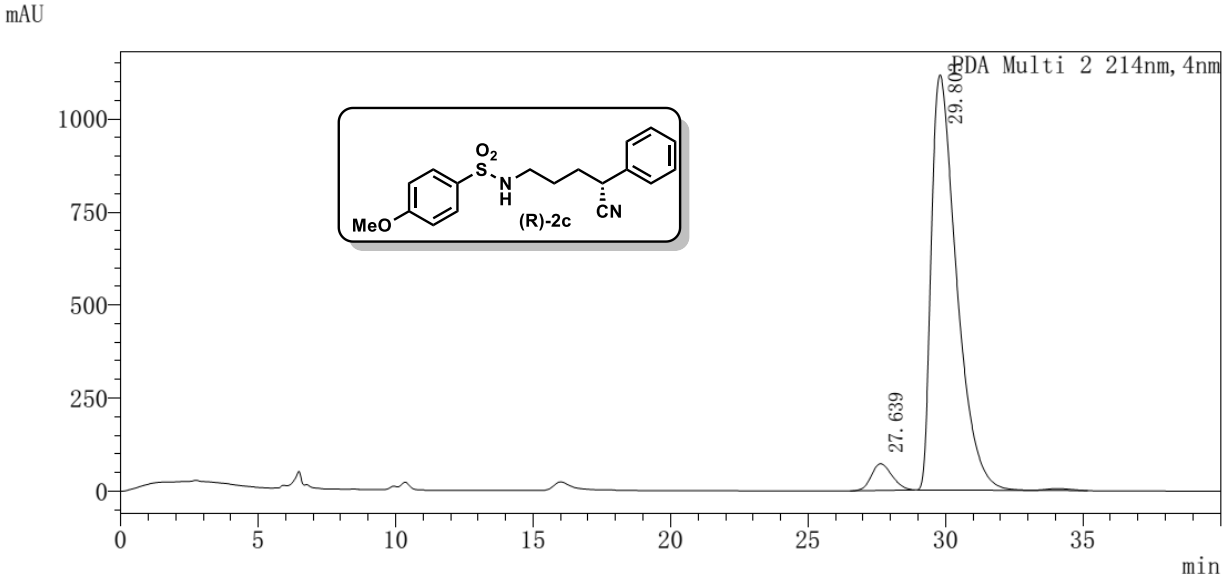

〈峰表〉

PDA Ch2 214nm

峰号	保留时间	面积%	面积	高度	标记
1	27.639	5.010	3779534	71868	M
2	29.803	94.990	71666231	1116770	M
总计		100.000	75445765	1188637	

Figure S148. HPLC data of **2c**, related to Figure 2.

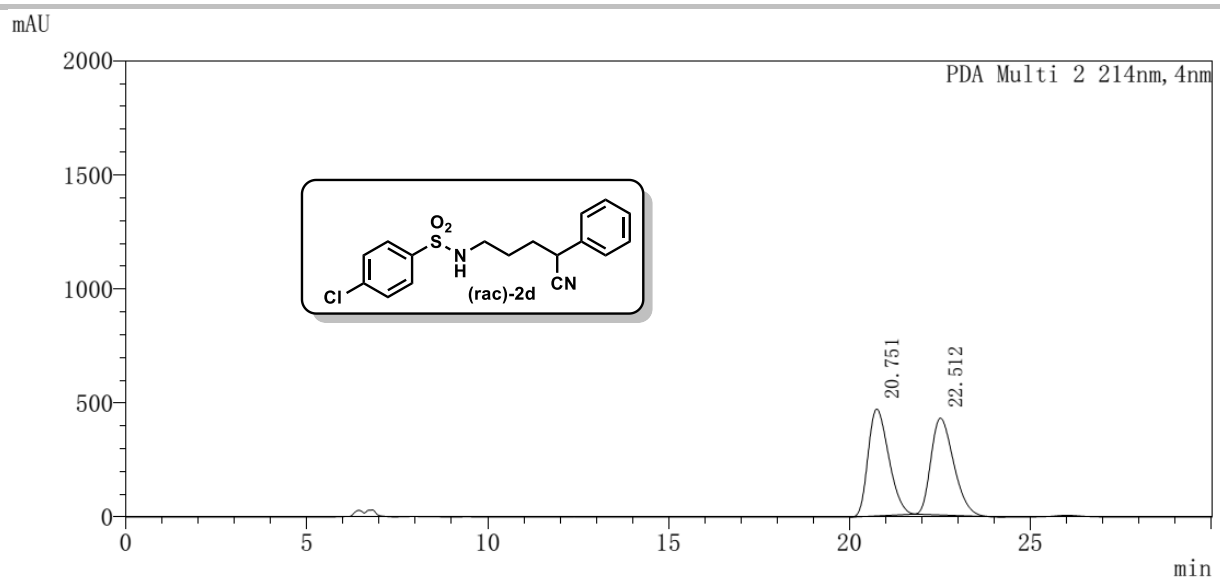

〈峰表〉

PDA Ch2 214nm

峰号	保留时间	面积%	面积	高度	标记
1	20.751	50.096	18614299	468420	M
2	22.512	49.904	18542951	424130	M
总计		100.000	37157250	892549	

Figure S149. HPLC data of rac-**2d**, related to Figure 2.

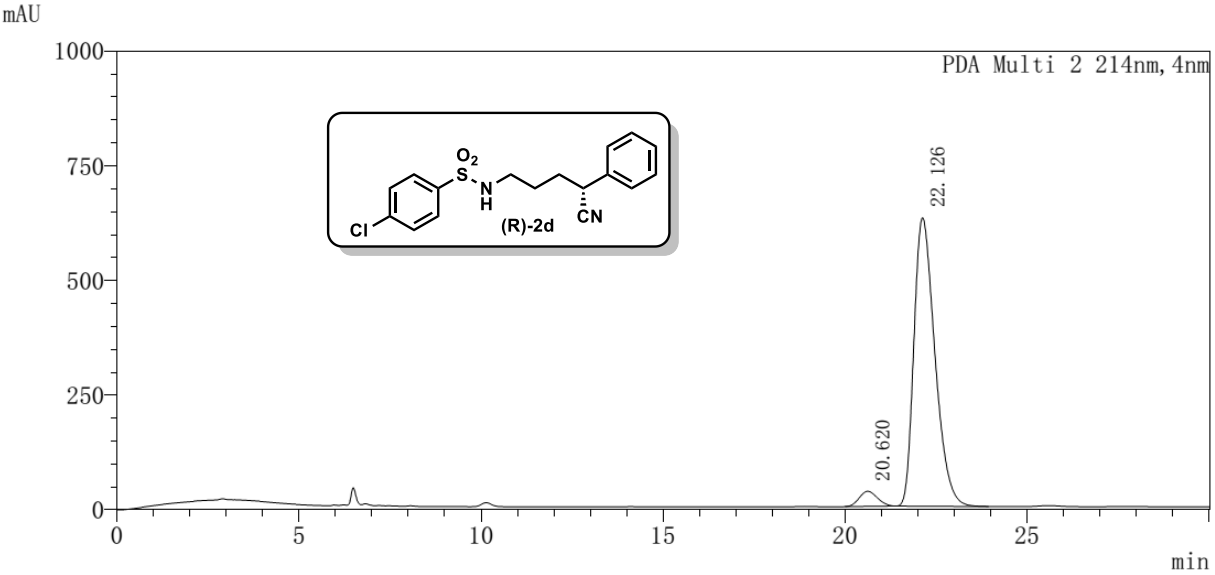

〈峰表〉

PDA Ch2 214nm

峰号	保留时间	面积%	面积	高度	标记
1	20.620	4.336	1142079	32901	M
2	22.126	95.664	25197262	628613	M
总计		100.000	26339341	661514	

Figure S150. HPLC data of **2d**, related to Figure 2.

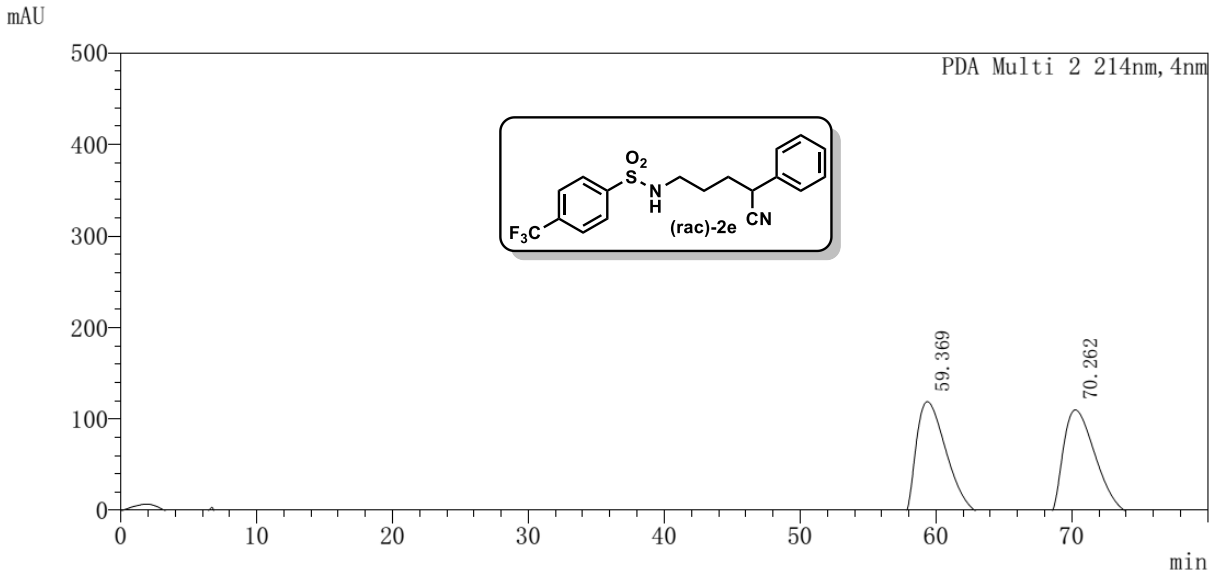

〈峰表〉

PDA Ch2 214nm

峰号	保留时间	面积%	面积	高度	标记
1	59.369	49.878	20451513	126967	M
2	70.262	50.122	20551907	118112	M
总计		100.000	41003420	245079	

Figure S151. HPLC data of rac-**2e**, related to Figure 2.

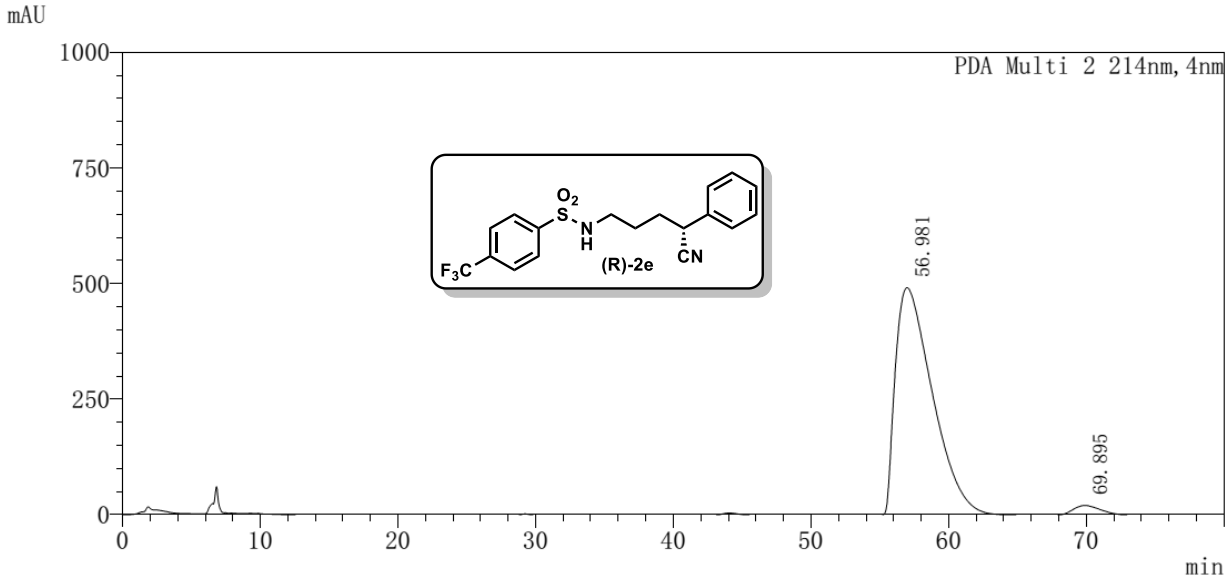

〈峰表〉

PDA Ch2 214nm

峰号	保留时间	面积%	面积	高度	标记
1	56.981	96.660	92704580	492493	M
2	69.895	3.340	3203036	21631	M
总计		100.000	95907615	514124	

Figure S152. HPLC data of **2e**, related to Figure 2.

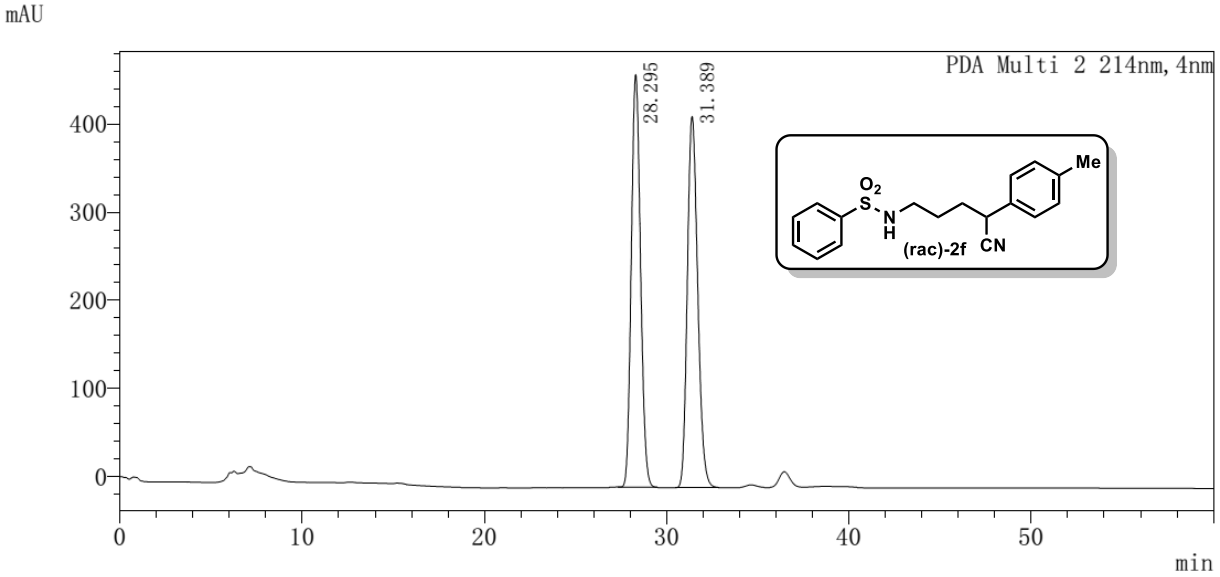

〈峰表〉

PDA Ch2 214nm

峰号	保留时间	面积%	面积	高度	标记
1	28.295	49.702	16469439	468564	M
2	31.389	50.298	16666635	421380	M
总计		100.000	33136074	889944	

Figure S153. HPLC data of rac-**2f**, related to Figure 2.

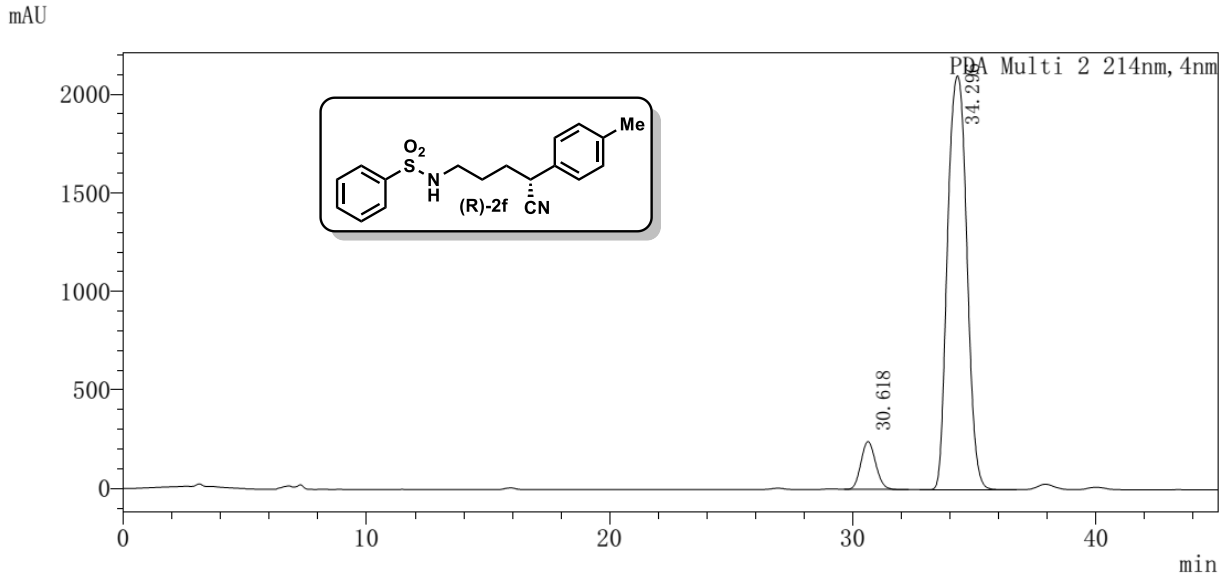

〈峰表〉

PDA Ch2 214nm

峰号	保留时间	面积%	面积	高度	标记
1	30.618	8.123	10228371	242480	M
2	34.296	91.877	115695045	2099657	M
总计		100.000	125923416	2342137	

Figure S154. HPLC data of **2f**, related to Figure 2.

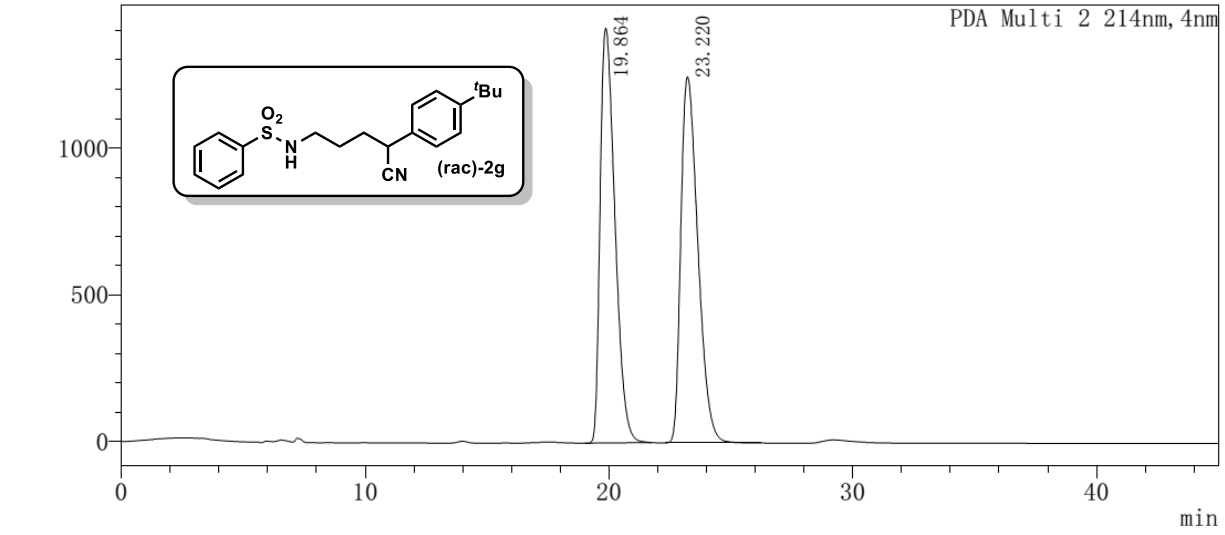

〈峰表〉

PDA Ch2 214nm

峰号	保留时间	面积%	面积	高度	标记
1	19.864	49.553	59567792	1412544	M
2	23.220	50.447	60641563	1246812	M
总计		100.000	120209356	2659356	

Figure S155. HPLC data of rac-**2g**, related to Figure 2.

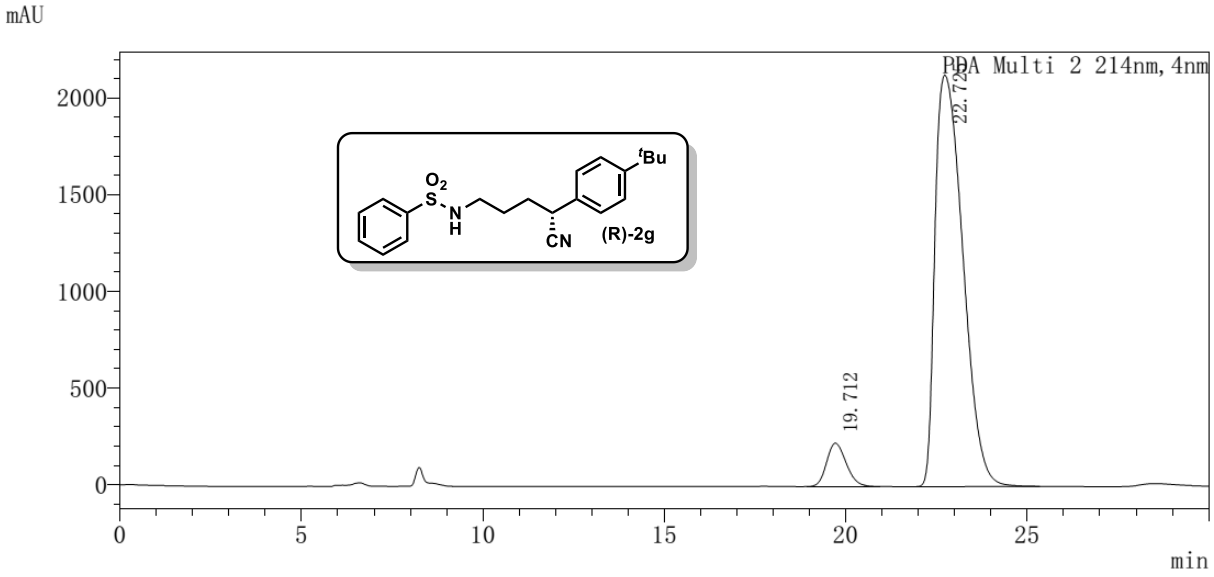

〈峰表〉

PDA Ch2 214nm

峰号	保留时间	面积%	面积	高度	标记
1	19.712	6.893	8399295	224284	M
2	22.725	93.107	113458703	2128436	M
总计		100.000	121857998	2352720	

Figure S156. HPLC data of **2g**, related to Figure 2.

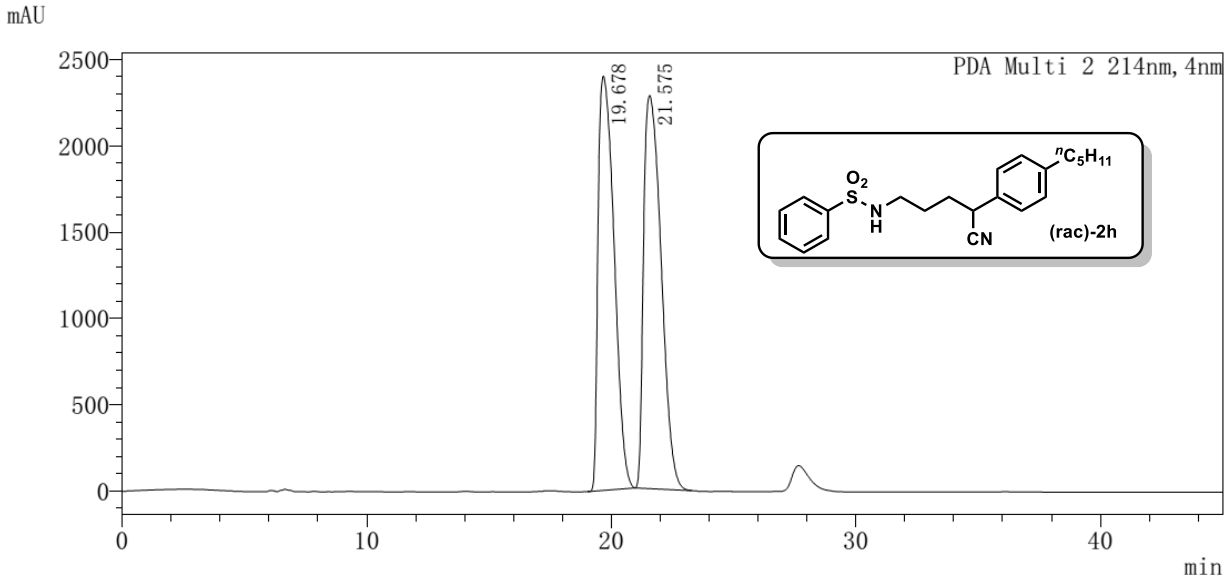

〈峰表〉

PDA Ch2 214nm

峰号	保留时间	面积%	面积	高度	标记
1	19.678	48.935	108938346	2400876	M
2	21.575	51.065	113679614	2278074	M
总计		100.000	222617960	4678950	

Figure S157. HPLC data of rac-**2h**, related to Figure 2.

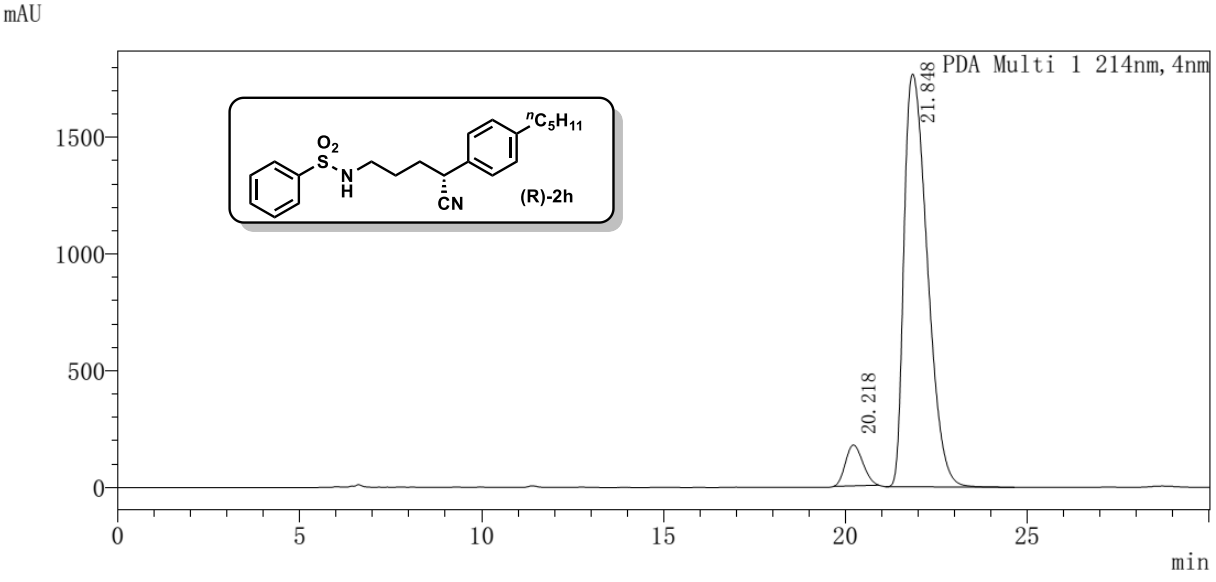

〈峰表〉

PDA Ch1 214nm

峰号	保留时间	面积%	面积	高度	标记
1	20.218	6.877	5823598	175191	M
2	21.848	93.123	78856066	1769621	M
总计		100.000	84679663	1944811	

Figure S158. HPLC data of **2h**, related to Figure 2.

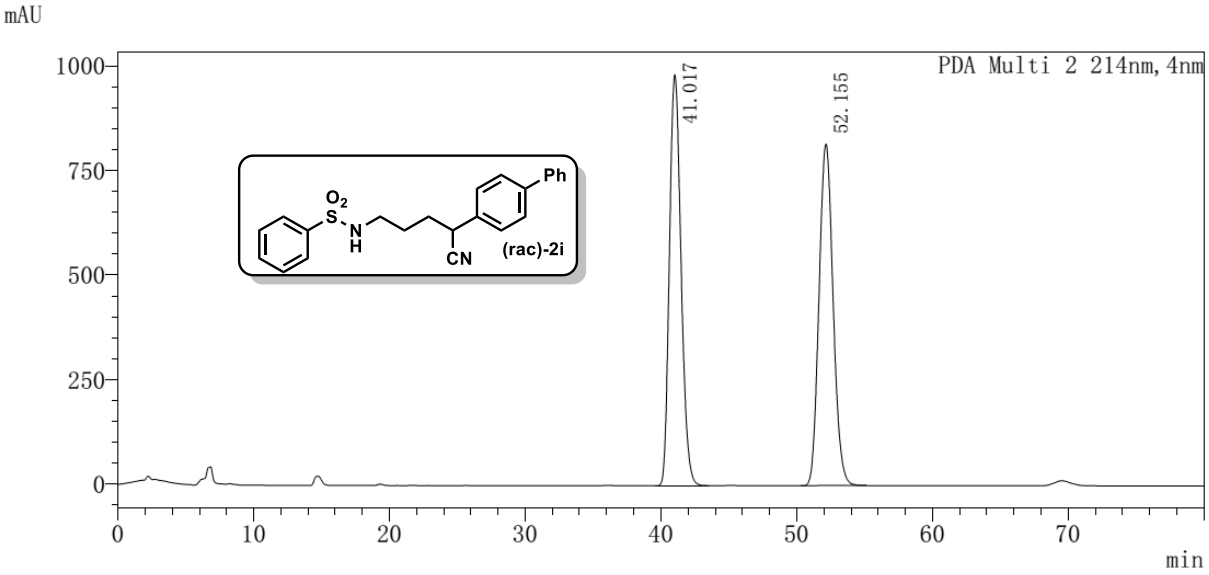

〈峰表〉

PDA Ch2 214nm

峰号	保留时间	面积%	面积	高度	标记
1	41.017	49.778	58363232	981928	M
2	52.155	50.222	58883604	816314	M
总计		100.000	117246835	1798242	

Figure S159. HPLC data of rac-**2i**, related to Figure 2.

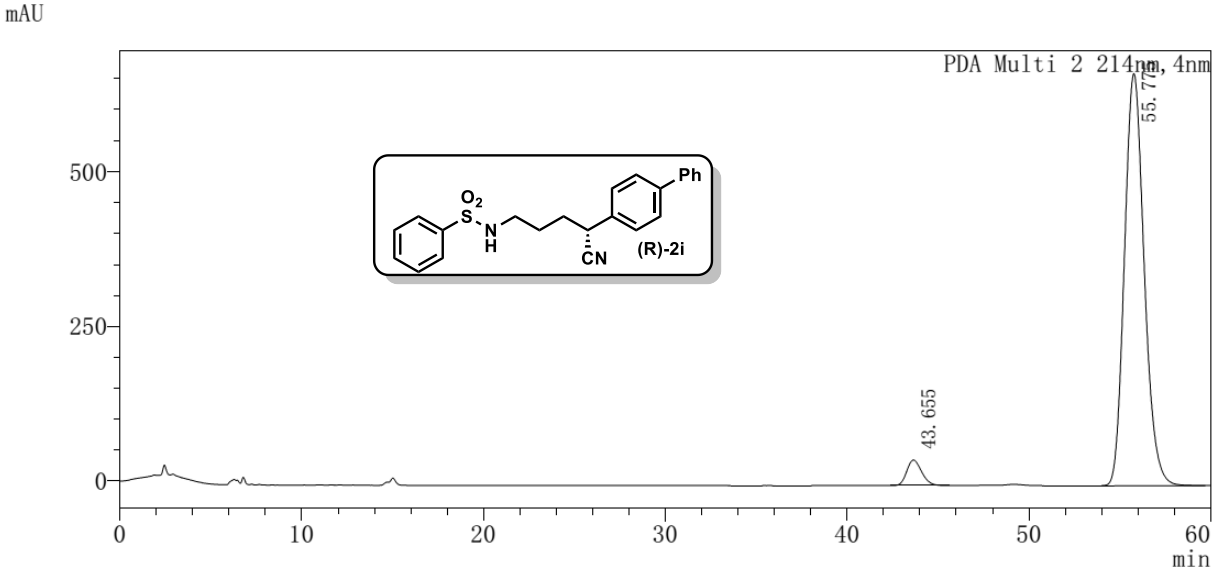

〈峰表〉

PDA Ch2 214nm

峰号	保留时间	面积%	面积	高度	标记
1	43.655	4.547	2394631	41482	M
2	55.775	95.453	50266186	665958	M
总计		100.000	52660817	707440	

Figure S160. HPLC data of **2i**, related to Figure 2.

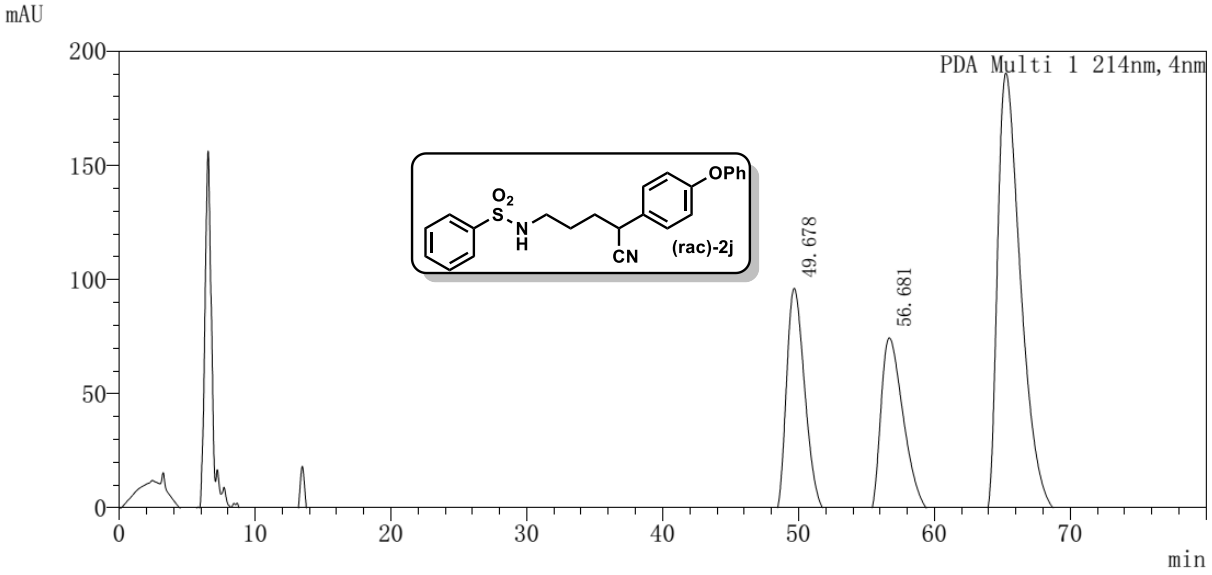

〈峰表〉

PDA Ch1 214nm

峰号	保留时间	面积%	面积	高度	标记
1	49.678	50.480	9955252	101420	M
2	56.681	49.520	9765884	79540	M
总计		100.000	19721136	180960	

Figure S161. HPLC data of rac-**2j**, related to Figure 2.

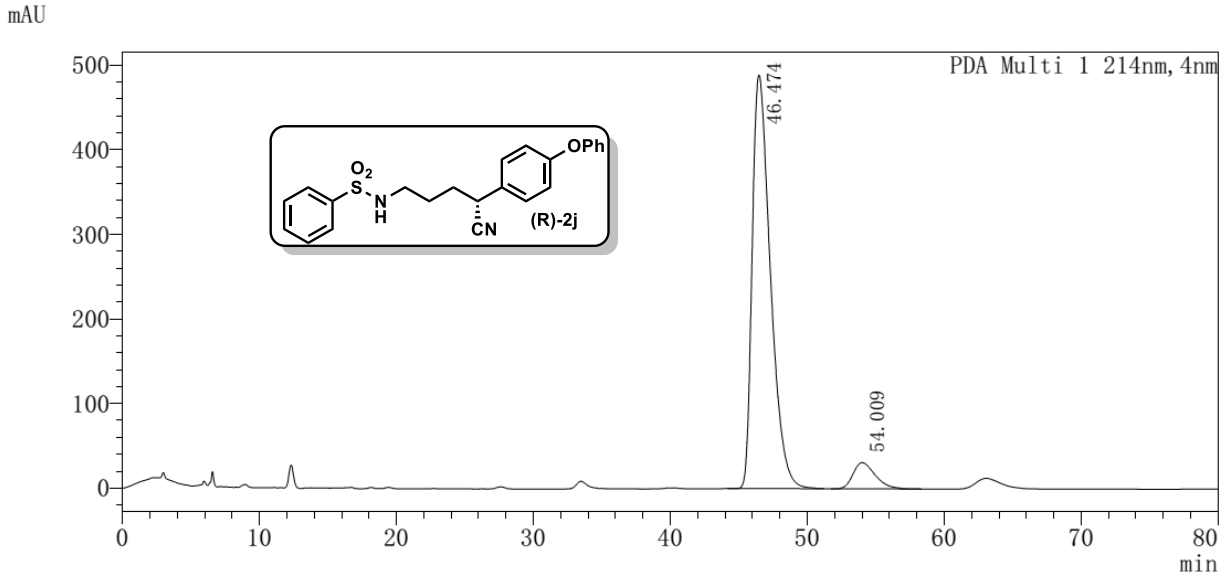

〈峰表〉

PDA Ch1 214nm

峰号	保留时间	面积%	面积	高度	标记
1	46.474	92.840	45064395	488400	M
2	54.009	7.160	3475575	30861	M
总计		100.000	48539971	519261	

Figure S162. HPLC data of **2j**, related to Figure 2.

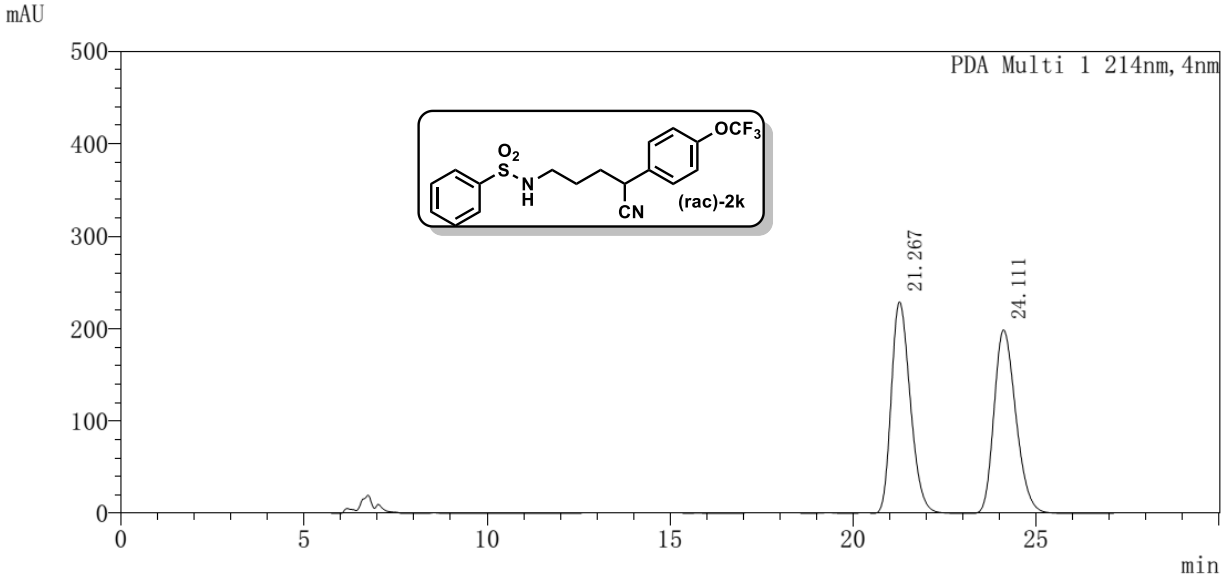

〈峰表〉

PDA Ch1 214nm

峰号	保留时间	面积%	面积	高度	标记
1	21.267	50.136	8305540	229277	M
2	24.111	49.864	8260588	198678	M
总计		100.000	16566128	427955	

Figure S163. HPLC data of rac-**2k**, related to Figure 2.

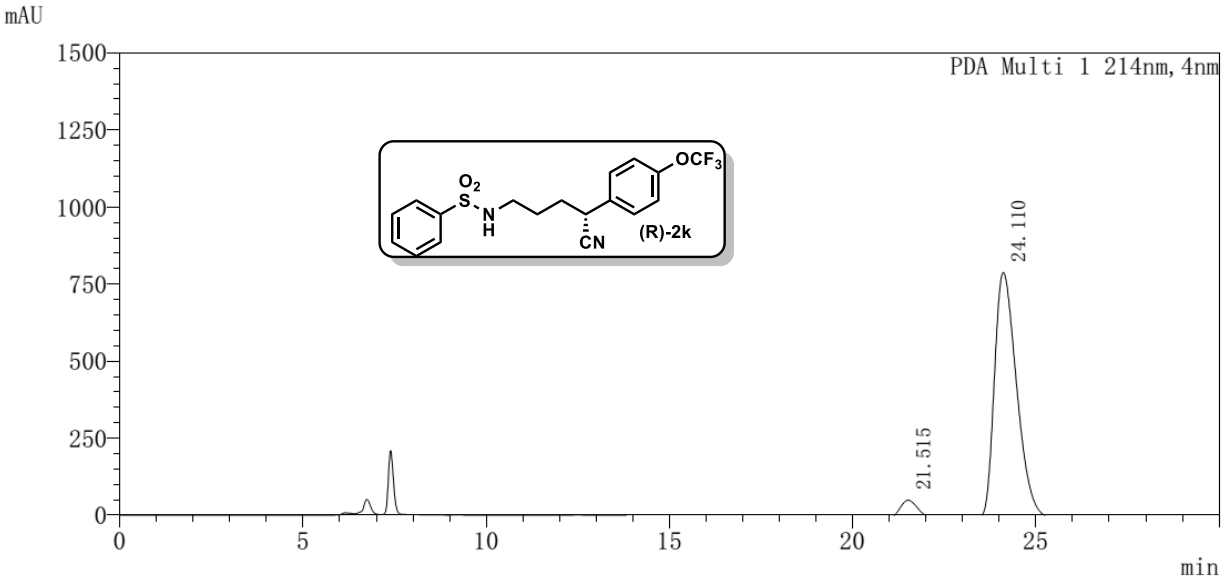

〈峰表〉

PDA Ch1 214nm

峰号	保留时间	面积%	面积	高度	标记
1	21.515	5.889	2112436	60582	M
2	24.110	94.111	33759792	799555	M
总计		100.000	35872228	860137	

Figure S164. HPLC data of **2k**, related to Figure 2.

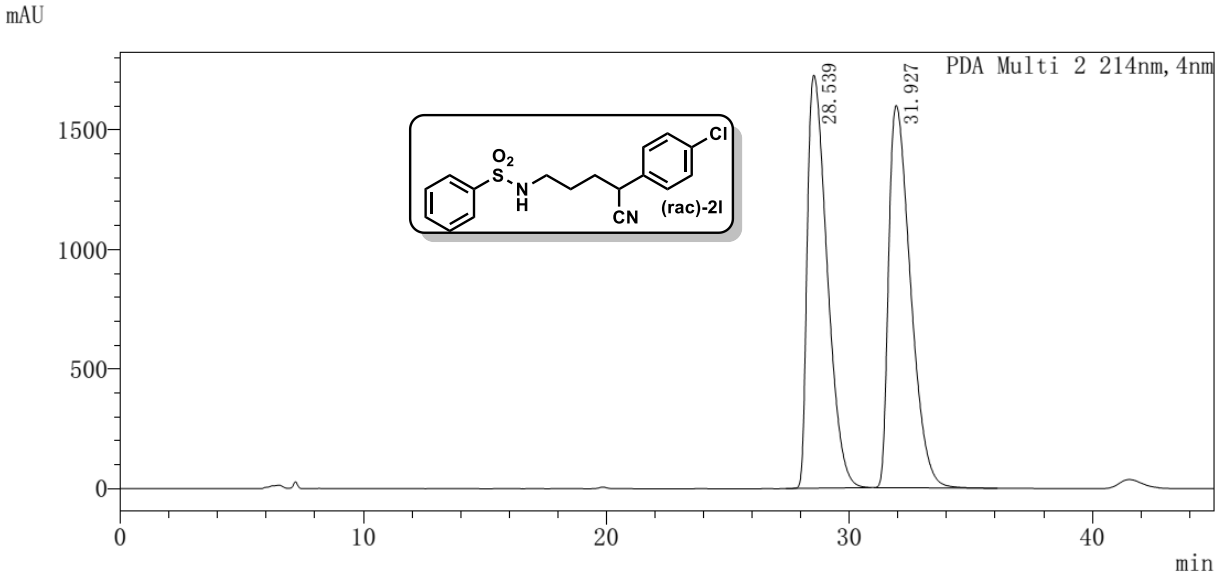

〈峰表〉

PDA Ch2 214nm

峰号	保留时间	面积%	面积	高度	标记
1	28.539	49.518	98209405	1728223	M
2	31.927	50.482	100119694	1600447	M
总计		100.000	198329099	3328670	

Figure S165. HPLC data of rac-**2l**, related to Figure 2.

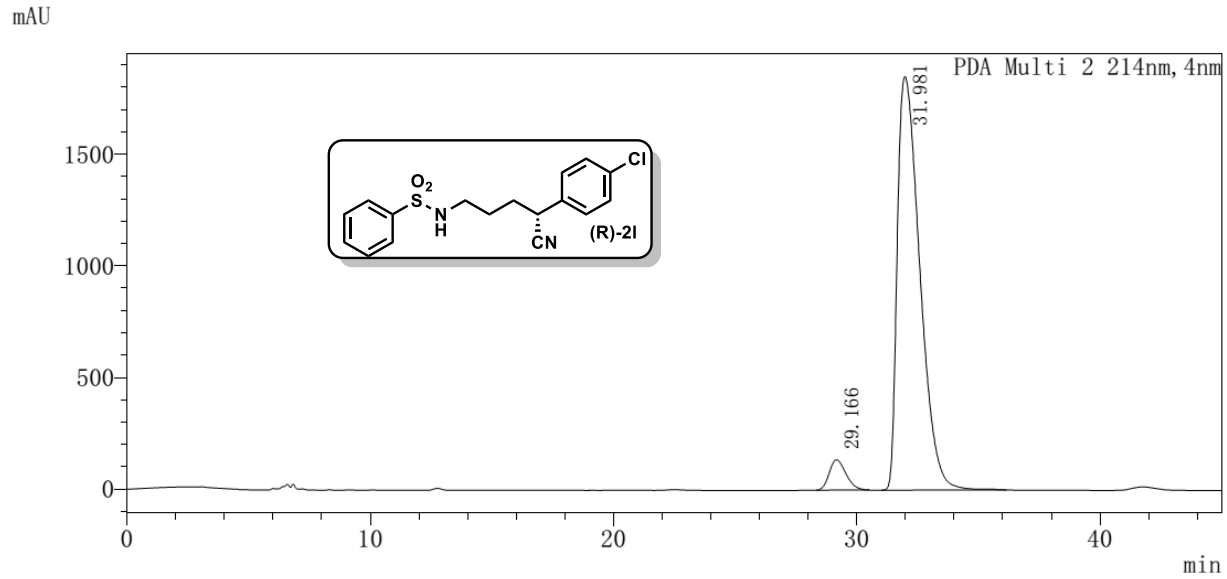

〈峰表〉

PDA Ch2 214nm

峰号	保留时间	面积%	面积	高度	标记
1	29.166	5.162	6478056	135587	M
2	31.981	94.838	119027655	1852317	M
总计		100.000	125505711	1987903	

Figure S166. HPLC data of **2l**, related to Figure 2.

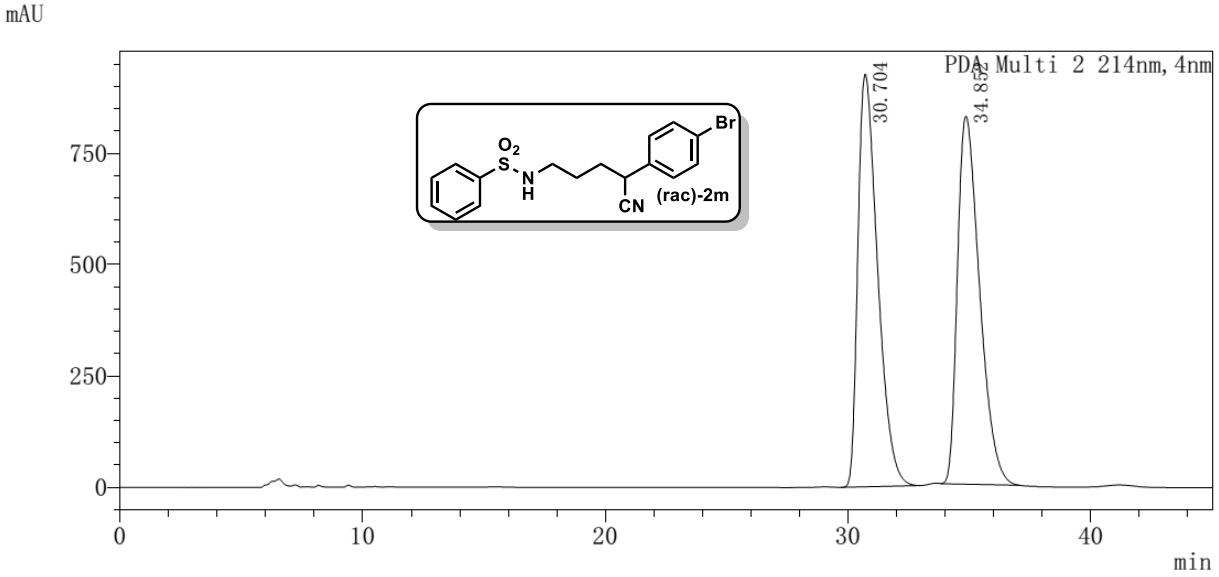

〈峰表〉

PDA Ch2 214nm

峰号	保留时间	面积%	面积	高度	标记
1	30.704	49.985	52284331	926355	M
2	34.852	50.015	52316159	826251	M
总计		100.000	104600490	1752606	

Figure S167. HPLC data of rac-**2m**, related to Figure 2.

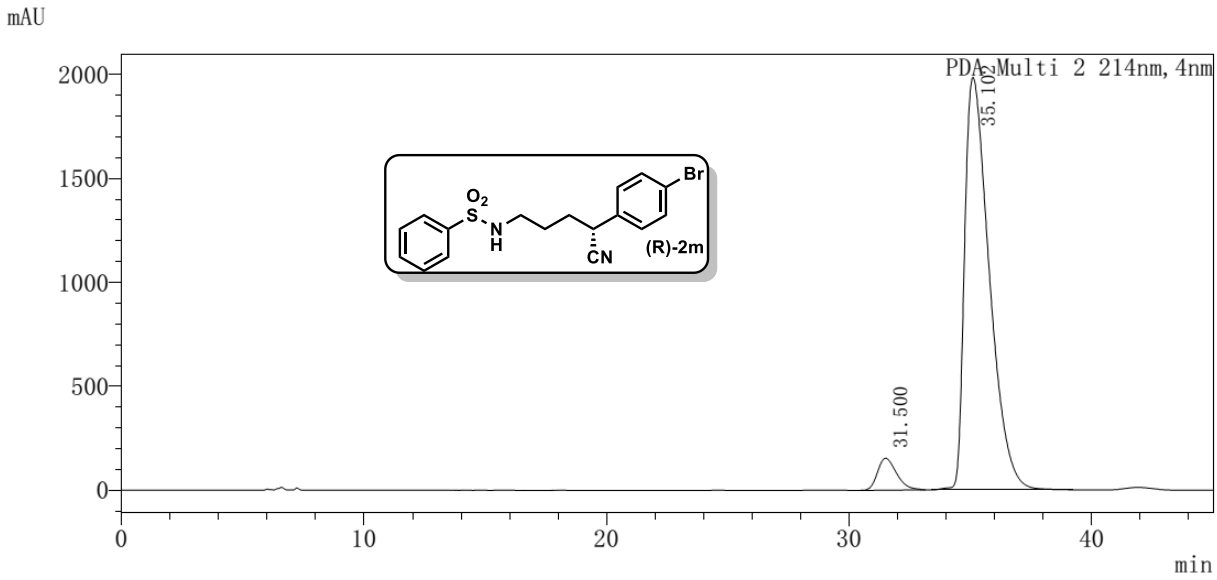

〈峰表〉

PDA Ch2 214nm

峰号	保留时间	面积%	面积	高度	标记
1	31.500	5.590	8315628	153043	M
2	35.102	94.410	140437709	1985740	M
总计		100.000	148753337	2138783	

Figure S168. HPLC data of **2m**, related to Figure 2.

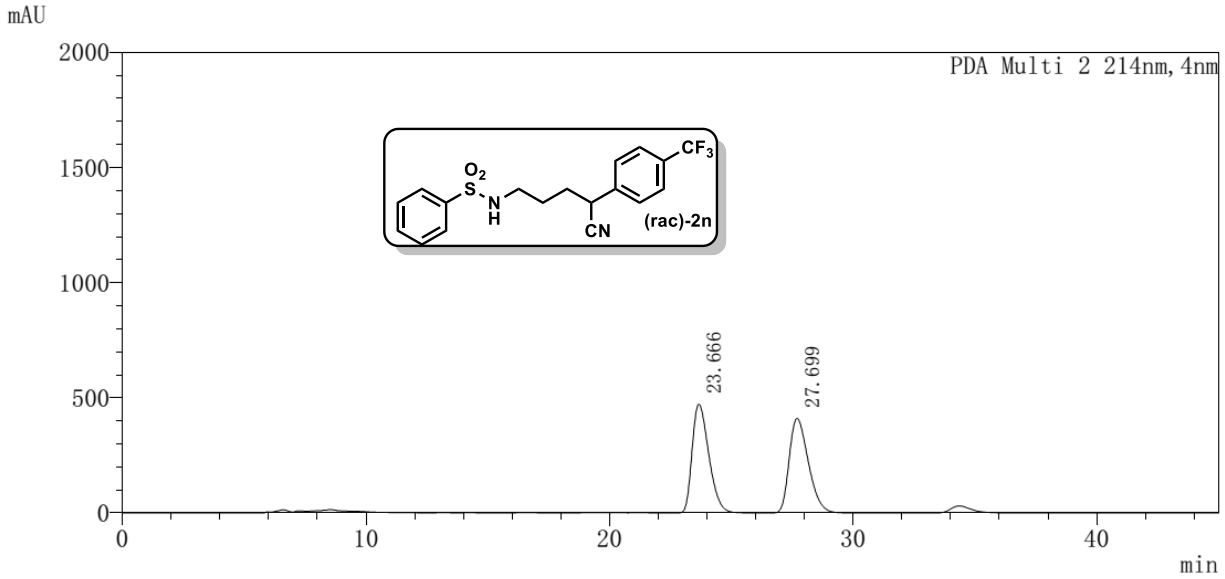

〈峰表〉

PDA Ch2 214nm

峰号	保留时间	面积%	面积	高度	标记
1	23.666	50.026	22610952	472965	M
2	27.699	49.974	22587473	411306	M
总计		100.000	45198425	884271	

Figure S169. HPLC data of rac-**2n**, related to Figure 2.

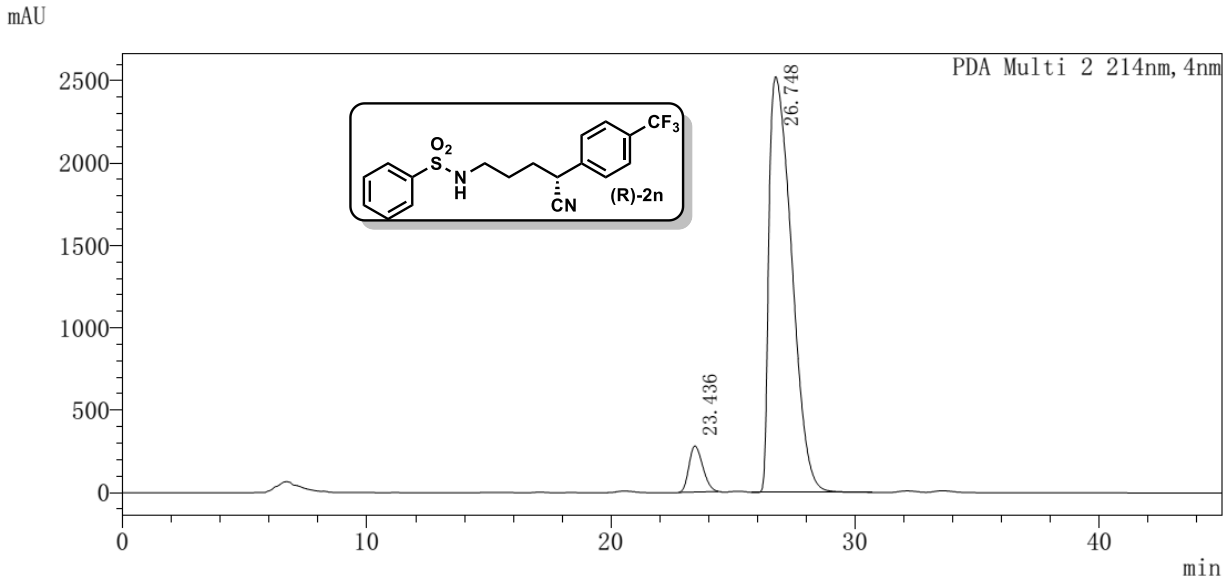

〈峰表〉

PDA Ch2 214nm

峰号	保留时间	面积%	面积	高度	标记
1	23.436	6.317	10941447	278729	M
2	26.748	93.683	162254017	2523147	M
总计		100.000	173195464	2801876	

Figure S170. HPLC data of **2n**, related to Figure 2.

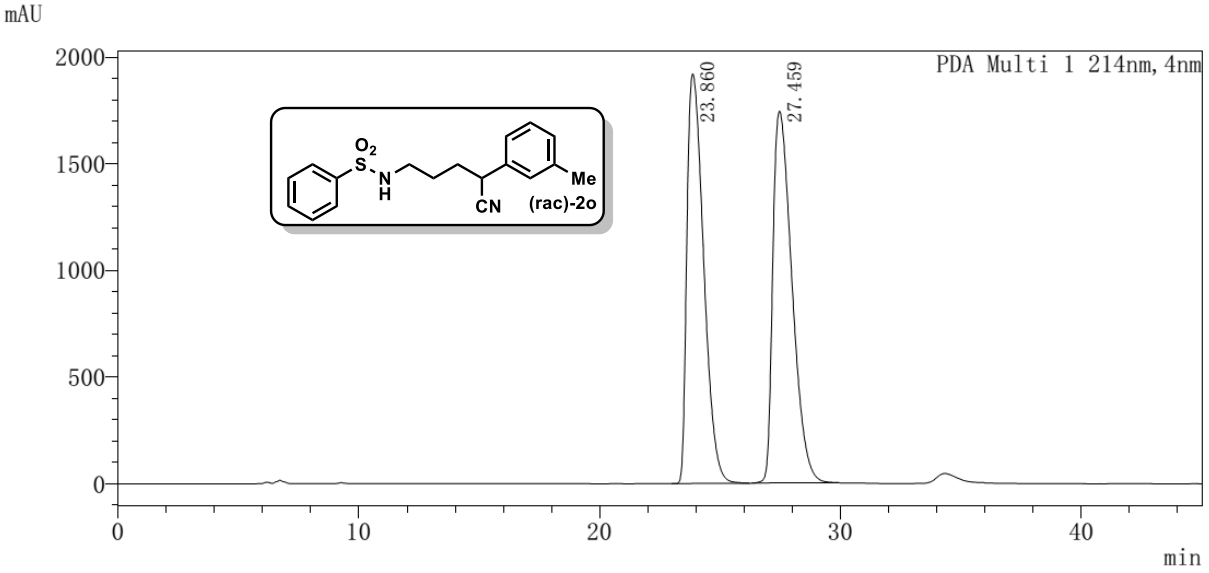

〈峰表〉

PDA Ch1 214nm

峰号	保留时间	面积%	面积	高度	标记
1	23.860	49.027	92799925	1921962	M
2	27.459	50.973	96483956	1744352	M
总计		100.000	189283880	3666314	

Figure S171. HPLC data of rac-**2o**, related to Figure 2.

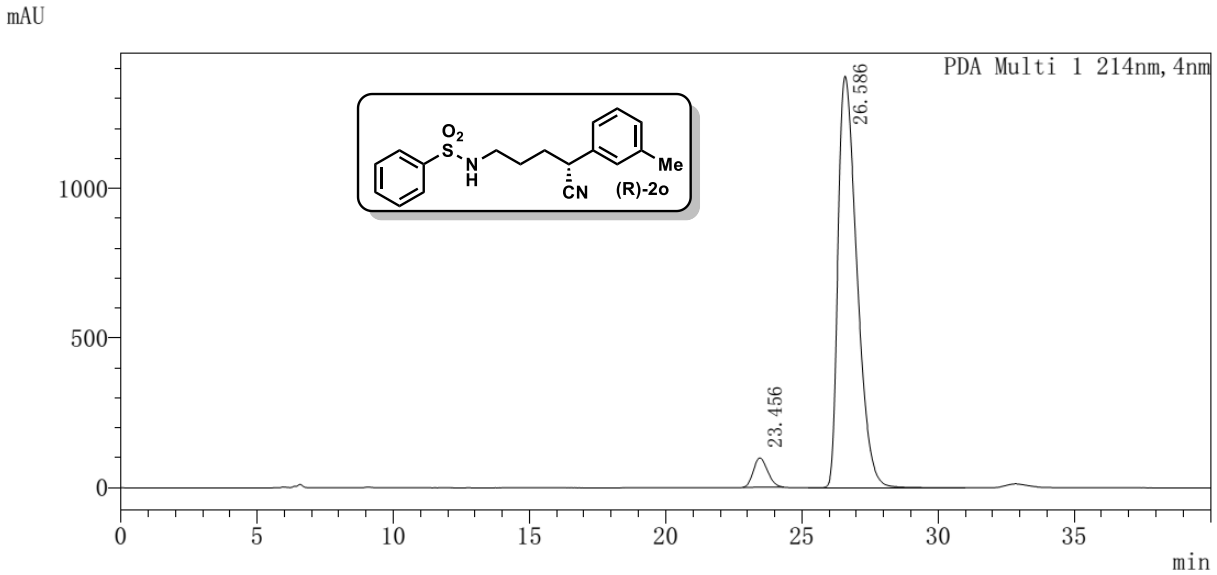

〈峰表〉

PDA Ch1 214nm

峰号	保留时间	面积%	面积	高度	标记
1	23.456	5.080	3541867	97645	M
2	26.586	94.920	66181350	1375977	M
总计		100.000	69723217	1473622	

Figure S172. HPLC data of **2o**, related to Figure 2.

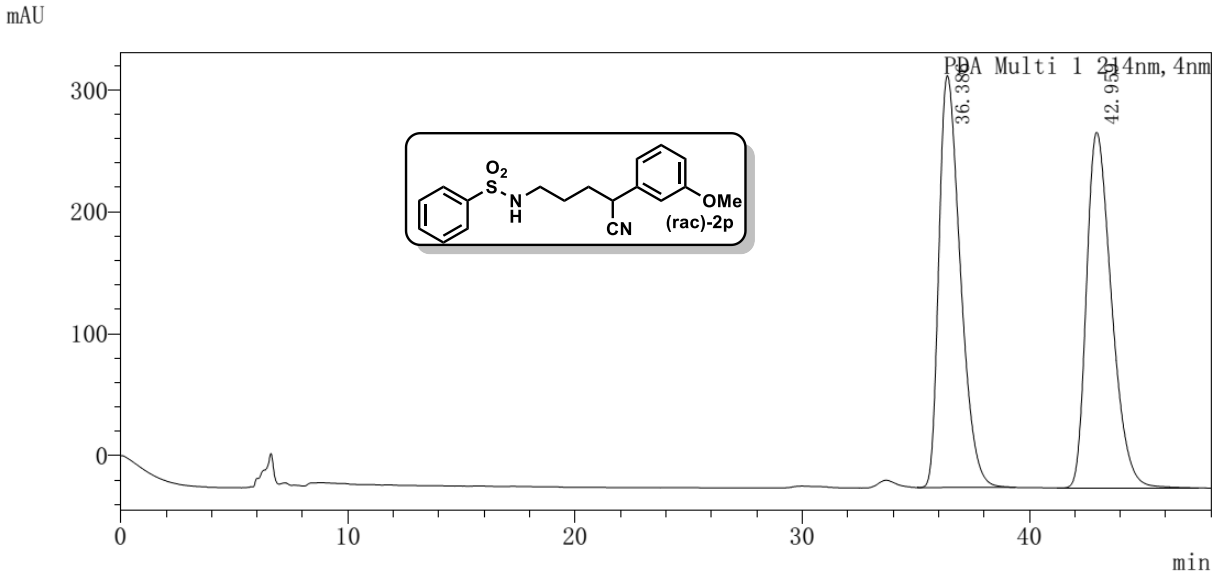

〈峰表〉

PDA Ch1 214nm

峰号	保留时间	面积%	面积	高度	标记
1	36.386	49.723	22109730	337653	M
2	42.959	50.277	22356073	291561	M
总计		100.000	44465803	629214	

Figure S173. HPLC data of rac-**2p**, related to Figure 2.

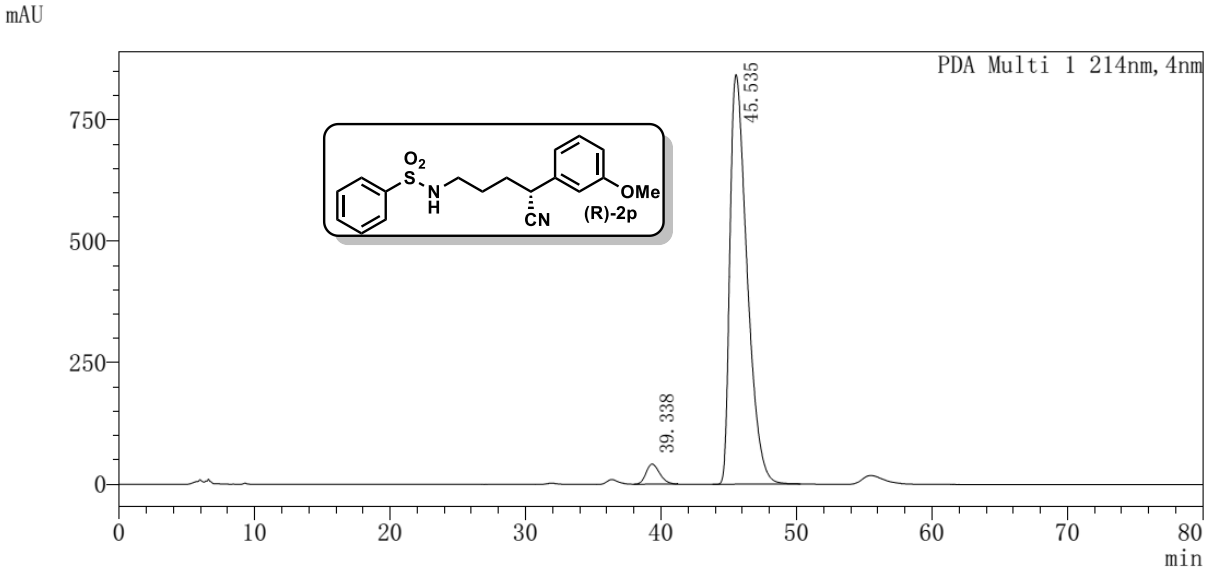

〈峰表〉

PDA Ch1 214nm

峰号	保留时间	面积%	面积	高度	标记
1	39.338	3.733	2881025	41233	M
2	45.535	96.267	74295852	843885	M
总计		100.000	77176877	885118	

Figure S174. HPLC data of **2p**, related to Figure 2.

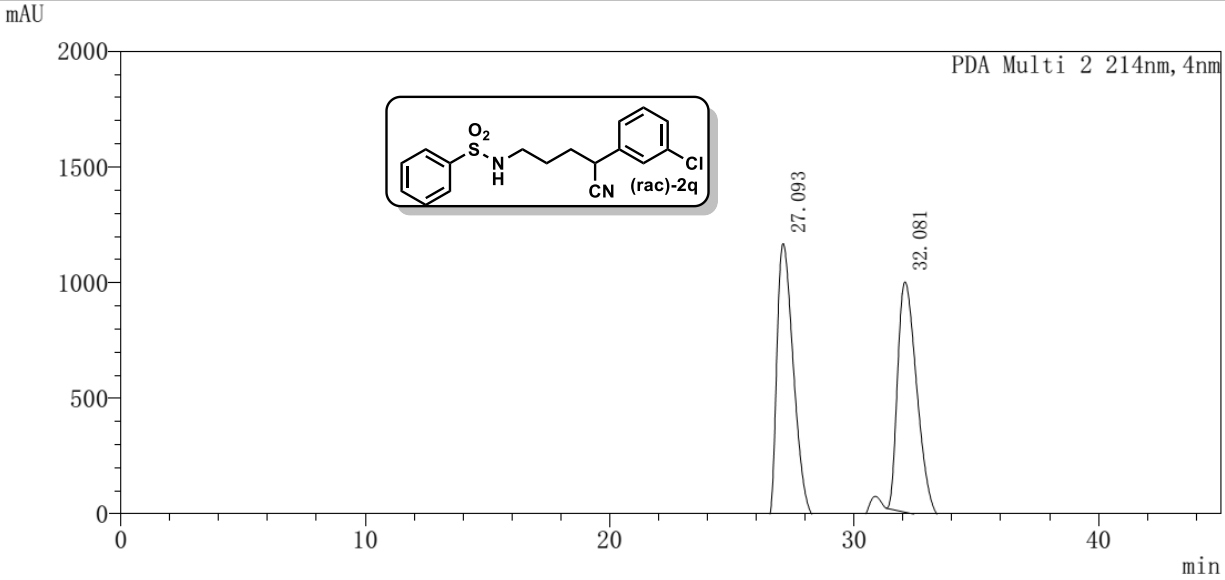

〈峰表〉

PDA Ch2 214nm

峰号	保留时间	面积%	面积	高度	标记
1	27.093	51.853	58740492	1211363	M
2	32.081	48.147	54542872	995634	M
总计		100.000	113283364	2206998	

Figure S175. HPLC data of rac-**2q**, related to Figure 2.

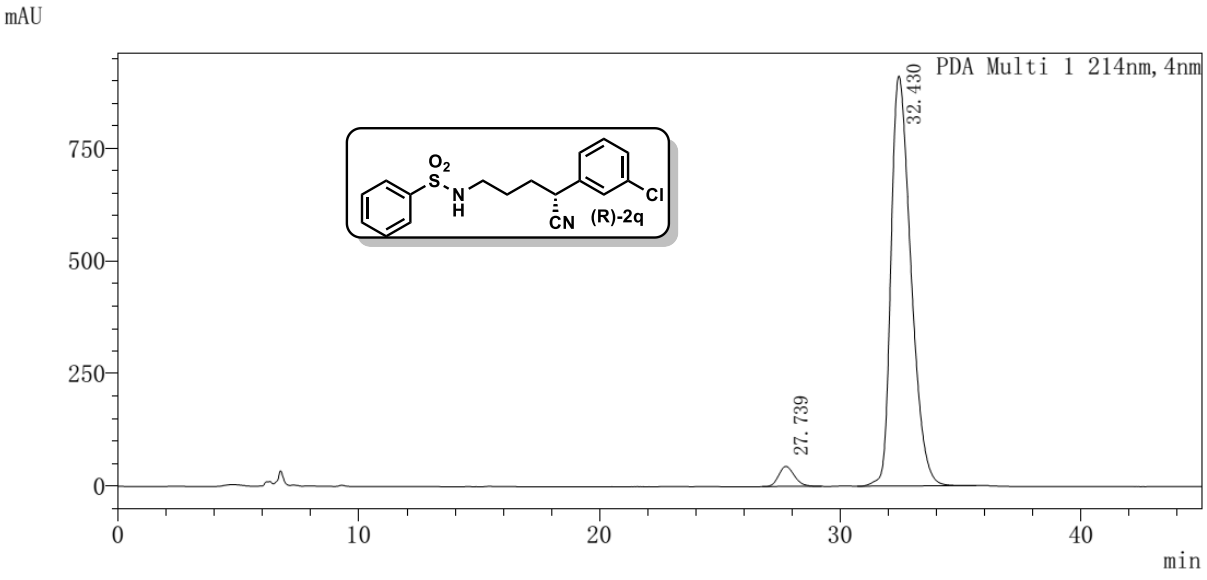

〈峰表〉

PDA Ch1 214nm

峰号	保留时间	面积%	面积	高度	标记
1	27.739	3.725	2027757	44497	M
2	32.430	96.275	52415512	910120	M
总计		100.000	54443269	954617	

Figure S176. HPLC data of **2q**, related to Figure 2.

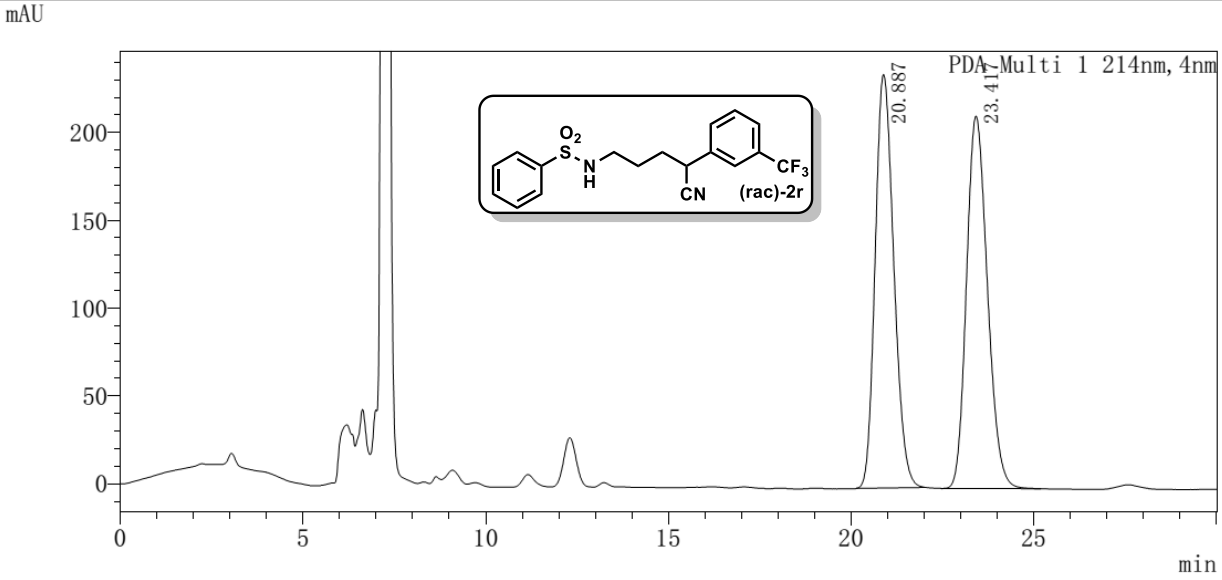

〈峰表〉

PDA Ch1 214nm

峰号	保留时间	面积%	面积	高度	标记
1	20.887	49.678	8346713	235618	M
2	23.417	50.322	8454788	212164	M
总计		100.000	16801501	447782	

Figure S177. HPLC data of rac-**2r**, related to Figure 2.

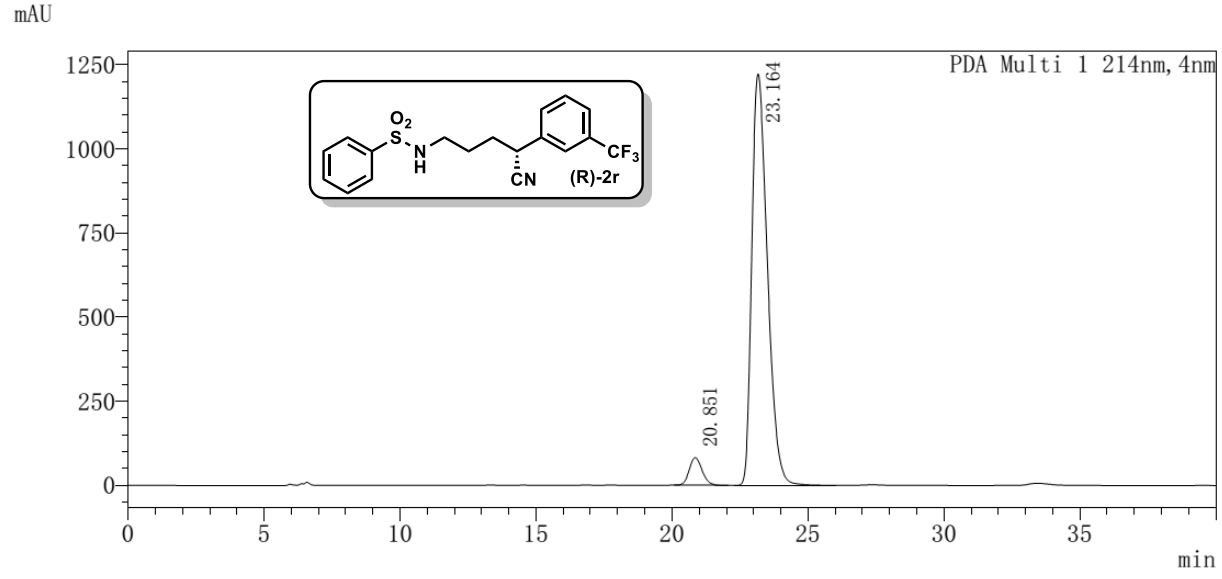

〈峰表〉

PDA Ch1 214nm

峰号	保留时间	面积%	面积	高度	标记
1	20.851	5.237	2696155	82019	
2	23.164	94.763	48783169	1222586	
总计		100.000	51479324	1304604	

Figure S178. HPLC data of **2r**, related to Figure 2.

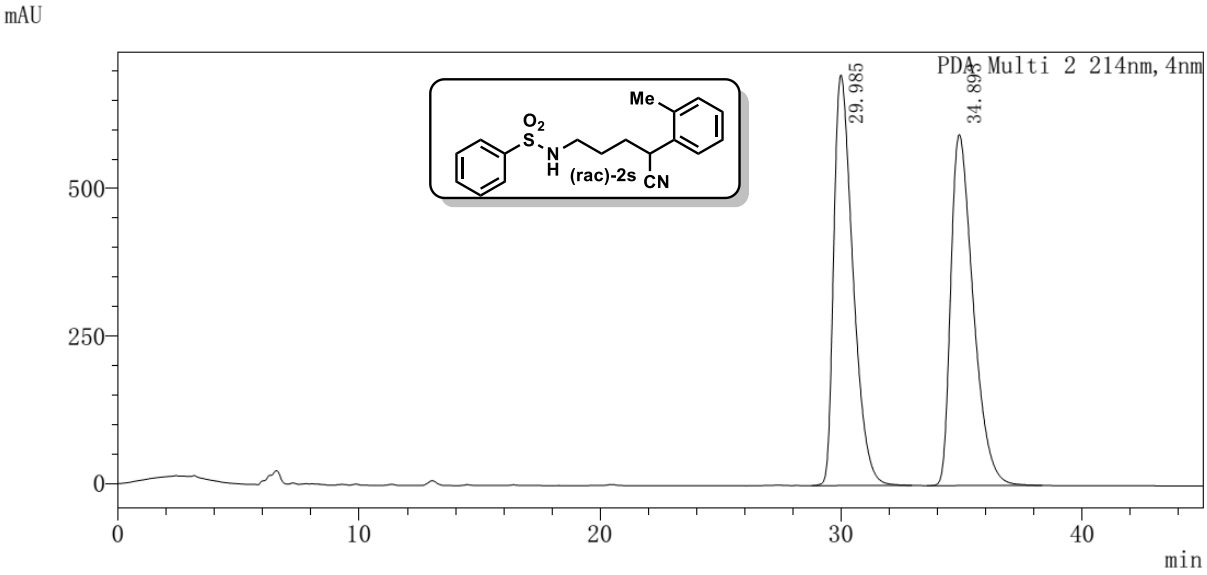

〈峰表〉

PDA Ch2 214nm

峰号	保留时间	面积%	面积	高度	标记
1	29.985	50.015	38540186	696223	M
2	34.893	49.985	38516638	595170	M
总计		100.000	77056824	1291393	

Figure S179. HPLC data of rac-**2s**, related to Figure 2.

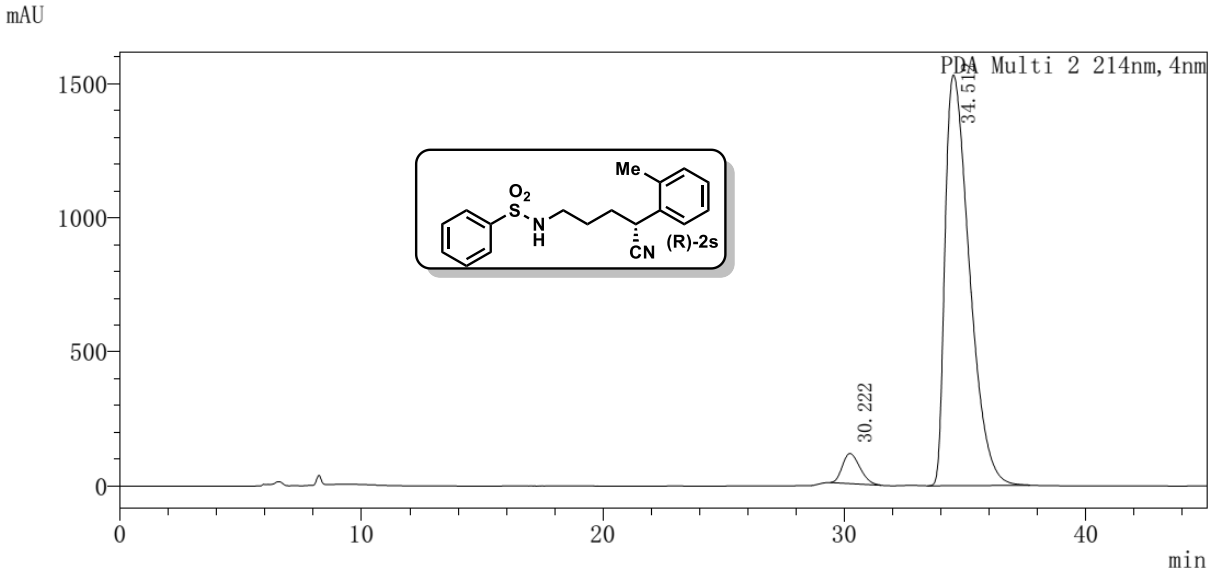

〈峰表〉

PDA Ch2 214nm

峰号	保留时间	面积%	面积	高度	标记
1	30.222	4.985	5637452	111750	M
2	34.512	95.015	107458751	1531766	M
总计		100.000	113096203	1643517	

Figure S180. HPLC data of **2s**, related to Figure 2.

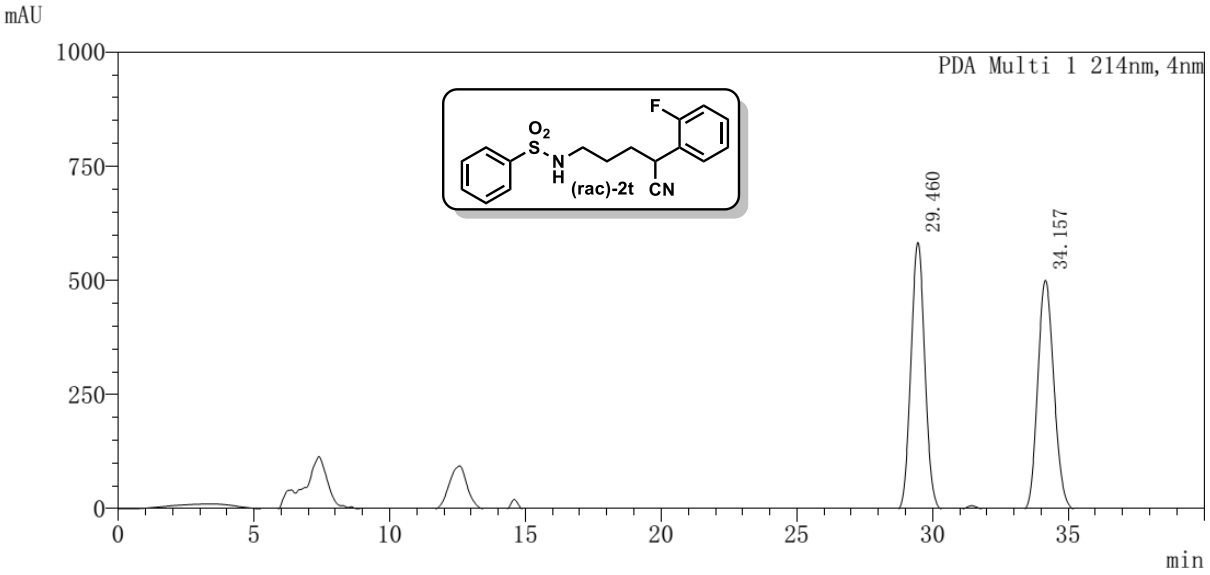

〈峰表〉

PDA Ch1 214nm

峰号	保留时间	面积%	面积	高度	标记
1	29.460	49.853	21095675	587941	M
2	34.157	50.147	21220385	505914	M
总计		100.000	42316060	1093855	

Figure S181. HPLC data of rac-**2t**, related to Figure 2.

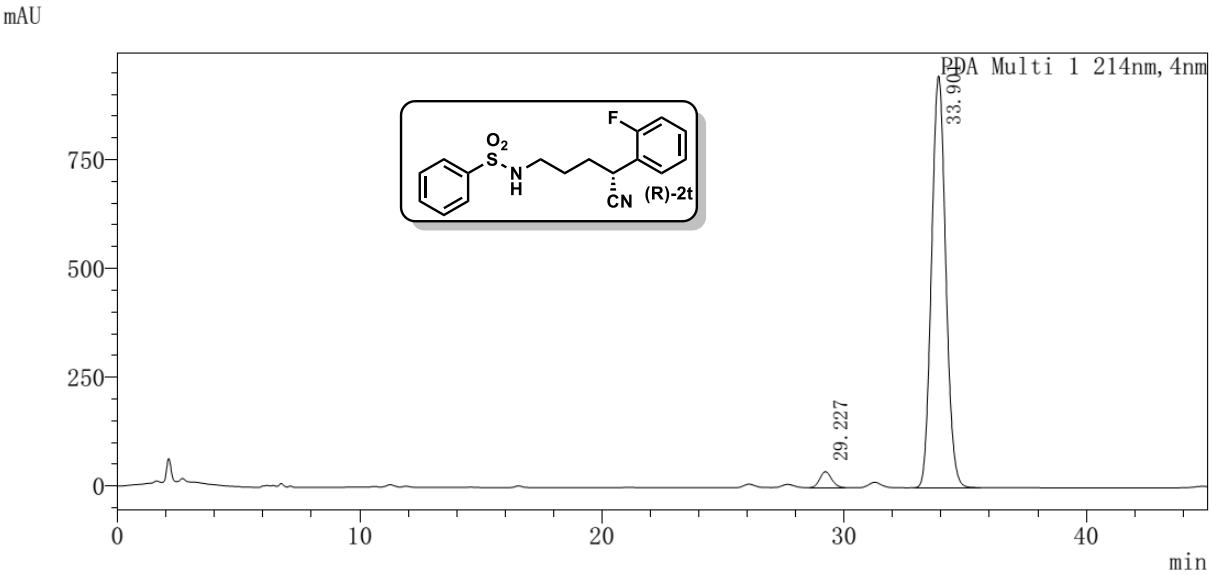

〈峰表〉

PDA Ch1 214nm

峰号	保留时间	面积%	面积	高度	标记
1	29.227	3.067	1220161	36392	M
2	33.901	96.933	38561063	946462	M
总计		100.000	39781224	982854	

Figure S182. HPLC data of **2t**, related to Figure 2.

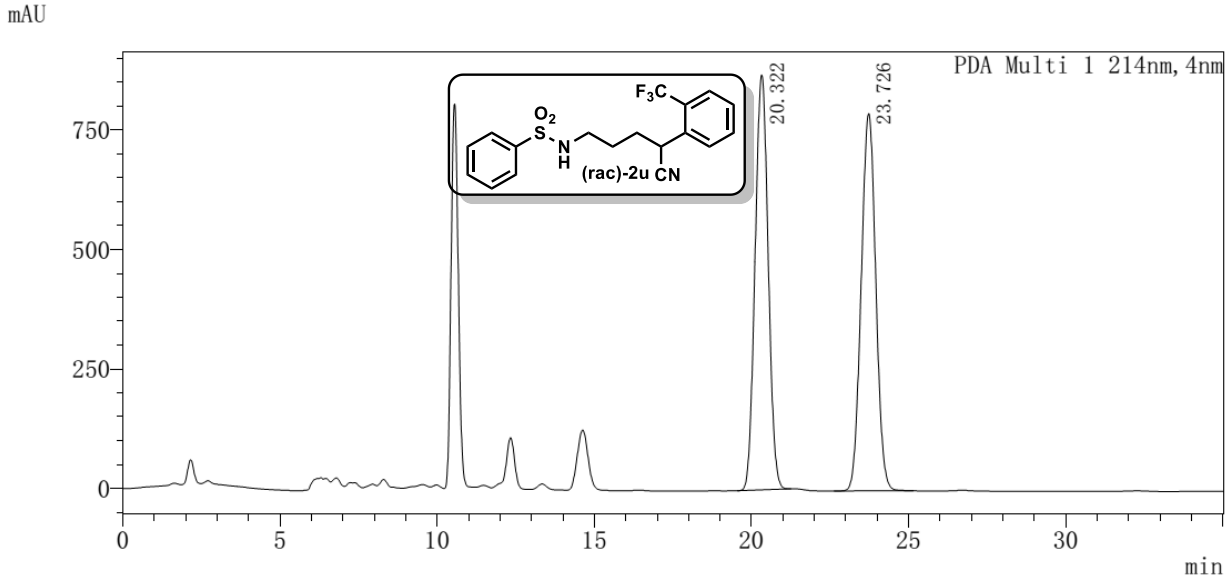

〈峰表〉

PDA Ch1 214nm

峰号	保留时间	面积%	面积	高度	标记
1	20.322	49.674	25217754	867979	M
2	23.726	50.326	25548249	789590	M
总计		100.000	50766003	1657569	

Figure S183. HPLC data of rac-**2u**, related to Figure 2.

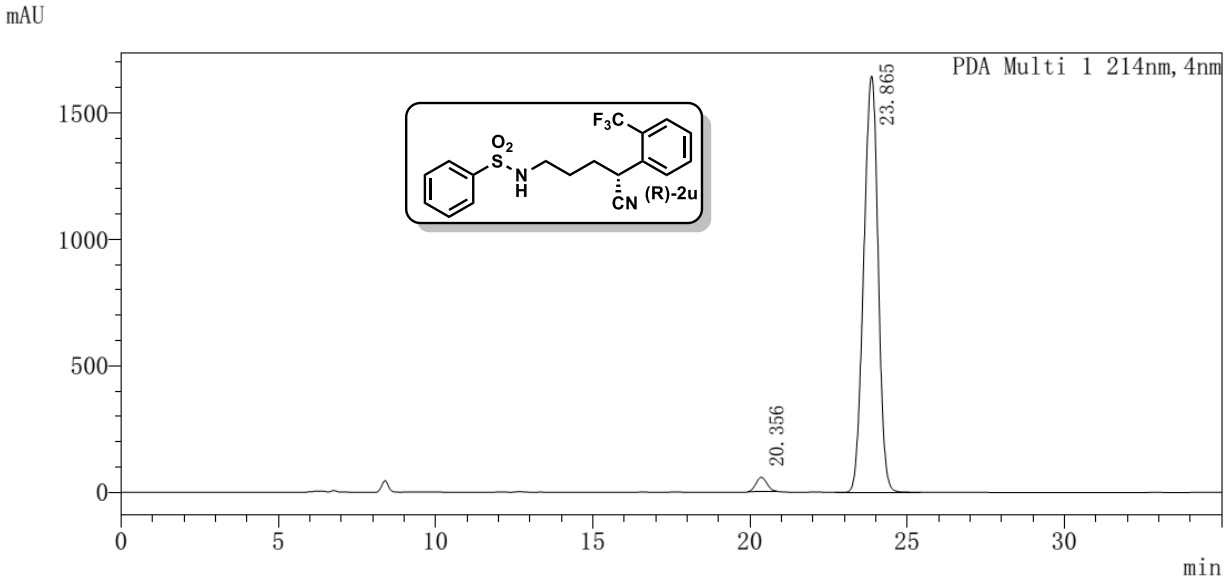

〈峰表〉

PDA Ch1 214nm

峰号	保留时间	面积%	面积	高度	标记
1	20.356	2.532	1361263	55964	M
2	23.865	97.468	52391437	1646995	M
总计		100.000	53752700	1702958	

Figure S184. HPLC data of **2u**, related to Figure 2.

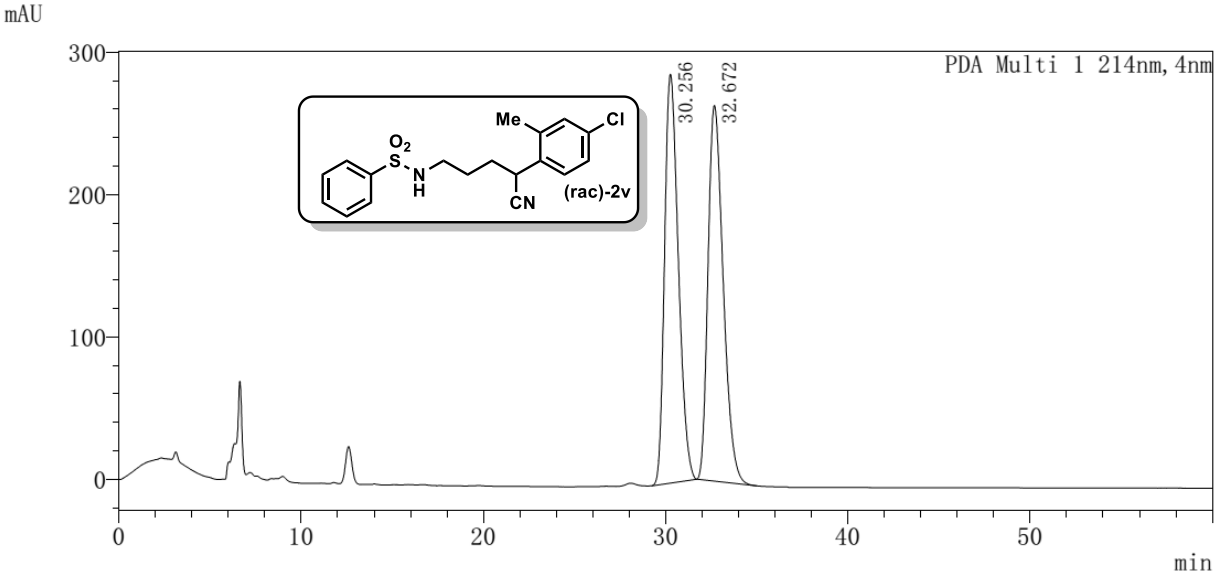

〈峰表〉

PDA Ch1 214nm

峰号	保留时间	面积%	面积	高度	标记
1	30.256	49.631	15059593	287218	M
2	32.672	50.369	15283631	264088	M
总计		100.000	30343224	551305	

Figure S185. HPLC data of rac-**2v**, related to Figure 2.

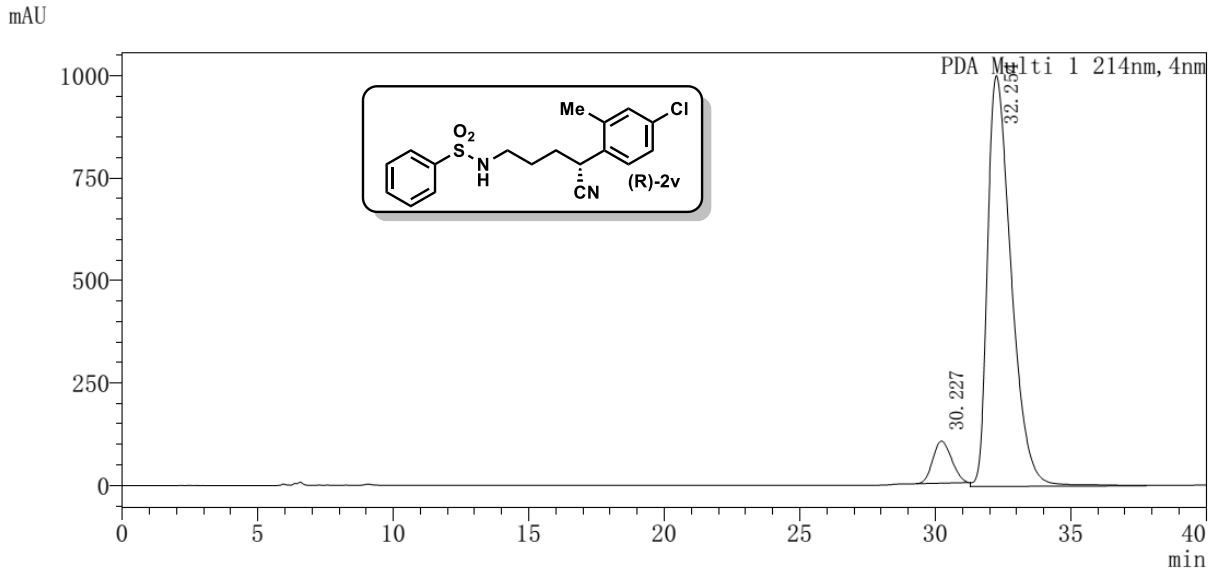

〈峰表〉

PDA Ch1 214nm

峰号	保留时间	面积%	面积	高度	标记
1	30.227	7.501	4960280	102400	M
2	32.254	92.499	61165750	1003022	M
总计		100.000	66126029	1105422	

Figure S186. HPLC data of **2v**, related to Figure 2.

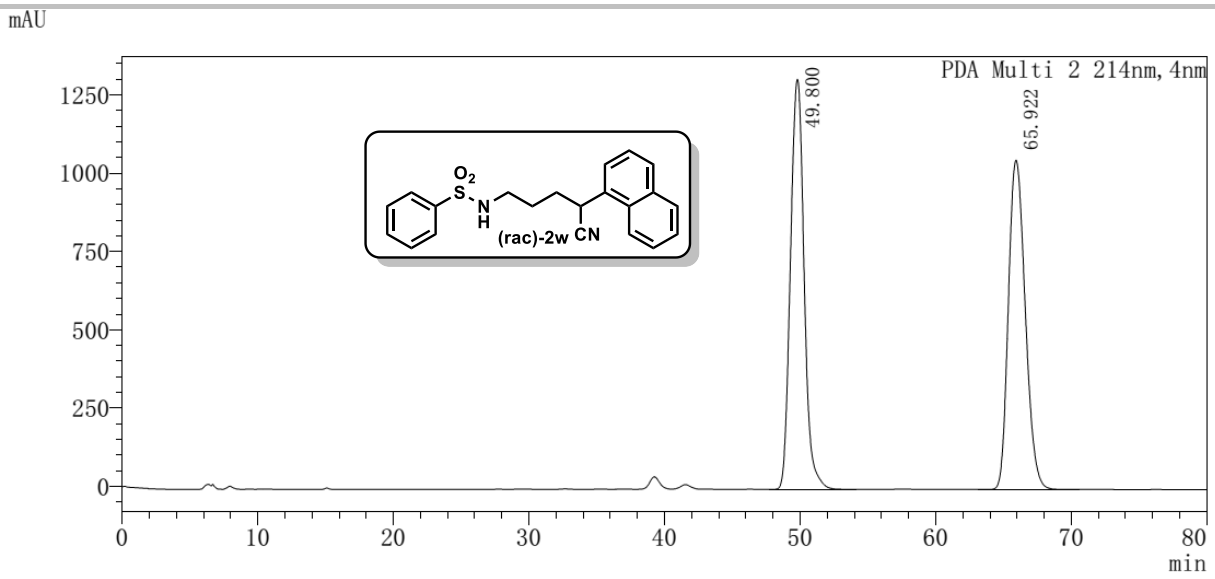

〈峰表〉

PDA Ch2 214nm

峰号	保留时间	面积%	面积	高度	标记
1	49.800	50.156	91530658	1309218	M
2	65.922	49.844	90963085	1051521	M
总计		100.000	182493743	2360739	

Figure S187. HPLC data of rac-**2w**, related to Figure 2.

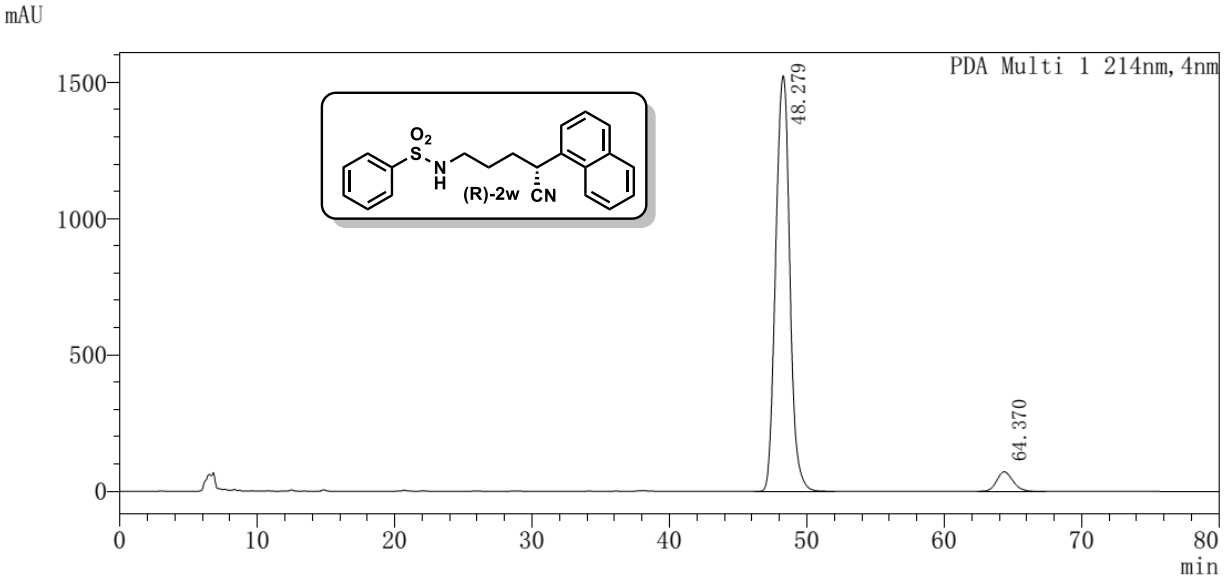

〈峰表〉

PDA Ch1 214nm

峰号	保留时间	面积%	面积	高度	标记
1	48.279	94.951	108846343	1524950	M
2	64.370	5.049	5787969	71077	M
总计		100.000	114634312	1596026	

Figure S188. HPLC data of **2w**, related to Figure 2.

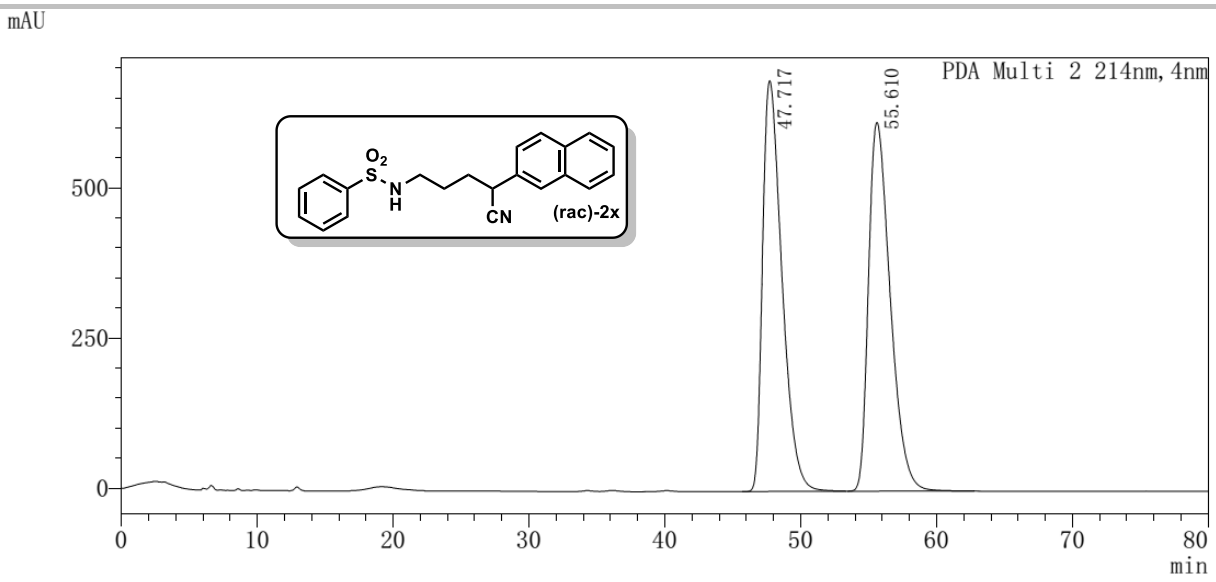

〈峰表〉

PDA Ch2 214nm

峰号	保留时间	面积%	面积	高度	标记
1	47.717	49.861	67827595	684001	M
2	55.610	50.139	68206149	613754	M
总计		100.000	136033745	1297755	

Figure S189. HPLC data of rac-**2x**, related to Figure 2.

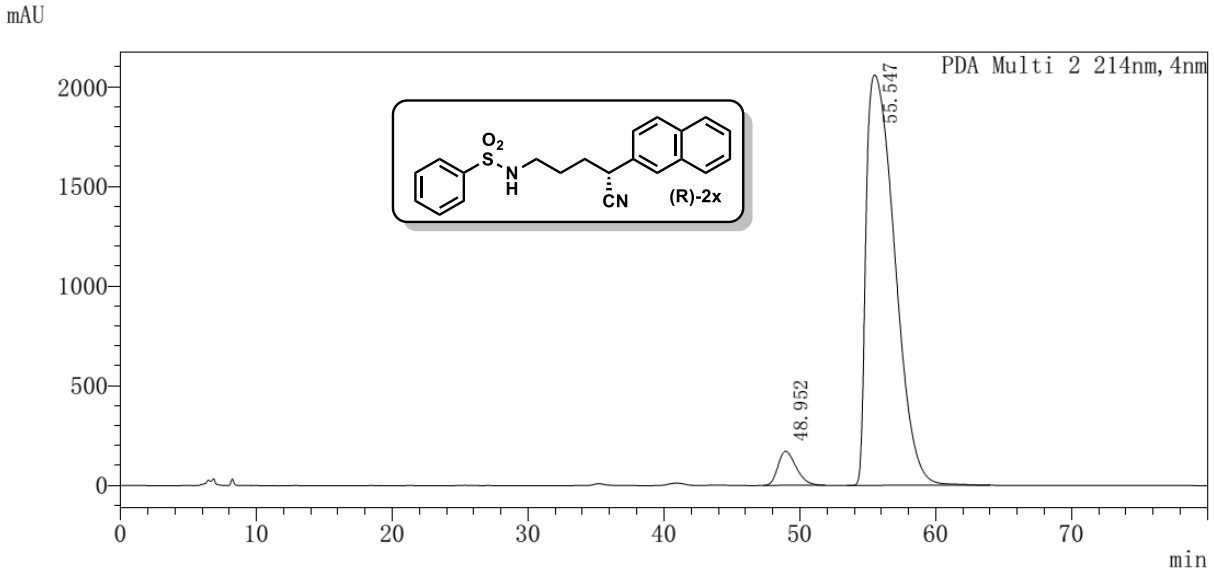

〈峰表〉

PDA Ch2 214nm

峰号	保留时间	面积%	面积	高度	标记
1	48.952	5.006	15883929	170849	M
2	55.547	94.994	301400880	2061728	M
总计		100.000	317284809	2232577	

Figure S190. HPLC data of **2x**, related to Figure 2.

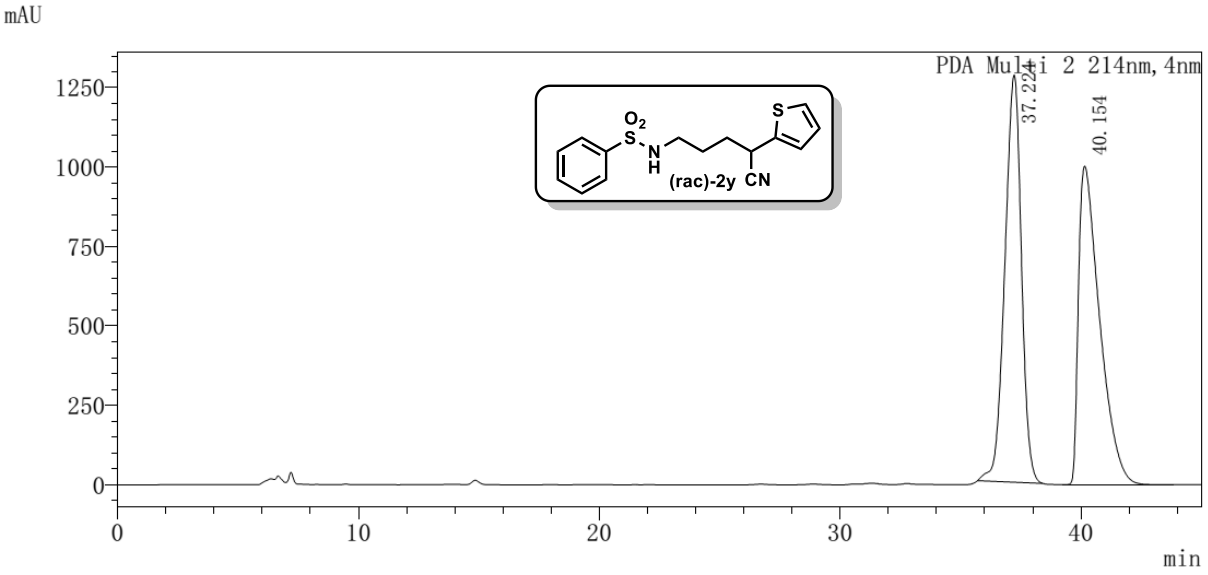

〈峰表〉

PDA Ch2 214nm

峰号	保留时间	面积%	面积	高度	标记
1	37.224	50.003	61233355	1282190	M
2	40.154	49.997	61226571	1002044	M
总计		100.000	122459926	2284234	

Figure S191. HPLC data of rac-**2y**, related to Figure 2.

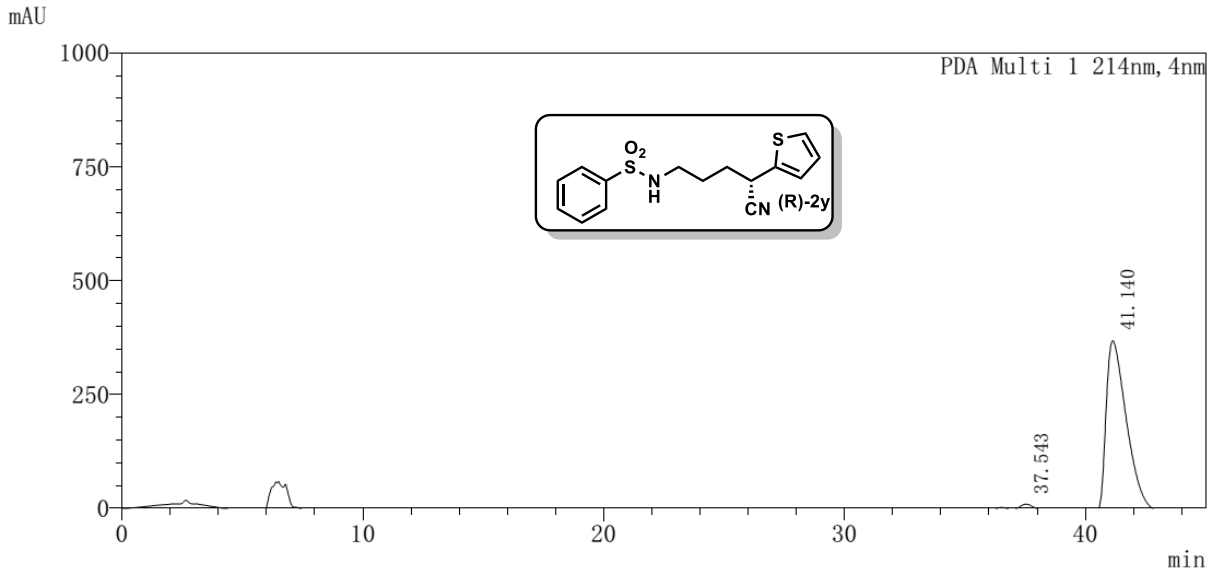

〈峰表〉

PDA Ch1 214nm

峰号	保留时间	面积%	面积	高度	标记
1	37.543	3.493	804551	16937	M
2	41.140	96.507	22229679	375833	M
总计		100.000	23034230	392770	

Figure S192. HPLC data of **2y**, related to Figure 2.

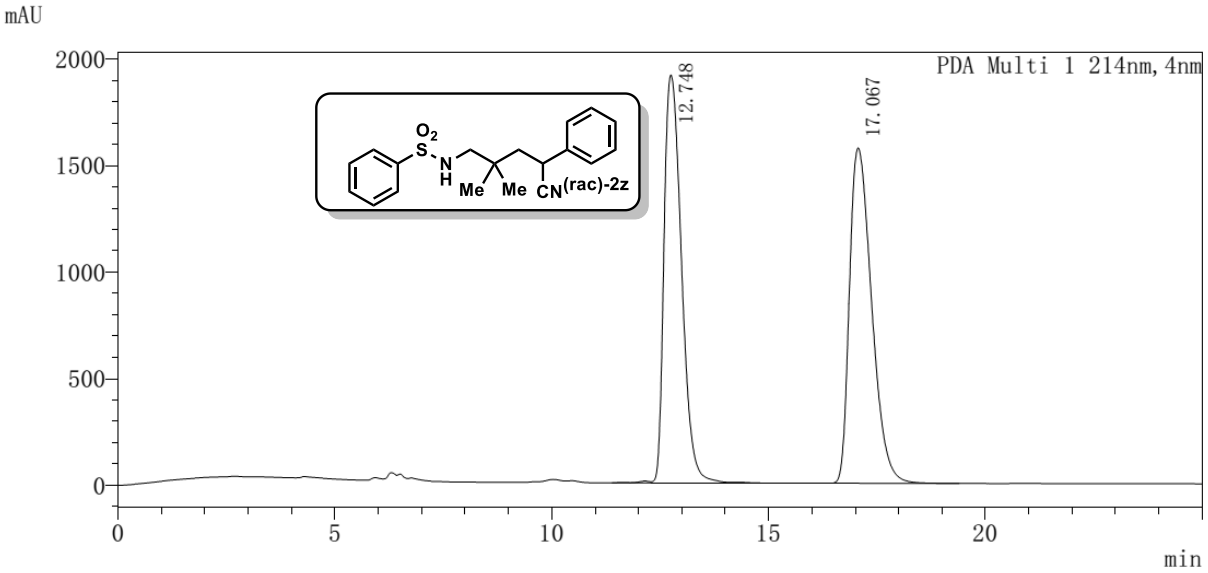

〈峰表〉

PDA Ch1 214nm

峰号	保留时间	面积%	面积	高度	标记
1	12.748	48.951	53812413	1915509	M
2	17.067	51.049	56118615	1575674	M
总计		100.000	109931028	3491183	

Figure S193. HPLC data of rac-**2z**, related to Figure 2.

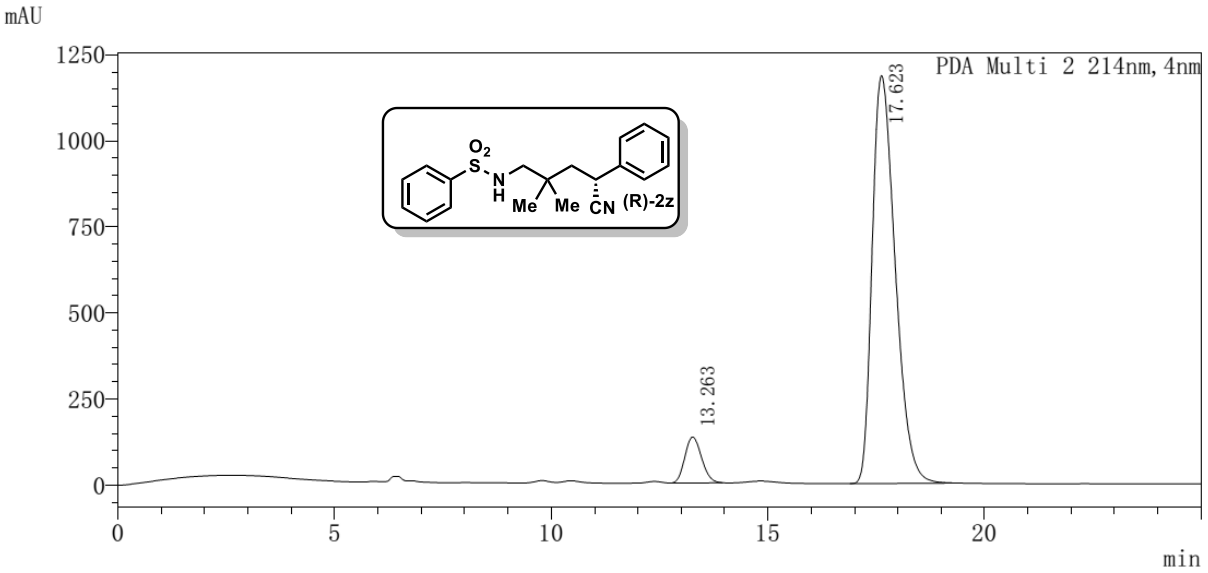

〈峰表〉

PDA Ch2 214nm

峰号	保留时间	面积%	面积	高度	标记
1	13.263	7.554	3582124	133245	M
2	17.623	92.446	43836613	1185247	M
总计		100.000	47418737	1318492	

Figure S194. HPLC data of **2z**, related to Figure 2.